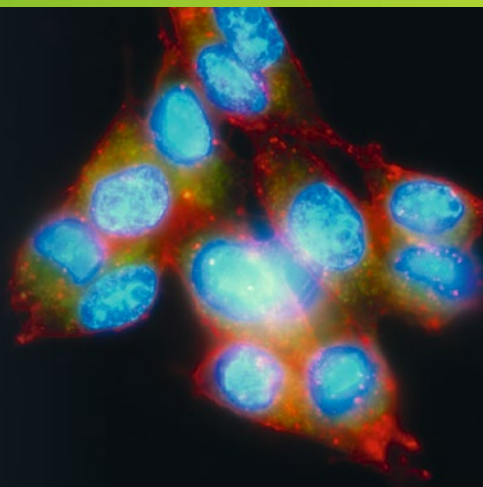


Methods in  
Molecular Biology 2622

Springer Protocols



Gerard G.M. D'Souza  
Hongwei Zhang *Editors*

# Liposomes

Methods and Protocols

*Third Edition*

Humana Press

# METHODS IN MOLECULAR BIOLOGY

*Series Editor*

John M. Walker

School of Life and Medical Sciences

University of Hertfordshire

Hatfield, Hertfordshire, UK

For further volumes:  
<http://www.springer.com/series/7651>

For over 35 years, biological scientists have come to rely on the research protocols and methodologies in the critically acclaimed *Methods in Molecular Biology* series. The series was the first to introduce the step-by-step protocols approach that has become the standard in all biomedical protocol publishing. Each protocol is provided in readily-reproducible step-by-step fashion, opening with an introductory overview, a list of the materials and reagents needed to complete the experiment, and followed by a detailed procedure that is supported with a helpful notes section offering tips and tricks of the trade as well as troubleshooting advice. These hallmark features were introduced by series editor Dr. John Walker and constitute the key ingredient in each and every volume of the *Methods in Molecular Biology* series. Tested and trusted, comprehensive and reliable, all protocols from the series are indexed in PubMed.

# **Liposomes**

**Methods and Protocols**

**Third Edition**

Edited by

**Gerard G. M. D'Souza and Hongwei Zhang**

*School of Pharmacy, MCPHS University, Boston, MA, USA*

 **Humana Press**

*Editors*

Gerard G. M. D'Souza  
School of Pharmacy  
MCPHS University  
Boston, MA, USA

Hongwei Zhang  
School of Pharmacy  
MCPHS University  
Boston, MA, USA

ISSN 1064-3745

ISSN 1940-6029 (electronic)

Methods in Molecular Biology

ISBN 978-1-0716-2953-6

ISBN 978-1-0716-2954-3 (eBook)

<https://doi.org/10.1007/978-1-0716-2954-3>

© The Editor(s) (if applicable) and The Author(s), under exclusive license to Springer Science+Business Media, LLC, part of Springer Nature 2017, 2023

This work is subject to copyright. All rights are solely and exclusively licensed by the Publisher, whether the whole or part of the material is concerned, specifically the rights of translation, reprinting, reuse of illustrations, recitation, broadcasting, reproduction on microfilms or in any other physical way, and transmission or information storage and retrieval, electronic adaptation, computer software, or by similar or dissimilar methodology now known or hereafter developed.

The use of general descriptive names, registered names, trademarks, service marks, etc. in this publication does not imply, even in the absence of a specific statement, that such names are exempt from the relevant protective laws and regulations and therefore free for general use.

The publisher, the authors, and the editors are safe to assume that the advice and information in this book are believed to be true and accurate at the date of publication. Neither the publisher nor the authors or the editors give a warranty, expressed or implied, with respect to the material contained herein or for any errors or omissions that may have been made. The publisher remains neutral with regard to jurisdictional claims in published maps and institutional affiliations.

This Humana imprint is published by the registered company Springer Science+Business Media, LLC, part of Springer Nature.

The registered company address is: 1 New York Plaza, New York, NY 10004, U.S.A.

---

## Preface

The first edition of *MiMB Liposomes Methods and Protocols* was a two-volume edition that compiled a diverse array of protocols for pharmaceutical nanocarriers and biological membrane models. The second edition on the other hand emerged as a single-volume collection of basic protocols that was intended to serve as a complimentary everyday companion for scientists at all levels interested in using liposomes for drug delivery purposes. The continued popularity of *MiMB Liposomes Methods and Protocols* led to this third edition being developed. In this edition, we have sought to continue with the theme of ensuring that fundamental protocols for the preparation and characterization of liposomes are maintained in a single convenient volume and ensuring that tried and tested protocols remain accessible to established and new investigators alike. The focus remains on entry-level protocols for the preparation of liposomes, physicochemical characterization of liposomes, lipid analysis, drug encapsulation, surface modification, stimuli response as well as cellular interaction, and biodistribution. Also essential to the continued health of the field of liposomology is an up-to-date history of its evolution. To this end, Chapter 1 from the second edition has been revised. The new version titled “From Olive Oil Emulsions to COVID-19 Vaccines: Liposomes Came First” is highly recommended as required reading for anyone interested in liposomology. We are extremely grateful to all the contributors to this edition and to Prof. John Walker the MiMB series editor for his guidance in the preparation of this edition. It is our hope that this volume will continue to serve as a convenient reference for graduate students, postdoctoral researchers, as well as established investigators utilizing lipid-based systems in the fields of cell and molecular biology, drug delivery, and physical chemistry.

*Boston, MA, USA*

*Gerard G. M. D'Souza  
Hongwei Zhang*

---

# Contents

|   |     |
|---|-----|
| <i>Preface</i> .....  | v   |
| <i>Contributors</i> .....   | ix  |
| <b>1</b> From Olive Oil Emulsions to COVID-19 Vaccines: Liposomes Came First .....                          | 1   |
| <i>Volkmar Weissig</i>  |     |
| <b>2</b> Preparation of DRV Liposomes .....   | 21  |
| <i>Sophia G. Antimisiaris</i>   |     |
| <b>3</b> Preparation of Small Unilamellar Vesicle Liposomes Using Detergent Dialysis Method .....           | 49  |
| <i>Qingyue Zhong and Hongwei Zhang</i>  |     |
| <b>4</b> Thin-Film Hydration Followed by Extrusion Method for Liposome Preparation .....                    | 57  |
| <i>Hongwei Zhang</i>  |     |
| <b>5</b> Ethanol Injection Method for Liposome Preparation .....  | 65  |
| <i>Guangsheng Du and Xun Sun</i>  |     |
| <b>6</b> Preparation of Giant Vesicles with Mixed Single-Tailed and Double-Tailed Lipids .....              | 71  |
| <i>Lauren A. Lowe and Anna Wang</i>   |     |
| <b>7</b> Scalable Liposome Synthesis by High Aspect Ratio Microfluidic Flow Focusing .....                  | 87  |
| <i>Jung Yeon Han, Zhu Chen, and Don L. Devoe</i>  |     |
| <b>8</b> Preparation of Doxorubicin Liposomes by Remote Loading Method .....                                | 95  |
| <i>Jian Chen</i>  |     |
| <b>9</b> Magnetic Thermosensitive Liposomes Loaded with Doxorubicin .....                                   | 103 |
| <i>Mohamad Alawak, Alice Abu Dayyih, Ibrahim Awak, Bernd Gutberlet, Konrad Engelhardt, and Udo Bakowsky</i> |     |
| <b>10</b> Preparation and Physical Characterization of DNA Binding Cationic Liposomes .....                 | 121 |
| <i>Vaibhav Saxena</i>   |     |
| <b>11</b> Tunable pH Sensitive Lipoplexes .....   | 127 |
| <i>Hélène Dhôtel, Michel Bessodes, and Nathalie Mignet</i>  |     |
| <b>12</b> Solid Lipid Nanoparticles for Drug Delivery .....   | 139 |
| <i>Wei-Chung Luo and Xiuling Lu</i>   |     |
| <b>13</b> Stable Discoidal Bicelles: Formulation, Characterization, and Functions .....                     | 147 |
| <i>Ying Liu, Yan Xia, Armin Tahmasbi Rad, Wafa Aresh, Justin M. Fang, and Mu-Ping Nieh</i>                  |     |

|    |  |     |
|----|--|-----|
| 14 | The Post-insertion Method for the Preparation of PEGylated Liposomes.....  | 159 |
|    | <i>Sherif E. Emam, Nehal E. Elsadek, Taro Shimizu, and Tatsuhiko Ishida</i>  |     |
| 15 | Click Chemistry for Liposome Surface Modification .....  | 173 |
|    | <i>Maria Vittoria Spanedda, Marcella De Giorgi, Béatrice Heurtault, Antoine Kichler, Line Bourel-Bonnet, and Benoît Frisch</i>                             |     |
| 16 | Surface Modification of Liposomes Using Folic Acid .....   | 191 |
|    | <i>Mengran Guo, Zhongshan He, Xi He, and Xiangrong Song</i>  |     |
| 17 | Preparation and Characterization of Trastuzumab Fab-Conjugated Liposomes (Immunoliposomes) .....   | 197 |
|    | <i>ShanShan Jin, Huimin Li, and Yubong Xu</i>  |     |
| 18 | Pyrophosphorylated-Cholesterol-Modified Bone-Targeting Liposome Formulation Procedure .....  | 207 |
|    | <i>Yanzhi Liu, Zhenshan Jia, Luoyang Ma, and Dong Wang</i>   |     |
| 19 | Method of Simultaneous Analysis of Liposome Components Using HPTLC/FID .....   | 221 |
|    | <i>Sophia Hatziantoniou and Costas Demetzos</i>  |     |
| 20 | High-Performance Liquid Chromatography Coupled with Tandem Mass Spectrometry Method for the Identification and Quantification of Lipids in Liposomes ..... | 227 |
|    | <i>Yujie Shi and Xiaona Li</i>   |     |
| 21 | DPH Probe Method for Liposome-Membrane Fluidity Determination.....   | 241 |
|    | <i>Wei He</i>  |     |
| 22 | Imaging of Liposomes by Negative Staining Transmission Electron Microscopy and Cryogenic Transmission Electron Microscopy .....                            | 245 |
|    | <i>Anand S. Ubbhe</i>  |     |
| 23 | Visualization and Characterization of Liposomes by Atomic Force Microscopy.....  | 253 |
|    | <i>Konrad Engelhardt, Eduard Preis, and Udo Bakowsky</i>   |     |
| 24 | Determination of the Subcellular Distribution of Fluorescently Labeled Liposomes Using Confocal Microscopy .....   | 265 |
|    | <i>Melani A. Solomon</i>   |     |
| 25 | Liposome Biodistribution via Europium Complexes.....   | 277 |
|    | <i>Nathalie Mignet and Daniel Scherman</i>   |     |
| 26 | Quantification of a Fluorescent Lipid DOPE-NBD by an HPLC Method in Biological Tissue: Application to Study Liposomes' Uptake by Human Placenta .....      | 289 |
|    | <i>Louise Fliedel, Nathalie Mignet, Thierry Fournier, Karine Andrieux, and Khair Albareth</i>  |     |
|    | <i>Index .....</i>   | 303 |

---

## Contributors

- MOHAMAD ALAWAK • *Department of Pharmaceutics and Biopharmaceutics, University of Marburg, Marburg, Germany*
- KHAIR ALHARETH • *Université Paris Cité, CNRS, INSERM, UTCBS, Unité des Technologies Chimiques et Biologiques pour la Santé, Paris, France*
- KARINE ANDRIEUX • *Université Paris Cité, CNRS, INSERM, UTCBS, Unité des Technologies Chimiques et Biologiques pour la Santé, Paris, France*
- SOPHIA G. ANTIMISIARIS • *Laboratory of Pharmaceutical Technology, Department of Pharmacy, University of Patras, Patras, Greece; Institute of Chemical Engineering Sciences, Foundation for Research and Technology Hellas, FORTH/ICE-HT, Patras, Greece*
- WAFA ARESH • *Department of Biomedical Engineering, University of Connecticut, Storrs, CT, USA*
- IBRAHIM AWAK • *Department of Pharmaceutics and Biopharmaceutics, University of Marburg, Marburg, Germany*
- UDO BAKOWSKY • *Department of Pharmaceutics and Biopharmaceutics, University of Marburg, Marburg, Germany*
- MICHEL BESSODES • *Université de Paris Cité, CNRS, INSERM, UTCBS, Unité des Technologies Chimiques et Biologiques pour la Santé, Faculté de Pharmacie, Paris, France*
- LINE BOUREL-BONNET • *Laboratoire de Conception et Applications des Molécules Bioactives, UMR 7199 CNRS/Université de Strasbourg, équipe 3BIO, Faculté de Pharmacie, Illkirch, France*
- JIAN CHEN • *School of Pharmacy, Shanghai Jiao Tong University, Shanghai, China*
- ZHU CHEN • *Department of Mechanical Engineering, University of Maryland, College Park, MD, USA*
- ALICE ABU DAYYIH • *Department of Pharmaceutics and Biopharmaceutics, University of Marburg, Marburg, Germany*
- MARCELLA DE GIORGI • *Laboratoire de Conception et Applications des Molécules Bioactives, UMR 7199 CNRS/Université de Strasbourg, équipe 3BIO, Faculté de Pharmacie, Illkirch, France*
- COSTAS DEMETZOS • *Faculty of Pharmacy, Department of Pharmaceutical Technology, National and Kapodistrian University of Athens, Athens, Greece*
- DON L. DEVOE • *Department of Mechanical Engineering, University of Maryland, College Park, MD, USA*
- HÉLÈNE DHOTEL • *Université de Paris Cité, CNRS, INSERM, UTCBS, Unité des Technologies Chimiques et Biologiques pour la Santé, Faculté de Pharmacie, Paris, France*
- GUANGSHENG DU • *West China School of Pharmacy, Sichuan University, Chengdu, China*
- NEHAL E. ELSADEK • *Department of Pharmacokinetics and Biopharmaceutics, Institute of Biomedical Sciences, Tokushima University, Tokushima, Japan*
- SHERIF E. EMAM • *Department of Pharmacokinetics and Biopharmaceutics, Institute of Biomedical Sciences, Tokushima University, Tokushima, Japan; Faculty of Pharmacy, Department of Pharmaceutics and Industrial Pharmacy, Zagazig University, Zagazig, Egypt*

- KONRAD ENGELHARDT • *Department of Pharmaceutics and Biopharmaceutics, University of Marburg, Marburg, Germany*
- JUSTIN M. FANG • *Department of Biomedical Engineering, University of Connecticut, Storrs, CT, USA*
- LOUISE FLIEDEL • *Université Paris Cité, CNRS, INSERM, UTCBS, Unité des Technologies Chimiques et Biologiques pour la Santé, Paris, France; Université Paris Cité, INSERM, Pathophysiology and Pharmacotoxicology of the Human Placenta, Pre and Postnatal Microbiota Unit (3PHM), Paris, France*
- THIERRY FOURNIER • *Université Paris Cité, INSERM, Pathophysiology and Pharmacotoxicology of the Human Placenta, Pre and Postnatal Microbiota Unit (3PHM), Paris, France*
- BENOÎT FRISCH • *Laboratoire de Conception et Applications des Molécules Bioactives, UMR 7199 CNRS/Université de Strasbourg, équipe 3BIO, Faculté de Pharmacie, Illkirch, France*
- MENGRAN GUO • *Department of Critical Care Medicine, State Key Laboratory of Biotherapy and Cancer Center, West China Hospital, Sichuan University, Chengdu, China*
- BERND GUTBERLET • *Department of Pharmaceutics and Biopharmaceutics, University of Marburg, Marburg, Germany*
- JUNG YEON HAN • *Department of Mechanical Engineering, University of Maryland, College Park, MD, USA*
- SOPHIA HATZANTONIOU • *Department of Pharmacy, Laboratory of Pharmaceutical Technology, School of Health Sciences, University of Patras, Rion, Greece*
- WEI HE • *School of Pharmacy, China Pharmaceutical University, Nanjing, China*
- Xi HE • *Department of Critical Care Medicine, State Key Laboratory of Biotherapy and Cancer Center, West China Hospital, Sichuan University, Chengdu, China*
- ZHONGSHAN HE • *Department of Critical Care Medicine, State Key Laboratory of Biotherapy and Cancer Center, West China Hospital, Sichuan University, Chengdu, China*
- BÉATRICE HEURTAULT • *Laboratoire de Conception et Applications des Molécules Bioactives, UMR 7199 CNRS/Université de Strasbourg, équipe 3BIO, Faculté de Pharmacie, Illkirch, France*
- TATSUHIRO ISHIDA • *Department of Pharmacokinetics and Biopharmaceutics, Institute of Biomedical Sciences, Tokushima University, Tokushima, Japan*
- ZHENSHAN JIA • *Department of Pharmaceutical Sciences, College of Pharmacy, University of Nebraska Medical Center, Omaha, NE, USA*
- SHANSHAN JIN • *Hangzhou Highfield Bipharaceuticals Inc., Hangzhou, China*
- ANTOINE KICHLER • *Laboratoire de Conception et Applications des Molécules Bioactives, UMR 7199 CNRS/Université de Strasbourg, équipe 3BIO, Faculté de Pharmacie, Illkirch, France*
- HUIMIN LI • *Yunnan Key Laboratory of Screening and Research on Anti-pathogen Plant Resources in Western Yunnan, Dali University, Dali, China*
- XIAONA LI • *Department of Pharmacy, Peking University Third Hospital, Beijing, People's Republic of China*
- YANZHI LIU • *Department of Pharmaceutical Sciences, College of Pharmacy, University of Nebraska Medical Center, Omaha, NE, USA; Zhanjiang Central Hospital, Guangdong Medical University, Zhanjiang, PR China*
- YING LIU • *Department of Chemical and Biomolecular Engineering, University of Connecticut, Storrs, CT, USA*

- LAUREN A. LOWE • *School of Chemistry, UNSW Sydney, Sydney, NSW, Australia; Australian Centre for Astrobiology, UNSW Sydney, Sydney, NSW, Australia*
- XIULING LU • *School of Pharmacy, University of Connecticut, Storrs, CT, USA*
- WEI-CHUNG LUO • *School of Pharmacy, University of Connecticut, Storrs, CT, USA*
- LUOYANG MA • *Zhanjiang Central Hospital, Guangdong Medical University, Zhanjiang, PR China*
- NATHALIE MIGNET • *Université de Paris Cité, CNRS, INSERM, UTCBS, Unité des Technologies Chimiques et Biologiques pour la Santé, Faculté de Pharmacie, Paris, France*
- MU-PING NIEH • *Department of Chemical and Biomolecular Engineering, University of Connecticut, Storrs, CT, USA; Department of Biomedical Engineering, University of Connecticut, Storrs, CT, USA; Polymer Program, Institute of Materials Science, University of Connecticut, Storrs, CT, USA*
- EDUARD PREIS • *Department of Pharmaceutics and Biopharmaceutics, University of Marburg, Marburg, Germany*
- ARMIN TAHMASBI RAD • *Department of Biomedical Engineering, University of Connecticut, Storrs, CT, USA*
- VAIBHAV SAXENA • *Pharmaceutical Development, Sage Therapeutics, Cambridge, MA, USA*
- DANIEL SCHERMAN • *Université Paris Cité, CNRS, INSERM, UTCBS, Unité des Technologies Chimiques et Biologiques pour la Santé, Faculté de Pharmacie, Paris, France*
- YUJIE SHI • *School of Pharmaceutical Sciences, Peking University, Beijing, People's Republic of China*
- TARO SHIMIZU • *Department of Pharmacokinetics and Biopharmaceutics, Institute of Biomedical Sciences, Tokushima University, Tokushima, Japan*
- MELANI A. SOLOMON • *Catalent Cell and Gene Therapy, Gaithersburg, MD, USA*
- XIANGRONG SONG • *Department of Critical Care Medicine, State Key Laboratory of Biotherapy and Cancer Center, West China Hospital, Sichuan University, Chengdu, China*
- MARIA VITTORIA SPANEDDA • *Laboratoire de Conception et Applications des Molécules Bioactives, UMR 7199 CNRS/Université de Strasbourg, équipe 3BIO, Faculté de Pharmacie, Illkirch, France*
- XUN SUN • *West China School of Pharmacy, Sichuan University, Chengdu, China*
- ANAND S. UBHE • *AbbVie, Irvine, CA, USA*
- ANNA WANG • *School of Chemistry, UNSW Sydney, Sydney, NSW, Australia; Australian Centre for Astrobiology, UNSW Sydney, Sydney, NSW, Australia*
- DONG WANG • *Department of Pharmaceutical Sciences, College of Pharmacy, University of Nebraska Medical Center, Omaha, NE, USA*
- VOLKMAR WEISSIG • *Midwestern University College of Pharmacy Glendale, Department of Pharmaceutical Sciences, Glendale, AZ, USA*
- YAN XIA • *Department of Chemical and Biomolecular Engineering, University of Connecticut, Storrs, CT, USA*
- YUHONG XU  • *Yunnan Key Laboratory of Screening and Research on Anti-pathogen Plant Resources in Western Yunnan, Dali University, Dali, China*
- HONGWEI ZHANG • *Department of Pharmaceutical Sciences, School of Pharmacy-Boston, MCPHS University, Boston, MA, USA*
- QINGYUE ZHONG • *Department of Pharmaceutical Sciences, School of Pharmacy-Boston, MCPHS University, Boston, MA, USA*



# Chapter 1

## From Olive Oil Emulsions to COVID-19 Vaccines: Liposomes Came First

Volkmar Weissig

### Abstract

It has been a long journey from Pliny the Elder (23–79 AD) to the FDA approval of the first injectable nanomedicine in 1997. A journey powered by intellectual curiosity, which began with sprinkling olive oil on seawater and culminated in playing around with smears of egg lecithin on microscopic slides. This brief review highlights how a few pairs of gifted hands attached to highly motivated brains have turned a curious discovery made under a microscopic lens into novel nanotherapeutics including liposome-based anti-cancer drugs and potent liposomal vaccines given to millions.

**Key words** Liposomes, Phospholipids, Biological membranes, Drug delivery, Membrane models, Vaccines, COVID-19

---

### 1 Pliny the Elder, Benjamin Franklin, Singer, and Nicolson

Following the first observations of living cells under a simple light microscope by Anton van Leeuwenhoek in the late 1600s, the question ultimately arose as to what holds such microscopic structures all together. The history of trying to understand biological membranes [1] can arguably be traced back to Pliny the Elder (23–79 AD) who noted that “...sea water is made smooth by olive oil, and so they sprinkle oil on their faces because it calms the rough element...” [1, 2]. Being aware of Pliny’s observation or not, about 1700 years later in 1774, Benjamin Franklin sprinkled oil droplets on water in a pond in Clapham Common and saw the oil spreading on the water surface until it was “smooth as a looking glass.” He subsequently published his observation in the *Philosophical Transactions of the Royal Society* [1, 2]. The same experiment was repeated again, i.e., for the third time in the span of almost 2000 years in 1890 by Lord Raleigh who was able to measure the area to which a defined volume of oil would expand and in addition also to calculate the thickness of the oil film [1, 2]. Approximately

during the same time Lord Raleigh was investigating oil films, Charles Ernest Overton, a young doctoral student at the University of Zurich, found that the chemical nature of a substance, i.e., oily versus watery, determines whether it passes through the membrane into a cell which lead him to the conclusion that there are similarities between cell membranes and lipids such as olive oil [1, 2]. In 1917, Langmuir described cell membranes as a layer of lipids one molecule thick [3]. Eight years later, Gorter and Grendel concluded from their studies that “the phospholipid molecules that formed the cell membrane were arranged in two layers to form a lipid bilayer” [4], and Danielli along with Robertson in 1935 proposed a model wherein bilayer of lipids were sequestered between two monolayers of unfolded proteins [5]. The currently still accepted fluid mosaic model was finally proposed by Singer and Nicolson in 1972 [6, 7].

---

## 2 The Penny Dropped: Membranes Came First

Among those landmarks of biomembrane history, a serendipitous observation made by Alec Bangham during the early 1960s deserves undoubtedly a special place. In the early 1960s, biological membranes were increasingly being visualized through the use of electron microscopy. Following appropriate staining, membranes showed up in electron micrographs as two dark bands separated by a light region [8] which David Robertson interpreted correctly as two opposed phospholipid monolayers [9]. According to Alec Bangham “the concept of the bimolecular sheet of phospholipids surrounding cells and cell organelles became compulsive, and soon anyone who had an oscilloscope and enough patience was making black lipid membranes (BLM)” [10]. Preparing a BLM must have been quite challenging and apparently also requires some level of experience [11]. Moreover, long-term experiments using BLM are almost impossible due to the very limited life time of around 1 h or less for any given BLM. Even nowadays, work is still continuing to enhance the stability of BLMs in order to extend their life span [12, 13]. Therefore, the design and development of a stable and easy to prepare model for a biological membrane was highly called for, something Alec Bangham might have been aware of but certainly did not plan on doing. During that time, i.e., the very early 1960s, Bangham was interested in studying the role biological membranes, in particular phospholipids play in the process of blood clotting. While doing so, he in his own words “played around with smears of egg lecithin on microscope slides and became fascinated by the way in which they reacted with water to

form mobile fronds<sup>1</sup> of delicate and intricate structure” [10]. Around 1962 Alex Bangham got easy access to a newly acquired electron microscope because its operator, Bob Horne, was his sailing friend [10]. During the very first session at the microscope, when looking at Bangham’s lipid dispersions in negatively stained samples, they saw “unmistakable vesicles all over the place” [10]. In Bangham’s own words “the penny dropped, phospholipids in aqueous negatively stained samples were spontaneously forming closed membrane systems” [10]. As much logical as it appears to us today, the simple observation that phospholipids when exposed to water spontaneously self-assemble into vesicular structures surrounded by membranes has profound philosophical implications, something which generally seems to be somewhat underappreciated in the literature dealing with Bangham’s body of work. As obvious as it now seems, there is no life without membranes. “Membranes Came First” was the title of a talk Alec Bangham gave at the beginning of the 1970s at Bristol University proposing that “something like liposomes must have been available to house the first forms of cellular life” [14]. This talk and a subsequent sabbatical in Bangham’s lab inspired David Deamer who soon found that phospholipid molecules could actually be synthesized under simulated prebiotic conditions [15]. Moreover, membrane forming amphiphilic molecules could also be found in the meteorite which crashed down in Australia in September 1969 [16].

---

### 3 Multilamellar Smectic Mesophases

To prove this self-assembly behavior of hydrated phospholipids, however, Bangham and Horne had to work two more years and “at no time did (they) imagine that (their) model system would prove to be anything like as useful as the BLM” [10]. They published their findings in 1964 in the Journal of Molecular Biology [17], referring to what they saw under the microscope as “multilamellar smectic mesophases.” Shortly thereafter Alec Bangham provided evidence for the ability of lipid bilayers to maintain concentration gradients of ions, which were disrupted upon adding detergents to this system [18, 19]. According to David Deamer, “this evidence, along with the planar bilayer models being developed at the same time, established that lipid bilayers are the primary permeability barrier of all cell membranes. It was the membrane equivalent of finding the double helix structure of DNA...” [14]. Unfortunately, only one of these two groundbreaking discoveries in life sciences was honored with the Nobel Prize. An early

---

<sup>1</sup> Frond: A large leaf (palm, fern) with many divisions (Merriam Webster)

visitor in Bangham's lab was Gerald Weissmann [14] who proposed to call Bangham's smectic mesophases "liposomes" which are defined as microscopic vesicles composed of one or more lipid bilayers [20]. Upon Weissmann's return to the USA, he "proceeded to evangelize (liposomes) prodigiously" [10]. Another early guest in Bangham's lab during that time was Demetrios Papahadjopoulos who intended to study the role of phospholipids in the process of blood coagulation. But "he never had a chance, and in no time at all was publishing papers [21, 22] on liposomes" [10].

In the following years, Alec Bangham kept demonstrating the usefulness of liposomes as a membrane model for studying fundamental membrane properties such as permeation but also adhesion and fusion [23–25]. During the following four decades, biological membrane models have grown in complexity and functionality [26], but nevertheless, liposomes are, besides supported bilayers, membrane nanodiscs and hybrid membranes, still an indisputably important tool for membrane biophysicists and biochemists. Ever since Bangham's early studies, liposomes remain an essential and basic model for the study of any biological, biochemical, biophysical, pharmacological, or pharmaceutical phenomenon which in one way or another involves phospholipid membranes. Just to give a few examples, liposomes are being used to study drug transfer and drug uptake [27], cytochrome p450-dependent drug metabolism [28], cellular osmosensors [29], as well as mechanosensitive ion channels [30]. The amino acid transport through membranes [31], the interactions of soluble proteins with membranes [32], and properties of integral membrane proteins [33] have been investigated employing liposomes as a membrane model or as a model of lysosomes by incorporating lysozyme into these vesicles [34]. Using liposomes, actin polymerization [35], lipid domains [36], respiratory cytochromes [37], antioxidant activities [38–40], colloidal aggregation [41], membrane translocation [42], protein folding [43], vesicular transport [44], and lipid organization in biological membranes [45, 46] have been investigated. The list could go on.

In addition to using liposomes as a membrane model, Alec Bangham extended the use of liposomes to the study of the mechanism of action of drugs such as local anesthetics [47]. In 1989, on the occasion of his paper about the "Diffusion of univalent ions across the lamellae of swollen phospholipids" [18] being highlighted by Current Contents as "This Week's Citation Classic," Bangham summarized "...liposomes proved not only to be a most useful and revealing model of the passive areas of a cell membrane... but also a pharmacological punching bag, notably with regard to the action of anesthetics, a favored field of my own before I retired" [10]. Bangham's key finding about anesthetics, published together with Sheena Johnson and Keith Miller [48], was the fact that liposomes become permeable to ionic solutes in

the presence of general anesthetics, implying these drugs somehow seem to insert themselves into phospholipid membranes or at least disturb their integrity. Ten years later, Keith Miller commented: “To a field whose most powerful model nearly seven decades ago had been a jar of olive oil, the liposome’s arrival was a liberating force” [14, 49]. Remarkably, Alec Bangham’s “creative instincts” [14] became further apparent when he suggested to use liposomes composed mainly of dipalmitoylphosphatidylcholine (DPPC) for the treatment of infantile respiratory distress syndrome. He was hoping that such lipid formulation could easily be delivered to the airways of newborns and replenish the occasionally insufficient amount of DPPC in the lungs of newborns. Notably, Alec Bangham called such a lipid mixture “ALEC” which stands for “artificial lung expanding compound” [14]. A paper summarizing a clinical trial to evaluate ALEC states that “artificial surfactant (ALEC) given to premature babies at birth significantly reduces their mortality ... and should prove a valuable addition to treatment” [14, 50].

One year before his death, in his very last publication at the age of 88 as the sole author (!), Alec Bangham sums up the impact of his serendipitous observation from the beginning of the 1960s on his scientific career by writing “it was the odd pattern of a well-drawn drop of blood that initiated my curiosity and eased my career away from morbid anatomy to that of the physical chemistry of cell surfaces” [51]. But not only did this odd pattern of a well-drawn drop of blood change Alec Bangham’s career and not only made his peculiar observation of multilamellar smectic mesophases on a microscopic slide biological membranes experimentally easily accessible, his serendipitous discovery was to be followed later by an entirely new sub-discipline in pharmaceutical science and technology. His observation that the lamellar structures formed by phospholipids exposed to aqueous buffers are able to sequester small buffer molecules has led to the development of the entire colloidal (nowadays called nano) drug delivery concept. It started by the realization that liposomes, in addition to entrapping salts present in the buffer solutions used to prepare liposomes, could also entrap other molecules, for instance, pharmacologically active agents.

During that time, Brenda Ryman at the Royal Free Hospital School of Medicine in London (UK) was working on glycogen storage disease [52–54], in search of a system for the delivery of glycosidase (a glycogen degrading enzyme) to hepatocytes. At that time, Gregory Gregoriadis, based at the Albert Einstein College of Medicine in New York, was working on a newly discovered [55, 56] property of desialylated glycoproteins to home to the hepatocytes after *i.v.* injection, thus enabling the transport of glycosidase chemically linked to a desialylated glycoprotein to home to the liver. Because of their common scientific interests, Ryman invited Gregoriadis to carry out postdoctoral work in her laboratory. The plan

was to test both, desialylated peptides linked to glycosidase and liposomes, a hitherto untested system used by the Head of the department (Jack Lucy) as a model for cell membranes. It was eventually decided to start with liposomes which have never been used in animal work nor had they ever been proposed as a drug delivery system. Gregory Gregoriadis himself described his entry into the at that time untested field of liposomes and its technology in a poetic fashion [57] (reprinted with permission from Elsevier):

Albert Einstein, The Bronx, New York.  
 Gentiles and Jews (impartial to pork),  
 Academic discussions and ifs and buts  
 Ceroloplasmin and test tubes, decapitated rats.  
 Exciting sequel of a previous discovery.  
 One could deduce from the total recovery  
 Of counts injected by the parenteral route  
 Into the blood stream or the pad of the foot:  
 Desialylated proteins home to the liver!  
 Will drugs be targeted? Post-doctoral fever...  
 November of sixty-nine, still in New York,  
 expiring visa, in search of work.  
 Abandoned reagents of forgotten adventure,  
 unfinished note books. An issue of Nature,  
 classified advertisement, turn of fate  
 Dear Madam of London, U.K.  
 I am flying to join you, if I may.

Based on their initial work on the liposomal encapsulation of amyloglucosidase, Gregory Gregoriadis together with the “Madam of London”, i.e., Brenda Ryman proposed in 1971 liposomes as carriers of enzymes or drugs as a new approach for the treatment of diseases, including storage diseases [58]. With an entrapment efficiency of between 4% and 10%, they succeeded in entrapping *Aspergillus niger* amyloglucosidase (EC 3.2.1.3) together with  $^{131}\text{I}$ -labelled albumin into liposomes composed of phosphatidyl-choline, cholesterol, and dicetyl phosphate. Considering they had prepared liposomes via probe sonication with an MSE 60 W sonicator [59], the encapsulation efficiency of proteins with up to 10% was very good even by today’s standards. Thirteen years later, in 1984, he published together with Chris Kirby a protocol for “high yield drug entrapment in liposomes” [60] which they called dehydration–rehydration vesicles (DRVs). Over the following 30 years, the list of potentially therapeutic agents which have been encapsulated into DRV’s has grown tremendously [61]. The type of liposomes as made by Gregoriadis and Ryman via probe sonication of a lipid suspension was years later named Small Unilamellar Vesicles (SUVs), which have become known for their generally low encapsulation efficiency.

Back to 1971, Gregoriadis and Ryman injected the amyloglucosidase and labeled albumin containing liposomes intravenously into rats. About 60% of all liposomes were eliminated from the circulation within 10 min. Remarkably, using [ $^3\text{H}$ ]-cholesterol

labeled and  $^{131}\text{I}$ -albumin-loaded liposomes, they found that circulating liposomes seemed to stay intact; no measurable leakage of  $^{131}\text{I}$ -albumin was found. Most of the radioactivity was recovered in the liver and to some extent in the spleen, with a maximum of 56% of the injected dose after the first 15 min. This rapid clearance of i.v. injected liposomes via organs of the RES system, as firstly described by Gregoriadis and Ryman in 1971, proved to become the major and almost insurmountable hurdle for getting liposome-based drugs into the clinic. Subsequently, during the middle and late 1980s, the extreme short half-life of liposomes in circulation contributed to a general waning of the original enthusiasm associated with liposomes as a potentially universal drug carrier except for when the liver and spleen are the target tissues. This barrier toward the clinical application of liposomes fell in 1990, when Alexander Klibanov, who obtained his Ph.D. degree in Vladimir Torchilin's lab in Moscow and at that time worked as a Postdoc in Leaf Huang's lab then in Nashville, Tennessee, grafted polyethylene glycol (PEG) chains onto the surface of liposomes in order to significantly prolong their circulation time [62]. Such flexible long PEG chains literally shield liposomes from interacting with opsonins, thereby significantly slowing down their clearance from circulation via the RES system [63, 64]. In addition, what is extremely important from the pharmaceutical manufacturer's view of point, these PEG chains also minimize vesicle to vesicle interactions thereby reducing vesicle aggregation, which in turn dramatically improves the stability of such liposomal formulations [65]. Only 5 years later, in 1995, the FDA (USA) approved the first injectable liposomal drug, Doxil, which are doxorubicin-loaded liposomes the surface of which is protected by a layer of PEG chains [66]. But again back to 1971, after subcellular fractionation of the liver following i.v. injection of radiolabeled and enzyme-loaded liposomes into rats, Gregoriadis and Ryman recovered most of the liposomes and their content in the mitochondrial-lysosomal fraction as well as the cytosol of both, liver parenchymal and Kupffer cells. In other words, liposomes indeed revealed themselves as "a promising vehicle for the direction of enzymes and drugs to the liver and spleen" [58]. Following this very first biodistribution study of liposomes containing radiolabeled cargo ( $^{131}\text{I}$ -albumin and [ $^3\text{H}$ ] cholesterol), Gregoriadis traced i.v. injected liposomes based on enzyme activity [67]. He encapsulated yeast beta-fructofuranosidase (invertase) or, in control experiments,  $^{131}\text{I}$ -labeled albumin into liposomes composed of phosphatidylcholine, cholesterol, and phosphatidic acid. Liposomal encapsulation of invertase almost completely shielded the enzyme from substrate added to the liposome suspension, i.e., the beta-fructofuranosidase activity in the liposomal preparations was latent. Following injection, the beta-fructofuranosidase activity in blood retained its latency, but the activity declined to 50% of the injected dose in

1 h. After 6 h, much of this activity was recovered in the liver and spleen. After 21 h, most of the hepatic beta-fructofuranosidase activity was located in the lysosomal fraction. Gregoriadis concluded in 1972 that “the lysosomal localization of injected liposome-entrapped material can probably be utilized in the treatment of certain disorders in man” [67].

---

## 4 Liposomes as Immunological Adjuvants

Shortly after the concept of using liposomes for drug delivery had been established, Gregory Gregoriadis extended the potential utilization of liposomes to a very different biomedical application. In a landmark paper published in *Nature* in November 1974 [68], he together with Anthony Allison reported “the use of liposomes, concentric spheres consisting of phospholipid bilayers separated by aqueous compartments, as immunological adjuvants.” Disregarding the lack of detailed knowledge at that time about the mechanism by which a protein antigen triggers an immune response, Allison and Gregoriadis hypothesized, as Lee Leserman put it in his “Gregoriadyssey” [69], “that the efficient encapsulation of protein in liposomes might reduce the amount of antigen required to induce a response and might also reduce the chance of an allergic reaction to the antigen” [69]. Indeed, Allison and Gregoriadis demonstrated that liposome-encapsulated diphtheria toxoid induced a higher antibody titer than the same amount of free antigen [68], and moreover, animals boosted with free antigen died of serum sickness, while those which received liposomal encapsulated diphtheria toxoid did not [68]. A few years later Gregoriadis incorporated hepatitis B surface antigen (HBsAg) into liposomes [70], he studied the impact of the mode of antigen incorporation into liposomes on their adjuvanticity [71], and he evaluated liposomal adjuvants against a variety of other widely used adjuvants [72]. In the early 1990s, Gregoriadis’ lab demonstrated that liposomes enhance the immunogenicity of reconstituted influenza virus A/PR/8 envelopes as well as the formation of protective antibody by influenza virus A/Sichuan/87 (H3N2) surface antigen [73]. They also showed that liposome-entrapped T-cell peptide provides help for a co-entrapped B-cell peptide to overcome genetic restriction in mice and induce immunological memory [74].

The outstanding immunological adjuvant properties of liposomes were commercially used during the 1990s by Berna Biotech Pharma GmbH (Switzerland) with the production of two liposomal vaccines. First, the influenza virus surface antigens neuraminidase and hemagglutinin incorporated into phospholipid bilayers produced Inf�xal® V [75, 76], and second, formalin inactivated hepatitis A virus particles adsorbed to the surface of liposomes (or virosomes) lead to the production of Epaxal, “a virosomal

vaccine to prevent hepatitis A infection” [77]. It should be noted that liposomes with surface-bound viral antigens are also called “virosomes” due to their morphological resemblance to virus particles.

The author was fortunate enough to be given the opportunity of getting involved in Gregory’s work on liposomal adjuvants when he was spending 3 months back in 1988 in his laboratory at the Royal Free Hospital in London. Coming from Juergen Lasch’s laboratory in Halle, Germany, he brought with him radiolabeled N-glutaryl-phosphatidylethanolamine (NGPE), which he simply carried in his hand luggage through airport security, an unthinkable security violation under today’s travel restrictions. Together with Sascha Klibanov mentioned earlier in connection with PEGylated liposomes, the author developed and synthesized NGPE in 1984 in Vladimir Torchilin’s laboratory in Moscow. They described NGPE as a new hydrophobic anchor for the attachment of proteins to liposomal membranes in FEBS Letters in 1986 [78]. This paper was accepted 3 months before Kung and Redemann’s paper describing the same new type of liposomal anchor was accepted by BBA [79]. Around 1988 a company in Alabama, Avanti Polar Lipids, started to commercialize NGPE for the functionalization of liposomes and is still selling it today. Unfortunately (for the author) back in 1986, he was only able to patent protect his development in East Europe due to the lack of convertible currency. Upon his arrival in Gregory’s lab, the author suggested to use NGPE for the covalent binding of peptide antigens to the surface of liposomes. Results were published in 1991 [80]. Weissig and co-workers assessed the adjuvants effect of liposomes using two different modes of presentation of polio virus subunit peptides by incorporating two poorly immunogenic synthetic polio peptides into the internal space of DRVs or by covalently linking the peptides to the surface of DRVs. It was found that for both peptides, liposome association in either mode boosted the primary and secondary IgG1 responses against 5 µg peptide as compared to controls in which free peptide was administered. Liposomal surface-linkage of both peptides exhibited an initially more rapid rise in antibody levels, as compared to internal entrapment of the peptides, but elicited no observable secondary response. It was concluded that it may be advantageous to administer liposomal virus subunit vaccines in both surface-linked and internally entrapped formulations to achieve adequate initial antibody levels followed by an anamnestic response [80].

---

## 5 Liposomes and Targeted Drug Delivery

Back to Gregory’s *Nature* paper from 1974 [68]: If liposomes could reduce the antigen dose while inducing higher titers, shouldn’t it also be possible to increase the efficacy of drugs by

encapsulating them into liposomes [69]? Only 1 year later, Gregoriadis and Neerunjun published their finding that injection of actinomycin D after its entrapment into liposomes prolonged the survival of tumor-bearing mice to a greater extent than did similar amounts of free actinomycin D [81]. The following year, Gregory Gregoriadis outlined the tremendous carrier potential of liposomes for potential drug therapies in two *New England Journal of Medicine* landmark papers [82, 83]. Two years later, in 1978, Gregoriadis deliberated on potential problems which might be involved when transposing results obtained from his early studies in rodents to human patients, in particular with respect to enzyme replacement therapies [84]. Among the issues which still needed to be addressed were the potential immunogenicity of the enzyme, its failure to reach its intended targets, which are (in this order) first the organ, then the tissue, followed by the cell, and finally a specific site inside the cell [69]. The final level of this “drug targeting hierarchy,” which is the subcellular or organelle-specific targeting, has recently emerged as a new frontier in drug delivery [85]. However, the question whether liposomes could be directed to specific organs or cells via attaching targeting ligands like specific antibodies to the liposomal surface was raised by Gregoriadis in a *Nature* review in 1977 [86]. During the same time Gregoriadis wrote his review, Koehler and Milstein were developing techniques based on B- and T-cell fusions for preparing monoclonal antibodies of potentially any desired antigen specificity [87–89]. Following Gregoriadis’ idea and considering the solved problem of obtaining highly specific antibodies, three liposome laboratories simultaneously published only 3 years later quite simple techniques for coupling antibodies to the liposomal surface. These three papers appeared in *Science* [90], *Nature* [91], and the *Journal of Biology* [92] indicating the weight such technologies were considered to have during that time. Even before these three landmark papers came out, Vladimir Torchilin’s group in Moscow (formerly Soviet Union) published first comparative studies on covalent and noncovalent immobilization of protein molecules on the surface of liposomes [93] and second demonstrated in an animal experiment the preservation of antimyosin antibody activity after covalent coupling to liposomes [94]. Taking such early development of targeted liposomes into account, it is quite stunning that as of today, almost 40 years later, no single therapy based on targeted liposomes has either reached the clinic [95] nor is under clinical development [96]. However, as mentioned earlier, Klibanov’s work [62] and the work of other liposome pioneers [97–100] about extending the circulation time of liposomes opened up the way for liposomes into the clinic. Subsequently, as expressed by Gregoriadis, “the 1990s were clearly the decade of clinic trials, approved injectable products... and of new horizons” [101].

---

## 6 Liposomal DNA Vaccines and Non-viral Transfection Vectors

In light of the most recent advent of Pfizer's and Moderna's COVID-19 vaccines, both of which are liposome-based (see below under 8.), it is quite remarkable that the use of liposomes for the cellular delivery of nucleic acids was already predicted over 50 years ago [67]. In 1972 Gregory Gregoriadis and Brenda Ryman (the "Madam of London", see above) wrote: "Administration of messenger RNA or DNA... appears to be the ultimate therapeutic approach for at least some of the genetic disorders...The possibility of employing liposomes to introduce segments of genetic material to defective cells... is worth considering" [67].

Following his own foresight, Gregoriadis extended the use of liposomes to the development of liposomal DNA vaccines in the 1990s [102, 103]. His work about liposomes for immunization and vaccine development has led him to found Xenetic BioScience [104], a biopharmaceutical company developing next-generation biologic drugs, novel oncology therapeutics, and vaccinations. The company's IP portfolio includes ImuXen®, which is a "liposomal technology platform designed to improve the delivery and effectiveness of DNA, protein and polysaccharide vaccines" [104]. ImuXen® technology has been demonstrated to generate rapid onset of protective immune responses, in some cases following just a single dose [104]. In 2008, Gregoriadis reflected with hindsight on his earlier papers describing the potentiation of immune responses to liposomal entrapped antigens, he wrote: "Seen from today's perspective, these 30-odd-year-old papers would appear courageously naïve in their claims, and their optimism vulnerably assertive. Yet it is an arresting thought that those innocent flights of fancy have ended up... on the desk of hard-nosed lawyers, eagle-eyed patent attorneys and worried CEOs, or hidden in the high and low numbers of the NASDAQ stock list" [101].

First attempts to use liposomes for nucleic acid transfer into mammalian cells have already been made in the 1980s. Interestingly though, the huge majority of papers describing the use of liposomes for DNA-based cell transfection were published mainly by one laboratory [105–114]. This is quite noteworthy, since throughout the 1980s, there wasn't hardly any drug or any other potentially therapeutic agent which was not by one or the other laboratory encapsulated into liposomes. But the encapsulation of negatively charged pDNA with an average hydrodynamic diameter roughly between 300 and 500 nm into charge-neutral or even negative charged liposomes having a diameter between 100 and 500 nm was generally considered as rather challenging. Reported findings of a high efficiency of liposome-mediated gene transfer

in vivo following the intravenously injection of a liposomal encapsulated recombinant plasmid encoding rat preproinsulin into rats [110] appear therefore as very remarkable. Nevertheless, the landscape completely changed almost overnight with the publication of Phillip Felgner's landmark paper in 1987 [115]. Felgner and his group developed a DNA-transfection protocol that makes use of a synthetic cationic lipid, N-[1-(2,3-dioleyloxy)propyl]-N,N,N-trimethylammonium chloride (DOTMA). The authors found that small unilamellar liposomes containing DOTMA interact spontaneously with DNA to form lipid-DNA complexes with 100% association of the DNA. They found that DOTMA facilitates fusion of the complex with the plasma membrane of tissue culture cells which eventually results in both uptake and expression of the DNA. Felgner's technique was simple and highly reproducible and effective for both transient and stable expression of transfected DNA. They reported at that time that depending upon the cell line, lipofection is from 5- to greater than 100-fold more effective than either the calcium phosphate or the DEAE-dextran transfection technique.

As if having anticipated the use of cationic liposomes for the development of RNA vaccines 20 years later, Felgner and his team described already in 1989 [116] the cationic liposome-mediated transfection of NIH3T3 mouse cells with mRNA resulting in the functional expression of *Photinus pyralis* luciferase. In the same paper, the authors also investigated the impact of RNA capping on the transfection efficiency [116].

The invention of cationic liposome-forming lipids (which are non-existent in nature) triggered a boom in the area of gene therapy during the 1990s. Cationic liposomes emerged as valuable alternative to viral transfection vectors, numerous gene therapy companies have been founded, and hundreds of clinical trials have been conducted ever since. A thorough discussion of this particular application of liposomes is however beyond the scope of this review.

---

## 7 COVID-19 Vaccines

With the most recent FDA approval of the Pfizer/BioNTech and Moderna COVID-19 vaccines, so-called lipid nanoparticles (LNP) became world famous almost overnight. The term "particle" arguably appears to demarcate LNP from liposomes, even more so due to the existence of numerous nanoparticles such as gold nanoparticles (AuNP), numerous other metal nanoparticles (copper, iron, zinc, platinum, selenium to name a few), polymeric nanoparticles, quantum dots, and others. Though it is debatable, but in contrast to a "vesicle," which has an aqueous inner space, the term "particle" may imply the presence of a solid inner core. To add to a conceivable confusion, also solid lipid nanoparticles (SLN®) and

nanostructured lipid carriers (NLC®) have been described [117, 118]. So, what are LNP? How much different are they from liposomes? What are SLNs?

According to Tenchov et al. [119], liposomes can be considered as the earliest generation of LNP: “The term ‘liposome’ was coined in the 1960s, shortly after it was found that closed lipid bilayer vesicles form spontaneously in water. The term ‘Lipid Nanoparticle’ came into use much later, in the early 1990s, with the beginning of the era of nanoscience and nanotechnology” [119].

The author characterized the impact of the emerging field of nanoscience on the terminology used in pharmaceutical science as follows: “The adoption of nanoscience terminology by pharmaceutical scientists resulted in the advent of nanopharmaceuticals. The term “nano” became tantamount to “cutting-edge” and was quickly embraced by the pharmaceutical science community. Colloidal drug delivery systems reemerged as nanodrug delivery systems; colloidal gold became a suspension of nano gold particles” [95].

SLNPs and NLCs are undoubtedly distinct from liposomes and LNP, already in so far as they first do not possess an aqueous inner core and, second, they do not (at least in most cases) even contain phospholipids. They are composed of a “solid” or “liquid” lipid inner core made up, for example, of triglycerides, waxes, “hard fats” like stearic acid, palmitic acid, or paraffin, which is surrounded aka emulsified by detergents like sodium cholate, different polysorbates, sodium oleate, cremophore EL or, in a few cases of lecithin, a phospholipid [119, 120].

Liposomes have been extensively described above. In brief, one or more phospholipid bilayers (with or without incorporated cholesterol) surround one or more aqueous compartments, namely, the inner core and the space between phospholipid bilayers in multilamellar liposomes. In the case of long-circulating liposomes, a small amount of a pegylated lipid is a component of the phospholipid bilayer (see above Klibanov, Huang, and Torchilin [62]), and liposomes made for the delivery of nucleic acids carry an artificial cationic lipid in their membranes (see above Felgner [115]). The morphology/structure of cationic liposome–nucleic acid (CL-NA) complexes, commonly called “lipoplexes,” has been extensively studied already in the early 1990s by Cyrus Safinya [121, 122] who most recently summarized the knowledge in this field [123]. In particular, in his paper from 2021, Safinya emphasizes that the choice of lipids determines “the structure of their CL-NA self-assemblies, which constitute distinct liquid crystalline phases” [123] and that in turn these structures play a vital role for the efficacy of nucleic acid delivery.

LNP are considered as the enabling technology of Onpattro, the first FDA-approved RNAi therapeutic, and of both the Pfizer/BioNTech and Moderna COVID-19 vaccines [124, 125]. The

exact composition of both COVID-19 vaccines is given in [119]. In both vaccines, the major lipid components responsible for forming lipid layers/bilayers are distearoylphosphatidylcholine (a phospholipid) and cholesterol. To prevent rapid clearing by the RES system, both vaccines contain pegylated lipids, though different ones. Finally, to enable the successful incorporation of negatively charged nucleic acids, i.e., mRNA, both formulations use ionizable cationic lipids, which are positively charged at pH around 4 and charge-neutral at physiological pH. The procedure and mechanism of RNA entrapment into LNP, i.e., a formulation comprised of an ionizable cationic lipid, a PEG-lipid, cholesterol, and a phospholipid, has been discussed in detail in [125]. The first step involves the formulation of “positively charged bilayer structures” at pH 4 followed by adding negatively charged RNA, which results in “vesicle aggregation.” One can imagine such vesicle aggregation by comparing the polyanion (RNA) “acting as a zipper between multiple membrane surfaces” [125]. The growing contact between the negatively charged nucleic acid and the positively charged vesicle membrane eventually causes membrane areas of high strain which results in membrane rupture and “reformation into planarized stacked membranes” [125]. This proposed mechanism of trapping RNA into LNPs has been illustrated by the authors with a drawing depicting in detail all abovementioned components. Interestingly, the final product as drawn by the authors shows a liposome composed of two bilayer membranes with RNA incorporated into the aqueous space between these two membranes (Fig. 3 in [125]). This depicted vesicular (liposomal) structure RNA-containing LNPs is remarkably confirmed by their own cryo-TEM images (Fig. 1 in [125]).

---

## 8 Conclusion

The bearing of Alec Bangham having played around with smears of egg lecithin on microscope slides and of Brenda Ryman and Gregory Gregoriadis on the development of cell and membrane biology, pharmacology, philosophy, and pharmacy and medicine is remarkable. Nowadays, “liposomes are successfully utilized in all imaginable drug delivery approaches and their use to solve various biomedical problems is steadily increasing” [126]. Liposomes came first, then variations of the system followed. “Liposomes present the prototype of all nanoscale drug delivery vectors... (and) lessons learned in the history of over 40 years of Liposome Technology should be heeded by new investigators in the emerging field of pharmaceutical and biomedical nanotechnology” [127].

## Acknowledgments

The author would like to sincerely thank Professor Gregory Gergiadiis for many useful discussions in preparing the manuscript as well as Dr. Medha Joshi (Midwestern University, Glendale, AZ) for critically reading the final text.

## References

1. Eichman P. From the lipid bilayer to the fluid mosaic: a brief history of membrane models. <http://www1.umn.edu/ships/9-2/membrane.htm>. Accessed 26 May 2015
2. Tanford C (2004) Ben Franklin stilled the waves. Oxford University Press, Oxford
3. Langmuir I (1917) The constitution and structural properties of solids and liquids. II. Liquids. *J Am Chem Soc* 39:1848–1906
4. Gorter E, Grendel F (1925) On bimolecular layers of lipoids on the chromocytes of the blood. *J Exp Med* 41:439–443
5. Danielli JF (1935) The thickness of the wall of the red blood corpuscle. *J Gen Physiol* 19:19–22
6. Singer SJ (1972) A fluid lipid-globular protein mosaic model of membrane structure. *Ann N Y Acad Sci* 195:16–23
7. Singer SJ, Nicolson GL (1972) The fluid mosaic model of the structure of cell membranes. *Science* 175:720–731
8. Sjostrand FS, Andersson-Cedergren E, Dewey MM (1958) The ultrastructure of the intercalated discs of frog, mouse and guinea pig cardiac muscle. *J Ultrastruct Res* 1:271–287
9. Robertson JD (1960) The molecular structure and contact relationships of cell membranes. *Prog Biophys Mol Biol* 10:343–418
10. Bangham AD (1989) The first description of liposomes. *Curr Content* 13:14
11. Mueller P, Rudin DO, Tien HT, Wescott WC (1962) Reconstitution of cell membrane structure in vitro and its transformation into an excitable system. *Nature* 194:979–980
12. Beerlink A, Wilbrandt PJ, Ziegler E, Carbone D, Metzger TH, Salditt T (2008) X-ray structure analysis of free-standing lipid membranes facilitated by micromachined apertures. *Langmuir* 24:4952–4958
13. Malmstadt N, Jeon T-J, Schmidt JJ (2007) Long-lived planar lipid bilayer membranes anchored to an in situ polymerized hydrogel. *Adv Mater* 20:84–89
14. Deamer DW (2010) From “banghasomes” to liposomes: a memoir of Alec Bangham, 1921–2010. *FASEB J* 24:1308–1310
15. Hargreaves WR, Mulvihill SJ, Deamer DW (1977) Synthesis of phospholipids and membranes in prebiotic conditions. *Nature* 266: 78–80
16. Deamer DW, Pashley RM (1989) Amphiphilic components of the Murchison carbonaceous chondrite: surface properties and membrane formation. *Orig Life Evol Biosph* 19:21–38
17. Bangham AD, Horne RW (1964) Negative staining of phospholipids and their structural modification by surface-active agents as observed in the electron microscope. *J Mol Biol* 8:660–668
18. Bangham AD, Standish MM, Watkins JC (1965) Diffusion of univalent ions across the lamellae of swollen phospholipids. *J Mol Biol* 13:238–252
19. Bangham AD, Standish MM, Weissmann G (1965) The action of steroids and streptolysin S on the permeability of phospholipid structures to cations. *J Mol Biol* 13:253–259
20. Sessa G, Weissmann G (1968) Phospholipid spherules (liposomes) as a model for biological membranes. *J Lipid Res* 9:310–318
21. Papahadjopoulos D, Bangham AD (1966) Biophysical properties of phospholipids. II. Permeability of phosphatidylserine liquid crystals to univalent ions. *Biochim Biophys Acta* 126:185–188
22. Bangham AD, Papahadjopoulos D (1966) Biophysical properties of phospholipids. I. Interaction of phosphatidylserine monolayers with metal ions. *Biochim Biophys Acta* 126:181–184
23. Bangham AD, Standish MM, Watkins JC, Weissmann G (1967) The diffusion of ions from a phospholipid model membrane system. *Protoplasma* 63:183–187
24. Bangham AD, Greville GD (1967) Osmotic properties and water permeability of phospholipid crytsals. *Chem Phys Lipids* 1: 225–246

25. Bangham AD, Hill MW, Miller NG (1974) Preparation and use of liposomes as models of biological membranes. In: Korn ED (ed) Methods in membrane biology, vol 1. Plenum Press: New York, pp 1–68
26. Chan YH, Boxer SG (2007) Model membrane systems and their applications. *Curr Opin Chem Biol* 11:581–587
27. Fahr A, Liu X (2010) Utilization of liposomes for studying drug transfer and uptake. *Methods Mol Biol* 606:1–10
28. Reed JR (2010) The use of liposomes in the study of drug metabolism: a method to incorporate the enzymes of the cytochrome p450 monooxygenase system into phospholipid, bilayer vesicles. *Methods Mol Biol* 606:11–20
29. Kramer R, Nicklisch S, Ott V (2010) Use of liposomes to study cellular osmosensors. *Methods Mol Biol* 606:21–30
30. Martinac B, Rohde PR, Battle AR, Petrov E, Pal P, Foo AF, Vasquez V, Huynh T, Kloda A (2010) Studying mechanosensitive ion channels using liposomes. *Methods Mol Biol* 606: 31–53
31. Indiveri C (2010) Studying amino acid transport using liposomes. *Methods Mol Biol* 606: 55–68
32. Hofer CT, Herrmann A, Muller P (2010) Use of liposomes for studying interactions of soluble proteins with cellular membranes. *Methods Mol Biol* 606:69–82
33. MirAfzali Z, DeWitt DL (2010) Liposomal reconstitution of monotopic integral membrane proteins. *Methods Mol Biol* 606:83–94
34. Sessa G, Weissmann G (1970) Incorporation of lysozyme into liposomes. A model for structure-linked latency. *J Biol Chem* 245: 3295–3301
35. Stammes M, Xu W (2010) The reconstitution of actin polymerization on liposomes. *Methods Mol Biol* 606:95–103
36. Montes LR, Ahyayauch H, Ibarguren M, Sot J, Alonso A, Bagatollo LA, Goni FM (2010) Electroformation of giant unilamellar vesicles from native membranes and organic lipid mixtures for the study of lipid domains under physiological ionic-strength conditions. *Methods Mol Biol* 606:105–114
37. Nantes IL, Kawai C, Pessoto FS, Mugnol KC (2010) Study of respiratory cytochromes in liposomes. *Methods Mol Biol* 606:147–165
38. Brittes J, Lucio M, Nunes C, Lima JL, Reis S (2010) Effects of resveratrol on membrane biophysical properties: relevance for its pharmacological effects. *Chem Phys Lipids* 163: 747–754
39. Lucio M, Lima JL, Reis S (2010) Drug-membrane interactions: significance for medicinal chemistry. *Curr Med Chem* 17: 1795–1809
40. Reis S, Lucio M, Segundo M, Lima JL (2010) Use of liposomes to evaluate the role of membrane interactions on antioxidant activity. *Methods Mol Biol* 606:167–188
41. Sabin J, Prieto G, Sarmiento F (2010) Studying colloidal aggregation using liposomes. *Methods Mol Biol* 606:189–198
42. Broecker J, Keller S (2010) Membrane translocation assayed by fluorescence spectroscopy. *Methods Mol Biol* 606:271–289
43. Fiedler S, Broecker J, Keller S (2010) Protein folding in membranes. *Cell Mol Life Sci* 67: 1779–1798
44. Takei K, Yamada H, Abe T (2010) Use of liposomes to study vesicular transport. *Methods Mol Biol* 606:531–542
45. Raguz M, Mainali L, Widomska J, Subczynski WK (1808) The immiscible cholesterol bilayer domain exists as an integral part of phospholipid bilayer membranes. *Biochim Biophys Acta* 2011:1072–1080
46. Subczynski WK, Raguz M, Widomska J (2010) Studying lipid organization in biological membranes using liposomes and EPR spin labeling. *Methods Mol Biol* 606: 247–269
47. Bangham AD, Hill MW (1986) The proton pump/leak mechanism of unconsciousness. *Chem Phys Lipids* 40:189–205
48. Johnson SM, Miller KW, Bangham AD (1973) The opposing effects of pressure and general anaesthetics on the cation permeability of liposomes of varying lipid composition. *Biochim Biophys Acta* 307:42–57
49. Miller KW (1983) Anaesthetized liposomes. Academic Press, London
50. (1987) Ten centre trial of artificial surfactant (artificial lung expanding compound) in very premature babies. Ten Centre Study Group. *Br Med J (Clin Res Ed)* 294:991–996
51. Bangham A (2009) The physical chemistry of self/non-self: jigsaws, transplants and fetuses. *FASEB J* 23:3644–3646
52. Gruener R, McArdle B, Ryman BE, Weller RO (1968) Contracture of phosphorylase deficient muscle. *J Neurol Neurosurg Psychiatry* 31:268–283
53. Leathwood PD, Ryman BE (1970) The use of skin biopsy in the diagnosis of the glycogen-storage diseases. *Biochem J* 117:34P

54. Palmer TN, Ryman BE, Whelan WJ (1968) The action pattern of amyloglucosidase. FEBS Lett 1:1–3
55. Gregoriadis G, Morell AG, Sternlieb I, Scheinberg IH (1970) Catabolism of desialylated ceruloplasmin in the liver. J Biol Chem 245:5833–5837
56. Morell AG, Gregoriadis G, Scheinberg IH, Hickman J, Ashwell G (1971) The role of sialic acid in determining the survival of glycoproteins in the circulation. J Biol Chem 246:1461–1467
57. Gregoriadis G (1983) How liposomes changed my life and got away with it. In: Bangham AD (ed) Liposome letters. Academic Press, London, pp 405–407
58. Gregoriadis G, Ryman BE (1971) Liposomes as carriers of enzymes or drugs: a new approach to the treatment of storage diseases. Biochem J 124:58P
59. Gregoriadis G, Leathwood PD, Ryman BE (1971) Enzyme entrapment in liposomes. FEBS Lett 14:95–99
60. Kirby C, Gregoriadis G (1984) Dehydration-rehydration vesicles: a simple method for high yield drug entrapment in liposomes. Biotechnology 2:979–984
61. Antimisiaris SG (2010) Preparation of DRV liposomes. In: Weissig V (ed) Liposomes: methods and protocols. Springer Science +Business Media, pp 51–75. [Walker JM (Series Editor), vol I]: New York Dordrecht Heidelberg London
62. Klibanov AL, Maruyama K, Torchilin VP, Huang L (1990) Amphiphatic polyethylene-glycols effectively prolong the circulation time of liposomes. FEBS Lett 268:235–237
63. Blume G, Cevc G (1993) Molecular mechanism of the lipid vesicle longevity in vivo. Biochim Biophys Acta 1146:157–168
64. Senior JH, Delgado C, Fisher D, Tilcock C, Gregoriadis G (1991) Influence of surface hydrophilicity of liposomes on their interaction with plasma proteins and clearance from the circulation. Studies with polyethylene glycol-coated vesicles. Biochim Biophys Acta 1062:77–82
65. Needham D, McIntosh TJ, Lasic DD (1992) Repulsive interactions and mechanical stability of polymer-grafted lipid membranes. Biochim Biophys Acta 1108:40–48
66. Barenholz Y (2012) Doxil(R)--the first FDA-approved nano-drug: lessons learned. J Control Release 160:117–134
67. Gregoriadis G, Ryman BE (1972) Lysosomal localization of -fructofuranosidase-containing liposomes injected into rats. Biochem J 129: 123–133
68. Allison AG, Gregoriadis G (1974) Liposomes as immunological adjuvants. Nature 252:252
69. Leserman L (2008) The Gregoriadis: from smetic mesophases to liposomal drug carriers, a personal reflection of Gregory Gregoriadis. J Drug Target 16:525–528
70. Manesis EK, Cameron CH, Gregoriadis G (1978) Incorporation of hepatitis-B surface antigen (HBsAg) into liposomes. Biochem Soc Trans 6:925–928
71. Gregoriadis G, Davis D, Davies A (1987) Liposomes as immunological adjuvants: antigen incorporation studies. Vaccine 5:145–151
72. Gregoriadis G, Panagiotidi C (1989) Immunoadjuvant action of liposomes: comparison with other adjuvants. Immunol Lett 20:237–240
73. Gregoriadis G, Tan L, Ben-Ahmed ET, Jennings R (1992) Liposomes enhance the immunogenicity of reconstituted influenza virus A/PR/8 envelopes and the formation of protective antibody by influenza virus A/Sichuan/87 (H3N2) surface antigen. Vaccine 10:747–753
74. Gregoriadis G, Wang Z, Barenholz Y, Francis MJ (1993) Liposome-entrapped T-cell peptide provides help for a co-entrapped B-cell peptide to overcome genetic restriction in mice and induce immunological memory. Immunology 80:535–540
75. Mischler R, Metcalfe IC (2002) Inflexal® V a trivalent virosome subunit influenza vaccine: production. Vaccine 20:B17–B23
76. Herzog C, Hartman K, Kuenzi V, Kuersteiner O, Mischler R, Lazar H, Glueck R (2009) Eleven years of Inflexal® V – a virosomal adjuvanted influenza vaccine. Vaccine 27:4381–4387
77. Bovier PA (2008) Epaxal: a virosomal vaccine to prevent hepatitis A infection. Expert Rev Vaccines 7(8):1141–1150
78. Weissig V, Lasch J, Klibanov AL, Torchilin VP (1986) A new hydrophobic anchor for the attachment of proteins to liposomal membranes. FEBS Lett 202:86–90
79. Kung VT, Redemann CT (1986) Synthesis of carboxyacyl derivatives of phosphatidylethanolamine and use as an efficient method for conjugation of protein to liposomes. Biochim Biophys Acta 862:435–439
80. Tan L, Weissig V, Gregoriadis G (1991) Comparison of the immune response against polio peptides covalently-surface-linked to and

- internally-entrapped in liposomes. *Asian Pac J Allergy Immunol* 9:25–30
81. Gregoriadis G, Neerunjun ED (1975) Treatment of tumour bearing mice with liposome-entrapped actinomycin D prolongs their survival. *Res Commun Chem Pathol Pharmacol* 10:351–362
  82. Gregoriadis G (1976) The carrier potential of liposomes in biology and medicine (second of two parts). *N Engl J Med* 295:765–770
  83. Gregoriadis G (1976) The carrier potential of liposomes in biology and medicine (first of two parts). *N Engl J Med* 295:704–710
  84. Gregoriadis G (1978) Liposomes in the therapy of lysosomal storage diseases. *Nature* 275: 695–696
  85. D’Souza GG, Weissig V (2009) Subcellular targeting: a new frontier for drug-loaded pharmaceutical nanocarriers and the concept of the magic bullet. *Expert Opin Drug Deliv* 6:1135–1148
  86. Gregoriadis G (1977) Targeting of drugs. *Nature* 265:407–411
  87. Milstein C (1977) Kohler G: [clonal variations of myelomatous cells (proceedings)]. *Minerva Med* 68:3453
  88. Kohler G, Pearson T, Milstein C (1977) Fusion of T and B cells. *Somatic Cell Genet* 3:303–312
  89. Milstein C, Adetugbo K, Cowan NJ, Kohler G, Secher DS, Wilde CD (1977) Somatic cell genetics of antibody-secreting cells: studies of clonal diversification and analysis by cell fusion. *Cold Spring Harb Symp Quant Biol* 41(Pt 2):793–803
  90. Heath TD, Fraley RT, Papahdopoulos D (1980) Antibody targeting of liposomes: cell specificity obtained by conjugation of F(ab')<sub>2</sub> to vesicle surface. *Science* 210:539–541
  91. Leserman LD, Barbet J, Kourilsky F, Weinstein JN (1980) Targeting to cells of fluorescent liposomes covalently coupled with monoclonal antibody or protein A. *Nature* 288:602–604
  92. Huang A, Huang L, Kennel SJ (1980) Monoclonal antibody covalently coupled with fatty acid. A reagent for in vitro liposome targeting. *J Biol Chem* 255:8015–8018
  93. Torchilin VP, Goldmacher VS, Smirnov VN (1978) Comparative studies on covalent and noncovalent immobilization of protein molecules on the surface of liposomes. *Biochem Biophys Res Commun* 85:983–990
  94. Torchilin VP, Khaw BA, Smirnov VN, Haber E (1979) Preservation of antimyosin antibody activity after covalent coupling to liposomes. *Biochem Biophys Res Commun* 89:1114–1119
  95. Weissig V, Pettinger TK, Murdock N (2014) Nanopharmaceuticals (part 1): products on the market. *Int J Nanomedicine* 9:4357–4373
  96. Weissig V, Guzman-Villanueva D (2015) Nanopharmaceuticals (part 2): products in the pipeline. *Int J Nanomedicine* 10:1245–1257
  97. Blume G, Cevc G, Crommelin MD, Bakker-Woudenberg IA, Kluft C, Storm G (1993) Specific targeting with poly(ethylene glycol)-modified liposomes: coupling of homing devices to the ends of the polymeric chains combines effective target binding with long circulation times. *Biochim Biophys Acta* 1149:180–184
  98. Gabizon A, Papahadjopoulos D (1988) Liposome formulations with prolonged circulation time in blood and enhanced uptake by tumors. *Proc Natl Acad Sci U S A* 85:6949–6953
  99. Allen TM, Chonn A (1987) Large unilamellar liposomes with low uptake into the reticuloendothelial system. *FEBS Lett* 223:42–46
  100. Park YS, Maruyama K, Huang L (1992) Some negatively charged phospholipid derivatives prolong the liposome circulation in vivo. *Biochim Biophys Acta* 1108:257–260
  101. Gregoriadis G (2008) Liposome research in drug delivery: the early days. *J Drug Target* 16:520–524
  102. Gregoriadis G, Saffie R, de Souza JB (1997) Liposome-mediated DNA vaccination. *FEBS Lett* 402:107–110
  103. Gregoriadis G, McCormack B, Obrenovich M, Perrie Y (2000) Entrapment of plasmid DNA vaccines into liposomes by dehydration/rehydration. *Methods Mol Med* 29:305–311
  104. Gregoriadis G. Xenetic webpage. <http://www.xeneticbio.com/about-us>. Accessed 26 June 2015
  105. Nandi PK, Legrand A, Nicolau C (1986) Biologically active, recombinant DNA in clathrin-coated vesicles isolated from rat livers after in vivo injection of liposome-encapsulated DNA. *J Biol Chem* 261: 16722–16726
  106. Nicolau C (1984) Liposomes for gene transfer and expression in vivo. *Biochem Soc Trans* 12:349–350
  107. Nicolau C, Cudd A (1989) Liposomes as carriers of DNA. *Crit Rev Ther Drug Carrier Syst* 6:239–271

108. Nicolau C, Le Pape A, Soriano P, Fargette F, Juhel MF (1983) In vivo expression of rat insulin after intravenous administration of the liposome-entrapped gene for rat insulin I. *Proc Natl Acad Sci U S A* 80:1068–1072
109. Nicolau C, Legrand A, Grosse E (1987) Liposomes as carriers for in vivo gene transfer and expression. *Methods Enzymol* 149:157–176
110. Nicolau C, Legrand A, Soriano P (1984) Liposomes for gene transfer and expression in vivo. *Ciba Found Symp* 103:254–267
111. Nicolau C, Rottem S (1982) Expression of a beta-lactamase activity in *Mycoplasma capricolum* transfected with the liposome-encapsulated *E.coli* pBR 322 plasmid. *Biochem Biophys Res Commun* 108:982–986
112. Nicolau C, Sene C (1982) Liposome-mediated DNA transfer in eukaryotic cells. Dependence of the transfer efficiency upon the type of liposomes used and the host cell cycle stage. *Biochim Biophys Acta* 721:185–190
113. Soriano P, Dijkstra J, Legrand A, Spanjer H, Londos-Gagliardi D, Roerdink F, Scherphof G, Nicolau C (1983) Targeted and nontargeted liposomes for in vivo transfer to rat liver cells of a plasmid containing the preproinsulin I gene. *Proc Natl Acad Sci U S A* 80:7128–7131
114. Wong TK, Nicolau C, Hofsneider PH (1980) Appearance of beta-lactamase activity in animal cells upon liposome-mediated gene transfer. *Gene* 10:87–94
115. Felgner PL, Gadek TR, Holm M, Roman R, Chan HW, Wenz M, Northrop JP, Ringold GM, Danielsen M (1987) Lipofection: a highly efficient, lipid-mediated DNA-transfection procedure. *Proc Natl Acad Sci U S A* 84:7413–7417
116. Malone RW, Felgner PL, Verma IM (1989) Cationic liposome-mediated RNA transfection. *Proc Natl Acad Sci U S A* 86:6077–6081
117. Mueller RH, Radtke M, Wissing SA (2002) Solid lipid nanoparticles (SLN) and nanostructured lipid carriers (NLC) in cosmetic and dermatological preparations. *Adv Drug Deliv Rev* 54:S131–S155
118. Mueller RH, Radtke M, Wissing SA (2002) Nanostructured lipid matrices for improved microencapsulation of drugs. *Int J Pharm* 242:121–128
119. Tenchov R, Bird R, Curtze AE, Zhou Q (2021) Lipid nanoparticles – from liposomes to mRNA vaccine delivery, a landscape of research diversity and advancement. *ACS Nano* 15:16982–17015
120. Montoto SS, Muraca G, Ruiz ME (2020) Solid lipid nanoparticles for drug delivery: pharmacological and biopharmaceutical aspects. *Front Mol Biosci* 7:1–24
121. Safinya CR, Sirota EB, Bruinsma RF, Jeppesen C, Plano RJ, Wenzel LJ (1993) Structure of membrane surfactant and liquid crystalline lamellar phases under flow. *Science* 261(5121):588–591
122. Chiruvolu S, Warriner HE, Naranjo E, Idziak SH, Raedler JO, Plano RJ, Zasadzinski JA, Safinya CR (1994) A phase of liposomes with entangled tubular vesicles. *Science* 266(5188):1222–1225
123. Ewert KK, Scodeller P, Simon-Graccia L, Steffes VM, Wonder EA, Teesalu T, Safinya CR (2021) Cationic liposomes as vectors for nucleic acid and hydrophobic drug therapeutics. *Pharmaceutics* 13:1365
124. Akine A, Maier MA, Manoharan M, Fitzgerald K, Jayaraman M, Barros S, Ansell S, Du C, Hope MJ, Madden TD, Mui BL, Semple SC, Tam YK, Ciufolini M, Witzigmann D, Kulkarni JA, van der Meel R, Cullis PR (2019) The Onpattro story and the clinical translation of nanomedicines containing nucleic acid-based drugs. *Nat Nanotechnol* 14:1084–1087
125. Kulkarni JA, Thomson SB, Zaifman J, Leung J, Wagner PK, Hill A, Tam YYC, Cullis PR (2020) Spontaneous, solvent-free entrapment of siRNA within lipid nanoparticles. *Nanoscale* 12:23959–23966
126. Elbayoumi TA, Torchilin VP (2010) Current trends in liposome research. *Methods Mol Biol* 605:1–27
127. Weissig V (2010) Liposomes – methods and protocols. Preface. *Methods Mol Biol* v–vi



# Chapter 2

## Preparation of DRV Liposomes

Sophia G. Antimisiaris

### Abstract

Dried reconstituted vesicle (DRV) liposomes are formulated under mild conditions. The method has the capability to entrap substantially higher amounts of hydrophilic solutes, compared to other passive-loading liposome preparation methods. These characteristics make this liposome type ideal for entrapment of labile substances, such as peptides, proteins, or DNA's (or other nucleotides or oligonucleotides), or in general biopharmaceuticals and sensitive drugs. In this chapter, all possible types of DRV liposomes (in respect to the encapsulated molecule characteristics and/or their applications in therapeutics) are introduced, and preparation methodologies (for each type) are described in detail.

**Key words** DRV, Protein, Peptide, Hydrophilic drug, Encapsulation efficiency, Vaccine, DNA, Biopharmaceuticals, Particulate, Bacteria, Cyclodextrin

### Abbreviations

|                |   |
|----------------|---|
| BisHOP         | 1,2-bis(hexadecylcycloxy)-3-trimethylaminopropane   |
| CD             | Cyclodextrin  |
| CF             | 5, 6 -carboxyfluorescein  |
| CFA            | Complete Freund's adjuvant  |
| Chol           | Cholesterol   |
| DMPC           | 1,2-dimyristoyl- <i>sn</i> -glyceroyl-3-phosphocholine  |
| DC-Chol        | 3b-( <i>N,N</i> -dimethylaminoethane)carbamylcholesterol  |
| DOTAP          | 1,2-dioleyloxy-3-trimethylammonium propane  |
| DOTMA          | <i>N</i> -[1-(2,3-dioleyloxy) propyl]- <i>N,N,N</i> -triethylammonium                                   |
| DPPC           | 1,2-dipalmitoyl- <i>sn</i> -glyceroyl-3-phosphocholine  |
| DPPE-PEG2000   | 1,2-dipalmitoyl- <i>sn</i> -glyceroyl-3-phosphoethanolamine conjugated to polyethylene glycol (MW 2000) |
| DRV            | Dried rehydrated vesicles; dehydrated reconstituted vesicles  |
| DSPC           | 1,2-distearoyl- <i>sn</i> -glyceroyl-3-phosphocholine   |
| HP $\beta$ -CD | Hydroxypropyl-beta-CD   |
| HPC            | Hydrogenated PC   |
| IONP           | Iron oxide nanoparticle   |
| iv             | Intravenous   |
| MLV            | Multilamellar vesicles  |

|        |  |
|--------|--|
| MW     | Molecular weight                       |
| PA     | Phosphatidic acid                      |
| PB     | Phosphate buffer                       |
| PBS    | Phosphate-buffered saline              |
| PC     | Phosphatidylcholine                    |
| PCS    | Photon correlation spectroscopy        |
| PEG    | Polyethylene glycol                    |
| PG     | Phosphatidylglycerol                   |
| PRE    | Prednisolone                           |
| PS     | Phosphatidylserine                     |
| RCM    | Radiographic contrast media            |
| rgp63  | Recombinant glycoprotein of leishmania |
| SA     | Stearylamine                           |
| SM     | Sphingomyelin                          |
| SUV    | Small unilamellar vesicles             |
| Tc     | Lipid transition temperature           |
| TO     | Triolein                               |
| USPIOs | Ultra small paramagnetic iron oxides   |

## 1 Introduction

Dried reconstituted vesicles (DRVs) (*see Note 1*) were initially developed in 1984 by Kirby and Gregoriadis [1]. They are oligolamellar or multilamellar liposomes with capability of encapsulating high amounts of aqueous soluble molecules. The fact that the DRV technique involves vesicle formation under mild conditions (e.g., conditions that do not cause decomposition or loss of activity of labile active substances) makes the DRV method the method of choice for preparation of liposomal formulations of sensitive active substances, such as peptides, proteins, enzymes, or biopharmaceuticals in general.

High entrapment efficiency is a valuable advantage for any liposome type, since it results in economy of lipids and active substances. This parameter is very important when functionalized lipids are included in the liposome composition (for vesicle targeting to specific receptors) and/or when expensive synthetic drugs are used. In addition to economy, high liposome entrapment yields minimize the amount of lipids required to deliver a given amount of drug, reducing the possibility for (i) saturation of cells with lipids and (ii) lipid-related toxicity.

The high entrapment capability of DRV liposomes is due to the fact that preformed “empty” small unilamellar vesicles are disrupted during a freeze-drying cycle, and subsequently, controlled rehydration is carried out in the presence of high concentration of the solute(s) destined for entrapment; during the rehydration step, the vesicles fuse into large oligolamellar (or multilamellar) vesicles

entrapping high amounts of the solute(s). The size of the initial liposome dispersion used and the solute(s) solution characteristics, together with the conditions applying during rehydration of the freeze-dried product, are all important parameters which determine the final size and entrapment efficiency of the DRV liposomes that are finally produced. The presence of cryoprotectants during the initial freeze-drying step of DRV preparation, results in reduced solute entrapment as previously proven [2], due to the fact that cryoprotectants preserves the integrity of “empty” vesicles, preventing disruption and subsequent fusion. It has been reported that by controlling the sugar (cryoprotectant)/lipid mass ratio, different entrapment efficiencies and final vesicle sizes can be achieved [2].

From 1984, when they were first developed by Kirby and Gregoriadis [1], the DRV liposome preparation method has been used for liposomal encapsulation of various active substances which may be divided in three main categories [3]: (i) low MW drug molecules (mainly hydrophilic drugs) [4–37]; (ii) proteins, peptides, enzymes, or antigens [38–47]; and (iii) DNA or oligonucleotides [48–54]. From these categories the last two are primarily used as liposomal vaccines. In addition to soluble materials, the DRV method can be applied for formation of liposomes that entrap particles, such as bacteria spores [55, 56] or iron oxide nanoparticles (IONPs) [57, 58]. Additionally, recently the DRV method was found to be advantageous for engineering of cellular vesicles, in order to achieve high drug loading into them [59, 60]. Some examples of substances entrapped in DRV liposomes from the last 20-year literature are presented in Table 1.

At this point, it should be clarified that the DRV method can indeed confer very high loading of drugs into liposomes, compared to other passive loading techniques; however when compared with remote of active loading methods, in cases of drugs that can be loaded into liposomes with such methods, the active loading methods attain higher loading efficiencies compared to the DRV methods, as recently reported for moxicloxacin [61].

In addition to hydrophilic drugs, the DRV method has been used for the production of stable liposomal formulations of amphiphilic/lipophilic or else membrane-permeable drugs, after the formation of appropriate aqueous soluble cyclodextrin [CD]-drug complexes which are finally encapsulated in the aqueous vicinity of the DRV vesicles [16, 18, 19, 22, 26, 29]. Cyclodextrins are cyclic oligosaccharides (composed of at least six D-(+) glucopyranose units) that form torus-like molecules or truncated cones. CD molecules have a hydrophilic surface and a hydrophobic interior, in which lipophilic drugs can be accommodated to form aqueous soluble CD-drug complexes. Several applications have been investigated for CD-drug complex encapsulating DRV liposomes.

**Table 1****List of compounds that have been entrapped in DRV liposomes for therapeutic applications**

| <b>Encapsulated substance</b>  | <b>Study objective</b>  | <b>Ref</b>                                  |
|--|---|---|
| <b>Low MW drugs</b>  |   |   |
| Daunorubicin/doxorubicin/riboflavin; contrast agents; gentamycin; Hepes; thioguanine; aminoglycoside and macrolide antibiotics; arsenic-trioxide; calcein/PRE; dehydroepiandrosterone/retinol/retinoic acid; curcumin; ibuprofen | Encapsulation efficiency, physicochemical parameter optimization; formulation studies; control encapsulation yield, and size of DRV | [2–5, 7, 8, 12, 13, 15, 16, 18, 19, 22, 26] |
| CF, vancomycin   | Development of targeted liposomes   | [6, 10]                                     |
| Dexamethasone; low-MW- heparin   | Biomaterial coating with liposomes  | [14, 20]                                    |
| Carboxyfluorescein (CF) or calcein   | Liposome–cell interaction studies; exosome engineering  | [17, 59, 60]                                |
| Rifampicin (RIF)   | Development of liposomes for nebulization   | [21]  |
| Pirarubicin, gentamicin, glucosamine, Cuphen, ciprofloxacin; hypericin; chloramphenicol, diclofenac, azithromycin, fullerol, moxifloxacin  | Enhancement of therapeutic effect of drugs  | [11, 23, 24, 27–31, 34, 35, 61]             |
| Raloxifene, leuprolide, dopamine, ranibizumab  | Carrier for protection, barrier passage   | [25, 32, 33, 36]                            |
| <b>Proteins</b>  |   |   |
| Bovine serum albumin, glucose oxidase (GO), human gamma-globulin; t-PA   | Immunization; entrapment optimization; biodistribution studies; freeze-drying studies   | [38, 40–42]                                 |
| Tetanus toxoid and IgG   | Coupling ligands to preformed DRVs  | [39]  |
| Protein 1  | Delivery carrier and protection by DRVs   | [43]  |
| Transmembrane proteins   | Protein reconstruction into membranes   | [46]  |
| Antigenic peptides   | Vaccine development   | [47]  |
| DNA – oligonucleotides   |   |   |
| <i>Candida albicans</i> ribosomes  | Vaccine development   | [48]  |
| Plasmid DNA or naked DNA   | Vaccine development; compare carriers   | [49–51]                                     |
| CpG oligodeoxynucleotides (CpG ODN) and glycoprotein (rgp63)   | Evaluation of immune response   | [52]  |
| Plasmid DNA  | Preservation as dried formulations  | [53]  |

### 1.1 Drug Encapsulating DRVs

Various hydrophilic molecules have been entrapped in DRV liposomes, as radiographic contrast media [RCM] [4], gentamycin [5, 23], thioguanine [8], bupivacaine hydrochloride [9], vancomycin [10], pirarubicin [11], arsenic trioxide [12], aminoglycosides and macrolide antibiotics [13], low molecular weight heparin [14], ciprofloxacin [28], chloramphenicol [31], dopamine [32], etc. In several studies in which the parameters that influence DRV stability and/or encapsulation efficiency are investigated, model molecules are encapsulated in DRVs. In such cases, and especially when the integrity of the liposomes is to be evaluated, it is preferable to use fluorescent dyes, such as calcein or 5, 6-carboxyfluorescein (CF), that are entrapped in the vesicles at quenched concentrations, and thus their release can be continuously monitored due to the de-quenching of the dye's fluorescence intensity upon its release from the vesicles and its dilution in the liposome dispersion media [1, 2, 15–17, 59, 60].

As mentioned above, the entrapment efficiencies and size distribution of the DRV liposomes produced can be tuned by controlling the sugar/lipid mass ratio, during DRV preparation [1–3].

Amphiphilic or lipophilic drug encapsulating DRV liposomes have also been prepared [16–22]. Nevertheless, in most cases amphiphilic or lipophilic drugs (depending on their lipid permeability and their aqueous solubility) rapidly leak out from their liposomal formulations upon dilution of the liposome suspension (the leakage rate being determined by the lipid permeability and aqueous solubility of the drug together with the dilution factor) [16]. This is highly likely to occur immediately after i.v. administration of liposomes when the liposome suspension is diluted in the bloodstream. As mentioned above, a method to overcome the latter problem is to entrap an aqueous soluble complex of the drug with cyclodextrin in the aqueous vicinity of DRV liposomes, instead of the drug itself which will probably be located in the lipid bilayers of the liposomes [16, 18, 18, 22, 26, 29]. Criticism has been raised about the final result of this approach in terms of its ability to improve the drug retention in the vesicles. In fact it has been demonstrated earlier for prednisolone (PRE), and more recently for curcumin, that the encapsulation of PRE-HP-beta-CD complex, or curcumin-CD complexes, does not improve the retention of the drugs in the liposomes significantly (compared to liposomes that incorporate the plain drug) but only results in increased drug encapsulation [16, 22]. The former failure was attributed to the rapid displacement of the drug from the CD complex by other components of the multicomponent drug-in-CD-in-liposome system, as phospholipids and cholesterol that usually have higher affinity for the CD cavity (compared to the drug). It was in fact demonstrated [15], that specific CD molecules can extract cholesterol molecules and in some cases also phospholipids from

liposomal membranes. Thereby, it is important to consider the affinity of the specific drug molecule for the specific cyclodextrin as well as the affinity of the cyclodextrin for the lipid components of the liposomes and select the cyclodextrin type and the lipid components of the drug-in-cyclodextrin-in-liposome system accordingly, when designing such complex systems, in order to achieve maximum drug retention in the vesicles.

Another application of the drug-in-CD-in-liposome complex system is the construction of liposomal formulations of photosensitive drugs (i.e., drugs that degrade on exposure to light and lose their activity), such as riboflavin [19]. For this, one or more lipid-soluble UV absorbers, as oil-red-O, oxybenzone, or dioxybenzone, can be entrapped into the lipid phase, while water-soluble ones, such as sulisobenzene, can be entrapped in the aqueous phase of liposomes together with the drug-CD complex. Study results suggest that such liposome-based multicomponent systems could be developed for the protection of photolabile agents.

## 1.2 Antigen Encapsulating DRVs

The immunological adjuvant properties of liposomes have been demonstrated more than 40 years ago [62], and extensive research on this subject has shown that liposome adjuvanticity applies to a large variety of protozoan, viral, bacterial, tumor, and other antigens [63, 64]. Thereby, the use of liposomes for the encapsulation of protein and DNA vaccines has been extensively studied [48–54, 62–64]. As mentioned before, the DRV technique is the method of choice for the preparation of liposomal formulations of labile compounds that may—partly or completely—lose their activity when exposed to the conditions applying for the preparation of liposome formulations by other techniques (as contact with organic solvents or sonication). In the case of vaccines, the easy scale-up and high yield entrapment of DRV's are additional assets that make this technique highly advantageous. For these reasons, DRV liposomes have been formulated and tested for their ability to encapsulate and retain a number of different types of vaccines (antigens), such as peptides, proteins, plasmid DNA, and other macromolecules or even particulates, as attenuated bacteria and spores [55, 56, 65]. Furthermore the immunological results of such formulations have been studied, and in most of the cases, the liposomal vaccines have been demonstrated to perform as good or even better than other adjuvants [54, 66, 67].

In addition to their adjuvanticity, another advantage of antigen-containing DRV suspensions is that they can be freeze-dried in the presence of a cryoprotectant for product shelf life prolongation, without losing significant amounts of entrapped material upon reconstitution with physiological saline [55, 56, 65–67]. However, it is very important to take special care during the initial rehydration of the freeze-dried material: *the water added at this stage should be kept to a minimum.*

In the following part of this chapter, the methodologies for preparation of DRVs for encapsulation of (i) low molecular weight drugs (mainly hydrophilic), (ii) CD–drug complexes, and (iii) vaccines (DRVs containing protein, peptide, particulate antigens, or DNA/oligonucleotides [for DNA-vaccines]), are discussed in detail.

---

## 2 Materials

### 2.1 Low MW Drug Encapsulating DRV

1. Egg L- $\alpha$ -phosphatidylcholine [PC] (grade 1) (Lipid Products, Nutfield, UK, or Lipoid, DE) is used in solid state or dissolved (20 mg/mL or 100 mg/mL) in a mixture of CHCl<sub>3</sub>/CH<sub>3</sub>OH (2:1 v/v) and stored in aliquots at –80 °C. The 99% purity of the lipid is verified by thin layer chromatography (*see Note 2*).
2. Hydrogenated egg phosphatidylcholine [HPC], sphingomyelin [SM], phosphatidic acid [PA], 1,2-dimyristoyl-*sn*-glyceroyl-3-PC [DMPC], 1,2-dipalmitoyl-*sn*-glyceroyl-3-PC [DPPC], or 1,2-distearoyl-*sn*-glyceroyl-3-PC [DSPC] (synthetic- grade 1) (Lipid Products, Nutfield, UK, or Lipoid, DE or Avanti Polar Lipids, USA). Storage conditions and purity tests (*see Note 2*) are the same as mentioned above for PC (with the difference that only 20 mg/mL solutions are made for these lipids).
3. Cholesterol [Chol] (pure) (Sigma-Aldrich, Athens, Greece). Chol is stored desiccated at –20 °C. Chol is used for liposome preparation in solid state (powder) or after being dissolved (20 mg/mL or 100 mg/mL) in a mixture of CHCl<sub>3</sub>/CH<sub>3</sub>OH (2:1 v/v) and stored in aliquots at –80 °C.
4. The water used in all solutions is deionized and then distilled [d.d. H<sub>2</sub>O].
5. Phosphate-buffered saline (PBS), pH 7.4.: 10 mM sodium phosphate, 3 mM potassium phosphate, 140 mM NaCl, and 0.2 g sodium azide (to a final concentration of 0.02% w/v; for prevention of bacterial growth). Before adjusting the volume (to 1 L), the pH of the solution is adjusted to 7.40. Sodium azide is not added if the buffer will be used for preparation of liposomes for *in vivo* studies.
6. Diluted PBS or phosphate buffer pH 7.40, for preparation of CF (or calcein) solution. This buffer is prepared by diluting PBS buffer 10 times with d.d. H<sub>2</sub>O (*see item 5*). This buffer is used for preparation of CF (or calcein) solution, prepared for encapsulation in DRV liposomes.
7. Solution of 5,(6)-carboxyfluorescein [CF] (Eastman Kodak, USA) or calcein (Sigma-Aldrich, Athens, Greece). The solid is dissolved in phosphate buffer pH 7.40 to make a solution of 100 mM, which can be diluted with the same buffer if lower concentration (17 mM) should be used (*see Note 3*).

8. Triton X-100 (Sigma-Aldrich, Athens, Greece). Triton is used as a 10% v/v solution in the liposome preparation buffer (see below). Usually 1 L solution is prepared, stored at room temperature, and used for up to 3 months.
9.  $\beta$ -Cyclodextrin [ $\beta$ -CD] (Sigma-Aldrich, Athens GR).
10. Hydropropyl-  $\beta$ -cyclodextrin (HP  $\beta$ -CD) (Sigma-Aldrich, Athens GR).
11. Prednisolone (PR) (99%) pure, (Sigma-Aldrich, Athens GR).
12. Sephadex G-50 (medium) (Phase Separations, Pharmacia, Sweden). The powder is dispersed in PBS buffer for swelling, and the dispersion is subsequently degassed under vacuum. Gel chromatography columns are packed and used for DRV liposome separation from non-encapsulated molecules (as described in detail below).
13. Stewart assay reagent (for determination of phospholipid concentration): For preparation dissolve 27.03 g of  $\text{FeCl}_3 \times 6\text{H}_2\text{O}$  and 30.4 g of  $\text{NH}_4\text{SCN}$  in 1 L of d.d.  $\text{H}_2\text{O}$ . The reagent is stored in dark glass bottles at room temperature and used for up to 1 month.

## **2.2 Protein (or Peptide) and/or Particulate Encapsulating DRV**

1. Egg phosphatidylcholine (PC), phosphatidic acid (PA), phosphatidylglycerol (PG), phosphatidylserine (PS), DSPC, and Chol (for lipid sources and storage, see Subheading 2.1 (1–3), and for purity testing, see Note 2).
2. Triolein (TO) (Sigma-Aldrich, Athens, Greece).
3. Stearylamine (SA) (Sigma-Aldrich, Athens, Greece).
4. 1,2-Bis(hexadecylcycloxy)-3-trimethylaminopropane (BisHOP) (Sigma-Aldrich, Athens, Greece).
5. *N*-[1-(2,3-Dioleyloxy) propyl]-*N,N,N*-triethylammonium (DOTMA) (Avanti Polar Lipids, USA).
6. 1,2-Dioleyloxy-3-(trimethylammonium propane) (DOTAP) (Avanti Polar Lipids, USA).
7. 3b-(*N,N*-Dimethylaminoethane)carbamylcholesterol (DC-Chol) (Sigma-Aldrich, Athens, Greece).
8. Sepharose CL-4B (Phase Separations, Pharmacia, Sweden).
9. Polyethylene glycol 6000 (PEG 6000) (Sigma-Aldrich, Athens, Greece).

## **2.3 Entrapment of Large Particles, Viruses, or Bacteria into Giant Liposomes**

1. *Solution 1*: PC or DSPC, CHOL, PG, and TO (4:4:2:1 molar ratio, 9 mmol total lipid) in 1.0 mL  $\text{CHCl}_3$ .
2. *Solution 2*: The same lipids as in solution 1, but dissolved in 0.5 mL diethyl ether.
3. *Solutions 3 and 4*: Sucrose (Sigma-Aldrich, Athens, Greece): 0.15 M (Sol. 3) and 0.2 M (Sol. 4) in  $\text{H}_2\text{O}$ .

4. *Solution 5:* Glucose 5% (w/v) in H<sub>2</sub>O.
5. *Solution 6:* Sodium phosphate buffer (PBS) 0.1 M, pH 7.0, containing 0.9% NaCl.
6. *Solution 7:* Discontinuous sucrose gradient prepared by the use of two solutions containing 59.7 and 117.0 g of sucrose, respectively, per 100 mL H<sub>2</sub>O, in swing-out bucket centrifuge tubes.

### 3 Methods

In this section of the chapter, the general methodology used to encapsulate any type of material (mostly applying for hydrophilic drugs, peptides or proteins) will be described in detail. After this, special considerations and methodologies that should be applied for encapsulation of other types of molecules or for special types of applications (such as liposomal vaccines) will be given in detail.

**3.1 General Methodology for DRV Preparation:**  
**Preparation of Hydrophilic Compound or Small Molecule Encapsulating DRV Liposomes [1–3, 16, 18, 19, 25, 28, 31–36]**

**3.1.1 Preparation of CF-Encapsulating DRV's with High Entrapment Yield [1]**

**Thin Film Formation (Step 1)**

For the preparation of DRV liposomes, empty (*see Note 4*) SUV liposomes dispersed in d.d. H<sub>2</sub>O with the appropriate lipid composition and concentration are initially prepared (*see Note 5*). SUV liposomes can be formulated by several techniques, depending on the specific lipid composition and concentration required, the most convenient and easiest to use being (i) probe sonication in one step (*see Note 6*) and (ii) size reduction of MLV liposomes (most applied technique).

1. Weight the required lipid or lipids and Chol (if included in the liposome composition) quantities for the preparation of 1 mL of liposomes and place them in a 50 mL round-bottomed flask; 16.5 µmole of lipid (PC) or 12.5 mg is the amount per each mL of aqueous phase that results in the highest encapsulation yield for CF [1].
2. Dissolve the lipids in 1 mL (or more if needed) of a CHCl<sub>3</sub>/CH<sub>3</sub>OH (2:1 v/v) mixture. Alternatively place the appropriate volumes of pre-formed lipid solutions (*see Note 7*) in the flask and mix.
3. Connect the flask to a rotor evaporator in order to evaporate the organic solvent under vacuum, until total evaporation and formation of a thin lipid film on the sides of the flask (*see Note 8*).
4. Flush the thin film with N<sub>2</sub> for at least 10 min and connect the flask (overnight) to a vacuum pump or lyophilizer for total removal of any traces of organic solvents.
5. If desired the thin films can be sealed with parafilm under N<sub>2</sub> and stored at –20 °C for a few days, until being used.

- Hydration of Thin Film: MLV Formation (Step 2)**
1. Add 1 mL of d.d. H<sub>2</sub>O in the flask that contains the thin film.
  2. If lipids with high T<sub>c</sub> are used as DPPC, DSPC, etc., then the H<sub>2</sub>O has to be preheated above the lipid T<sub>c</sub>, and the hydration procedure should be performed at that temperature, in a heated water bath.
  3. Hydrate the lipid film by repeated vortex agitation.
  4. Add glass beads in the flask if needed, in order to facilitate the removal of the lipid from the flask. (In the current case in which plain PC is used the lipid film, hydration should be done very easily at room temperature).
- SUV Formation (Step 3)**
1. Place the MLV suspension produced by the method described above, in a small test tube for vesicle size reduction by probe sonication.
  2. Subject the suspension to high intensity sonication using a Vibra Cell Probe Sonicator (Sonics and Materials, UK) or other.
  3. If a small volume of liposomes are to be prepared (1–3 mL), a tapered micro tip is used, but for larger volumes the conventional tip should be used.
  4. Apply sonication (*see Note 9*) for two 10 min cycles, at least, or until the vesicle dispersion becomes completely transparent.
  5. Following sonication, leave the SUV suspensions for 1–2 h at a temperature higher than the T<sub>c</sub> of the lipid used in each case, in order to anneal any structural defects of the vesicles.
  6. Remove the titanium fragments (extracted from the probe) and any remaining multilamellar vesicles or liposomal aggregates from the SUV dispersion, by centrifugation at 10,000 rpm for 15 min.
- Preparation of SUV–Solute Mixture (Step 4)**
1. Mix the SUV suspension with a solution of the solute that is to be entrapped in the DRVs.
  2. Usually 1 mL of SUV suspension is mixed with 1 mL of the solute solution (or 2 mL + 2 mL, etc.).
  3. CF-encapsulating DRV's 1 mL of the empty SUVs are mixed with 1 mL of a 17 mM CF solution in diluted PBS (*see Subheading 2.1*).
  4. The characteristics of the solute solution are important for the final encapsulation yield; especially the concentration and ionic strength (*see Note 10*). Some examples of entrapment yields of some substances in DRVs and the conditions applying in each case are presented in Table 2.

**Table 2**  
**Examples of encapsulation efficiencies of DRV liposomes**

| Solute entrapped <sup>a</sup>                          | Lipid composition/lipid concentration <sup>b</sup>                                      | Special consideration   | Yield  | EE (%)   | Ref. |
|--|---|---|--|--|------|
| CF   | PC/Chol (1:1) /16.5<br>PC / 16.5  | Solute conc.  |  |  |      |
|  |   | 17 mM<br>17 mM  |  | 40.2<br>54.0   | [1]  |
| Glucose  | PC/Chol(1:1) /16.5  | 50 mM   |  | 40.0   |      |
| Albumin  | PC/Chol(1:1) /16.5  | 10 mg/mL  |  | 40.6   |      |
|  |   | Solute type/vol.  | Amount entrapped <sup>a</sup>  |  |      |
| PRE<br>(plain = PL<br>or as<br>HP $\beta$ -CD complex) | PC / 6.5<br>PC/Chol (2:1) / 6.5<br>PC/Chol (2:1) / 6.5<br>PC /6.5<br>PC/Chol (2:1) /6.5 | PL (1 mg in lipid phase)<br>PL (1 mg in lipid phase)<br>HP $\beta$ -CD/PRE (6:1) / 2 mL<br>HP $\beta$ -CD/PRE (2:1) / 2 mL<br>HP $\beta$ -CD/PRE (2:1) / 2 mL | 1.3 mg<br>1.5 mg<br><sup>c</sup> 1.3 mg<br><sup>d</sup> 1.7 mg<br><sup>d</sup> 3.8 mg<br><sup>d</sup> 3.7 mg | 1.3 mg<br>1.5 mg<br><sup>c</sup> 1.3 mg<br><sup>d</sup> 1.7 mg<br><sup>d</sup> 3.8 mg<br><sup>d</sup> 3.7 mg | [16] |
| Penicillin G<br>(5 mg)                                 | PC/Chol (1: 1) /16.5  | Sucrose/lipid (mass ratio)  | EE (%)/vesicle diameter (nm)   | 30.5 / 213 nm<br>19.5 / 195 nm<br>15.5 / 198 nm  | [2]  |
| Riboflavin (1 mg)                                      | PC/Chol (1: 1) /16.5  | 1<br>3<br>5   | 78 / 591 nm<br>47.8 / 168 nm<br>34.8 / 145 nm  |  |      |

(continued)

**Table 2**  
(continued)

| Solute entrapped <sup>a</sup> | Lipid composition/lipid concentration <sup>b</sup>   | Special consideration | Yield                | Ref.             |
|-------------------------------|--|-----------------------|----------------------|------------------|
| Tetanus toxoid                | PC/Chol (1:1) /16.5  | Solute amount<br>2 mg | EE (%)<br>40-82      | [39, 49, 53, 65] |
| BSA                           |  | 2 mg                  | 40-45%               | [38, 39, 53, 65] |
| Plasmid DNA                   | PC/DOPE (1:0.5)<br>PC/DOPE /PS (1.00:0.50:0.25) / 16.5<br>PC/DOPE /SA (1.00:0.50:0.25) /16.5 | 10-500 µg             | 44.2<br>57.3<br>74.8 | [53, 65]         |

<sup>a</sup>Or incorporated

<sup>b</sup>µm total lipid /mL (of final liposome suspension)

<sup>c</sup>Diluted to 3 mL before freeze-drying

<sup>d</sup>Diluted to 3 mL before freeze-drying

**Freeze-Drying (Step 5)**  
*(See Note 11)*

1. Place the mixture in a test tube or a 20 mL screw capped bottle or round-bottomed flask for freeze-drying.
2. Freeze the empty SUV–solute mixture by swirling the container in the cold liquid containing Dewar flask (taking care not to freeze your fingertips) in order to form a thin layer of frozen liquid on the sides of the container. For freezing, it is advisable to use liquid N<sub>2</sub> or crushed dry ice in acetone (placed in a Dewar flask), whatever is available.
3. If the solute is not sensitive to a slow freezing process, the mixture can also be frozen by placing in a freezer for the time period required to achieve complete freezing (depending on the volume and salt content of a sample and the thickness of the layer in the container, this may need from a few hours to overnight freezing [usually most convenient]).
4. Connect the sample to a freeze-drier (as a Labconco laboratory lyophilizer) and dry under vacuum (vacuum level below 5 Pa).

**Rehydration or  
 Reconstitution: DRV  
 Formation (Step 6)**

1. Add 100 µL of d.d. H<sub>2</sub>O (if applying, this should be pre-heated above the lipid T<sub>c</sub>), and rehydrate the mixture by vortex agitation, taking care to hydrate the full quantity of the lyophilized powder.
2. It is very important and actually determines the encapsulation yield of the DRVs produced to use the smallest possible volume of d.d. H<sub>2</sub>O for first step of rehydration of the dried liposome–solute mixture. The typical volume added is 1/10 of the solute (solution) volume, in the current case 100µL (solutions of 1 mL).
3. After total hydration, leave the mixture to stand for 30 min at room temperature (or higher than the lipid T<sub>c</sub>).
4. Replace the remaining volume (900 µL) by adding PBS buffer, and vigorously vortex the mixture. The buffer used should have a tenfold greater osmolarity than the initial solute concentration.
5. In some cases, it is advisable to repeat the first step of rehydration (addition of small volume of water, vortex, annealing) before the final volume adjustment.
6. Keep the suspension above T<sub>c</sub> for 30 min.

It is important to understand that when the lyophilized material is hydrated with a tenth of the original solute volume, this results in a tenfold increase in the overall concentration of the solute. And since the liposomes formed are osmotically active, their exposure to hypotonic solutions will result in material loss. This is the reason why a buffer with at least tenfold greater osmolarity of the solute solution should be used (*see Note 10*).

**DRV Separation from Non-entrapped Solutes (Step 7)**

(In order to use the DRV liposomes, and/or measure the entrainment or encapsulation efficiency (or yield), they should first be separated or purified from not entrapped solute. Depending on the MW of the entrapped solute and on the final size of the DRV liposomes, this can be done by centrifugation or size exclusion chromatography of ultrafiltration).

For separation of the non-encapsulated CF (or calcein) from the DRVs on Sephadex G-50 chromatography columns (*see Note 12*) eluted with PBS, pH 7.40, the following steps are used:

1. Pre-saturate the column with lipids by eluting a liposome sample through the column, in order to finally have lipid recovery >95%.
2. For lipid recovery calculation, measure the lipid concentration in the liposome sample loaded on the column, and the lipid concentration in the liposomal fractions eluted, by a colorimetric assay for phospholipids, such as the Stewart assay (described below) [68], and calculate the percent of the loaded lipid which is finally eluted from the column.
3. After assuring that the column has been saturated, load the liposome sample on the column, and separate the liposomes from the non-liposome encapsulated molecules.
4. Calculate the amount of CF (or calcein) entrapped in a given volume of vesicles and the amount of lipid in the same volume of the DRV dispersion, as described below.

**Determination of Entrapped CF (or Calcein)**

1. Disrupt the DRVs with a 10% v/v Triton X-100 solution. For this, mix an appropriate volume of the Triton solution in a sample of the DRV dispersion, so that the final concentration of Triton X-100 is at least 1% v/v.
2. Vigorously mix the dispersion by vortex for at least 2 min (*see Note 13*).
3. After total disruption of the vesicles, measure the fluorescence intensity (FI) of the sample at 37 °C, at EM – 470 nm and EX – 520 nm and slit band widths 10-10.
4. Finally, calculate the amount of CF (or calcein) entrapped in the DRVs with the help of an appropriate calibration curve of the dye.

**Determination of Lipid Concentration**

The phospholipid content of the liposomes is measured by the Stewart assay [68], a colorimetric technique that is widely used for phospholipid content determination. For this:

1. Mix a sample from the liposome dispersion (20–50 µL, depending on the lipid concentration) with 2 mL Stewart reagent (ammonium ferrothiocyanate 0.1 M) and 2 mL chloroform, in a 2.5 × 10 cm (or higher) test tube.

2. Vortex the mixture vigorously for at least 3 min, in order to extract the complex formed between phospholipid and Stewart reagent in the chloroform phase.
3. Centrifuge the two-phase mixture at 1000 rpm for 5 min, in order to separate the two phases.
4. Remove the top (red) aqueous phase from the test tube by aspiration.
5. Take the chloroform phase out and measure its OD at 485 nm.
6. Finally calculate the lipid concentration of the sample or samples by comparison of the measured OD-485, with a standard curve (prepared from known concentrations of PC) (*see Note 14*).

*3.1.2 Preparation of Amphiphilic/Lipophilic Drug Incorporating or Encapsulating DRVs (as Reported for PRE [16], Curcumin [22], Ibuprofen [26], and Hypericin [29])*

For the preparation of amphiphilic or lipophilic drug incorporating DRVs (this may be needed for comparison between plain drug containing DRVs and CD–drug complex entrapping DRVs), the general DRV technique (as described in Subheading 3.1.1) should be modified as follows:

1. *In Step 1:* If the aqueous solubility of the drug is low, it is advisable to add the drug at this stage, as a concentrated solution in MeOH or CHCl<sub>3</sub>. In the case of prednisolone (PRE), 100 µL of a 10,000 ppm solution of PRE in MeOH are mixed in the lipid solution.
2. *In Step 2:* After hydration of the thin film (**step 2**), the MLV suspension prepared is filtered (Whatmman no. 5) to remove precipitated (non-incorporated in liposomes) drug.
3. *In Step 4:* 1 mL of the SUV liposomes is mixed with 1 mL of buffer (diluted phosphate buffer), and the mixture is freeze-dried overnight.
4. All following steps are the same with those presented in Subheading 3.1.1. Care has to be taken to use the appropriate buffers before freeze-drying and after the initial rehydration step.

*3.1.3 Preparation of Drug/CD Complex Encapsulating DRVs (as Reported in [16, 19, 22, 26, 29])*

Formation of Drug–CD Inclusion Complexes [69]

As mentioned in the introduction part (Subheading 1.1), amphiphilic or lipophilic drugs can be encapsulated in the aqueous compartments of DRV in the form of soluble inclusion complexes with CD molecules. Thereby, a required initial step of this modified DRV technique is the formation of the CD–drug inclusion complex.

1. Mix drug, as example prednisolone PRE (2 mg) is used, with 1 mL of d.d. H<sub>2</sub>O containing 185 mg β-CD or 50 mg HPβ-CD or 16.7 mg HPβ-CD, and place in a screw capped

test tube or bottle. Higher amount of complexes can be formed by increasing the compound amounts proportionally.

2. Stir the mixtures for 3 days at 20 °C (this can be done by placing the screw capped container on a tumbling or circular mixing device). Water-soluble inclusion complexes are formed.
3. Centrifuge the milky solution formed with  $\beta$ -CD at 51,000 $\times g$  for 2 h, or filter the almost clear (or clear) solutions formed with HP $\beta$ -CD through polycarbonate filters (0.22 mm, Millipore).
4. Calculate the amount of cyclodextrin-solubilized drug spectrophotometrically, by measuring its absorption at 256 nm and constructing an appropriate calibration curve, from solutions of known drug concentration.
5. Calculate the final cyclodextrin-to-drug molar ratio by taking into account the initial amount of CD added and the final amount of drug measured.

The molar ratio of CD/drug (in this case PRE) plays a significant role in the final vesicle encapsulation efficiency. When an initial HP $\beta$ -CD–PRE molar ratio of 2:1 is used for complex preparation, it is calculated that all the drug is in the complex, giving thus a final HP  $\beta$ -CD–PR complex with a CD/PRE molar ratio of 2:1.

*Other methods can be used for the formation of drug/CD complexes*, as the co-precipitation method used in the case of curcumin (see reference [22]).

#### Preparation of DRVs

1. Mix 1 mL of empty SUV with 1 mL of the CD–drug complex (as in **step 4**, of Subheading 3.1.1).
2. Dilute the mixture (by adding an appropriate volume of d.d. H<sub>2</sub>O), before freeze-drying (*see Note 15*).
3. Freeze-dry the mixture and rehydrate as described in detail in Subheading 3.1.1.
4. In this case, again, care has to be taken to adjust the osmolarity of the mixture before freeze-drying and to use the appropriate buffer for dilution of the rehydrated DRVs, making sure that the CD concentration in the solute solution is considered.
5. Separate the non-entrapped inclusion complex and/or free drug from the vesicles by gel-exclusion chromatography.
6. Measure the lipid concentration of the produced liposomes by an appropriate technique (as the Stewart assay presented above).
7. Measure the concentration of encapsulated drug in the DRVs, after dissolving DRV samples in MeOH or 2-propanol and constructing an appropriate calibration curve.

### **3.1.4 Preparation of Multicomponent DRVs for Photolabile Drugs**

The preparation of DRV multicomponent systems of photolabile drugs is achieved by a similar procedure as the one described above (Subheading 3.1.3) [18]. For this:

1. The lipid-soluble light absorbers are added in the lipid phase during thin lipid film preparation (**step 1** of procedure described in Subheading 3.1.1).
2. Aqueous soluble light absorbers are mixed together with the CD–drug complex and the empty SUVs (**step 4** of procedure described in Subheading 3.1.1).

### **3.1.5 Preparation of DRV Liposomes with Controlled Entrapment Yield and Vesicle Size (as Reported in 2)**

Since the addition of cryoprotectants during the freeze-drying step (**step 5** in procedure of Subheading 3.1.1) may reduce liposome disruption/fusion and result in decreased encapsulation yield and mean vesicle size of the DRVs produced, it has been demonstrated that by adding specific amounts of sugars in the SUV/solute mixtures prior to freeze-drying and by controlling their final concentration therein, the former two DRV characteristics can be controlled accordingly. For this:

1. Add the specified amount of sucrose in the mixture of empty SUV (with mean diameters between 60 and 80 nm) in **step 4** of the general DRV preparation procedure (Subheading 3.1.1), in order to obtain a final sugar-to-lipid mass ratio between 1 and 5 (or else 1–5 mg of sucrose per each mg of phospholipid).
2. Adjust the mixture sugar molarity to a predetermined value by the addition of the appropriate amount of d.d. H<sub>2</sub>O (sugar molarity values between 30 and 50 mM were found to give good vesicle encapsulation and considerably small vesicle size, when the sugar/lipid mass ratio was set at 3 [2]).
3. Freeze-dry the mixtures overnight. After this, all other steps of the procedure are similar to those described above (in Subheading 3.1.1).

After separation of the DRVs from the non-encapsulated solute molecules and measurement of the entrapment, it is found that as sugar/lipid mass ratio increases, vesicle size decreases together with the encapsulation yield. Some of the solutes studied and the results obtained [2] are presented in Table 2.

## **3.2 Preparation of Protein (or Peptide) and DNA Vaccines (as Reported in [1, 47, 63, 70])**

This procedure is similar to the general procedure described in Subheading 3.1.1, for DRV preparation. A few special considerations—suggestions are mentioned below.

**3.2.1 Lipid Compositions  
for Protein and DNA  
Vaccines**

1. Phospholipid (32 mmol) and Chol (32 mmol).
2. Negatively charged liposomes containing 3.2 mmol of PA, PS, or PG.
3. Positively charged liposomes containing 3.2–8 mmol of SA, BisHOP, DOTMA, DOTAP, or DC-CHOL.
4. Depending on the amount of vesicle surface charge required, greater quantities of charged lipids can be added.
5. *In all cases*, the appropriate quantities of the lipids are dissolved in 2–5 mL of chloroform during **step 1** of the general procedure for DRV preparation (see procedure Subheading 3.1.1).

**3.2.2 Liposome  
Preparation Procedure:  
Vaccine Material Addition**

If the sonication step (**step 3** in Subheading 3.1.1) is not detrimental to the vaccine material, the vaccine solution may be added instead of H<sub>2</sub>O during the hydration of the thin film (general DRV preparation procedure—**step 2**). For this:

1. Dissolve (up to) 10 mg of the water-soluble vaccine in 2 mL d.d. H<sub>2</sub>O or 10 mM sodium phosphate buffer, pH 7.2 [phosphate buffer (PB)].
2. The buffer used can be varied with respect to composition, pH, and molarity, as long as this does not interfere with liposome formation or entrapment yield (*see Note 10*).
3. The amount of vaccine material added can be increased proportionally to the total amount of lipid.
4. Apply sonication and let the produced SUVs to stand for annealing (as described in Subheading 3.1.1).
5. Mix the SUV suspension with water (if the vaccine was added in **step 2** of this procedure) or with the vaccine solution (prepared as described above).
6. For the rehydration step (**step 6** in Subheading 3.1.1), it is advised to use 0.1 mL of H<sub>2</sub>O per 32 mmol of phospholipid (but enough H<sub>2</sub>O to ensure complete dissolution of the powder) and keep the sample above T<sub>c</sub> for 30 min. Then repeat this step (add another 0.1 mL of water; vortex and keep for 30 min above T<sub>c</sub>) before bringing the DRV suspension to volume, with 0.8 mL PB (which is pre-warmed to a temperature above the lipid T<sub>c</sub>).
7. The sample is finally allowed to stand for extra 30 min above T<sub>c</sub>.

**3.2.3 Separation of DRVs  
from Non-entrapped  
(Vaccine) Material**

This is done by centrifugation:

1. Centrifuged the DRV suspension that contains entrapped and non-entrapped vaccine at 40,000*g* for 60 min (4 °C).

2. Resuspend the pellet obtained (vaccine containing DRVs) in H<sub>2</sub>O or PB and centrifuge again under the same conditions.
3. Repeat the above process once more for total removal of the remaining non-entrapped material.
4. Finally suspend the pellet in 2 mL H<sub>2</sub>O or PB.

#### *3.2.4 Vaccine Entrapment Yield Estimation*

1. The entrapment yield is calculated by measuring the vaccine in the suspended pellet and the combined supernatants.
2. The easiest way to monitor entrapment is by using a radiolabeled vaccine. If a radiolabel is not available or cannot be used, appropriate quantitative techniques should be employed.
3. To determine the vaccine by such techniques, a sample of the liposome suspension is mixed with Triton X-100 (up to 5% final concentration) or 2-propanol (1:1 volume ratio) in order to liberate the entrapped material.
4. If Triton X-100 or the solubilized liposomal lipids interfere with the assay of the material, lipids must be extracted using appropriate techniques.
5. Entrapment yields of this technique range between about 20% and 100%, depending on the amounts of lipid and vaccine used.
6. Highest values are achieved when solutes for entrapment bear a net charge that is opposite of that of the charged lipidic component of liposomes (*see Note 16*).

#### *3.2.5 Vaccine-Containing DRV Size Reduction*

If vaccine-containing DRV liposomes must be converted to smaller vesicles (down to about 100 nm z-average diameter), the following procedure is used:

1. Dilute the liposomal suspension obtained in **step 6** (of the general procedure described in Subheading [3.1.1](#)) prior to separation of the entrapped from the non-entrapped vaccine, to 10 mL with H<sub>2</sub>O.
2. Pass the dispersion for a specific number of full cycles through a Microfluidizer 110S (microfluidics), with the pressure gauge set at 60 PSI throughout the procedure to give a flow rate of 35 mL/min [39]. The number of cycles used depends on the vesicle size required and the sensitivity of the entrapped vaccine (e.g., plasmid DNA) [70].
3. The greater the number of cycles, the smaller the amount of drug retained by the vesicles [70] (*see Note 17*).
4. The microfluidized sample volume (appr. 10 mL) may be reduced, if needed, by placing the sample in dialysis tubing and then in a flat container filled with PEG 6000. Removal of excess H<sub>2</sub>O from the tubing is relatively rapid (within

30–60 min), and it is therefore essential that the sample be inspected regularly.

5. When the required volume has been reached, the sample is treated for the separation of entrapped from non-entrapped vaccine, by molecular sieve chromatography using a Sepharose CL-4B column, in which case vaccine-containing liposomes are eluted at the end of the void volume (*see Note 12*).
6. Minimum vesicle diameters obtained after ten cycles of microfluidization are about 100–160 nm, depending on whether microfluidization was carried out in H<sub>2</sub>O or PB, using unwashed or washed liposomes.
7. Alternatively to microfluidization, downsizing of the vaccine-entrapping DRV liposomes may be carried out by extrusion method, as recently reported [47].

### **3.3 Preparation of Giant Liposome DRVs that Entrap Large Particles, Viruses, or Bacteria (as Described in [55, 56, 65])**

#### **3.3.1 Giant Liposome Preparation**

1. Mix 1 mL of *solution 3* with 1 mL of *solution 1* by vortex agitation. Then mix (vortex for 15 s) the resulting water-in-chloroform emulsion with a similar mixture composed of *solution 2* and *solution 4* (2.5 mL).
2. Place the water-in-oil-in-water double emulsion formed in a 250 mL conical flask.
3. Place the flask under a stream of nitrogen (N<sub>2</sub>) and in a shaking incubator (at 37 °C) under mild agitation, in order to evaporate the organic solvents. This leads to the generation of (sucrose-containing) giant liposomes.
4. Wash the giant liposomes by centrifugation (in a typical bench centrifuge at 1000*g*) for 5 min over *solution 5*.
5. Resuspend the liposomal pellet in 1 mL PBS.
6. Mix the suspended pellet with 1 mL of a particulate matter suspension (could be killed or live *B. subtilis* spores; killed bacille Calmette–Guerin (BCG) bacteria, etc.), and freeze-dry the mixture under vacuum, overnight.
7. Rehydrate the freeze-dried material, with 0.1 mL H<sub>2</sub>O at 20 °C (*see Note 18*), by vigorous mixing. Let the suspension at peace for 30 min above the lipid T<sub>c</sub>.
8. Repeat the previous step with addition of 0.1 mL PBS.
9. Finally bring the sample to volume by adding 0.8 mL PBS, 30 min later (1 mL total suspension volume).

As mentioned above, *small particles or nanoparticles, such as USPIOs or IONPs*, can be successfully encapsulated in liposomes, using the classical DRV technique (as described above in Subheading 3.1.1). For more details, see [57, 58].

### 3.3.2 Giant DRV Liposome Separation from Non-entrapped Particulates

Entrapped particulate material is separated from non-entrapped material (bacteria spores, etc.) by sucrose gradient centrifugation. For this:

1. Place 1 mL of the suspension which contains entrapped and non-entrapped particulates, on top of a sucrose gradient (see *solution 7* in Subheading 2.3).
2. Centrifuge for 2 h at 90,000*g*, using a swing-out bucket rotor.
3. Following centrifugation, continuously take out 1 mL fractions from the top of the gradient, and assay each fraction for particulate content (it is convenient to use radiolabeled (e.g.,  $^{125}\text{I}$ -labeled) particulates).
4. The non-entrapped particulates are recovered at the bottom fractions of the gradient, whereas entrapped material is recovered mostly in the top seven fractions of the gradient where liposomes remain [55].
5. Finally pool the fractions that contain the entrapped spores or bacteria and dialyze them exhaustively against PBS, after placing them in a dialysis tubing (MW-cutoff 10,000), until all sucrose has been eliminated.
6. Centrifuge the dialyzed material and resuspend the liposomal pellet in 1 mL PBS for further use.

Typical values of *B. subtilis* or BCG entrapment range between 21 and 27% of the material used [55, 56].

---

## 4 Notes

1. The abbreviation DRV stands for *dehydration–rehydration vesicles* as initially named by the inventors of this liposome preparation technique [1, 3]. However, one will find several other explanations in the relevant literature as *dried (or dehydrated) rehydrated vesicles* and *dried reconstituted vesicles*, which are actually the same type of liposomes.
2. The 99% purity of the lipids can be verified by thin layer chromatography on silicic acid precoated plates (Merck, Germany), using a  $\text{CHCl}_3/\text{CH}_3\text{OH}/\text{H}_2\text{O}$  65:25:4 v/v/v mixture for plate development, and iodine staining for visualization. Pure lipids give single spots.
3. Calcein (as well as CF) is not easily dissolved in buffer with pH 7.40. Therefore, the weighted solid is initially dissolved in NaOH (1 M) which is added dropwise until the full quantity is dissolved and subsequently the resulting solution is diluted with the appropriate volume of buffer (in order to achieve the required calcein concentration). The pH of the final solution

should be checked and re-adjusted if required, while care has to be taken so that calcein does not precipitate.

4. For the formation of DRV liposomes entrapping solutes that are not sensitive to the conditions used for MLV and/or SUV preparation, it is possible to prepare drug containing liposomes in the initial step of DRV formation. This is particularly important if amphiphilic/lipophilic or in general substances with low aqueous solubility are to be entrapped. However when there is interest to have a method that can be easily up-scaled for large batch manufacturing, this approach can be a problematic.
5. It has been reported that DRV liposomes with comparably high encapsulation efficiency (compared to plain MLVs) can be produced even by using MLV liposomes for the initial drying step [1]. Indeed a EE% of 21% for CF was reported when empty MLV liposomes were used (compared to 1.8% when plain MLV were formed using the same CF hydrating concentration), while a 30% EE% was reached when starting from SUV.
6. For “one-step” probe sonication (SUV formation), the lipid or lipids in solid form are placed in an appropriate test tube (with dimension that ensure proper placement on the probe) together with the hydration solution. The mixture is heated above the lipid transition temperature and subsequently probe sonicated. This method may not be applicable in some cases of lipids and when high lipid concentrations are used (>20 mg/mL).
7. The lipids could also be used in the form of solutions in CHCl<sub>3</sub>/CH<sub>3</sub>OH 2:1 v/v that can be initially prepared and stored at -80 °C. In this case the appropriate volume of lipid solution (or each lipid solutions; if several lipids are used in the form of organic solution) is (or are) used. If one-step probe sonication is used, the organic solvent is evaporated by a stream of N<sub>2</sub>, and the preparation proceeds as described above.
8. If the film has irregularities, it is advisable to re-dissolve in CHCl<sub>3</sub> (or other easily evaporated organic solvent depending on the solubility of the lipids) and evaporate the organic solvent again, until a nice and even thin film is formed.
9. For probe sonication, the probe tip (or tapered microtip) is immersed into the MLV or lipid dispersion by approximately 1.2–1.5 cm from the surface, taking care so that no part of the tip is in contact with the vial (a mirror is used to be sure). The vial is placed in an ice-cold water tank, to prevent overheating of the liposome dispersion during probe sonication. Alternatively a glycerol bath which has been pre-heated above the lipid transition temperature can be used in order to prevent overheating of the sample. A simple method for size reduction of

MLV liposomes if a probe sonicator is not available is by extrusion through stacked polycarbonate filters with appropriate pore dimensions. For this, the filters are placed on a double-syringe apparatus (several are commercially available), and the liposome dispersions are passed through the filters from the one syringe to the other several times (at least 10), until the vesicle dispersion size has been appropriately reduced. The system can be immersed in a heated water bath if lipids with high Tcs are used.

10. The solute solution concentration has been demonstrated to influence DRV encapsulation efficiency differently, depending on the solute. As an example although glucose and CF entrapment values were found to decrease with increasing solute solution concentration, the same was not found true for encapsulation of sodium chloride and potassium chloride [1]. For CF, best encapsulation yields in DRVs are demonstrated when a 17 mM solution in a tenfold dilution of an isotonic PBS buffer is used. The ionic strength of the buffer used to dissolve the solute added at this step should be at least 10 times less of that of the buffer used for DRV dilution after the hydration step (see below) in order to reduce material losses, due to osmotic activity of liposomes.
11. Although we do not have experience of this in our lab, it has been reported that similar encapsulation yields for DRVs may be obtained by drying down the SUV–solute mixture using other procedures, as drying non-frozen mixtures at 20 °C under vacuum or under a stream of N<sub>2</sub> (at 20 °C or 37 °C).
12. A column with dimensions 1 × 35 cm is sufficient to separate 1 mL of liposome or the DRV liposome dispersion. The column is pre-calibrated and at the same time saturated with a dispersion of empty liposomes mixed with a quantity of the encapsulated material (in each case). The void volume of such columns should be between 7 and 13 mL and the bed volume between 17 and 21 mL.
13. In some cases, especially when rigid liposomes that contain DSPC and Chol are used, the liposomes are difficult to disrupt by using 1% v/v final concentration of Triton X-100 detergent. Then the liposome mixture with Triton can be heated by rapidly immersing in boiling water (in which case care should be taken in order to perform the final measurement after the sample is cooled, in order to avoid mistakes). Another possibility is to use higher final concentration of detergent (in which case the extra dilution of the sample has to be taken into account during calculations).

14. The linear region for a calibration curve by the Stewart assay is between 10 and 100 µg of PC (DPPC; DSPC can also be used at this range).
15. This is a *very important step*, in order to avoid low encapsulation yields that may be caused by the presence of high CD concentrations in the sample (which as an oligosaccharide will act as a cryoprotectant). For PRE-CD complexes when the mixtures are diluted up to 10 mL final volume before the freeze-drying step, the final encapsulation of PRE is increased by 30% (Table 2) [16].
16. Part of the liposome-associated solute may have interacted with the liposomal surface during the entrapment procedure. Thereby, it is essential that actual entrapment of the solute (as opposed to surface-bound solute) is determined. In the case of DNA or proteins, this can be achieved by using deoxyribonuclease [70] and a proteinase [6], respectively, which will degrade the external material.
17. Microfluidization of the sample can also be carried out after removal of non-entrapped vaccine (after **step 7** of the general procedure in Subheading 3.1). However, drug retention in this case is reduced. It appears that the presence of non-entrapped drug during micro-fluidization diminishes solute leakage, probably by reducing the osmotic rupture of vesicles and/or the initial concentration gradient across the bilayer membranes [71].
18. It has been observed in this case that rehydration of liposomes which contain “high-melting” DSPC above Tc (50 °C) does not have a significant effect on the percentage entrapment of materials [56, 65].

## References

1. Kirby C, Gregoriadis G (1984) Dehydration-rehydration vesicles: a simple method for high yield drug entrapment in liposomes. *Biotechnology* 2:979–984
2. Zadi B, Gregoriadis G (2000) A novel method for high-yield entrapment of solutes into small liposomes. *J Liposome Res* 10:73–80
3. Antimisiaris SG (2017) Preparation of DRV liposomes. *Methods Mol Biol* 1522:23–47
4. Seltzer SE, Gregoriadis G, Dick R (1988) Evaluation of the dehydration-rehydration method for production of contrast-carrying liposomes. *Investig Radiol* 23:131–138
5. Cajal Y, Alsina MA, Busquets MA, Cabanes A, Reig F, Garcia-Anton JM (1992) Gentamicin encapsulation in liposomes: factors affecting the efficiency. *J Liposome Res* 2:11–22
6. Senior J, Gregoriadis G (1989) Dehydration-rehydration vesicle methodology facilitates a novel approach to antibody binding to liposomes. *Biochim Biophys Acta* 1003:58–62
7. Du Plessis J, Ramachandran C, Weiner N, Müller DG (1996) The influence of lipid composition and lamellarity of liposomes on the physical stability of liposomes upon storage. *Int J Pharm* 127:273–278
8. Casals E, Gallardo M, Estelrich J (1996) Factors influencing the encapsulation of thioguanine in DRV liposomes. *Int J Pharm* 143:171–177
9. Grant GJ, Barenholz Y, Piskoun B, Bansinath M, Turndorf H, Bolotin EM (2001) DRV liposomal bupivacaine:

- preparation, characterization, and in vivo evaluation in mice. *Pharm Res* 18:336–343
10. Anderson KE, Eliot LA, Stevenson BR, Rogers JA (2001) Formulation and evaluation of a folic acid receptor-targeted oral vancomycin liposomal dosage form. *Pharm Res* 18:316–322
  11. Kawano K, Takayama K, Nagai T, Maitani Y (2003) Preparation and pharmacokinetics of pirarubicin loaded dehydration-rehydration vesicles. *Int J Pharm* 252:73–79
  12. Kallinteri P, Fatouros D, Klepetsanis P, Antimisiaris SG (2004) Arsenic trioxide liposomes: encapsulation efficiency and in vitro stability. *J Liposome Res* 14:27–38
  13. Mugabe C, Azghani AO, Omri A (2006) Preparation and characterization of dehydration-rehydration vesicles loaded with aminoglycoside and macrolide antibiotics. *Int J Pharm* 307:244–250
  14. Koromila G, Michanetzis GPA, Missirlis YF, Antimisiaris SG (2006) Heparin incorporating liposomes as a delivery system of heparin from PET-covered metallic stents: effect on haemocompatibility. *Biomaterials* 27:2525–2533
  15. Hatzi P, Mourtas S, Klepetsanis PG, Antimisiaris SG (2007) Integrity of liposomes in presence of cyclodextrins: effect of liposome type and lipid composition. *Int J Pharm* 333:167–176
  16. Fatouros DG, Hatzidimitriou K, Antimisiaris SG (2001) Liposomes encapsulating prednisolone and prednisolone-cyclodextrin complexes: comparison of membrane integrity and drug release. *Eur J Pharm Sci* 13:287–296
  17. Manconi M, Isola R, Falchi AM, Sinico C, Fadda AM (2007) Intracellular distribution of fluorescent probes delivered by vesicles of different lipidic composition. *Coll Surf B Biointerf* 57:143–151
  18. Loukas YL, Jayasekera P, Gregoriadis G (1995) Novel liposome-based multicomponent systems for the protection of photolabile agents. *Int J Pharm* 117:85–94
  19. McCormack B, Gregoriadis G (1994) Drugs-in-cyclodextrins-in liposomes: a novel concept in drug delivery. *Int J Pharm* 112:249–258
  20. Kallinteri P, Antimisiaris SG, Karnabatidis D, Kalogeropoulou C, Tsota I, Siablis D (2002) Dexamethasone incorporating liposomes: an in vitro study of their applicability as a slow releasing delivery system of dexamethasone from covered metallic stents. *Biomaterials* 23: 4819–4826
  21. Zaru M, Mourtas S, Klepetsanis P, Fadda AM, Antimisiaris SG (2007) Liposomes for drug delivery to the lungs by nebulization. *Eur J Pharm Biopharm* 67:655–666
  22. Matloob AH, Mourtas S, Klepetsanis P, Antimisiaris SG (2014) Increasing the stability of curcumin in serum with liposomes or hybrid drug-in-cyclodextrin-in-liposome systems: a comparative study. *Int J Pharm* 476:108–115
  23. Atashbeyk DG, Khameneh B, Tafaghodi M, Fazly Bazzaz BS (2014) Eradication of methicillin-resistant *Staphylococcus aureus* infection by nanoliposomes loaded with gentamicin and oleic acid. *Pharm Biol* 52:1423–1428
  24. Malaekeh-Nikouei B, Golmohammadzadeh S, Salmani-Chamanabad S, Mosallaei N, Jamialahmadi K (2013) Preparation, characterization, and moisturizing effect of liposomes containing glucosamine and N-acetyl glucosamine. *J Cosm Dermatol* 12:96–102
  25. Patel A, Dhande R, Thakkar H (2021) Development of intravaginal rod insert bearing liposomal raloxifene hydrochloride and Leuprolide acetate as a potential carrier for uterine targeting. *J Pharm Pharmacol* 73(5):653–663
  26. Angelini G, Campestre C, Boncompagni S, Gasbarri C (2017) Liposomes entrapping β-cyclodextrin/ibuprofen inclusion complex: role of the host and the guest on the bilayer integrity and microviscosity. *Chem Phys Lipids* 209:61–65
  27. Nave M, Castro RE, Rodrigues CM, Casini A, Soveral G, Gaspar MM (2016) Nanoformulations of a potent copper-based aquaporin inhibitor with cytotoxic effect against cancer cells. *Nanomedicine (Lond)* 14:1817–1830
  28. Bandara HM, Herpin MJ, Kolacny D Jr, Harb A, Romanovicz D, Smyth HD (2016) Incorporation of farnesol significantly increases the efficacy of liposomal ciprofloxacin against *Pseudomonas aeruginosa* biofilms in vitro. *Mol Pharm* 13(8):2760–2770
  29. Plenagl N, Seitz BS, Duse L, Pinnapireddy SR, Jedelska J, Brüßler J, Bakowsky U (2019) Hypericin inclusion complexes encapsulated in liposomes for antimicrobial photodynamic therapy. *Int J Pharm* 570:118666
  30. Plenagl N, Duse L, Seitz BS, Goergen N, Pinnapireddy SR, Jedelska J, Brüßler J, Bakowsky U (2019) Photodynamic therapy - hypericin tetraether liposome conjugates and their anti-tumor and antiangiogenic activity. *Drug Deliv* 1:23–33
  31. Dias-Souza MV, Soares DL, Dos Santos VL (2017) Comparative study of free and liposome-entrapped chloramphenicol against biofilms of potentially pathogenic bacteria

- isolated from cooling towers. *Saudi Pharm J* 7: 999–1004
32. Trapani A, Mandracchia D, Tripodo G, Cometa S, Cellamare S, De Giglio E, Klepetsanis P, Antimisiaris SG (2018) Protection of dopamine towards autoxidation reaction by encapsulation into non-coated- or chitosan- or thiolated chitosan-coated-liposomes. *Colloids Surf B Biointerfaces* 170:11–19
  33. Lopalco A, Cutrignelli A, Denora N, Lopedota A, Franco M, Laquintana V (2018) Transferrin functionalized liposomes loading dopamine HCl: development and permeability studies across an in vitro model of human blood-brain barrier. *Nanomaterials (Basel)* 8(3):178
  34. Ferreira H, Silva R, Matamá T, Silva C, Gomes AC, Cavaco-Paulo AA (2016) Biologically active delivery material with dried-rehydrated vesicles containing the anti-inflammatory diclofenac for potential wound healing. *J Liposome Res* 26(4):269–275
  35. Solleti VS, Alhariri M, Halwani M, Omri A (2015) Antimicrobial properties of liposomal azithromycin for *Pseudomonas* infections in cystic fibrosis patients. *J Antimicrob Chemother* 70(3):784–796
  36. Joseph RR, Tan DWN, Ramon MRM, Natarajan JV, Agrawal R, Wong TT, Venkatraman SS (2017) Characterization of liposomal carriers for the trans-scleral transport of Ranibizumab. *Sci Rep* 7(1):16803
  37. Ramos GS, Vallejos VMR, Ladeira MS, Reis PG, Souza DM, Machado YA, Ladeira LO, Pinheiro MBV, Melo MN, Fujiwara RT, Frézard F (2021) Antileishmanial activity of fullerol and its liposomal formulation in experimental models of visceral leishmaniasis. *Biomed Pharmacother* 134:111120
  38. Gregoriades G, Panagiotidi C (1989) Immunoadjuvant action of liposomes: comparison with other adjuvants. *Immunol Lett* 20:237–240
  39. Skalko N, Bouwstra J, Spies F, Gregoriadis G (1996) The effect of microfluidization of protein-coated liposomes on protein distribution on the surface of generated small vesicles. *Biochim Biophys Acta* 1301:249–254
  40. Rodriguez-Nogales JM, Pérez-Mateos M, Bustó MD (2004) Application of experimental design to the formulation of glucose oxidase encapsulation by liposomes. *J Chem Technol Biotechnol* 79:700–705
  41. García-Santana MA, Duconge J, Sarmiento ME, Lanio-Ruiz ME, Becquer MA, Izquierdo L, Acosta-Domínguez A (2006) Biodistribution of liposome-entrapped human gamma-globulin. *Biopharm Drug Disp* 27: 275–283
  42. Ntimenou V, Mourtas S, Christodoulakis EV, Tsilimbaris M, Antimisiaris SG (2006) Stability of protein-encapsulating DRV liposomes after freeze-drying: a study with BSA and t-PA. *J Liposome Res* 16:403–416
  43. Badiie A, Jaafari MR, Khamesipour A (2007) Leishmania major: immune response in BALB/c mice immunized with stress-inducible protein 1 encapsulated in liposomes. *Exp Parasitol* 115:127–134
  44. Bhowmick S, Mazumdar T, Sinha R, Ali N (2010) Comparison of liposome based antigen delivery systems for protection against Leishmania donovani. *J Control Release* 141:199–207
  45. Ariaee FM, Tafaghod M (2012) Mucosal adjuvant potential of Quillaja saponins and cross-linked dextran microspheres, co-administered with liposomes encapsulated with tetanus toxoid. *Iranian J Pharm Res* 11: 723–732
  46. Garten M, Aimon S, Bassereau P, Toombes GE (2015) Reconstitution of a transmembrane protein, the voltage-gated ion channel, KvAP, into giant unilamellar vesicles for microscopy and patch clamp studies. *J Vis Exp* 95:52281
  47. Heuts J, Varypataki EM, van der Maaden K, Romeijn S, Drijfhout JW, van Schelting AT, Ossendorp F, Jiskoot W (2018) Cationic liposomes: a flexible vaccine delivery system for physicochemically diverse antigenic peptides. *Pharm Res* 35(11):207
  48. Eckstein M, Barenholz Y, Bar LK, Segal E (1997) Liposomes containing *Candida albicans* ribosomes as a prophylactic vaccine against disseminated candidiasis in mice. *Vaccine* 15: 220–224
  49. Perrie Y, Frederik PM, Gregoriadis G (2001) Liposome-mediated DNA vaccination: the effect of vesicle composition. *Vaccine* 19: 3301–3310
  50. Perrie Y, Barralet JE, McNeil S, Vangala A (2004) Surfactant vesicle-mediated delivery of DNA vaccines via the subcutaneous route. *Int J Pharm* 284:31–41
  51. Pupo E, Padrón A, Santana E, Sotolongo J, Quintana D, Dueñas S, Duarte C, de la Rosa MC, Hardy E (2005) Preparation of plasmid DNA-containing liposomes using a high-pressure homogenization-extrusion technique. *J Control Release* 104:379–396
  52. Jaafari MR, Badiie A, Khamesipour A, Samiei A, Soroush D, Kheiri MT, Barkhordari F, McMaster WR, Mahboudi F

- (2007) The role of CpG ODN in enhancement of immune response and protection in BALB/c mice immunized with recombinant major surface glycoprotein of Leishmania (rgp63) encapsulated in cationic liposome. *Vaccine* 25: 6107–6117
53. Maitani Y, Aso Y, Yamada A, Yoshioka S (2008) Effect of sugars on storage stability of lyophilized liposome/DNA complexes with high transfection efficiency. *Int J Pharm* 356:69–75
54. Bayyurt B, Gürsel I (2013) Inflammasome induction and immunostimulatory effects of CpG-ODN loaded liposomes containing DC-cholesterol. *Turk J Immunol* 2:21–28
55. Antimisiaris SG, Jaysekera P, Gregoriadis G (1993) Liposomes as vaccine carriers. Incorporation of soluble and particulate antigens in giant vesicles. *J Immun Methods* 166:271–280
56. Gurcel I, Antimisiaris SG, Jaysekera P, Gregoriadis G (1995) Liposomes in biomedical applications (Shek, P., Ed.), pp. 35–50, Harwood Academic, Chur
57. Skouras A, Mourtas S, Markoutsa E, De Goltstein M-C, Catoen S, Antimisiaris SG (2011) Magnetoliposomes with high USPIO entrapping efficiency, stability and magnetic properties. *Nanomedicine* 7:572–579
58. Cruz N, Pinho JO, Soveral G, Ascensão L, Matela N, Reis C, Gaspar MMA (2020) Novel hybrid nanosystem integrating cytotoxic and magnetic properties as a tool to potentiate melanoma therapy. *Nanomaterials* (Basel) 10(4):693
59. Marazioti A, Papadia K, Kannavou M, Spella M, Basta A, de Lastic AL et al (2019) Cellular vesicles: new insights in engineering methods, interaction with cells and potential for brain targeting. *J Pharmacol Exp Ther* 370(3):772–785
60. Kannavou M, Marazioti A, Stathopoulos GT, Antimisiaris SG (2021) Engineered versus hybrid cellular vesicles as efficient drug delivery systems: a comparative study with brain targeted vesicles. *Drug Deliv Transl Res* 11(2): 547–565
61. Natsaridis E, Gkartziou F, Mourtas S, Stuart MCA, Kolonitsiou F, Klepetsanis P, Spiliopoulou I, Antimisiaris SG (2022) Moxifloxacin liposomes: effect of liposome preparation method on physicochemical properties and antimicrobial activity against *Staphylococcus epidermidis*. *Pharmaceutics* 14:370
62. Allison AC, Gregoriadis G (1974) Liposomes as immunological adjuvants. *Nature* 252:252
63. Gregoriadis G (1990) Immunological adjuvants: a role for liposomes. *Immunol Today* 11:89–97
64. Gregoriadis G, Saffie R, De Souza JB (1997) Liposome-mediated DNA vaccination. *FEBS Lett* 402:107–110
65. Gregoriadis G, McCormack B, Obrenovic M, Roghieh S, Zadi B, Perrie Y (1999) Vaccine entrapment in Liposomes. *Methods* 19:156–162
66. Vangala A, Bramwell VW, McNeil S, Christensen D, Agger EM, Perrie Y (2007) Comparison of vesicle based antigen delivery systems for delivery of hepatitis B surface antigen. *J Control Release* 119:102–110
67. Lanio ME, Luzardo MC, Alvarez C, Martínez Y, Calderon L, Alonso ME, Zadi B et al (2008) Humoral immune response against epidermal growth factor encapsulated in dehydration rehydration vesicles of different phospholipid composition. *J Liposome Res* 18:1–19
68. Stewart JCM (1980) Colorimetric determination of phospholipids with ammonium ferrothiocyanate. *Anal Biochem* 104:10–14
69. Loftsson T, Brewster ME (1996) Pharmaceutical applications of cyclodextrins. I. Drug solubilization and stabilization. *J Pharm Sci* 85: 1017–1025
70. Gregoriadis G, Saffie R, Hart SL (1996) High field incorporation of plasmid DNA within liposomes: effect on DNA integrity and transfection efficiency. *J Drug Target* 3:469–475
71. Gregoriadis G, Da Silva H, Florence AT (1990) A procedure for the efficient entrapment of drugs in dehydration-rehydration liposomes (DRVs). *Int J Pharm* 65:235–242



# Chapter 3

## Preparation of Small Unilamellar Vesicle Liposomes Using Detergent Dialysis Method

**Qingyue Zhong and Hongwei Zhang**

### Abstract

Small unilamellar liposomes are commonly used as model biomembranes and carriers for drug and gene delivery. Although methods which employ mechanical forces or organic solvents can be used to reduce the liposome size and the number of lipid bilayers, they are not suitable options when the purpose is to incorporate biologically active proteins into lipid bilayers or to encapsulate nucleic acid into liposomes. Detergent dialysis is a simple and inexpensive procedure to produce homogeneous small unilamellar vesicles (SUVs). Lipids are solubilized by detergent at a concentration much higher than its critical micellar concentration (CMC) in an aqueous dispersion medium. Free monomer detergent molecules in the dispersion medium are removed during dialysis, while the supramolecular detergent–lipid mixed micelles (MMs) are kept inside the dialysis tubing, leading to dissociation of detergent molecules from MMs. SUVs are formed after the micelle to vesicle transition (MVT).

**Key words** Liposome, Small unilamellar vesicles, Detergent, Dialysis, Phospholipid, Mixed micelle

---

### 1 Introduction

SUVs are commonly used as tools in biomedical research and drug delivery. Although traditional mechanical procedures, such as microfluidization, high-pressure homogenization, and probe sonication, may be used to prepare SUVs, they employ strong shearing forces and generate excessive heat that can cause the degradation of the payloads. Methods utilizing organic solvents may also be used to produce SUVs, but biologically active protein and nucleic acid molecules may be denatured or degraded when they are in contact with solvents. For researchers who study protein incorporated biomembranes, proteoliposomes, and lipid-based nucleic acid delivery, a mild preparation condition and an easy procedure without strong shearing force, overheating, and organic solvents would be most appropriate. SUVs are desired liposomes for these researchers due to their spherical shape, small particle size, and narrow size

distribution. In this chapter, a simple detergent dialysis procedure is described to prepare SUVs in a laboratory setting.

When amphiphilic lipid molecules are dispersed in an aqueous solution in the presence of a suitable detergent at a concentration way above its CMC, the lipid and detergent molecules spontaneously form disk-shaped MMs [1–3]. Equilibrium is reached between detergent molecules which reside at the edges of the micelles and monomer detergent molecules which are dissolved in the aqueous dispersion medium [4]. When the monomer detergent molecules are removed from the dispersion medium through a dialysis membrane, detergent molecules at the edges of the MMs dissociate and become free monomers to maintain the concentration equilibrium. This molecular re-organization increases the packing of lipid molecules and the size of the MMs, leading to a curvature in the disks. Eventually, the curved lipid bilayers close and small unilamellar vesicles are formed after the MVT process.

Different strategies have been studied to remove detergent from the MMs. These methods include direct dilution [5, 6], membrane dialysis [7, 8], gel exclusion chromatography [9, 10], and tangential filtration [11]. Direct dilution is the simplest method to trigger an MVT. It also provides an accurate final concentration of the detergent and a definite sample volume. However, it just lowers the detergent concentration but does not remove the detergent from the sample. The sample must be dramatically diluted in order to achieve a very low detergent concentration. Gel exclusion chromatography is another simple method, but elution also dilutes the sample. In addition, the liposome and/or the payloads may adsorb to the column, resulting in the loss of lipids and/or materials to be incorporated. The membrane dialysis method is very easy to conduct, and it does not require expensive materials and tools to remove detergents from the sample. However, this method takes a long time because it requires multiple changes of the dialysis buffer. Additionally, it cannot control the detergent removal rate well. For that reason, tangential filtration has been used to enable controlled dialysis [12].

Detergent dialysis method has been used to prepare empty liposomes [13–15] and proteoliposomes [16–18]. It is also used to make lipid nanoparticles (LNPs) for the delivery of plasmid DNA (pDNA) and antisense oligonucleotides (ASOs) [19–21]. It is worth noting that an LNP encapsulating pDNA or ASOs are structurally different from an SUV, even when both are prepared using the detergent dialysis method. Unlike an SUV, an LNP does not have a central aqueous pool inside the nanoparticle [22].

---

## 2 Materials and Equipment

1. Dimethyldioctadecylammonium bromide (DDAB).
2. 1,2-Dioleoyl-sn-glycero-3-phosphoethanolamine (DOPE).
3. 10 mL of glass vial.
4. Plastic spatula.
5. Chloroform.
6. Methanol.
7. 10 mL volumetric flask.
8. Glass pipet tip and rubber bulb.
9. Ultrapure water obtained from Millipore water system.
10. Vortex mixer.
11. Nitrogen gas tank.
12. Vacuum desiccator.
13. Parafilm.
14. Rotary evaporator.
15. Water bath.
16. Deoxycholate sodium solution, 0.5 M in distilled water.
17. Rotary incubator shaker.
18. Water bath sonicator.
19. Dialysis tubing (Dianorm, cut-off molecular weight 10 kDa).
20. Dialysis tubing closure.
21. PBS: Dissolve 8 g of NaCl, 0.2 g of KCl, 1.44 g of Na<sub>2</sub>HPO<sub>4</sub>, and 0.24 g of KH<sub>2</sub>PO<sub>4</sub> in 800 mL distilled water. Adjust the pH to 7.4 with HCl. Adjust the volume to 1 L with additional distilled water.
22. Magnetic stirrer.
23. Stirrer bar.
24. Disposable low-volume polystyrene cuvette (ZEN0118, Malvern).
25. Malvern Zetasizer Nano ZS90.
26. 1 mL slip tip syringe (309659, BD).
27. Disposable folded capillary cells and stoppers (DTS1070, Malvern).
28. Syringe filter unit, 0.22 µm.
29. Filtered PBS: PBS filtered through a 0.22 µm syringe filter unit.

---

### 3 Methods

#### 3.1 Preparation of a Dry Lipid Film

1. Rinse a 10 mL glass vial using 2 mL of chloroform. Let the glass vial dry.
2. Weigh 6.31 mg of DDAB and 66.96 mg of DOPE in the 10 mL glass vial (*see Notes 1 and 2*). Add 7 mL of chloroform/methanol (2:1, v/v) to the glass vial to completely dissolve the lipids. Transfer the lipid solution to a 10 mL volumetric flask using a glass pipet tip with a rubber bulb (*see Note 3*). Rinse the glass vial using 1 mL of chloroform/methanol (2:1, v/v), and transfer the solvent to the volumetric flask. Repeat this step three times. Adjust the total volume to 10 mL by adding an appropriate amount of solvent. A DDAB/DOPE (1:9, mol/mol) mixed lipid solution in the organic solvent is obtained. Tightly close the storage container, and wrap the cap with parafilm. Store the solution at -20 °C after each use.
3. Rinse a 25 mL round-bottom flask using 3 mL of chloroform. The round-bottom flask may be used immediately after rinsing.
4. Transfer 1 mL of the mixed lipid solution to the 25 mL round-bottom flask. In a chemical hood, rotate the flask at 50 revolutions per minute (RPM), and provide a steady stream of nitrogen into the flask to evaporate the organic solvents. A thin and even lipid film can be obtained on the bottom of the flask. Place the flask in a desiccator overnight under a high vacuum to remove residue solvents (*see Notes 4 and 5*).

#### 3.2 Rehydration of the Dry Lipid Film

1. Add 2 mL of deoxycholate sodium solution to the dried lipid film (*see Note 6*).
2. Place the round-bottom flask on a rotary incubator at 20 RPM at room temperature. Adjust the rotation speed and rotate the flask to make sure the entire lipid film is hydrated by the detergent solution. An optically clear lipid/surfactant solution will be obtained within ~20 min (*see Notes 7–10*).

#### 3.3 Detergent Removal by Dialysis

1. Soak a dialysis tubing (~8 cm long) in water overnight at room temperature. Thoroughly rinse the dialysis tubing using filtered PBS before use. Remove residue PBS inside the dialysis tubing as much as possible.
2. Transfer the aqueous sample from **step 2** in Subheading 3.2 to the dialysis tubing. Remove air from the dialysis tubing as much as possible. Tightly close both sides of the dialysis tubing using dialysis tubing closures.
3. Place the dialysis tubing in a glass beaker containing 500 mL of PBS. Dialyze the sample while stirring on a magnetic stirrer at room temperature for 40 h (*see Note 11*). Change the PBS

three times during the dialysis procedure at 8 h, 16 h, and 24 h. An almost clear colloidal dispersion will be obtained at the end of dialysis (*see Notes 12 and 13*). The average particle size of this DDAB/DOPE (1:9, mol/mol) formulation is typically 55–70 nm with a polydispersity index of 0.2 or lower, determined by dynamic light scattering (*see Note 14*).

4. Transfer the liposome dispersion to a glass vial (*see Note 15*). Displace the air in the vial with nitrogen gas, and store the sample at 4 °C. The total lipid concentration of this DDAB/DOPE (1:9, mol/mol) formulation is 5 µmol/mL or 3.66 mg/mL.

#### **3.4 Particle Size Determination**

Transfer 60 µL of the liposome sample to a ZEN0118 disposable polystyrene cuvette and cap the cuvette. Determine the average particle size using a Malvern Zetasizer Nano ZS90 at 25 °C and a 90° scattering angle.

#### **3.5 Surface Charge Determination**

Load the liposome sample into a 1 mL syringe, and insert the syringe into one of the openings of a disposable folded capillary cell. Slowly fill the cell to avoid generating air bubbles. Remove the syringe from the cell, and tightly close each opening of the cell using a stopper. Carefully wipe and clean the measuring windows of the cell using Kimwipes paper. Insert the cell into Malvern Zetasizer Nano ZS90, and measure the zeta potential three times (*see Notes 16 and 17*).

---

## **4 Notes**

1. Use a plastic spatula instead of a metal spatula to avoid introducing metal into the SUV preparation.
2. Other cationic lipids, anionic lipids, helper phospholipids, and cholesterol can also be used to prepare cationic, anionic, or neutral SUVs.
3. The glass vial, the volumetric flask, the glass pipette tip, and the round-bottom flask should be rinsed three times with filtered water and then thoroughly dried.
4. Cover the flask with a parafilm and poke some small holes. Removing organic solvents can be also conducted using rotary evaporation.
5. The size of the flask should be appropriate to the amount of total lipids and the volume of the dispersion medium to be added in Subheading 3.1. If the total volume of the dispersion medium is only 1 mL, adding it to a 100 mL round-bottom flask will result in a significant loss of sample when the sample is transferred to a dialysis bag.

6. Non-ionic detergents such as octylglucoside can also be used. The concentration of the detergent and the detergent removal rate should be optimized because they have different CMC, micelle sizes, critical packing parameters, etc. Dialysis can easily remove detergents with high CMC.
7. Although a slightly warmed (e.g., 37 °C) deoxycholate sodium solution may accelerate the lipid dissolving process, it is not recommended to warm the whole flask containing lipids and deoxycholate sodium solution at 37 °C, because the solubility of lipids and the CMC of the detergent will change. Also, if the total volume is small, water evaporation may significantly elevate the concentration of the solution in the flask.
8. Make sure the entire lipid film is completely dissolved so that the detergent to lipid ratio in the aqueous solution is as designed.
9. Briefly vortex the solution if there are any difficulties in dissolving the lipid film. A brief (5 s) sonication in a water bath can also help. If there are still visible particles in this solution, the detergent may be insufficient, and more detergent should be added.
10. A drug or protein solution containing an equal concentration of the same detergent can be added to prepare drug-loaded liposomes or proteoliposomes. An antisense oligonucleotide or pDNA solution in a small volume can also be added to prepare nucleic acid-loaded LNPs.
11. More efficient and controllable flow-through dialysis cells can also be used.
12. The dialysis condition, including the temperature of the dialysis buffer and the volume ratio of dialysis buffer to the sample, affects the removal rate of the detergent and the particle size of SUVs. It is recommended that the volume of dialysis buffer should be at least 100-fold compared with the volume of the liposome sample.
13. SUVs are formed after a few hours of dialysis. However, at least another 24 h are needed to further reduce the concentration of the detergent in the liposome sample.
14. The average particle size can be tailored by changing the detergent species, the initial ratio of detergent to lipids, the liposome formulation (the total lipid concentration, the lipid species, and the ratio between lipids), and the dialysis buffer (volume, temperature, ionic strength, and pH).
15. When an appropriate amount of polyethylene glycol (PEG) lipid is included in the formulation, the liposome sample can maintain stable for a prolonged period.

16. It is highly recommended to use a brand new cell for each sample for zeta potential determination. The entire sample channel of the cell should be rinsed using a filtered dispersion medium before use. The majority amount of the rinsing solution can be removed using a 1 mL syringe. The cell does not have to be dry before loading a sample because the minimum remaining dispersion medium does not significantly dilute the sample.
17. Zeta potential of SUVs is dependent on the surface properties of the nanoparticles, the concentration of the nanoparticles, the pH, the composition of the dispersion medium, and the temperature. If the concentration of the nanoparticles works well for the particle size determination, it typically also works well for zeta potential determination.

## References

1. Helenius A, Simons K (1975) Solubilization of membranes by detergents. *Biochim Biophys Acta* 415(1):29–79
2. Lichtenberg D, Robson RJ, Dennis EA (1983) Solubilization of phospholipids by detergents. Structural and kinetic aspects. *Biochim Biophys Acta* 737(2):285–304
3. Lichtenberg D, Ahyayauch H, Goni FM (2013) The mechanism of detergent solubilization of lipid bilayers. *Biophys J* 105(2): 289–299
4. Schubert R, Schmidt KH (1988) Structural changes in vesicle membranes and mixed micelles of various lipid compositions after binding of different bile salts. *Biochemistry* 27(24):8787–8794
5. Schurtenberger P, Mazer N, Waldvogel S, Kanzig W (1984) Preparation of monodisperse vesicles with variable size by dilution of mixed micellar solutions of bile salt and phosphatidylcholine. *Biochim Biophys Acta* 775(1): 111–114
6. Ollivon M, Eidelman O, Blumenthal R, Walter A (1988) Micelle-vesicle transition of egg phosphatidylcholine and octyl glucoside. *Biochemistry* 27(5):1695–1703
7. Rhoden V, Goldin SM (1979) Formation of unilamellar lipid vesicles of controllable dimensions by detergent dialysis. *Biochemistry* 18(19):4173–4176
8. Kagawa Y, Racker E (1971) Partial resolution of the enzymes catalyzing oxidative phosphorylation. *J Biol Chem* 246(17):5477–5487
9. Brunner J, Skrabal P, Hauser H (1976) Single bilayer vesicles prepared without sonication. Physico-chemical properties. *Biochim Biophys Acta* 455(2):322–331
10. Allen TM, Romans AY, Kercet H, Segrest JP (1980) Detergent removal during membrane reconstitution. *Biochim Biophys Acta* 601(2): 328–342
11. Peschka R, Purmann T, Schubert R (1998) Cross-flow filtration—an improved detergent removal technique for the preparation of liposomes. *Int J Pharm* 162(1–2):7
12. Ollivon M, Lesieur S, Grabielle-Madelmont C, Paternostre M (2000) Vesicle reconstitution from lipid-detergent mixed micelles. *Biochim Biophys Acta* 1508(1–2):34–50
13. Zumbuehl O, Weder HG (1981) Liposomes of controllable size in the range of 40 to 180 nm by defined dialysis of lipid/detergent mixed micelles. *Biochim Biophys Acta* 640(1): 252–262
14. Lasch J, Berdichevsky VR, Torchilin VP, Koelsch R, Kretschmer K (1983) A method to measure critical detergent parameters. Preparation of liposomes. *Anal Biochem* 133(2): 486–491
15. Schwendener RA, Asanger M, Weder HG (1981) n-Alkyl-glucosides as detergents for the preparation of highly homogeneous bilayer liposomes of variable sizes (60–240 nm phi) applying defined rates of detergent removal by dialysis. *Biochim Biophys Res Commun* 100(3):1055–1062
16. Paternostre MT, Roux M, Rigaud JL (1988) Mechanisms of membrane protein insertion into liposomes during reconstitution procedures involving the use of detergents. 1. Solubilization of large unilamellar liposomes

- (prepared by reverse-phase evaporation) by triton X-100, octyl glucoside, and sodium cholate. *Biochemistry* 27(8):2668–2677
17. Rigaud JL, Paternostre MT, Bluzat A (1988) Mechanisms of membrane protein insertion into liposomes during reconstitution procedures involving the use of detergents. 2. Incorporation of the light-driven proton pump bacteriorhodopsin. *Biochemistry* 27(8): 2677–2688
  18. Levy D, Gulik A, Bluzat A, Rigaud JL (1992) Reconstitution of the sarcoplasmic reticulum Ca(2+)-ATPase: mechanisms of membrane protein insertion into liposomes during reconstitution procedures involving the use of detergents. *Biochim Biophys Acta* 1107(2): 283–298
  19. Stuart DD, Allen TM (2000) A new liposomal formulation for antisense oligodeoxynucleotides with small size, high incorporation efficiency and good stability. *Biochim Biophys Acta* 1463(2):219–229
  20. Zhang HW, Zhang L, Sun X, Zhang ZR (2007) Successful transfection of hepatoma cells after encapsulation of plasmid DNA into negatively charged liposomes. *Biotechnol Bioeng* 96(1):118–124
  21. Wheeler JJ, Palmer L, Ossanlou M, MacLachlan I, Graham RW, Zhang YP, Hope MJ, Scherrer P, Cullis PR (1999) Stabilized plasmid-lipid particles: construction and characterization. *Gene Ther* 6(2):271–281
  22. Tam P, Monck M, Lee D, Ludkovski O, Leng EC, Clow K, Stark H, Scherrer P, Graham RW, Cullis PR (2000) Stabilized plasmid-lipid particles for systemic gene therapy. *Gene Ther* 7(21):1867–1874



# Chapter 4

## Thin-Film Hydration Followed by Extrusion Method for Liposome Preparation

Hongwei Zhang

### Abstract

One of the simplest ways to prepare liposomes in a research laboratory is the thin-film hydration method followed by extrusion. This method involves making a thin lipid film in a round-bottom flask by the removal of organic solvent. Upon the addition and agitation of the dispersion medium, heterogeneous liposomes are formed. Finally, after extrusion through polycarbonate membranes, homogeneous small liposomes are obtained.

**Key words** Liposomes, Thin-film hydration, Extrusion, Phase transition temperature, Drug delivery

---

### 1 Introduction

Since the historic observation by Alex Bangham in the 1960s [1], liposomes have found their applications in a variety of areas in the past century. Except for the use as model biological membranes, liposomes are extensively used in drug delivery [2–4], vaccine delivery [5, 6], gene delivery [7], molecular imaging [8], cosmetics [9, 10], and food industry [11, 12]. Most recently, liposomes were also used in genome editing [13]. Although these applications and the advantages of liposomes are well-known, many new comers to the world of liposomes often feel it is difficult to prepare liposomes by themselves. This short protocol aims to provide a detailed guideline to researchers with little or zero experience in liposome preparation so that they can prepare liposomes successfully.

Liposomes can be made from different natural and/or synthetic phospholipids as well as cholesterol. At high concentrations, amphiphilic phospholipid molecules spontaneously form lipid bilayers surrounding an aqueous pool [14]. Hydrophobic drug molecules and imaging agents can reside in the lipid bilayers, while hydrophilic compounds can be carried by liposomes in the aqueous pool. Different natural and synthetic phospholipids have

different phase transition temperature ( $T_M$ ), which is a very important parameter influencing drug encapsulation efficiency, storage stability, and in vivo stability. When the environment temperature is higher than their  $T_M$ , phospholipids exhibit a fluid state which is more permeable to water and is favorable for drug encapsulation during preparation. When used in vivo, if  $T_M$  is lower than the body temperature, the phospholipids in drug-loaded liposomes are in fluid state. The leaky lipid bilayer will result in premature drug release. Therefore, phospholipids whose  $T_M$  is higher than the body temperature are often used to prepare more stable liposomes as drug delivery carriers for in vivo use. In addition, cholesterol is routinely added to liposome formulations to stabilize the lipid bilayer by inhibiting the flip-flop of phospholipids. However, while cholesterol increases the lipid membrane rigidity, higher contents of cholesterol also increases the particle size of liposomes [15].

Liposomes can be categorized in different ways. Based on the diameter and the number of lipid bilayers, liposomes are often classified as small unilamellar vesicles (SUVs, 20–100 nm), large unilamellar vesicles (LUVs, 100–1000 nm), giant unilamellar vesicles (GUVs, >1000 nm), and multilamellar vesicles (MLVs, >500 nm). Liposomes can be negatively charged, neutral, or positively charged by the addition of other materials at a certain pH environment. For the delivery of nucleic acids, positively charged liposomes containing cationic lipids, such as N-[1(2,3-dioleoyloxy)propyl]-N,N,N-trimethylammonium chloride (DOTAP), are often used. Cationic liposomes can form lipid complexes (lipoplexes) with negatively charged nucleic acids due to electrostatic interaction and protect them from enzymatic degradation [16]. Because mammalian cell membrane is negatively charged, the positively charged liposomes and lipoplexes can also facilitate cellular internalization via electrostatic interaction [17]. When stored in dispersion medium, charged liposomes are more stable than neutral liposomes because of electrorepulsion between the particles.

Ideally, the liposome formulation should be optimized in terms of the species and contents of lipids as well as preparation parameters in order to achieve desired properties, such as particle size, surface charge, encapsulation efficiency, stability, etc.

---

## 2 Materials and Equipment

1. 50 mL round-bottom flask.
2. Sterile ultrapure water.
3. Phosphate-buffered saline (PBS): Dissolve 8 g of NaCl, 0.2 g of KCl, 1.44 g of Na<sub>2</sub>HPO<sub>4</sub>, and 0.24 g of KH<sub>2</sub>PO<sub>4</sub> in 800 mL

distilled H<sub>2</sub>O. Adjust pH to 7.4 with HCl. Adjust volume to 1 L with additional distilled H<sub>2</sub>O.

4. Sterilize by autoclaving.
5. N<sub>2</sub> (or argon) gas tank.
6. Rotary evaporator.
7. Water bath sonicator.
8. L- $\alpha$ -Phosphatidylcholine (PC).
9. Cholesterol.
10. Chloroform (containing ~1% ethanol).
11. Phospholipid stock solution in chloroform (10 mg/mL).
12. Cholesterol stock solution in chloroform (10 mg/mL).
13. Vortex mixer.
14. LiposoFast™ extruder, with 1.0 mL syringes (Avestin, Ottawa ON, Canada).
15. Polycarbonate membranes with the pore sizes of 400 nm, 200 nm, 100 nm, and 50 nm (Avestin, Ottawa ON, Canada).
16. Malvern Zetasizer Nano ZS90 (Malvern instruments Ltd., Malvern, Worcestershire, UK).
17. Vacuum desiccator.

---

### 3 Methods

#### 3.1 Preparation of the Thin Film

1. Add 5 mL of chloroform to rinse a 50 mL glass round-bottom flask. The round bottle flask may be used immediately after rinsing.
2. To prepare 2 mL of 10 mg/mL PC/cholesterol (1:1, molar ratio), add 670  $\mu$ L of 10 mg/mL PC stock solution and 1330  $\mu$ L of 10 mg/mL cholesterol stock solution, and mix them briefly in a chemical hood. Then evaporate the organic solvent on a rotary evaporator. The flasks may be dipped in a warm water bath, usually 40–45 °C, to make the evaporation process faster (*see Notes 1–5*).
3. Put the flask in a vacuum desiccator overnight to remove organic solvent residue. Cover the opening of a flask by a piece of stretched parafilm to prevent the entry of dusts or contaminants, and poke some small holes in the parafilm by a needle.

#### 3.2 Hydration of the Thin Film

1. Add 2 mL of PBS to the dry lipid film (*see Note 6*).
2. Vortex the solution for 10 s on maximum speed 3 times to suspend the lipid materials in the solution. Some lipid materials on the edge of the dry lipid film may stay on the flask and form

a ring. In this case, sonicate the lipids in a water bath sonicator for 15 s to help the lipids suspend in the solution.

3. Once all lipid materials are suspended in the solution, allow the suspension to stand at 4 °C overnight to efficiently hydrate the lipid materials.

### 3.3 Extrusion

1. Sonicate the liposome preparation in a water bath for 10–20 min to remove all visible precipitates. The obtained milky crude liposome sample contains mostly MLVs. The particle size will decrease with prolonged sonication time (*see Notes 7 and 8*).
2. Place two polycarbonate membranes with the pore size of 400 nm in the extruder.
3. Before pushing the plunger of the loaded syringe, make sure the plunger of the receiving syringe is inserted into the barrel to the zero position. Extrude the liposome preparation by passing the suspension through the polycarbonate membranes 5 times. The sample will look semitranslucent (*see Notes 9–11*).
4. Depending on the desired particle size, repeat steps 2–3 using 200 nm, 100 nm, and 50 nm polycarbonate membranes sequentially to obtain small unilamellar liposomes. After the series of extrusion, the mean particle size of extruded liposomes is usually within 200–300 nm, 100–200 nm, and 70–100 nm, respectively.
5. After extrusion through 100 nm polycarbonate membranes, the sample will look more translucent.
6. Inject the sample from the syringe to a storage vial. Displace the air in the vial by N<sub>2</sub> (or argon) gas to reduce lipid oxidation. Store the liposome sample at 4 °C.

### 3.4 Particle Size and Surface Charge Measurement

Mix 0.25 mL of the liposome sample with 2.25 mL of PBS in a cuvette, and determine the particle size by photon correlation spectroscopy (PCS) at 25 °C at an angle of 90°. The surface charge of the sample can also be determined by PCS using a disposable folded capillary cell (*see Note 12*).

---

## 4 Notes

1. To avoid introducing metal ions which may catalyze the oxidation of phospholipids [18], it is strongly suggested that plastic disposable spatula should be used for weighing lipids.
2. The containers of lipid stock solutions should be tightly closed, wrapped by parafilm, and restored at –20 °C after each use to prevent the loss of volatile chloroform.

3. Brand new glass flasks may have very smooth interior surface with little adhesion by lipid molecules, making it difficult to obtain a thin, even, and large dry lipid film. Based on the experience of my research group, it is helpful to make better thin lipid film using glass flasks with slightly coarser interior surface. The coarser interior surface may be easily obtained by filling the glass flasks using 1 M NaOH overnight and then rinsing it thoroughly using distilled water.
4. Both normal round-bottom flasks and pear-shaped round-bottom flasks may be used when the organic solvent is to be evaporated out on the rotary evaporator. Alternatively, 50 mL glass centrifuge tube with a round bottom may be used when the organic solvent is to be evaporated out by blowing inert gas ( $N_2$  or argon) flow into the tube while rotating the tube. Chloroform fume is toxic to human. It is always suggested to use chloroform in a chemical hood.
5. The quality of the dry film is very important to make good quality of the liposome products. Boiling of the organic solvent in the flasks should be prevented because it makes the lipid dry film uneven. In addition, boiling of organic solvent may result in the loss of lipid materials due to splashing into the condenser. The rapidity of solvent evaporation, which is affected by the motor rotation speed, the depth of dipping into the water bath, and the water bath temperature, as well as the size of the flask and the aqueous dispersion medium can influence the particle size and size distribution of the liposome preparation.
6. Except for the PBS listed in Subheading 2, other physiological buffers can also be used to prepare liposomes. The pH value, ionic species, and ionic strength may affect the properties of the liposome products, such as particle size, surface charge, drug encapsulation efficiency, stability, etc. It is recommended to pass the buffer through a 220 nm filter membrane to sterilize and remove any particulates.
7. Sonication of the suspension in a water bath sonicator for 5–10 min will generally produce relatively large liposomes, including MLVs, with wide particle size distribution, from several hundred nanometers to several micrometers.
8. To obtain SUVs, probe sonication using a titanium probe inserted into a crude liposome sample may be an alternative method. However, this method should be used with caution because it has some obvious limitations. Although probe sonication converts LUVs and MLVs to SUVs much faster than extrusion, the excessive heat generated by the probe tip may cause chemical degradation of both phospholipids and other

ingredients. In addition, the SUV product may be contaminated by metal particles.

9. Sonicate and extrude liposomes at a temperature higher than the  $T_M$  of the lipids is usually recommended to improve the encapsulation efficiency when the aim is to prepare drug-loaded liposomes. It also makes the extrusion easier with less resistance and shortens the time needed to reduce the particle size to the desired level. Liposome extruder syringes may be quickly heated to the desired temperature in an oven. Coarse liposome sample may be heated in a water bath at the same predetermined temperature.
10. Extrusion is usually necessary to obtain homogeneous SUVs. For the delivery of small hydrophilic molecules, extrusion may lead to decreased drug loading efficiency because a SUV has a much smaller aqueous pool surrounded by the lipid bilayer.
11. The first one or two extrusion of liposomes through polycarbonate membranes with each given pore size usually meet more resistance. In this case, it is important to be patient and push the plunger consistently but slowly. Pushing the plunger too hard will result in the rupture of the polycarbonate membranes. A brand new syringe and plunger usually fit tightly with each other and make it more difficult to push. To decrease the resistance, it is recommended to pre-wet the syringe barrel and plunger using the dispersion medium of the liposome before inserting the plunger into the barrel.
12. When PCS is used for particle size measurement, concentrated samples should be diluted by dispersion medium used in sample preparation so that the samples should be only slightly turbid. For a highly concentrated sample, the measured particle size by PCS is inaccurate due to multiple scattering and/or viscosity effects. In this case, it is recommended to dilute the sample to 1–10 mg/mL.

## References

1. Bangham AD, Horne RW (1964) Negative staining of phospholipids and their structural modification by surface-active agents as observed in the electron microscope. *J Mol Biol* 8:660–668
2. Sessa G, Weissmann G (1970) Incorporation of lysozyme into liposomes. A model for structure-linked latency. *J Biol Chem* 245: 3295–3301
3. Gregoriadis G (1976) The carrier potential of liposomes in biology and medicine (first of two parts). *N Engl J Med* 295:704–710
4. Gregoriadis G (1976) The carrier potential of liposomes in biology and medicine (second of two parts). *N Engl J Med* 295:765–770
5. van Rooijen N (1990) Liposomes as carrier and immunoadjuvant of vaccine antigens. *Adv Biotechnol Process* 13:255–279
6. Richards RL, Hayre MD, Hockmeyer WT, Alving CR (1988) Liposomes as carriers for a human malaria sporozoite vaccine. *Biochem Soc Trans* 16:921–922
7. Felgner PL, Gadek TR, Holm M, Roman R, Chan HW, Wenz M, Northrop JP, Ringold GM, Danielsen M (1987) Lipofection: a highly efficient, lipid-mediated DNA-transfection

- procedure. *Proc Natl Acad Sci U S A* 84:7413–7417
8. Silindir M, Erdogan S, Ozer AY, Maia S (2012) Liposomes and their applications in molecular imaging. *J Drug Target* 20:401–415
  9. Weiner N, Lieb L, Niemiec S, Ramachandran C, Hu Z, Egbaria K (1994) Liposomes: a novel topical delivery system for pharmaceutical and cosmetic applications. *J Drug Target* 2:405–410
  10. Betz G, Aeppli A, Menshutina N, Leuenberger H (2005) In vivo comparison of various liposome formulations for cosmetic application. *Int J Pharm* 296:44–54
  11. Taylor TM, Davidson PM, Bruce BD, Weiss J (2005) Liposomal nanocapsules in food science and agriculture. *Crit Rev Food Sci Nutr* 45: 587–605
  12. Mozafari MR, Johnson C, Hatziantoniou S, Demetzos C (2008) Nanoliposomes and their applications in food nanotechnology. *J Liposome Res* 18:309–327
  13. Zuris JA, Thompson DB, Shu Y, Guilinger JP, Bessen JL, Hu JH, Maeder ML, Joung JK, Chen ZY, Liu DR (2015) Cationic lipid-mediated delivery of proteins enables efficient protein-based genome editing in vitro and in vivo. *Nat Biotechnol* 33:73–80
  14. Lasic DD (1988) The mechanism of vesicle formation. *Biochem J* 256:1–11
  15. Lopez-Pinto JM, Gonzalez-Rodriguez ML, Rabasco AM (2005) Effect of cholesterol and ethanol on dermal delivery from DPPC liposomes. *Int J Pharm* 298:1–12
  16. Harries D, May S, Gelbart WM, Ben-Shaul A (1998) Structure, stability, and thermodynamics of lamellar DNA-lipid complexes. *Biophys J* 75:159–173
  17. Mislick KA, Baldeschwieler JD (1996) Evidence for the role of proteoglycans in cation-mediated gene transfer. *Proc Natl Acad Sci U S A* 93:12349–12354
  18. Lang JK, Vigo-Pelfrey C (1993) Quality control of liposomal lipids with special emphasis on peroxidation of phospholipids and cholesterol. *Chem Phys Lipids* 64:19–29



# Chapter 5

## Ethanol Injection Method for Liposome Preparation

Guangsheng Du and Xun Sun

### Abstract

Ethanol injection method is one of the preferred methods for liposome preparation due to its advantages including rapidity, safety, and reproducibility. This method involves the injection of phospholipid solution of ethanol into a stirred aqueous solution. Due to the diffusion of ethanol in aqueous solution, the dissolved phospholipids precipitate to form bilayer phospholipid fragments, which further fuse to form closed liposomal structures. After evaporation of ethanol, the liposomes can be finally obtained. In this chapter, we will describe the details of ethanol injection method for preparing liposomes and discuss issues that need to be considered during the fabrication process.

**Key words** Ethanol injection method, Liposomes, Drug delivery, Lipid bilayer, Nano-sizing

---

### 1 Introduction

Liposomes are sphere-shaped vesicles formed by self-assembling of natural or synthetic phospholipids and normally have a size from 30 nm to several micrometers [1, 2]. Due to the amphipathic property of phospholipids (both hydrophobic and hydrophilic), the lipids can self-assemble into closed bilayer structures when they are hydrated in aqueous phase. In liposomes, the hydrophobic tails of the phospholipids face each other inside of the bilayer, while the polar heads face outward [3]. Benefited by the favorable size, hydrophobic and hydrophilic properties, and superior biocompatibility, liposomes have been extensively investigated as drug delivery systems, including for small-molecule drugs and biologics [4, 5]. Hydrophobic drugs can be encapsulated inside of the bilayers, while hydrophilic drugs can be placed into the inner aqueous phase. Very often, cholesterol is added for fabrication of liposomes, which is expected to improve the stability and decrease the permeability of the liposomes [6].

Ethanol injection method for preparing liposomes was first reported by Batzri et al. in the 1980s and is used as an alternative fabrication method to thin-film hydration followed by

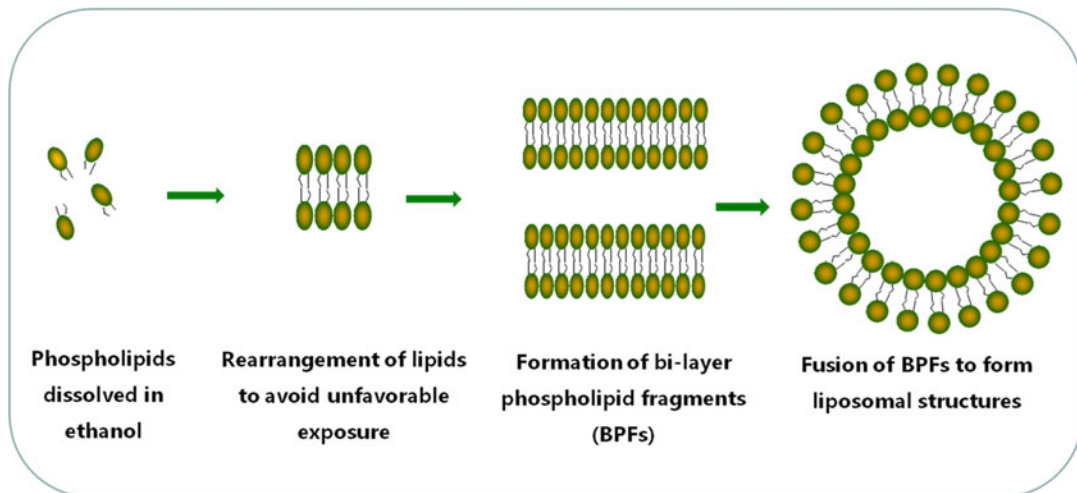


**Fig. 1** Mechanism of ethanol injection method for liposome preparation. Upon injection of ethanol solution, the hydrophobic groups of phospholipids rearrange to avoid unfavorable exposure to aqueous phase, which results in the formation of bilayer phospholipid fragments (BPFs). Along with the diffusion and evaporation of ethanol, BPFs fuse with each other to form closed liposomal structures

extrusion [7]. Ethanol injection method involves the injection of phospholipid solution of ethanol into aqueous phase. After diffusion and evaporation of ethanol, liposomes with a small size and a good uniformity can be obtained. The proposed mechanism of ethanol injection method for preparing liposomes is illustrated in Fig. 1. Upon the injection of ethanol into the aqueous solution, ethanol rapidly diffuses into the aqueous phase. During this process, the unfavorable exposure of phospholipids to aqueous phase leads to fast precipitation of the phospholipids in the form of bilayer phospholipid fragments (BPFs) [8, 9]. As the two end sides of BPFs face to unfavorable aqueous phase, they tend to further fuse with each other to form closed phospholipid bilayer structures (Fig. 1). This self-fusion process is preferred by the system as it encompasses the energy minimization principle, and the system selects the lowest energy demanding option. On the other hand, the rapid diffusion of ethanol results in very small ethanol droplets which contain small amount of BPFs. As a result, the liposomes prepared by ethanol injection method normally have a relatively small size [6, 10].

As compared to thin-film hydration followed by extrusion, ethanol injection method has several advantages [6, 11, 12]. Firstly, ethanol injection method uses safer ethanol as organic solvent and therefore possesses better safety and biocompatibility as compared to thin-film hydration followed by extrusion, which depends on more hazardous solvents such as chloroform and methanol. Secondly, the liposome fabrication efficiency of ethanol injection method is higher than thin-film hydration followed by extrusion. In the later one, the production efficiency could be limited by steps

of thin-film preparation and water hydration. Lastly, the ethanol injection method is relatively easy to scale up due to their rapidity, better safety, and reproducibility. Nowadays, many modifications on the ethanol injection method have been reported to improve the production capacity and uniformity of liposomes. For instance, microfluidic technology has been used for precisely controlling over the mixing and interdiffusion of ethanol in the aqueous phase. Particularly, microfluidic technology can create a continuous and steady-state mixing of the two miscible liquids [13, 14]. Consequently, the production efficiency and the reproducibility of liposomes can be significantly improved, which provides advantages for industrial production. In other modified methods, for example, multi-time ethanol injection or automated ethanol injection methods, the ethanol injection and ethanol removal steps are optimized in order to increase the production speed and the reproducibility [15, 16].

Although the liposomes prepared by ethanol injection method could have a smaller particle size and better uniformity as compared to that fabricated by thin-film hydration followed by extrusion, additional nano-sizing steps are often used to improve the uniformity of the liposomes. There are generally four types of nano-sizing methods for liposomes, including probe sonication, extrusion, homogenization, and shearing. In these strategies, extrusion and homogenization have a better potential to achieve industrial production of liposomes. In the research laboratory, probe sonication and small-volume extrusion are mostly used for the nano-sizing of liposomes. In this chapter, we will describe the details of ethanol injection method for liposome preparation and discuss points of caution that need to be considered.

---

## 2 Materials

1. Anhydrous ethanol 99.8%.
2. 2-Dioleoyl-sn-glycero-3-phosphocholine (DOPC) >99%, stored in –20 °C freezer. Dissolve DOPC in anhydrous ethanol to prepare stock solutions with a concentration of 63.60 mM.
3. Cholesterol >99%, stored in –20 °C freezer. Dissolve cholesterol in anhydrous ethanol to prepare stock solutions with a concentration of 25.86 mM.
4. Phosphate-buffered saline (PBS) is prepared from PBS granular powder: 17.6 g NaCl, 6 g Na<sub>2</sub>PO<sub>4</sub>, 0.3 g NaH<sub>2</sub>PO<sub>4</sub>. Dissolve the powder in 2000 mL deionized water. Sterilize the buffer with autoclave.
5. PB buffer: 10 mM phosphate buffer (pH 7.4). Prepare 10 mM Na<sub>2</sub>HPO<sub>4</sub> and NaH<sub>2</sub>PO<sub>4</sub> solutions by dissolving 1.42 g

Na<sub>2</sub>HPO<sub>4</sub> and 1.20 g NaH<sub>2</sub>PO<sub>4</sub>, respectively, in 1000 mL distilled water. Add the Na<sub>2</sub>HPO<sub>4</sub> solution slowly into NaH<sub>2</sub>PO<sub>4</sub> solution under stirring until the pH reaches 7.4.

6. Deionized water (18 MΩ/cm).
7. 1 mL syringe with 26 G hypodermic needle.
8. 25 mL glass beaker.
9. 25 mL round bottom flask.
10. IKA® C-MAG MS magnetic stirrer.
11. Rotary evaporator.
12. Branson Sonifier 250.
13. Nano ZS® Zetasizer (Malvern Instruments, Worcestershire, U.K.).

---

### 3 Methods

#### 3.1 Preparation of Working Solutions

1. Pipette 200 μL DOPC and 100 μL cholesterol solutions into a 1 mL Eppendorf tube. Add 700 μL anhydrous ethanol to obtain a 1 mL working solution.
2. Pipette 4 mL PBS into the 25 mL glass beaker which contains a magnetic stirrer. Heat the solution to 45 °C.

#### 3.2 Fabrication of Liposomes by Ethanol Injection Method

1. Transfer the working solutions of DOPC and cholesterol into the 1 mL syringe equipped with 26 G needle. Remove possible air bubbles by gently tapping the syringe tube and pushing the plunger.
2. Stir the PBS at a speed of 700 rpm. Inject slowly the phospholipid solution of ethanol into the PBS with an injection speed of around 10 μL/s. Keep stirring the mixture solution for 1 h to remove ethanol.
3. Transfer the resultant liposomal vesicles into the 25 mL round-bottom flask. Evaporate residual ethanol with the rotary evaporator at 37 °C for 1 h. After this step, ethanol and some water will be evaporated.
4. Transfer the resultant suspension into a 10 mL Eppendorf tube. Sonicate the suspension with the probe sonicator at 200 W for 3 min, 5 s on and 5 s off. After this step, the liposomes will be obtained.
5. The liposomes can be further concentrated by centrifuging with a high speed (e.g., at 40,000g for 2 h).

### 3.3 Size and Surface Charge Characterization

1. Size measurement: Dilute the liposome suspension by 10 times with the PB buffer, and measure the size of the liposomes with dynamic laser scattering by the Nano ZS® Zetasizer.
2. Zeta potential measurement: Dilute the liposome suspension by 10 times with the PB buffer, and measure the zeta potential of the liposomes with laser Doppler velocimetry, by using the Nano ZS® Zetasizer.

---

## 4 Notes

1. For drug loading during ethanol injection method, hydrophobic or hydrophilic drug can be dissolved into ethanol or aqueous phase, respectively. To remove the excess drug that is not encapsulated, the obtained liposome suspension can be centrifuged or dialyzed against large volume of PBS. The encapsulation efficiency of drug can be measured by detecting the amount of the drug in the supernatant after centrifugation or that in the dialysis medium or by directly measuring the loaded drug in the purified liposome samples.
2. The phospholipids can be dissolved in anhydrous ethanol to prepare stock solutions and stored in –20 °C fridge for further use. The bottles should be closed tightly and sealed with parafilm.
3. During the ethanol injection step, the temperature of the aqueous buffer is better controlled to be higher than the glass transition temperature of the phospholipids. By doing this, the fluidity of the phospholipids and the diffusion of ethanol in the aqueous phase are faster, which could help to prepare liposomes with a smaller size and a better uniformity.
4. The stirring speed of the aqueous phase and the concentration of phospholipid solution of ethanol could significantly affect the quality of the liposomes. A faster stirring speed could result in a smaller size. Low concentration of phospholipids may make it difficult to form liposomes, while high concentration of phospholipids could cause aggregation of the lipids.
5. Surfactant can be added into the aqueous phase during the preparation process, which could help to decrease the size and increase the encapsulation efficiency of liposomes.
6. During the sonication of liposomes, ice is needed to protect the liposomes from being damaged or oxidized by the high temperature caused by the sonication.
7. When measuring the size and surface charge of the liposome samples, the concentration of the sample should be controlled between 0.1 mg/mL and 50 mg/mL. Too concentrated sample could interfere the detection.

8. When measuring the zeta potential of the samples, the concentrated samples in PBS need to be diluted with buffer without salt, for example, with low molar concentration of PB buffer. The presence of high concentration of salt could interfere the measurement of zeta potential.
9. To increase long-term storage stability, the liposomes can be freeze-dried. In order to avoid the aggregation of liposomes during freeze-drying, lyoprotectants such as trehalose, mannitol, or lactose need to be added.

## References

1. Akbarzadeh A, Rezaei-Sadabady R, Davaran S et al (2013) Liposome: classification, preparation, and applications. *Nanoscale Res Lett* 8: 102
2. Torchilin VP (2005) Recent advances with liposomes as pharmaceutical carriers. *Nat Rev Drug Discov* 4:145–160
3. Bozzuto G, Molinari A (2015) Liposomes as nanomedical devices. *Int J Nanomedicine* 10: 975–999
4. Eloy JO, Claro De Souza M, Petrilli R et al (2014) Liposomes as carriers of hydrophilic small molecule drugs: strategies to enhance encapsulation and delivery. *Colloid Surf B* 123:345–363
5. Swaminathan J, Ehrhardt C (2012) Liposomal delivery of proteins and peptides. *Expert Opin Drug Del* 9:1489–1503
6. Jaafar-Maalej C, Diab R, Andrieu V et al (2010) Ethanol injection method for hydrophilic and lipophilic drug-loaded liposome preparation. *J Liposome Res* 20:228–243
7. Batzri S, Korn ED (1973) Single bilayer liposomes prepared without sonication. *BBA-Biomembranes* 298:1015–1019
8. Lasic DD (1982) A molecular model for vesicle formation. *BBA-Biomembranes* 692:501–502
9. Lasic DD (1995) Mechanisms of liposome formation. *J Liposome Res* 5:431–441
10. Schubert MA, Müller-Goymann CC (2003) Solvent injection as a new approach for manufacturing lipid nanoparticles – evaluation of the method and process parameters. *Eur J Pharm Biopharm* 55:125–131
11. Sala M, Miladi K, Agusti G et al (2017) Preparation of liposomes: a comparative study between the double solvent displacement and the conventional ethanol injection—from laboratory scale to large scale. *Colloid Surf A* 524: 71–78
12. Gentine P, Bourel-Bonnet L, Frisch B (2013) Modified and derived ethanol injection toward liposomes: development of the process. *J Liposome Res* 23:11–19
13. Zizzari A, Bianco M, Carbone L et al (2017) Continuous-flow production of injectable liposomes via a microfluidic approach. *Materials* 10:1411
14. Carugo D, Bottaro E, Owen J et al (2016) Liposome production by microfluidics: potential and limiting factors. *Sci Rep* 6:25876
15. Wagner A, Vorauer-Uhl K, Kreismayr G et al (2002) Enhanced protein loading into liposomes by the multiple crossflow injection technique. *J Liposome Res* 12:271–283
16. Yang K, Delaney JT, Schubert US et al (2012) Fast high-throughput screening of temoporfin-loaded liposomal formulations prepared by ethanol injection method. *J Liposome Res* 22: 31–41



# Chapter 6

## Preparation of Giant Vesicles with Mixed Single-Tailed and Double-Tailed Lipids

Lauren A. Lowe and Anna Wang

### Abstract

Giant vesicles are model membrane systems that can be characterized with microscopy. Whereas most giant synthetic vesicles are created with a single phospholipid species, vesicles with mixed membrane compositions, including single-tailed and double-tailed lipids, serve as more accurate models of biological membranes and also have applications in the origins of life and drug delivery fields. Here we describe several approaches that can be used to create giant vesicles with mixed lipid compositions.

**Key words** Vesicles, Phospholipids, Fatty acids, Single-chain, Double-chain, Lipid bilayers, Membranes, GUVs

---

### 1 Introduction

Vesicles or liposomes are enclosed lipid bilayer membrane structures that encapsulate an aqueous core. Giant vesicles (GVs) are approximately cell-sized ( $>1\text{ }\mu\text{m}$ ), meaning that a large number of solute molecules can be encapsulated, and they can easily be studied using microscopy. Phospholipid GVs and, in particular, giant unilamellar vesicles (GUVs) have been used to model cell membranes and build artificial cells.

This chapter describes making GVs composed of a mixture of A) phospholipids (which have two acyl tails) and B) lipids that have a single acyl tail. The inclusion of these additional lipids can unveil the effect of such lipids on membranes, which includes promotion of stalk formation, membrane fusion, vesicle division, vesicle rupture, or conferral of new properties such as pH sensitivity.

An important consideration when preparing membranes of mixed lipid composition is the effect of different lipids on the bilayer packing. The critical packing parameter (CPP) is a measure of lipid geometry, defined as  $\text{CPP} = v/(\alpha * l)$  where  $v$  is the lipid volume,  $\alpha$  is the area of the lipid headgroup, and  $l$  is the length of

| Lipid            | CPP | Shape                        | Curvature              |
|------------------|-----|------------------------------|------------------------|
| POPC<br>         | ~1  | Cylinder<br>                 | Zero curvature<br>     |
| 18:1 Lyso PC<br> | <1  | Cone<br>                     | Positive curvature<br> |
| POPA<br>         | >1  | Inverted cone<br>            | Negative curvature<br> |
| Oleic Acid<br>   | ~1  | Cylinder<br>(see Note 1)<br> | Zero curvature<br>     |

**Fig. 1** Impact of lipids POPC (1-palmitoyl-2-oleyl-sn-glycero-3-phosphocholine), 18:1 Lyso PC (1-oleoyl-2-hydroxy-sn-glycero-3-phosphocholine), POPA (1-palmitoyl-2-oleyl-sn-glycero-3-phosphate), and oleic acid, which have different shapes, on membrane curvature

the lipid. Lipids with CPP  $\sim 1$  have a cylindrical shape and pack into lamellar structures (*see Note 1* and Fig. 1). Lipids with a CPP  $< 1$  have a conical shape; this leads to positive membrane curvature that can result in pore formation or micelle formation. Conversely, lipids with a CPP  $> 1$  have an inverted cone geometry, leading to negative membrane curvature.

Because vesicle formation primarily occurs when cylindrical lipids are used, the addition of lipids with cone or inverted cone geometries can generate curvature stresses in the membrane and be destabilizing at high concentrations. For example, the addition of high concentrations of lysolipids such as 18:1 Lyso PC to 1-palmitoyl-2-oleyl-glycero-3-phosphocholine (POPC) vesicles leads to vesicle destruction [1].

The different lipid species used in this chapter include phospholipids and single-tailed lipids such as:

- Fatty acids: These are key building blocks for the synthesis of a variety of lipids and play an important role in modulating membrane fluidity [2]. Free fatty acids are also found as products of phospholipid hydrolysis. Biology aside, fatty acids have been proposed as important components of model primitive cells [3, 4] and have drug delivery applications. The effect of combining fatty acids, such as oleic acid, and phospholipids such as POPC in bilayers has been explored in literature [5–7].
- Lysolipids: These are another product of phospholipid hydrolysis and play an important role in a variety of cellular processes [8]. They are present in relatively small amounts in cell membranes, but unlike phospholipids and fatty acids, lysolipids generally do not form bilayers on their own [8]. To explore the effect of lysolipids on phospholipid membranes, mixed membranes have been studied. In particular, lysolipids have been found to affect membrane curvature, vesicle hydration, and vesicle fusion [8, 9].

To make mixed-lipid GVs, the lipids can either be mixed before (“pre-mixed”) or after (“post-mixed”) vesicle formation. For pre-mixed membranes, there are several techniques used to make single-lipid GVs that can be extended to mixed membrane systems. For post-mixed membranes, additional lipids are added after the formation of single-lipid GVs.

Considerations when combining lipids include:

- Potential change in the melting temperature of the membrane. Mixing lipids can often lead to melting-temperature depression.
- Potential for complications from hydrophobic mismatch if the acyl tail lengths of the lipids differ significantly.

Additional considerations for post-mixing of lipids include:

- Small amounts of single-tailed lipid (much less than 10%) can be added via aqueous solution if the lipid solution is prepared below the critical micelle concentration of the single-tailed lipid [1].
- Upon lipid addition, any generated curvature stresses or excess surface area may be relieved by flip-flop, inward or outward budding, or vesicle–vesicle fusion. If outward budding occurs and leads to division, it may not be obvious that any change has occurred to the vesicles [10].
- Single-tailed lipids are more soluble in aqueous solution than phospholipids with similar acyl tail lengths. They also have a lower driving force for self-assembly [4]. As a result, lipid exchange between vesicles is unavoidable, and the system must be given time to equilibrate. Compared to phospholipid

membranes, membranes containing single-tailed lipids are kinetically less trapped.

- Lipid bilayer membranes are semi-permeable, which results in vesicle volumes being osmotically limited in the presence of solutes. When the surface area increases upon lipid addition, previously spherical vesicles may become elongated in shape. However, elongated structures may be easily damaged by shear from vortexing or other vigorous methods of mixing. We recommend gentler forms of mixing, such as inverting the tube a few times, if the morphology of the vesicles is intended to be maintained.

For many or all of the techniques, it is impossible to determine the homogeneity of the membranes or their composition by microscopy. Not all lipids will necessarily partition onto bilayer membranes in the same proportion. For example, some may remain in a micelle form, at an air–water interface, adhered to paper (if present) or in an oil phase (if present). Confirming the membrane composition with mass spectrometry is recommended.

---

## 2 Materials

### 2.1 General Materials

1. Milli-Q water.
2. Stock solutions: 1 M sucrose, 1 M glucose, 100 mM pyranine (*see Note 2*).
3. Stock solution of lipid dye: 1 mM rhodamine B in water (*see Note 3*).

### 2.2 Pre-mixed GVs

#### 2.2.1 Paper-Based Thin-Film Hydration

1. Buffer stock solution: 1 M bicine adjusted to pH 8.3 with NaOH (*see Note 4*).
2. 50 mM mixed POPC/oleic acid (1:1) in ethanol (*see Note 5*).
3. Hot plate in a fume hood.
4. Micropipettes.
5. Metal tweezers.
6. Filter paper (Whatman Grade 1, 20 mm circles).
7. 20 mL glass vial with flat bottom.
8. Microcentrifuge tube.

#### 2.2.2 Emulsion Transfer Method

1. Mineral oil (*see Note 6*).
2. Inner aqueous phase: 500 mM sucrose with 200 mM bicine, or 500 mM sucrose with 50 mM HEPES (*see Note 7*).
3. Subphase: 500 mM glucose with 200 mM bicine, or 500 mM glucose with 50 mM HEPES (*see Note 7*).

4. 20 mg/mL POPC:18:1 lyso PC (4:1, w/v) in chloroform (*see Note 8*).
5. Hot plate in fume hood.
6. Solvent-resistant syringe (250 µL) with needles (Hamilton Gastight syringe with PTFE Luer Lock) or micropipettes with 200 µL solvent-resistant pipette tips (Solvent Safe™ pipette tips).
7. 20 mL glass vial with flat bottom.
8. Magnetic stir bar.
9. Microcentrifuge tubes.
10. Microcentrifuge capable of 15,000 g (Eppendorf microcentrifuge 5425).

#### **2.2.3 Fatty Acid Self-Assembly Method**

1. Buffer stock solution: 1 M bicine adjusted to pH 8.1 with NaOH.
2. 125 mM NaOH solution.
3. Neat oleic acid at room temperature (*see Notes 9–12*).
4. Neat linoleic acid at room temperature (*see Notes 9–12*).
5. Micropipettes.
6. Microcentrifuge tubes.
7. Orbital shaker.
8. Vortexer.

### **2.3 Post-mixed GVs**

#### **2.3.1 Adding Lipid 2 Via Solvent**

1. Buffer stock solution: 1 M bicine adjusted to pH 8.3 with NaOH (*see Note 4*).
2. Single-lipid GVs: 50 mM POPC GVs.
3. Concentrated stock solution of lipid in solvent: 300 mM oleic acid in ethanol (*see Note 13*).
4. Micropipettes.
5. Microcentrifuge tubes.

#### **2.3.2 Adding Lipid 2 as Pre-formed Vesicles or Micelles**

1. Buffer stock solution: 1 M bicine adjusted to pH 8.3 with NaOH (*see Note 3*).
2. Single-lipid GVs: 50 mM POPC GVs.
3. Neat oleic acid at room temperature (*see Notes 9–12*).
4. Micropipettes.
5. Microcentrifuge tubes.
6. Optional: vesicle extruder (Avanti Mini-Extruder with Nucleopore track-etched membranes).

### 2.3.3 Phospholipase Incubation

1. Phospholipase: phospholipase-D from *Arachis hypogaea*.
2. Phosphate-buffered saline (PBS): 137 mM NaCl, 10 mM Na<sub>2</sub>HPO<sub>4</sub>, 1.8 mM KH<sub>2</sub>PO<sub>4</sub>, 2.7 mM KCl, pH 7.4.
3. Phosphate-buffered saline (PBS) with calcium: 137 mM NaCl, 10 mM Na<sub>2</sub>HPO<sub>4</sub>, 1.8 mM KH<sub>2</sub>PO<sub>4</sub>, 2.7 mM KCl, 0.5 mM CaCl<sub>2</sub>, pH 7.4.
4. Phospholipid GVs: 50 mM POPC GVs.
5. Micropipettes.
6. Microcentrifuge tubes.
7. Hotplate or incubator to maintain samples at 37 °C.

## 3 Methods

### 3.1 Pre-mixed GVs

#### 3.1.1 Paper-Based Thin-Film Hydration

This method is also known as the PAPYRUS method by Li et al. [11] and uses filter paper to spread the lipid and reduce the presence of dense, kinetically trapped lipid aggregates relative to traditional thin-film hydration methods. The method described here can be used to prepare mixed phospholipid (POPC) and fatty acid (oleic acid) GUVs (Fig. 2) with the presence of either lipid optional. For additional details, please see [12].

1. Using clean metal tweezers, hold the piece of filter paper over a hotplate at 100 °C. Make sure the paper is hovering 1–5 mm above the hot plate, but not touching the hot plate.

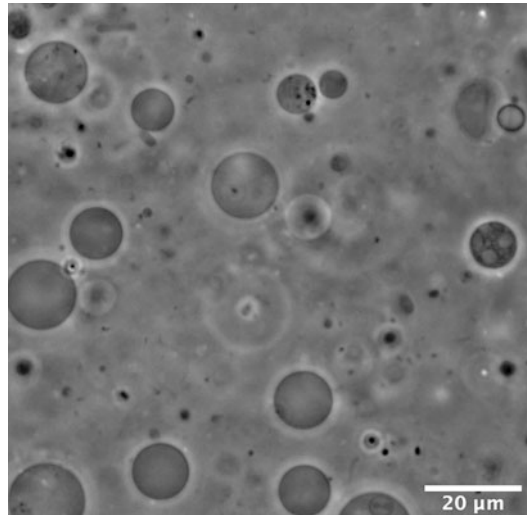


**Fig. 2** Phase contrast microscopy image of 1:1 POPC/oleic acid GVs prepared in 100 mM bicine using the paper-based thin-film hydration method (20 mM total lipid used). Vesicles encapsulating 100 mM sucrose, diluted into 100 mM glucose

2. Drip 50  $\mu\text{L}$  of 50 mM solvent–lipid solution slowly onto the filter paper (*see Note 14*). Allow the paper to dry between drips.
3. Put the paper into an uncapped 20 mL glass vial with a flat bottom (not concave). Heat at 65 °C under a gentle stream of nitrogen to remove residual solvent. Alternatively, use a vacuum desiccator.
4. Prepare 1 mL of hydration buffer in a microcentrifuge tube. Combine 100  $\mu\text{L}$  of 1 M bicine (pH 8.3), 100  $\mu\text{L}$  of 1 M sucrose, 10  $\mu\text{L}$  of 100 mM pyranine, and 790  $\mu\text{L}$  of water.
5. Add 1 mL of hydration buffer into the vial and tightly cap the vial.
6. Heat the vial for 1 h at 45–65 °C.
7. Tap vial firmly but carefully to allow any condensation to collect back into the vial.
8. Pipette up and down near the paper’s surface to release vesicles.
9. Aspirate to collect vesicles.

### 3.1.2 Emulsion Transfer Method

Also known as the inverted emulsion method, as developed by Pautot et al. [13], the emulsion transfer technique starts with creating an emulsion of aqueous droplets in a lipid-carrying oil. The surface-activity of the lipids results in droplets that are enveloped with a lipid monolayer. These droplets are then passed through an oil–water interface, adding an extra monolayer to the droplets and thus forming lipid bilayer vesicles (Fig. 3). The method described here can be used to prepare mixed phospholipid (POPC) and lysolipid (18:1 Lyso PC) GUVs (Fig. 4) with the presence of lysolipid being optional.

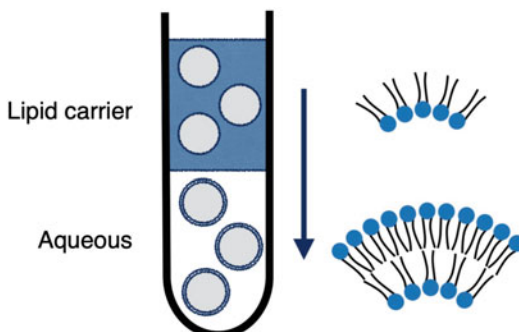


**Fig. 3** Emulsion transfer technique. Droplets with a single lipid monolayer in a lipid-carrying oil pass through an oil–water interface into the aqueous phase, adding an additional lipid monolayer to the droplets, forming vesicles

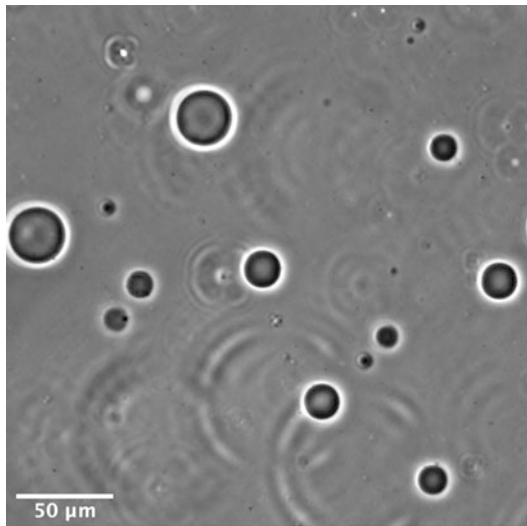


**Fig. 4** Phase contrast microscopy image of POPC and 18:1 Lyso PC GUVs prepared using the emulsion transfer method. Initial lipid-carrying oil mixture consisted of 1 mg/mL 4:1 POPC:Lyso PC in mineral oil

1. Prepare the lipid-carrying oil. Add 50  $\mu$ L of 20 mg/mL lipid in chloroform to 1 mL of mineral oil in an uncapped 20 mL glass vial.
2. Heat the vial at 80 °C for 30 min with a stir bar stirring to evaporate the chloroform, and then allow the mixture to cool to room temperature.
3. Next prepare the emulsion. Add 50  $\mu$ L of inner aqueous phase to a 2.0 mL microcentrifuge tube.
4. Add 400  $\mu$ L of the lipid-carrying oil from the 20 mL glass vial to the microcentrifuge tube.
5. Vortex the microcentrifuge tube well for at least 60 s to yield an emulsion. For some vortexers, a narrower microcentrifuge tube, such as 1.5 mL tubes, can also yield good emulsions.
6. In a separate 2.0 mL microcentrifuge tube, add 200  $\mu$ L of the subphase.
7. Layer 400  $\mu$ L of the emulsion onto the subphase before placing the tube in the microcentrifuge with a balance.
8. Wait 5–10 min to allow the interface to equilibrate and acquire a lipid monolayer.
9. Centrifuge the tube at 15,000 g for 5 min at a time, up to 30 min, until the emulsion layer no longer looks milky, indicating transfer of droplets into the aqueous phase. You may see a pellet form.

10. Pipette off the oil and the top of the aqueous phase, leaving approximately 150 µL of aqueous solution.
11. Gently pipette (deep, near the pellet if one forms) up and down to agitate the sample without disturbing the air–water/oil–water interface.
12. Remove 100 µL from the bottom of the tube and transfer into a clean microcentrifuge tube.
13. *Optional wash:* Add 400 µL of the subphase to the clean tube used in the previous step and mix with the vesicles by pipetting up and down. Centrifuge at 15,000 g for 1 min at a time to re-form the pellet (if a pellet previously formed; maximum 5 min); then remove approximately 400 µL from the top of the sample before flicking the tube gently or pipetting up and down to redisperse the vesicles.
14. For further details on encapsulating material and concentrating vesicles, please refer to [12].

### **3.1.3 Fatty Acid Self-Assembly Method**

This method relies on the particular self-assembly properties of fatty acids and can be extended to prepare unilamellar GVs of mixed fatty acid compositions. One example of a two-lipid-system, 1:1 oleic acid/linoleic acid, is described below. For more detail on buffer and lipid combinations, please see [12].

1. Make 100 µL of a 100 mM mixed lipid micelle solution in a 1.5 mL microcentrifuge tube, by pipetting 1.6 µL of oleic acid and 1.6 µL of linoleic acid into 100 µL of 125 mM NaOH solution. Pipette up and down in a controlled but rapid manner to ensure the pipette tip does not retain any fatty acid.
2. Mix well by vortexing the tube to form a clear solution of micelles.
3. Add 800 µL Milli-Q water to the microcentrifuge tube. Vortex for 3 s.
4. Add 100 µL 1 M bicine buffer (pH 8.1) to the microcentrifuge tube. Vortex for 3 s.
5. Leave the microcentrifuge tube on an orbital shaker at 90 rpm overnight, with the tube well-capped and lying sideways (without rocking) to form GUVs in high yield.

## **3.2 Post-mixed GVs**

### **3.2.1 Adding Lipid 2 Via Solvent**

This technique involves first making single-lipid GVs before adding a small amount of solvent that is rich in the second lipid. Upon dilution of the solvent, the lipids will partition into their own aggregates or onto pre-existing membranes. When working with fatty acids, for example during the addition of oleic acid to POPC

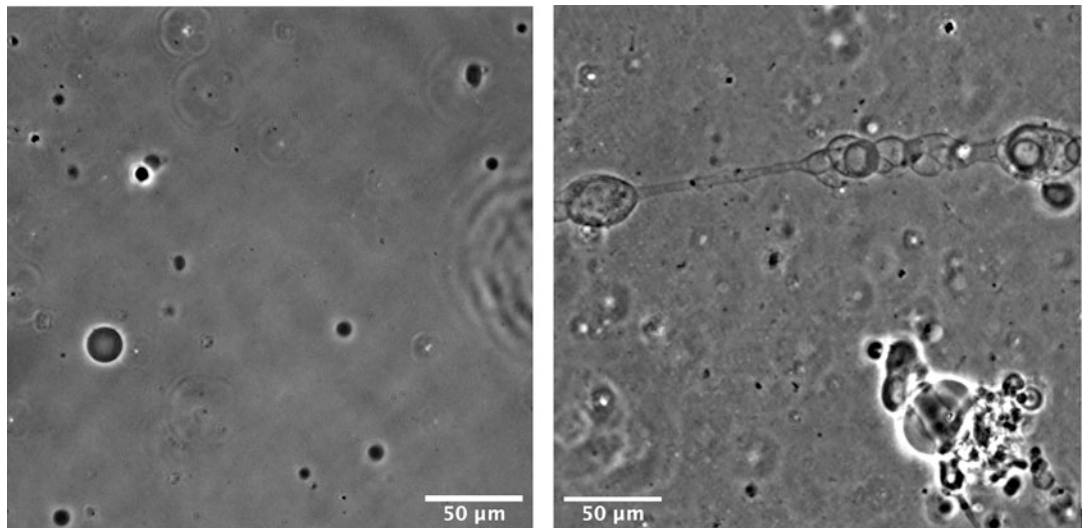


**Fig. 5** Phase contrast microscopy images of 5 mM POPC GVs without (left) and with (right) 1% (v/v) of 300 mM oleic acid in ethanol

GUVs (Fig. 5), the fatty acid can decrease the pH of the system and thus the pH of the system should be monitored. The changes in morphology and pH are both highly dependent on the concentration of fatty acid in ethanol added to the vesicles.

1. Prepare 50 mM POPC GUVs. This can be achieved using the paper-based method described in Subheading 3.1.1 (using a hydration buffer containing 100 mM bicine and 100 mM sucrose).
2. Prepare the dilution buffer. Mix 100  $\mu$ L of 1 M bicine (pH 8.3), 100  $\mu$ L of 1 M glucose, and 800  $\mu$ L of water in a microcentrifuge tube.
3. In a microcentrifuge tube, mix 900  $\mu$ L of the dilution buffer and 100  $\mu$ L of 50 mM POPC GUVs to give 5 mM POPC GUVs.
4. Add 1% by volume of 300 mM oleic acid in ethanol to the 5 mM POPC GUVs in a microcentrifuge tube and pipette up and down gently to mix (e.g., 20  $\mu$ L 5 mM POPC GUVs + 0.2  $\mu$ L 300 mM oleic acid in ethanol). Allow at least half an hour for the oleic acid to partition onto the POPC membranes.

### 3.2.2 Adding Lipid 2 as Pre-formed Vesicles or Micelles

This approach involves preparing GVs made of one lipid first before adding an aqueous solution of lipid that can partition onto the GVs. Here, POPC GUVs are prepared before micelles or extruded oleic acid vesicles are added to give mixed phospholipid and fatty acid GVs (Fig. 6). Extrusion is optional but could help speed up equilibration. For applications, see [14, 15].

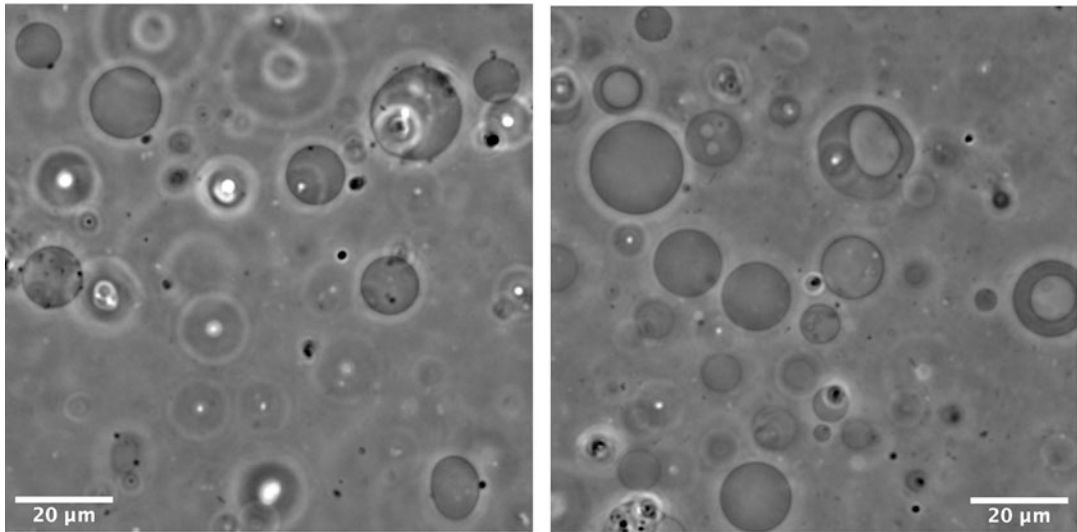


**Fig. 6** Phase contrast microscopy images of (left) 20 mM POPC GVs and (right) 20 mM 1:1 POPC GVs/oleic acid vesicles. The mixed vesicles (right) showed internal compartment formation after the POPC GVs incorporated the lipids from the oleic acid vesicles

1. Prepare 50 mM POPC GUVs. This can be achieved using the paper-based method described in Subheading 3.1.1 (using a hydration buffer containing 100 mM bicine and 100 mM sucrose).
2. Next prepare a 50 mM oleic acid vesicle solution (or for a micelle solution *see step 3*):
  - (a) In a microcentrifuge tube, mix 100  $\mu$ L of 1 M bicine (pH 8.3), 25  $\mu$ L of 1 M NaOH, and 875  $\mu$ L of water.
  - (b) Pipette 50  $\mu$ mol (15.8  $\mu$ L) of oleic acid into the tube. Pipette up and down in a controlled but rapid manner to ensure the pipette tip does not retain oleic acid; then vortex well to mix.
  - (c) Leave the tube on the orbital shaker at 90 rpm for a minimum of 1 h to yield multilamellar oleic acid vesicles.
  - (d) Optional: Extrude the sample at least 11 passes through 50 or 100 nm diameter polycarbonate membranes to give small, unilamellar oleic acid vesicles.
3. Alternatively for a 50 mM micelle solution:
  - (a) In a 1.5 mL microcentrifuge tube, prepare 1 mL of 75 mM NaOH solution.
  - (b) Pipette 50  $\mu$ mol (15.8  $\mu$ L) of oleic acid into the tube. Pipette up and down in a controlled but rapid manner to ensure the pipette tip does not retain any fatty acid.

- (c) Mix well by vortexing the tube to form a clear solution of micelles.

The final steps are to mix the POPC GUVs and the oleic acid vesicles (or micelles) in the desired ratio, though adding micelles in a high proportion will significantly increase the pH. Oleic acid (or oleate) will partition rapidly onto membranes and can generate curvature stresses leading to division [10] or other shape changes [16] (such as the inward budding shown in Fig. 6). To make 20 mM 1:1 POPC/oleic acid GV:

4. Prepare the dilution buffer by mixing 60  $\mu$ L of 1 M bicine (pH 8.3), 60  $\mu$ L of 1 M glucose, and 480  $\mu$ L of water in a microcentrifuge tube.
5. In two separate microcentrifuge tubes, mix 300  $\mu$ L of dilution buffer and 200  $\mu$ L of each vesicle (or micelle) species to give two tubes of 500  $\mu$ L 20 mM lipid solutions.
6. Finally, mix both vesicle (or micelle) species in a desired ratio to create mixed lipid GV with final lipid concentration 20 mM, i.e., 1:1 ratio to give 1:1 POPC/oleic acid GV.
7. Allow the sample 1 hour to equilibrate.

### 3.2.3 Phospholipase Incubation

This technique involves incubating phospholipid GUVs with a phospholipase, a class of enzymes that hydrolyze phospholipids. Phospholipases differ in the sites at which they cleave phospholipids, resulting in the formation of different products. It is important to consider what effect the cleavage reaction products will have on vesicle stability. This method describes incubating POPC vesicles with phospholipase D to yield vesicles containing POPA, a phosphatidic acid, in accordance with results from Holme et al. [17].

1. Prepare 1 mL of 50 mM POPC GUVs in PBS. This can be achieved using the paper-based method described in Subheading 3.1.1.
2. Dilute the POPC GUVs into a solution of phospholipase D (50 mU/mL) in PBS containing 0.5 mM  $\text{CaCl}_2$  so that the concentration of POPC GUVs is 4 mM.
3. Incubate the sample for 1 h at 37 °C.

---

## 4 Notes

1. The shape of the fatty acid depends on the protonation state of the headgroup, which is influenced by pH. At a pH significantly less than the apparent  $pK_a$  of the fatty acid, the fatty acid will be protonated. At a pH significantly above the apparent  $pK_a$ , the molecules will be deprotonated, meaning the headgroups will repel each other and will take up a larger area.

2. Encapsulating sucrose inside vesicles, then diluting them into an isotonic glucose buffer, is useful for concentrating vesicles using a density difference. Pyranine can be used to fluorescently label the interior of vesicles.
3. A lipid dye can be added to the vesicles after self-assembly to label the membranes for fluorescence imaging.
4. Bicine is used here because it has good buffering capacity at the pH of oleic acid GUV assembly (a pH slightly below the apparent  $pK_a$  of the fatty acid). Different buffers should be used for different fatty acids. The use of a buffer is not strictly necessary when using lipids that do not possess pH-dependent behavior.
5. Some potential solvents include ethanol, methanol, and chloroform. Considerations for the lipid–solvent solution (taken from [12]):
  - (a) The solution should be stored at  $-20\text{ }^{\circ}\text{C}$ .
  - (b) Choose a good solvent for the lipids to prevent the lipids from pre-organizing into undesired structures.
  - (c) Choose a solvent that is also miscible with the carrier oil, if using the emulsion transfer method.
  - (d) Store the solvent on molecular sieves if conductivity suggests substantial water content.
  - (e) Make sure the solvent is reasonably volatile. As a counter-example DMSO is a good lipid solvent but has an extremely high boiling temperature.
  - (f) If chloroform is used, use solvent-resistant syringes of different sizes (e.g., 10  $\mu\text{L}$ , 250  $\mu\text{L}$ , 1 mL) with needles (e.g., Hamilton Gastight syringe with PTFE Luer Lock) to prepare and transfer the stock solution or solvent-resistant pipette tips (e.g., Solvent Safe™ pipette tips).
  - (g) To image vesicles using fluorescence, 0.2 mol% of a phospholipid-conjugated membrane dye (e.g., TopFluor PC or Lissamine Rhodamine B (1,2-dioleoyl-sn-glycero-3-phosphoethanolamine-N-(lissamine rhodamine B sulfonyl))) can be incorporated into the lipid–solvent solution.
6. The choice of oil depends on a range of considerations:
  - (a) A good starting point for the viscosity of the oil is 10–50 mPas, e.g., light mineral oil. This is viscous enough such that the emulsion droplets do not sediment rapidly toward the interface without centrifugation, but not so viscous that the expected centrifugation time is unreasonably long.

- (b) It is harder to make smaller emulsion droplets with more viscous oils.
  - (c) The oil should be high grade and pure to minimize contaminants in the membrane.
  - (d) The oil should be kept on molecular sieves to prevent moisture absorption.
  - (e) The oil should not have any propensity to incorporate into a bilayer. Hexadecane, for instance, has a similar alkyl tail length as many membrane lipids and is thus likely to incorporate.
7. When choosing the two solution compositions, it is paramount for the inner aqueous phase to be denser than the subphase, hence sucrose in the inner aqueous phase and glucose in the subphase. Other considerations:
- (a) The inner aqueous phase and the subphase should be osmotically matched.
  - (b) If the solutions cannot be precisely matched, the inner aqueous phase should be at a slightly lower osmolarity such that newly formed vesicles can have some excess surface area to prevent buildup of membrane tension.
  - (c) Depending on the lipid and experiment, the presence of a buffering salt may not be necessary.
8. Whether the lipids will work using this method depends on two factors: (1) the lipid must be marginally soluble in the oil, and (2) the lipid must not be so soluble that it ceases to be interfacially active and readily coat any oil–water interfaces. The oil–water interfacial tension, with and without lipid, could be measured to verify the lipid’s interfacial activity. Alternatively, prepare a small quantity of the lipid–oil mixture and attempt to make an emulsion. If the emulsion does not split immediately, then the lipid may be interfacially active enough to proceed with the rest of the method.
9. After purchasing lipids, store at  $-20^{\circ}\text{C}$  and flush with nitrogen gas after opening. This is more critical for lipids containing unsaturated fatty acids because they are susceptible to oxidation. If unsure of lipid quality, use mass spectrometry to check that the molecular weight is as expected.
10. Making aliquots of lipids in small vials is recommended so that only a small amount is exposed to oxygen per experiment. Flush the tubes with nitrogen or argon after making the aliquots.
11. Fatty acids can be pipetted if heated above their  $T_m$ ; it is helpful to make aliquots in containers that can be heated in your desired apparatus (water bath, heat block).

12. When directly pipetting a liquid lipid such as fatty acids, some lipids may stick to the pipette tip. If the exact concentration of fatty acid is critical to know, weigh the vial before and after lipid addition to determine the exact amount added.
13. Suitable solvents include those suggested in **Note 5** as well as DMSO because the solvent is not being evaporated.
14. Do not attempt to put much more than 5 µmol of lipid onto a 1 cm × 1 cm area; otherwise the paper does not spread the lipids out as efficiently.

## References

1. Tanaka T, Sano R, Yamashita Y, Yamazaki M (2004) Shape changes and vesicle fission of Giant Unilamellar vesicles of liquid-ordered phase membrane induced by Lysophosphatidylcholine. *Langmuir* 20:9526–9534. <https://doi.org/10.1021/la049481g>
2. de Carvalho CCCR, Caramujo MJ (2018) The various roles of fatty acids. *Mol J Synth Chem Nat Prod Chem* 23:2583. <https://doi.org/10.3390/molecules23102583>
3. Chen IA, Walde P (2010) From self-assembled vesicles to protocells. *Cold Spring Harb Perspect Biol* 2:a002170. <https://doi.org/10.1101/cshperspect.a002170>
4. Wang A, Szostak JW (2019) Lipid constituents of model protocell membranes. *Emerg Top Life Sci* 3:537–542. <https://doi.org/10.1042/ETLS20190021>
5. Lonchin S, Luisi PL, Walde P, Robinson BH (1999) A matrix effect in mixed phospholipid/fatty acid vesicle formation. *J Phys Chem B* 103:10910–10916. <https://doi.org/10.1021/jp9909614>
6. Jin L, Kamat NP, Jena S, Szostak JW (2018) Fatty acid/phospholipid blended membranes: a potential intermediate state in protocellular evolution. *Small Weinh Bergstr Ger* 14: e1704077. <https://doi.org/10.1002/smll.201704077>
7. Cheng Z, Luisi PL (2003) Coexistence and mutual competition of vesicles with different size distributions. *J Phys Chem B* 107: 10940–10945. <https://doi.org/10.1021/jp034456p>
8. Fuller N, Rand RP (2001) The influence of lysolipids on the spontaneous curvature and bending elasticity of phospholipid membranes. *Biophys J* 81:243–254
9. Alves M, Bales BL, Peric M (2008) Effect of Lysophosphatidylcholine on the surface hydration of phospholipid vesicles. *Biochim Biophys Acta* 1778:414–422. <https://doi.org/10.1016/j.bbamem.2007.11.005>
10. Kindt JT, Szostak JW, Wang A (2020) Bulk self-assembly of giant, unilamellar vesicles. *ACS Nano* 14:14627–14634. <https://doi.org/10.1021/acsnano.0c03125>
11. Kresse KM, Xu M, Pazzi J et al (2016) Novel application of cellulose paper as a platform for the macromolecular self-assembly of biomimetic giant liposomes. *ACS Appl Mater Interfaces* 8:32102–32107. <https://doi.org/10.1021/acsmi.6b11960>
12. Lowe LA, Loo DWK, Wang A (2022) Methods for forming Giant Unilamellar fatty acid vesicles. In: Cranfield CG (ed) *Membrane lipids: methods and protocols*. Springer, New York, pp 1–12
13. Pautot S, Frisken BJ, Weitz DA (2003) Production of Unilamellar vesicles using an inverted emulsion. *Langmuir* 19:2870–2879. <https://doi.org/10.1021/la026100v>
14. Fujikawa SM, Chen IA, Szostak JW (2005) Shrink-wrap vesicles. *Langmuir* 21:12124–12129. <https://doi.org/10.1021/la052590q>
15. Budin I, Szostak JW (2011) Physical effects underlying the transition from primitive to modern cell membranes. *Proc Natl Acad Sci* 108:5249–5254. <https://doi.org/10.1073/pnas.1100498108>
16. Peterlin P, Arrigler V, Kogej K et al (2009) Growth and shape transformations of giant phospholipid vesicles upon interaction with an aqueous oleic acid suspension. *Chem Phys Lipids* 159:67–76. <https://doi.org/10.1016/j.chemphyslip.2009.03.005>
17. Holme MN, Rashid MH, Thomas MR et al (2018) Fate of liposomes in the presence of phospholipase C and D: from atomic to supramolecular lipid arrangement. *ACS Cent Sci* 4: 1023–1030. <https://doi.org/10.1021/acscentsci.8b00286>



# Chapter 7

## Scalable Liposome Synthesis by High Aspect Ratio Microfluidic Flow Focusing

Jung Yeon Han, Zhu Chen, and Don L. Devoe

### Abstract

Microfluidic flow focusing provides an efficient approach to the generation of nanoscale lipid vesicles of tunable size and low size variance. Scalable nanoliposome synthesis over a wide range of production rates can be readily achieved using a high aspect ratio flow focusing device fabricated by widely available additive manufacturing methods. Here we detail methods for the manufacture and operation of a 3D-printed microfluidic flow focusing technology enabling the synthesis of liposomes with modal diameters ranging from ca. 50–200 nm at production rates up to several hundred milligrams lipid per hour.

**Key words** Nanoliposomes, Nanomedicine, Hydrodynamic flow focusing, Nanoparticles, Lipids, Vesicles, Drug delivery, 3D printing, Additive manufacturing

---

### 1 Introduction

The microfluidic flow focusing technique [1] is a continuous-flow liposome production process that enables tunable control over the resulting vesicle size and low polydispersity without the need for additional post processing steps. By taking advantage of precisely defined laminar flow streams in a merging microchannel network, microfluidic flow focusing sheathes a stream of solvated lipids by two adjacent flows of aqueous buffer to focus the lipids into a narrow sheet with final width determined by buffer/lipid flow rate ratio [2]. The interplay between the diffusion of solvent, buffer, and lipid results in the focusing region allows a sharp lipid solubility gradient to be formed, thereby promoting rapid and uniform vesicle generation. By adjusting the flow rate ratio, the length scale of the focused lipid stream, and thus the size of the resulting vesicles, can be readily tuned by the operator [2, 3]. The technique can be

---

**Supplementary Information** The online version contains supplementary material available at [https://doi.org/10.1007/978-1-0716-2954-3\\_7](https://doi.org/10.1007/978-1-0716-2954-3_7).

further combined with additional microfluidic elements to enable liposome surface modification [4] together with passive [5, 6] and active [7] loading of therapeutic compounds within the resulting nanoparticles.

Production throughput for the microfluidic technique is limited by the small microchannel size scale required for effective lipid focusing. Higher synthesis rates have been demonstrated by extending the channel width while maintaining consistent dimensions in the focusing axis, but the fabrication and integration of the large aspect ratio features employed in these devices is challenging without sacrificing liposome size control [8]. To overcome these microfabrication challenges, the use of high-resolution additive manufacturing using stereolithography (SLA) with digital light processing (DLP) to pattern complex 3D features in a photosensitive polymer opens new opportunities for microfluidic devices with designs that cannot be achieved with conventional planar microfluidics [9–11]. We have leveraged SLA-DLP fabrication to design and manufacture high aspect ratio microfluidic flow focusing devices capable of high-volume liposome synthesis using an optimized design that can be replicated by any laboratory with access to a suitable SLA-DLP printer [12]. The resulting devices offer tunable vesicle dimensions below 100 nm and may be operated at volumetric flow rates of at least 30 mL/min, allowing liposome synthesis at production rates up to 4 mg/min from a single device. This production rate is suitable for common pilot-scale manufacture of liposomal nanomedicines, and higher rates may be readily achieved by operating multiple low-cost devices in parallel.

---

## 2 Materials

Use analytical grade reagents. Prepare all reagents at room temperature, unless indicated otherwise. Store lipids at –20 °C. Follow all applicable regulations when disposing waste materials.

### 2.1 Flow Focusing Device Fabrication

1. Microfluidic flow focusing device design file: see Supplementary Information stereolithography CAD design file (liposome\_flow\_focusing\_MiMB.stl).
2. SLA-DLP 3D printer: Perfactory 4 (EnvisionTEC Inc.) or similar instrument with a projected voxel size scale below 100 µm.
3. Photosensitive resin: HTM140 (EnvisionTEC Inc.) or similar high resolution SLA-DLP polymer resin.
4. Isopropanol (IPA).
5. Otoflash UV curing system.

## 2.2 Lipid Preparation

1. 1,2-Dimyristoyl-sn-glycero-3-phosphocholine (DMPC).
2. Cholesterol.
3. Dicetyl phosphate (DCP).
4. Lipophilic dye for imaging: 1,1'-dioctadecyl-3,3,3',3' tetra-methylindocarbocyanine perchlorate (DiIC<sub>18</sub>).
5. Chloroform.
6. Anhydrous ethanol.
7. Phosphate-buffered saline (PBS).
8. 0.22 µm syringe filter.

## 2.3 Flow Focusing Device Operation

1. Stainless steel blunt needle segments: 22 gauge, 1 in length (Hamilton Inc.).
2. Syringe pumps [3]: PHD 22/2000 (Harvard Apparatus Inc.).
3. Threaded tubing fittings: F-120, 10–32 thread, 1/16 in o.d. (IDEX LLC).
4. Tygon tubing: 0.02 in i.d., 0.06 in o.d.

## 3 Methods

Perform all procedures at room temperature unless otherwise noted. Filter all solvents and buffers except chloroform through a 0.22 µm syringe filter before use. Printing and developing must be performed in a light-protected environment.

### 3.1 Flow Focusing Device Fabrication

1. Prior to printing, convert the STL file containing the microfluidic flow focusing device design into a job file using appropriate software for the specific SLA-DLP printer to be used for printing (*see Note 1*). For the STL design presented in this chapter, the job file should be defined using a 25 µm slicing distance and using printing parameters selected for maximum printing resolution (*see Note 2*).
2. After printing is completed (*see Note 3*), remove the microfluidic device from the printer stage for developing. First, thoroughly rinse its exterior with IPA. Then connect a disposable syringe with an IDEX fitting and Tygon tubing to a threaded input port of the printed device, and flush the interior of the device with IPA to remove uncured resin (*see Note 4*). Continue to flow IPA until no residual solvent is observed in the effluent; then clear IPA from the device with air (*see Note 5*). Flush IPA through the same port at least one more time followed by air to ensure complete resin removal. Repeat the same flushing steps for all three input ports in sequence.
3. Expose the device in the UV curing system for 20 min to complete the resin polymerization process. Store the fully developed device in a desiccator before use.

### 3.2 Lipid Solution Preparation

1. Prepare an initial lipid mixture of DMPC, cholesterol, and DCP in chloroform at a molar ratio of 5:4:1 (*see Note 6*). Use a glass scintillation vial to prepare the solution while actively purging the vial with nitrogen.
2. Immediately place the uncapped vial in a vacuum desiccator for at least 24 h to achieve solvent removal.
3. Rehydrate the desiccated lipid mixture in anhydrous ethanol (*see Note 7*), with the ethanol volume selected to yield the desired total lipid concentration, typically between 1 to 20 mM (*see Note 8*).
4. If desired to allow fluorescent imaging of the resulting vesicles, add 0.025 wt% DiIC<sub>18</sub> to the initial lipid mixture.

### 3.3 Flow Focusing Device Operation

1. Connect IDEX fittings to each of the four threaded ports on the printed flow focusing device (*see Fig. 1*), with blunt needle segments firmly seated inside each fitting.

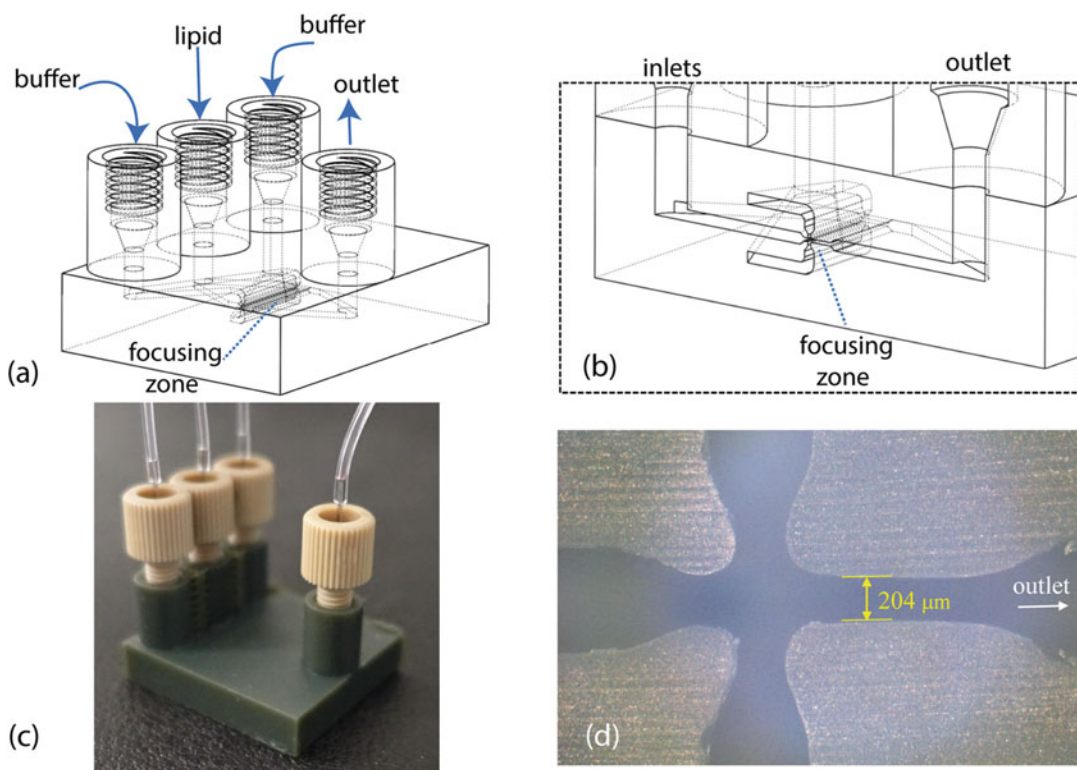


**Fig. 1** (a) Schematic of the high throughput microfluidic flow focusing device detailing the inlet and outlet ports for fluidic interfacing. (b) Detailed view of the flow focusing region. (c) Image of a flow focusing device fabricated by SLA-DLP. (d) Micrograph of the lipid focusing zone with critical dimensions on the order of 200  $\mu\text{m}$

2. Connect independent syringe pumps to the exposed needle segments on each of the lipid and buffer inlet ports using Tygon tubing.
3. Connect Tygon tubing to the waste port needle and temporarily route the opposite end to a waste vial.
4. Fill the syringe connected to the lipid inlet with the prepared lipid solution, and fill both syringes connected to the buffer inlets with phosphate-buffered saline as a hydration buffer.
5. Submerge the flow focusing device in a heated water bath at 40 °C, and wait at least 10 min for the entire device to reach the target temperature.
6. Start the flow from both buffer syringe pumps at the specified flow rate, typically between 1 and 30 mL/min. When the output visually stabilizes, initiate flow from the lipid pump at the flow rate required to reach the target ratio of buffer/lipid flow, with typical flow rate ratios in the range of 5–40 (*see Note 9*).
7. Immediately replace the waste vial with a liposome collection vial (*see Note 10*).
8. When the desired liposome solution volume has been collected, remove the outlet tube from the collection vial, and then turn off the pumps.
9. After liposome synthesis is complete, rinse the flow focusing device with isopropanol and deionized water. Store the device in a desiccator.

---

#### 4 Notes

1. When preparing the job file, orientation of the microfluidic device on the printing stage should be selected to align the length of focusing microchannel normal to the print stage. If the wide focusing channel is printed parallel to the stage, the channel ceiling can deform during printing. Depending on the SLA-DLP printer used, additional support structures may be required to prevent deformation of the inlet and outlet ports.
2. The SLA-DLP printing process should first be optimized to identify the light intensity required to achieve the desired feature resolution. In general, a lower light intensity will reduce the voxel volume and allow smaller channels to be realized. However, if the intensity is too low, the resulting print will be structurally unstable due to insufficient resin polymerization. Because print resolution can vary with ambient temperature and humidity as well as light source aging, the light intensity optimization process should be repeated periodically when fabricating multiple devices over time.

3. While printing time will depend on the specific print parameters used, a print time of approximately 5–10 h is typical. Throughput can be improved by printing multiple devices in a single run, provided that the SLA-DLP printer used for the process supports a sufficiently large working area.
4. Avoid exposing the printed devices to IPA for more than an hour before completing the secondary UV exposure. Extensive exposure to IPA at this stage may cause cracking or slight deformation of the final prints.
5. Do not attempt to flush IPA from the device using water or aqueous buffer, since any residual uncured resin can clog the fluidic channels when exposed to water. Compressed air or nitrogen is sufficient to clear the device after each IPA rinse.
6. While other lipid mixtures may be used, the resulting liposome size and size distribution may vary when working with different lipid species or lipid ratios.
7. Because unsaturated lipids are prone to oxidize in the presence of water or oxygen, dried lipid film vials must not be stored for more than a day after desiccation and should be sealed using parafilm after purging with nitrogen. Instead, the initial lipid mixture can be prepared in chloroform in larger quantity and aliquoted to smaller volume for storage at –20 °C.
8. The concentration of liposomes produced using the flow focusing process may be increased by working with a higher initial lipid concentration. However, it is important to note that higher lipid concentrations tend to yield larger vesicles and may also result in precipitation prior to vesicle formation. For the lipid mixture described here, precipitation is observed when the total lipid concentration exceeds approximately 30–40 mM.
9. Microfluidic flow focusing relies on the diffusive migration of lipids at the fluidic interface of two miscible laminar flows. At higher total flow rate, the laminar flow profile within the microfluidic system may be disrupted, negatively affecting liposome size control and size uniformity. Higher flow rate ratios generally yield smaller vesicles by more narrowly focusing the lipid stream at the fluidic junction, but at the cost of liposome productivity and concentration.
10. Liposome collection should begin as soon as the flow has stabilized after turning on the buffer and lipid pumps. Provided that the tubing connecting the syringe pumps to the flow focusing device are short (on the order of 15 cm), compliance within the flow network is minimal, and stabilization is nearly instantaneous. If longer tubing is used, or if other

sources of mechanical compliance are introduced in the fluidic system, it may be necessary to wait before moving the device outlet tube from the waste vial to the collection vial to avoid collecting effluent prior to flow stabilization.

## Acknowledgments

This work was supported by the US National Science Foundation through NSF grant CMMI1562468.

## References

1. Lu M, Ozcelik A, Grigsby CL, Zhao Y, Guo F, Leong KW, Jun T (2016) Microfluidic hydrodynamic focusing for synthesis of nanomaterials. *Nano Today* 11:778–792
2. Jahn A, Vreeland WN, Gaitan M, Locascio LE (2004) Controlled vesicle self-assembly in microfluidic channels with hydrodynamic focusing. *J Am Chem Soc* 126:2674–2675
3. Jahn A, Vreeland W, DeVoe DL, Locascio L, Gaitan M (2007) Microfluidic directed self-assembly of liposomes of controlled size. *Langmuir* 23:6289–6293
4. Hood RR, Shao C, Omiatek DM, Vreeland WN, DeVoe DL (2013) Microfluidic synthesis of PEG- and Folate-conjugated liposomes for one-step formation of targeted stealth Nano-carriers. *Pharm Res* 30:1597–1607
5. Jahn A, Reiner JE, Vreeland WN, DeVoe DL, Locascio LE, Gaitan M (2008) Preparation of nanoparticles by continuous-flow microfluidics. *J Nanopart Res* 10:893–1087
6. Jahn A, Reiner JE, Vreeland WN, DeVoe DL, Locascio LE, Gaitan M (2008) Controlled encapsulation of a hydrophilic drug simulant in Nano-liposomes using continuous flow microfluidics. *TechConnect Briefs* 1:684–687
7. Hood RR, Vreeland WN, DeVoe DL (2014) Microfluidic remote loading for rapid single-step liposomal drug preparation. *Lab Chip* 14:3359–3367
8. Hood RR, DeVoe DL (2015) High throughput continuous flow production of nanoscale liposomes by microfluidic vertical flow focusing. *Small* 11:5790–2799
9. Gong H, Woolley AT, Nordin GP (2016) High density 3D printed microfluidic valves, pumps, and multiplexers. *Lab Chip* 16:2450–2458
10. Waheed S, Cabot JM, Macdonald NP, Lewis T, Guijt RM, Paull B, Breadmore MC (2016) 3D printed microfluidic devices: enablers and barriers. *Lab Chip* 16:1993–2013
11. Macdonald NP, Cabot JM, Smejkal P, Guijt RM, Paull B, Breadmore MC (2017) Comparing microfluidic performance of three-dimensional (3D) printing platforms. *Anal Chem* 89:3858–3866
12. Chen Z, Han JYJY, Shumate L, Fedak R, DeVoe DL (2019) High throughput Nanoliposome formation using 3D printed microfluidic flow focusing chips. *Adv Mater Technol* 4: 1800511



# Chapter 8

## Preparation of Doxorubicin Liposomes by Remote Loading Method

Jian Chen

### Abstract

Doxorubicin liposome is one of the most important nano-drug formulations. DOXIL, the first FDA-approved doxorubicin liposomes, is also the first nano-drug product in market. Since it was approved in 1995, DOXIL have been widely used in the treatment of various tumors. Several important technologies used in the development of doxorubicin liposomes, especially the remote loading technology, have an extremely important impact on the later liposome research and development. This article describes a protocol to prepare doxorubicin liposomes by remote loading in a laboratory.

**Key words** Doxorubicin, Liposomes, Remote loading, Ammonium sulfate

---

### 1 Introduction

As the first nano-drug approved by the FDA, DOXIL®, the doxorubicin liposome, is a milestone for pharmaceutical area [1]. There are a number of novel methods applied in the manufacturing of DOXIL. For example, remote loading greatly improves the encapsulation rate and stability of liposomes for water-soluble drugs, and PEGylation significantly improves the retention time of drugs in the body and stability in vitro as well. These technologies have a great impact on the later development of liposomal dosage forms [2, 3]. So far, doxorubicin liposomes are still important therapeutic drug products for tumors such as Kaposi's sarcoma. In addition, doxorubicin with bright red color has a strong fluorescence signal under the excitation of visible light. Therefore, it can be used as an important drug model in studies of nano-pharmaceutical preparation. This article will describe the preparation and characterization of doxorubicin liposomes.

---

## 2 Materials

Zeta-sizer Nano ZS-90 (Malvern Instruments, Malvern, UK).  
Talos F200C G2 TEM (Thermo Fisher Scientific, USA).  
LIPEX® liposome extruder (Northern Lipids, Canada).  
Magnetic stirrer (Sile Instruments Co., LTD., Shanghai).  
Rotary evaporator (Zhengzhou Greatwall Scientific Industrial and Trade Co., LTD., China).  
UV-visible spectrophotometer (Thermo Fisher, USA).  
KQ-300DA ultrasonic cleaner (Kunshan Shumei Ultrasonic Instruments Co., LTD., China).  
FE20 pH meter (Mettler Toledo, Switzerland).  
Eppendorf Thermomixer Compact 5350 Mixer (Marshall Scientific LTD., USA).

### 2.1 Sucrose Solution (10% W/V)

Add an appropriate amount of deionized water to dissolve 1000 g sucrose followed by dilution to 10,000 mL. Store the solution at room temperature.

### 2.2 $(\text{NH}_4)_2\text{SO}_4$ Solution (250 mM, pH 4.0)

Use about 90 mL deionized water to dissolve 3.3 g  $(\text{NH}_4)_2\text{SO}_4$  (see Note 1). Adjust the pH of the solution to 4.0 by hydrochloric acid solution and then q.s to 100.0 mL with deionized water. Store the solution at room temperature.

### 2.3 Lipid Solution

Weigh 83.6 mg hydrogenated soybean phospholipids, 31.0 mg cholesterol, and 27.4 mg DSPE-PEG 2000 (molar ratio 55:40:5) in a 10 mL round-bottom flask. Add 2.0 mL chloroform to dissolve them. Store the solution at room temperature.

### 2.4 Doxorubicin Solution (10 mg/mL)

Use 10% sucrose solution to dissolve 100.0 mg of doxorubicin hydrochloride and dilute to 10.0 mL (see Note 2).

### 2.5 Triton X100 Solution (0.5%V/V)

Dissolve 50  $\mu\text{L}$  Triton X100 with 10% sucrose solution and dilute to 10.0 mL. Store the solution at room temperature.

---

## 3 Methods

### 3.1 Preparation of Blank Liposomes (Film Forming Method)

#### 3.1.1 Lipid Film Forming

Following Subheading 2.3, remove the chloroform and form lipid film using the rotary evaporator at 50 °C.

### 3.1.2 Blank Liposomes Forming

Preheat 2.0 mL of  $(\text{NH}_4)_2\text{SO}_4$  solution (250 mM, pH 4.0) to 60 °C. Add the solution to the bottle containing the lipid film followed by sonication in a water bath at 60 °C until the lipid film is fully hydrated. Continue to sonicate the liposomes for 10 more min, and extrude the liposomal suspension through 400, 100, and 50 nm pore diameter polycarbonate filters in sequence with a LIPEX® liposome extruder (*see Note 3*). Extrude the liposomes across each filter 5 times before using another filter (*see Notes 4 and 6*). Measure the PSD of liposomes by Zetasizer Nano ZS (Malvern, UK) at 25 °C and 90° refraction angle. Equilibrate for 120 s with three rounds of each data measurement (*see Note 5*).

### 3.1.3 Transmembrane Ion Gradient Formation

Place 2.0 mL of liposomes in a 10 kDa dialysis tubing and dialyze it with more than 200 mL of 10% sucrose solution at 4 °C for 4–6 h (*see Notes 7 and 8*). Keep magnetic stirring throughout the process to ensure sufficient liquid exchange. Repeat the procedure 3 times to completely remove ammonium sulfate in the outer water phase. Store the sample at 4 °C.

## 3.2 Drug Loading

1. Mix 1.0 mL blank liposomes (lipid concentration is about 70 mg/mL) with 0.7 mL doxorubicin hydrochloride solution (10.0 mg/mL). The ratio of lipid to drug is 10:1 w/w. Shake and incubate the suspension for 0.5 h at 60 °C to obtain doxorubicin liposomes (*see Note 10*).
2. Dialyze the doxorubicin liposome in a 10 kDa dialysis bag with 10% sucrose solution with a volume at least 100 times more than liposomal suspension at 4 °C for 4 h (*see Notes 7 and 9*). Repeat three times to completely remove free doxorubicin.

## 3.3 Characterize of Doxorubicin Liposomes

### 3.3.1 Size Detection

Dilute the liposomal sample 10–30 times with 10% sucrose solution. Add the diluted sample to measurement cell. Determine the hydrodynamic size (Z-average) and polydispersity index (PDI) of liposomes by dynamic light scattering (DLS) of Zetasizer Nano ZS (Malvern, UK) at 25 °C and 90° refraction angle. Equilibrate for 120 s with three rounds of each data measurement.

### 3.3.2 Encapsulation Efficiency

Prepare 0.5% v/v Triton X100 solution with 10% sucrose solution. Prepare a series of doxorubicin hydrochloride standard solutions of 10 to 40 µg/mL using the 0.5% v/v Triton X100 solution and measure their absorbance at 480 nM to establish a standard profile. Take 50 µL of liposome sample before and after dialysis to mix with 950 µL of 0.5% Triton X100. Put the mixture into thermomixer and shake it at 60 °C for 5 min to rupture the membrane. Then dilute it 10 times with 0.5% v/v Triton X100, and measure the OD480 of each sample with 10% sucrose solution as a reference and calculate the concentration of doxorubicin (*see Notes 11 and 14*).

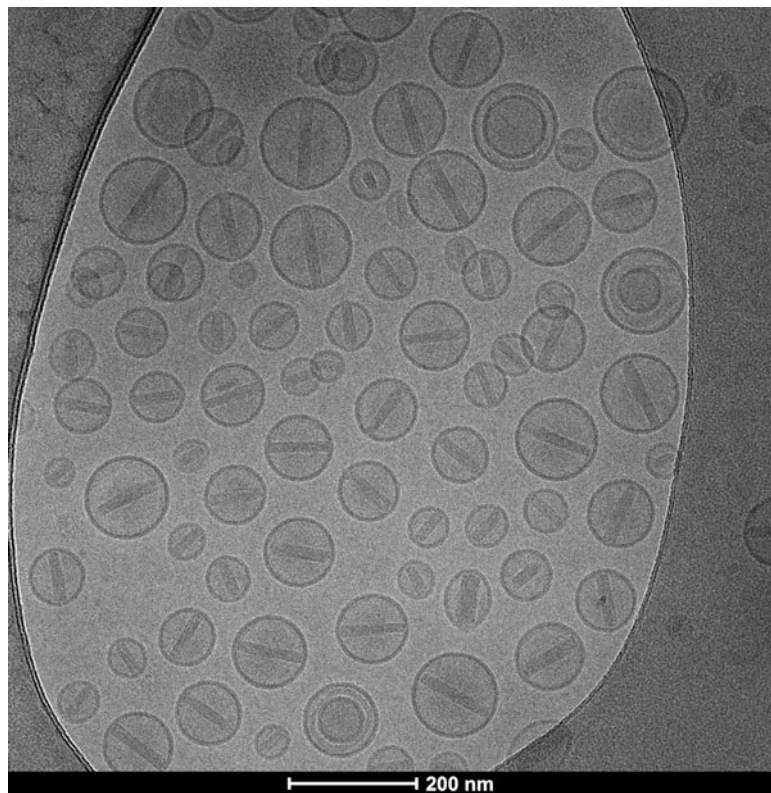


**Fig. 1** Cryo-TEM of doxorubicin liposomes

$$\text{Encapsulation efficiency} = \frac{\text{Volume after dialysis} \times \text{Concentration of doxorubicin after dialysis}}{\text{Volume before dialysis} \times \text{Concentration of doxorubicin before dialysis}}$$

### 3.3.3 Liposome Morphology by Cryo-TEM

Place the doxorubicin liposomes in a 10 kDa dialysis tubing and dialyze with deionized water with a volume more than 100 volumes greater than liposomal volume for 4 h. Repeat the procedure 5 times to completely remove sucrose in the outer water phase (*see Note 12*). Prepare the samples by placing 4.5  $\mu\text{L}$  of liposomes onto a lacey carbon-coated grid using single sided blotting for 2 s then waiting for 1 s and immersing the sample grid into nitrogen cooled ethane (100% ethane). Observe the liposome morphology using the Talos F200C G2 TEM (Thermo Fisher Scientific, USA) at liquid nitrogen temperature and 200 kV (Fig. 1) (*see Notes 1 and 13*).

---

## 4 Notes

1. This protocol is based on the ammonium sulfate gradient method, and the loading mechanism is illustrated (Fig. 2) [4–6].

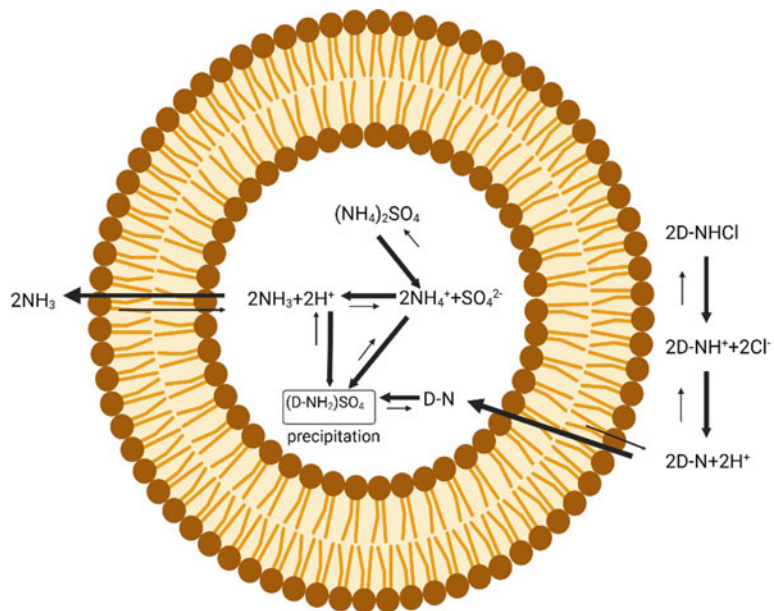


**Fig. 2** Mechanism of remote loading by ammonium sulfate gradient

By this method, doxorubicin and sulfate forms rod-like precipitates within the liposomes. Due to the support of this rod-like precipitates, some liposomes are elliptical or spindle-shaped, rather than the standard spherical shape [5].

2. Doxorubicin is very toxic and appropriate protection is necessary. Disposal of waste follows local regulations.
3. LIPEX® liposome extruder is a pressure equipment, and please handle it with care.
4. If Lipex extruder is not available in the lab, mini-extruder can also be used, and liposomes of less than 1 mL can be prepared each time. However, it will be difficult to pass through the filters if the lipid concentration is high. Moreover, the temperature control of the mini-extruder is not very convenient, and it is recommended to use a lipid formulation with a low phase transition temperature.
5. The size of blank liposomes should be around or smaller than 100 nm, and polydispersity index should be less than 0.2. Otherwise, the extruding of liposomes should be performed again.
6. Blank liposomes could be prepared by alternative methods, such as ethanol injection method, freeze-drying method, etc. If a microfluidic method is used, small unilamellar vesicles with uniform size distribution could be obtained directly and extrusion is not needed to reduce the liposomal size.

7. The dialysis tubing should be filled with liquid as possible as you can to ensure a good dialysis effect.
8. To form an ion gradient, the blank liposomes should be dialyzed with 100 volumes of dialysis medium for 3 times, each time for 4–6 h in this protocol. If the volume of deionized water for dialysis is further increased, or the number of dialysis times is increased, the encapsulation efficiency can be further improved.
9. Dialysis tubing could be replaced by dialysis cassette. The operators could also use Sephadex G-50 column to remove outer water phase or free doxorubicin.
10. The lipid formulation in this protocol is the same as DOXIL®. The operators can change formulation to fit their needs. Regardless of the formulation used, blank liposomes should be stored at temperature lower than phase transition temperature, and drug loading should be performed at temperature higher than phase transition temperature.
11. Doxorubicin is stable during the liposome preparation, and its concentration is high enough. Therefore, we use UV-visible spectrophotometer to quantify doxorubicin for convenience. HPLC method can also be used. It could not only quantify doxorubicin precisely but also detect possible degradation.
12. High concentrations of salt can reduce the contrast of the liposomal membrane. Therefore, sucrose should be removed from extra liposomal solution before perform Cryo-TEM to get better resolution of doxorubicin liposomes [7].
13. The pH gradient method can also be used, which also has a high encapsulation efficiency. However, the morphology and drug release rate of doxorubicin liposomes will vary [8, 9].
14. If the researcher wants to calculate the final drug loading rate, it is recommended to use the phosphoric acid quantitative method to determine the phospholipid content. The drug loading rate was calculated by the doxorubicin and phospholipid contents of the final doxorubicin liposomes.

## References

1. Barenholz Y (2012) Doxil®—the first FDA-approved nano-drug: lessons learned. *J Control Release* 160:117–134
2. Gubernator J (2011) Active methods of drug loading into liposomes: recent strategies for stable drug entrapment and increased *in vivo* activity. *Expert Opin Drug Deliv* 8:565–580
3. Barenholz Y (2001) Liposome application: problems and prospects. *Curr Opin Colloid Interface Sci* 6:66–77
4. Haran G, Cohen R, Bar LK et al (1993) Transmembrane ammonium sulfate gradients in liposomes produce efficient and stable entrapment of amphipathic weak bases. *Biochim Biophys Acta* 1151:201–215
5. Bolotin EM, Cohen R, Bar LK et al (1994) Ammonium sulfate gradients for efficient and stable remote loading of amphipathic weak bases into liposomes and ligandoliposomes. *J Liposome Res* 4:455–479

6. Abraham SA, Waterhouse DN, Mayer LD et al (2005) The liposomal formulation of doxorubicin. *Methods Enzymol* 391:71–97
7. Lasic DD, Frederik PM, Stuart MC et al (1992) Gelation of liposome interior. A novel method for drug encapsulation. *FEBS Lett* 312:255–258
8. Niu G, Cogburn B, Hughes J (2010) Preparation and characterization of doxorubicin liposomes. *Methods Mol Biol* 624:211–219
9. Tardi PG, Boman NL, Cullis PR (1996) Liposomal doxorubicin. *J Drug Target* 4:129–140



# Chapter 9

## Magnetic Thermosensitive Liposomes Loaded with Doxorubicin

**Mohamad Alawak, Alice Abu Dayyih, Ibrahim Awak, Bernd Gutberlet, Konrad Engelhardt, and Udo Bakowsky**

### Abstract

Liposome-mediated anticancer drug delivery has the advantage of limiting the massive cytotoxicity of chemotherapeutic agents. Doxorubicin (DOX) PEG-liposomal does however have a slow-release rate that hinders its therapeutic efficacy. In this study, an integrated therapeutic system based on magnetic thermosensitive liposomes was designed. The chelated gadolinium acquired magnetic properties in the liposomes. The hyperthermia induced by ultra-high-field magnetic resonance imaging (UHF-MRI) enhances the therapeutic effects of DOX. The DOX release from liposomes was facilitated over a narrow range of temperatures owing to the phase transition temperature of the liposomes. The magnetic properties of the liposomes were evident by the elevation of contrast after the exposure to UHF-MRI. Moreover, triple-negative breast cancer (TNBC) cells showed a significant decrease in cellular viability reaching less than 40% viability after 1 h of exposure to UHF-MRI. The liposomes demonstrated a physiological coagulation time and a minimal hemolytic potential in hemocompatibility studies; therefore, they were considered safe for physiological application. As a result, magnetic-thermosensitive liposomal guidance of local delivery of DOX could increase the therapeutic index, thereby reducing the amount of the drug required for systemic administration and the chance of affecting the adjacent tissues.

**Key words** Magnetic thermosensitive liposomes, DODA-DTPA, Ultra-high-field magnetic resonance imaging, Diagnostic, Doxorubicin, Drug delivery system

---

### 1 Introduction

Doxorubicin (DOX) is one of the most widely used antimitotic agents for the treatment of several neoplastic conditions in particular breast carcinomas [1]. DOX intercalates into DNA and disrupts topoisomerase-II-mediated DNA repair, which gives DOX its antimitotic and cytotoxic properties [2]. Additionally, DOX metabolites produce reactive oxygen species (ROS) that lead to lipid peroxidation and cellular membrane damage and would eventually trigger apoptotic pathways [3]. DOX, however, is associated with

different side effects including alopecia, nausea vomiting, extravasation reactions, and cardiotoxicity [4]. Chemotherapy treatment can be greatly improved by delivering a sufficiently accumulated dose of the drug to the tumor while reducing its systematic side effects. To overcome these challenges, PEGylated DOX liposomes were firstly introduced by Gabizon and Barenholz et al. [5]. These liposomes with prolonged circulation time were associated with a higher total accumulated dose of DOX in the tumor due to the EPR effect and appeared to have a low toxicity profile in preclinical and clinical studies. Despite these promising aspects, preclinical evidence suggests that slow and passive drug release from these stealth liposomes compromises their therapeutic efficacy [6]. Mild hyperthermia has frequently been used in the clinic owing to its ability to improve the outcome of chemotherapy with minimal side effects. Mild hyperthermia increases vascular permeability, interstitial extravasation, and blood flow. Thereby elevating intratumoral interstitial fluid flow and pressure in a manner that enhances nano-scale carrier extravasation and the EPR [7, 8].

Thermosensitive liposomes (TSL) are made from a blend of phospholipids with the possibility of triggered drug release around a tunable phase transition temperature ( $T_m$ ), typically 40–43 °C [9]. Incorporating DOX into stealth thermosensitive liposomes enables prolonged circulation and localized controlled release upon hyperthermia [10, 11]. Gadolinium, formerly known as gadolinium chloride, is a magnetic resonance contrast agent, which is designed to elevate the T1 signal of measurement by returning the protons to a more rapid “low-energy” state, resulting in a rapid increase in longitudinal magnetization [12]. As the ability to attain mild hyperthermic temperature uniformly within a tumor depends on its location and perfusion, technical advances nowadays enable precise heating above normal physiological temperature. Moreover, a magnetic resonance tomography, namely, ultra-high-field magnetic resonance tomograph (UHF-MRI), can be used to induce mild hyperthermia in tumor location after the accumulation of gadolinium encapsulated thermosensitive liposomes [13]. In this study, we examine a magnetic liposomal system that demonstrates high thermosensitivity as early as about 38 °C. With the application of UHF-MRI to our drug delivery system, we can obtain this temperature with reduced toxicity to normal tissues. Local hyperthermia induced by the applied magnetic field by using a diffusion sequence causes the liposomal bilayer to transition from the gel phase to the liquid crystal phase, resulting in DOX release.

## 2 Materials

Unless otherwise stated, all solutions were prepared with ultrapure water ( $0,05 \mu\text{S}/\text{cm}$  at  $25^\circ\text{C}$ ), and all reagents are of analytical quality. Prepare all reagents and store them at room temperature (unless otherwise noted). Sodium azide should not be added to the reagents.

### 2.1 Liposomes Formulation

1. 1,2-Dipalmitoyl-sn-glycero-3-phosphocholine (DPPC), 1,2-distearoyl-sn-glycero-3-phosphocholine (DSPC), cholesterol, and 1,2-distearoyl-sn-glycero-3-phosphoethanolamine-N-[methoxy (polyethyleneglycol) 2000] (DSPE-PEG-2000).
2. Doxorubicin hydrochloride as drug.
3. Gadolinium trichloride as a T1 magnetic resonance contrast agent.
4. DODA-DTPA (Fig. 1) as a chelator for the complexation of gadolinium  $\text{Ga}^{3+}$  ions: 2-[2-[2-[bis(carboxymethyl)amino]ethyl-[2-(dioctadecylamino)-2-oxoethyl]amino]ethyl-(carboxymethyl) amino] acetic acid [14] that has

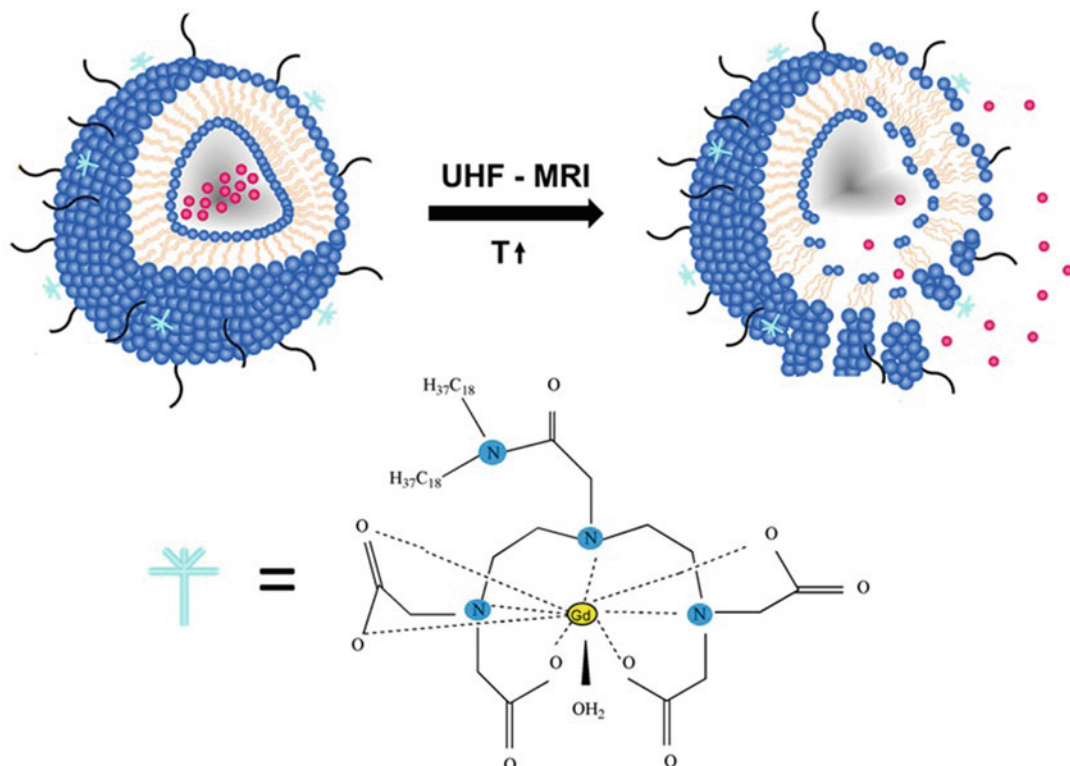


**Fig. 1** Schematic presentation of DOX release from the magnetic thermosensitive liposomes upon hyperthermia under UHF-MRI exposure by using the chelator gadolinium/DODA-DTPA complex

diethylenetriaminepentaacetic acid (DTPA) backbone that is modified with the addition of dioctadecylamine (DODA) (*see Note 1*).

5. Chloroform/methanol mixture (2:1 v/v).
  6. 250 mM ammonium sulfate solution including 0.5 mM gadolinium chloride.
  7. Extruder with polycarbonate membranes (200 nM and 100 nM).
  8. 25 mM 4-(2-hydroxyethyl)-1-piperazineethane sulfonic acid (HEPES) buffer (pH 8.4) containing 1.05 mg/mL doxorubicin hydrochloride, NaOH solution.
- 2.2 Dynamic Light Scattering (DLS)**
1. Hydrodynamic diameters of the liposomes [15] were analyzed by Zetasizer Nano ZS in a capillary cell (*see Note 2*).
  2. Ultrapure water for sample dilution (*see Note 3*).
- 2.3 Laser Doppler Velocimetry (LDV)**
1. The zeta potential of the prepared liposomes was measured by LDV using the Zetasizer Nano ZS.
  2. The measurements were performed in a clear disposable folded capillary cell.
  3. Ultrapure water was used to dilute the samples for the measurements (*see Note 3*).
- 2.4 Encapsulation Efficiency**
1. Free DOX has separated from DOX encapsulated liposomes by size-exclusion chromatography (SEC).
  2. Sephadex-G50 column was used to separate free DOX.
  3. The concentration of DOX in the liposomes after SEC was measured using UV/Vis spectrophotometry.
  4. The amount of encapsulated DOX was calculated using a calibration curve of DOX in 25 mM HEPES buffer (pH 7.4) [16].
- 2.5 Atomic Force Microscopy (AFM)**
1. The morphology and surface structure of the liposomes were visualized using AFM.
  2. Liposomes were diluted with ultrapure water.
  3. Silicon wafer for sample placement (*see Note 4*).
  4. Cantilever NSC14 Al/BS or comparable for tapping or intermittent contact mode measurements [17].
- 2.6 Transmission Electronic Microscopy (TEM)**
1. The surface structure and morphology of the prepared liposomes were investigated using the TEM (*see Note 5*).
  2. S160-3 copper grids are used as sample holders (*see Note 6*).
  3. 25 mM HEPES buffer (pH 7.4) and 2% uranyl acetate solution for sample preparation.

## **2.7 Differential Scanning Calorimetry (DSC)**

1. DSC measurements were performed to determine the phase transition of the prepared liposomes.
2. 25 mM HEPES buffer (pH 7.4) serves as a control.
3. The DSC measurements for the liposomes were performed on MicroCal VP-DSC (*see Note 7*).

## **2.8 Drug Release**

1. DOX release profile from the prepared liposomes was determined upon low hyperthermia.
2. 25 mM HEPES (pH 7.4) and dialysis bags with MWCO of 6000 to 8000.
3. A water bath and UHF-MRI were used to get the hyperthermia (*see Note 8*).
4. Samples after hyperthermia were analyzed by UV/Vis spectrophotometry.

## **2.9 Ultra-High-Field Magnetic Resonance Imaging (UHF-MRI)**

1. UHF-MRI measurements were performed on a 7 Tesla UHF-MRI.
2. A water bath was used during the measurements.

## **2.10 Cell Viability**

1. Triple-negative breast cancer (TNBC): MDA-MB-231 cell line was utilized in this project (*see Note 9*).
2. Dulbecco's Modified Eagle Medium (DMEM), 10% fetal calf serum, and a cell culture incubator were used for cultivation.
3. Dimethylsulfoxid (DMSO) and 3-(4,5-dimethylthiazol-2-yl)-2,5-diphenyltetrazolium bromide (MTT-reagent) were needed.
4. 96-well plates.
5. Plate reader at 570 nM (*see Note 10*).

## **2.11 Activated Partial Thromboplastin Time (aPTT)**

1. aPTT was used to measure the effect of the magnetic thermosensitive liposomes on the coagulation time (*see Note 11*).
2. Fresh blood samples were used in citrate tubes.
3. Coatron M1 coagulation analyzer.
4. aPTT-S Kit (TEClot) according to the manufacturer's instructions was used as described with some modifications [18].
5. aPTT reagent and calcium chloride (25 mM).

## **2.12 Ex Vivo Hemolysis Assay**

1. The hemolytic potential of the magnetic thermosensitive liposomes on blood was determined by using erythrocytes isolated from human blood [19].
2. Isolated human erythrocytes were used [18].

3. PBS buffer (pH 7.4): 137 mM sodium chloride (NaCl), 2.7 mM potassium chloride, 10 mM disodium hydrogen phosphate, and 1.8 mM potassium dihydrogenphosphate.
4. Ethylenediaminetetraacetic acid (EDTA), 0.9% NaCl, and Triton X-100® (1%) were used in this assay.
5. Centrifuge and FLUOstar Optima microplate reader were used to measure the hemolysis of the prepared liposomes.
6. An orbital shaker was used to incubate the samples in V-bottom microtiter plates.

---

### 3 Methods

Carry out all procedures at room temperature unless otherwise specified.

#### **3.1 Preparation of Magnetic Thermosensitive Liposomes**

1. Liposomes were prepared using the thin-film hydration method [16, 20].
2. Stock solutions of lipids and chelator were prepared in a chloroform/methanol mixture (2:1 v/v).
3. Lipids were mixed in a round-bottom flask (25 mL–250 mL, depending on the desired final volume) using the stock solutions. The concentrations of DPPC, DSPC, cholesterol, DSPE-mPEG2000, and the chelator were adjusted to molar ratios of 85:7.8:2:0.2:5 (*see Note 12*).
4. The organic solvents were evaporated using a rotary evaporator (*see Note 13*).
5. The formed lipid film was then hydrated in a 250 mM ammonium sulfate solution including 0.5 mM gadolinium to the total lipid concentration of 105 mg/mL [21].
6. After adding the liquid, the round bottom flask is shaken by hand (about 20 times).
7. It is then sonicated in a bath sonicator at 56 °C to obtain a uniform dispersion of liposomes (*see Note 14*).
8. The prepared liposomes were extruded using an extruder through polycarbonate membranes (200 nM and 100 nM) 21 times at 56 °C (*see Note 15*).
9. Encapsulation of DOX into the preformed liposomal core was achieved by ammonium sulfate gradient method (*see Fig. 2*) [16, 20].
10. The liposomal dispersion (105 mg/mL in ammonium sulfate) was diluted with 25 mM HEPES buffer at pH 8.4 containing 1.05 mg/mL DOX a to a molar ratio of 1:5 (DOX: total lipids).The loading process was carried out at 7 °C for 12 h [16, 22]. (*see Note 16*).

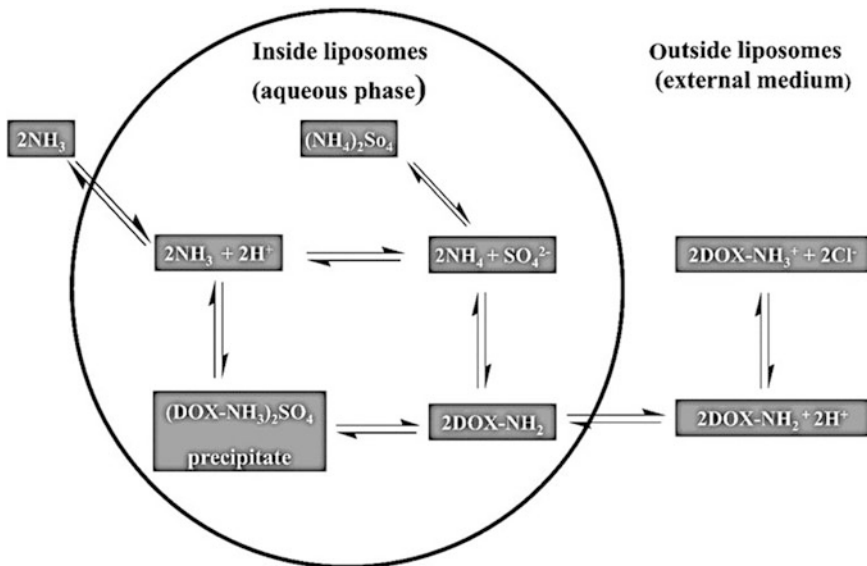


**Fig. 2** Schematic presentation of the remote loading process of DOX into liposomes via ammonium sulfate gradient method

11. The theoretical load of DOX was  $[\text{C}] \text{DOX} = 1 \text{ mg/mL}$ .
12. Purification of liposomes was done by gel filtration technique using size exclusion chromatography by Sephadex-G50 column (see also Subheading 3.3) [23].

### 3.2 Size and Zeta Potential of the Liposomes

1. The wavelength of the laser was 633 nm, and the temperature was 25 °C.
2. The scattered light was detected at an angle of 173°.
3. Before the measurement liposomes were diluted with demineralized water 1:100 [24].
4. The refractive index (1.33) and viscosity (0.88 mPa\*s) of liposomal dispersions were considered for data analysis [24] (see Note 17).
5. The obtained results were presented as an average value  $\pm$  standard deviation of three independent preparations with three replicate measurements of each preparation for at least 10 runs.
6. The prepared liposomes have a diameter of less than 200 nm with a PDI of less than 0.2 (see Note 18).
7. Zeta potential was about -14 mV.

### **3.3 Loading Efficiency of DOX**

1. The entrapment efficiency of DOX was measured by using size exclusion chromatography (SEC).
2. Sephadex-G50 column was saturated with empty liposomes to prevent loss of lipid material before adding DOX liposomes (*see Note 19*).
3. The concentration of DOX in the liposomes obtained after SEC was measured using UV/Vis spectrophotometry.
4. Encapsulation efficiency (EE) of DOX in the liposomes was calculated according to the following equation by using a calibration curve of DOX/HEPES buffer [25]:

$$\text{EE\%} = \frac{\text{DOX amount encapsulated}}{\text{Initial amount of DOX}} \times 100\% \quad (1)$$

### **3.4 Atomic Force Microscopy**

5. The encapsulation efficiency of DOX into the prepared liposomes should be greater than 50%.
1. 20 μL of prepared liposomes solution were diluted in demineralized water (1:1000) and transferred onto a piece of a silicon wafer.
2. They left for 5 min to dry.
3. AFM images have been performed on the atomic force microscope NanoWizard® 3 NanoScience.
4. A NSC14 Al/BS was used with a resonance frequency of 140 Hz and a force constant of 5 N/m.
5. AFM measurements were performed at room temperature and in a soundproof chamber (*see Note 20*).
6. The measurement was performed in intermittent contact mode (comparable to the tapping mode) with a scan speed of 0.5–1.5 Hz.
7. Liposomes have a round structure before heating (Fig. 3b), whereas they lost their structure after hyperthermia under UHF-MRI, which is shown in Fig. 3d.

### **3.5 Transmission Electronic Microscopy**

1. Liposomes were pipetted onto 300 mesh formvar-coated S160-3 copper grids and waited until they dry.
2. Liposomes were stained using uranyl acetate (2%) for 30 min (*see Note 21*).
3. Afterward, samples were heated to 37 °C or exhibited to UHF-MRI and left to be wiped before liposomes were visualized by TEM (80 kV) [26].

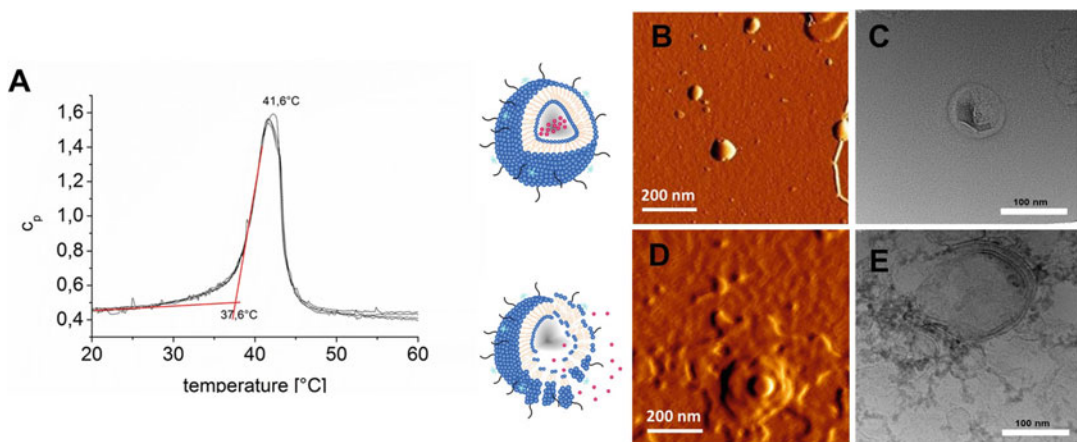


**Fig. 3** Differential scanning calorimetry thermogram of magnetic thermosensitive liposomes (a), visualization of the liposomes using AFM before heating (b) and after heating (d), transmission electron micrographs of the liposomes before heating (c) and after heating (e)

- 4. Liposomes showed a round structure, and Gd-chelate was encapsulated into the liposomes (Fig. 3c).
- 5. Liposomes were opened after hyperthermia and Gd-chelate was unlocked from the liposomes (Fig. 3e).
  
- 1. The scanned temperature range was between 20 and 60 °C.
- 2. The heating rate was 60 °C/h.
- 3. The baseline (25 mM HEPES buffer, pH 7.4) was deducted from the liposomes–thermograms.
- 4. 25 mM HEPES buffer was filled in the reference cells during the measurements [27].
- 5. The change in the phase transition of the prepared liposomes was started at approximately 38 °C, whereas a maximum value of about 42 °C (Fig. 3a).

### 3.7 Drug Release

- 1. The release profile of DOX from the magnetic liposomes was determined at different temperatures (37–40 °C) and after 1 h UHF-MRI exposure.
- 2. The calibration curve of DOX in 25 mM HEPES buffer (pH 7.4) was utilized.
- 3. DOX-magnetic liposomes (2 mL) were suspended in 25 mM HEPES buffer (pH 7.4) (1 mL).
- 4. The mixture was transferred into a dialysis bag with MWCO of 6000–8000 and incubated in 25 mM HEPES buffer (pH 7.4) (20 mL) pre-heated with stirring speed (100 rpm).

5. 1 mL from the 25 mM HEPES buffer (pH 7.4) (outer) was collected at different times and replaced with 1 mL of 25 mM HEPES buffer (pH 7.4).
6. The samples were measured by UV/Vis spectrophotometry at 480 nM.
7. Released DOX was calculated according to Eq. 2.

$$\text{Cumulative DOX release \%} = \frac{\text{DOX released}}{\text{Initial amount of DOX}} \times 100\% \quad (2)$$

8. The prepared liposomes showed no significant release at 37 °C, whereas DOX release after 1 h UHF-MRI exposure was about 68%.

### **3.8 Ultra-High-Field Magnetic Resonance Imaging**

1. UHF-MRI images of the magnetic and non-magnetic liposomes (Fig. 4a) were performed on a 7 Tesla UHF-MRI (*see Note 22*).
2. The images were acquired with a birdcage coil by applying a diffusion sequence for all images before heating and after heating exposure.

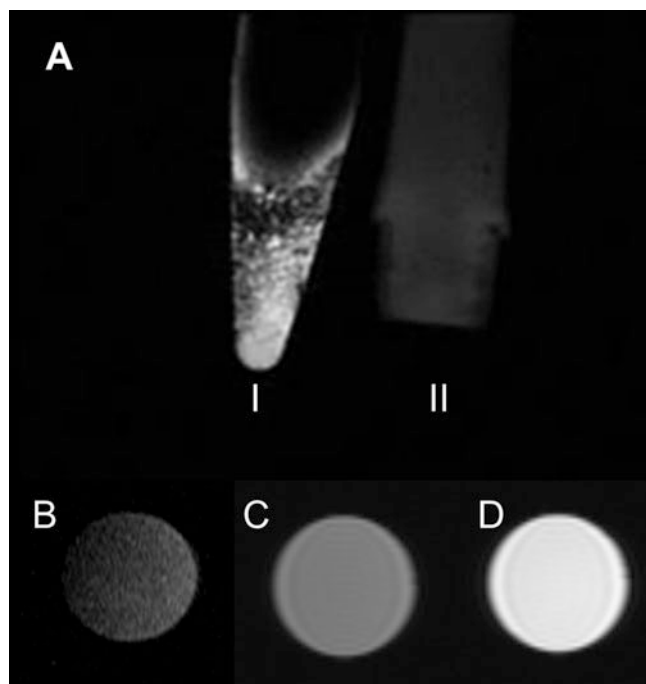


**Fig. 4** UHF-MRI of the liposomes. (A)I Magnetic liposomes and (A)II non-magnetic liposomes in an Eppendorf cap, (B) non-magnetic liposomes, (C) magnetic liposomes before heating, (D) magnetic liposomes after heating

3. To prevent hypothermia due to room temperature, samples were kept on temperature pads, which were contacted with heated water tubes to keep an initial point of 37 °C (*see Note 23*).
4. The contrast of the liposomes before heating (Fig. 4c) was lower than the contrast after heating (Fig. 4d).
5. Pure non-magnetic liposomes are visualized as control (Fig. 4b).

### **3.9 Thermal Therapy Under Magnetic Field**

1. MDA-MB-231-control cells were seeded in two-well chamber slides.
2. Cells were cultivated in DMEM at 37 °C and 7% CO<sub>2</sub> under humid conditions in a cell culture incubator.
3. The media were boosted with 10% fetal calf serum.
4. Cellular density was 20,000 cells/well.
5. Liposomes were incubated with the cells for 3 h at 37 °C, followed by cellular exposure to UHF-MRI field for 1 h.
6. The cells were further incubated for 24 h.
7. Control untreated cells were similarly incubated at the same incubation times and under UHF-MRI conditions.
8. Chamber slides were kept on temperature pads that were contacted with heated water tubes to keep 37 °C as a start temperature and prevent hypothermia due to room temperature during UHF-MRI exposure.

### **3.10 MTT Cell Viability Assay**

1. Cytotoxicity after thermal therapy was determined by measurement of cell viability based on the cellular redox potential as previously reported [28].
2. The medium was aspirated and MTT reagent was subsequently added.
3. Cells were further incubated for 4 h in the dark (*see Note 24*).
4. Actively respiring cells convert the water-soluble MTT to an insoluble purple formazan.
5. The formazan was then solubilized in DMSO, and its concentration was determined at 570 nM using a plate reader.
6. Untreated cells were used as a control representing 100% viability [29].
7. Cell viability after 1 h UHF-MRI exposure was less than 40%.

### **3.11 Activated Partial Thromboplastin Time**

1. Fresh whole blood samples were collected in citrate tubes.
2. Blood samples were centrifuged in a centrifuge at 1500 g for 10 min.

3. 25  $\mu$ L of blood plasma were mixed with 25  $\mu$ L of the sample preparation.
4. 50  $\mu$ L of aPTT reagent was mixed with the prepared sample (*see Note 11*).
5. Afterward, 50  $\mu$ L of warmed calcium chloride solution was added (25 mM).
6. A spectrophotometer was used to confirm the coagulation.
7. The time was measured in seconds; prepared liposomes showed a time of around 37 s.

### **3.12 Ex Vivo Hemolysis Assay**

1. Human blood was filled in tubes containing EDTA.
2. The filled tubes were centrifuged at 1500 g for 10 min.
3. The collected red blood cell pellet was washed three times with PBS buffer (pH 7.4) and diluted with 0.9% NaCl to a concentration of 1:50.
4. Afterward, the mixture was incubated with the samples in V-bottom microtiter plates at 37 °C for 1 h in an orbital shaker.
5. The plates were then centrifuged at 1500 g for 15 min, and absorbance of the collected supernatants was measured at 540 nM using FLUOstar Optima microplate reader.
6. PBS buffer (pH 7.4) was used as a negative control, whereas 1% Triton X-100® was used as a positive control.
7. Triton X-100® absorbance values were considered as 100% hemolysis.
8. Hemolytic potentials of the prepared liposomes were around 5%.

## **4 Notes**

1. Other chelators for positively charged metal ions such as Gd<sup>3+</sup> can also be used here. These only have to fulfill the structural features from Fig. 1: a hydrophilic head group for complexing the metal ions and a hydrophobic chain portion for insertion into the lipid membrane of the liposomes. DTPA is a diethylenetriamine backbone with five carboxymethyl groups, while DODA is a secondary amine, which is a fatty amine derivative. One of the OH groups in DTPA is substituted with a secondary amine. DODA has been utilized in the formulation of liposomes, polymeric conjugates, and others [30].
2. A device for determining the particle size diameter is required here; the measuring principle should apply to liposomes. We used the DLS method. You should always use fresh measuring

cuvettes. The device should always be calibrated beforehand and checked using standard samples.

3. Depending on the concentration of the sample and the sensitivity of the measuring device used, it should be diluted 20–100 times.
4. In principle, the use of different carriers for the sample is possible. Mica or glass microscopy slides are also common materials. For years we have been using silicon wafers from the semiconductor industry with a natural oxide thickness of 3.8 nM and a contact angle to water of >55°. If you use glass slides, you should make sure that the surface is as smooth as possible. Flame polished glasses are appropriate.
5. A TEM JEM-3010 with a retractable high-resolution slow-scan CCD camera was used in our investigations. In principle, any TEM with sufficient resolution can be used. With this method, you can visualize the lamellarity of the liposomes and the storage of the drug [31].
6. In principle, different holders can be used for the samples. Different polymer coatings can also be used. This depends on the type of TEM used itself and the measurement methodology used.
7. Any DSC that has the resolution to measure aqueous liposomal formulations can be used. The exact measurement of the phase transition is necessary for the use of thermosensitive liposomes since the exact phase transition must be known.
8. Here it is necessary to reach the phase transition temperature of the liposomes. When this is reached, the DOX release begins. To determine when the necessary temperature increase is reached by the UHF-MRI, a device is required that makes this possible. We used a commercial 7 Tesla UHF-MRI (Bruker BioSpin GmbH, Rheinstetten, Germany) for this. But you can also use a simple magnetic coil that generates a high-frequency alternating magnetic field [32].
9. We used the MDA-MB-231 cell line for our investigations. The investigations can also be carried out with other cell lines. Both adherently growing and cell suspensions can be used.
10. We used the Plate Reader FLUOstar Optima. Any plate reader with a measuring wavelength of 570 nM can be used.
11. Any comparable methodology for measuring activated partial thromboplastin time can be used here. We used the Coatron M1 coagulation analyzer (Teco, Neufahrn, Germany) using aPTT-S Kit (TEClot).
12. Maintaining the correct concentration ratios is very important. This ratio determines the phase transition temperature of the liposomes. One should use enough lipid to be able to carry out

all experiments with one batch of liposomes. The amount of lipid used depends on the number of experiments planned and the amount of lipid present. To be able to carry out all the specified experiments with triplicates, you should allow for around 500 mg of total lipids. It is best to do a trial run with a small amount of lipids.

13. The vacuum should be adjusted so that the solvent slowly evaporates without foaming. The rotation speed must be adjusted so that the lipid film formation takes place in the lower half of the round-bottom flask. At the end of the evaporation, the temperature can be increased up to 60 °C to remove residual solvent.
14. We used the Elmasonic P30 H bath sonicator (Elma Hans Schmidbauer, Singen, Germany) at the maximum level (about 50 W) with continuous ultrasound. Any other temperature-controlled bath sonicator should work as well. In any case, it should be ensured that the temperature selected is above the phase transition temperature of the individual lipid components. The sonication is ended when a white opalescent and highly viscous liposome dispersion has formed, which takes about 30 min. If the dispersion does not become homogeneous, increase the temperature slightly, and continue the sonication. In order to disperse the entire lipid film, it is often necessary to change the position of the round-bottom flask in the ultrasonic bath.
15. We used a mini extruder (Avanti Polar Lipids, Alabaster, USA) to adjust the size of the liposomes. While using the extruder, be sure to work on it slowly to avoid damaging the liposomes. The highly viscous liposome dispersion must always be heated during extrusion. With our mixture, 56 °C was sufficient. Because of the high viscosity, the process can take more than 1 h. Please make sure to use the filter with the pore diameter of 200 nM first and then the filter with 100 nm.
16. The pH of the HEPES buffer must be adjusted with sodium hydroxide solution (NaOH). The dilution is carried out slowly over a period of about 10 min.
17. Changes in the refractive index strongly affect the calculation of particle diameters. The dilution of the liposome dispersion is necessary to set the desired viscosity (0.88 mPa\*s).
18. If the PDI is significantly greater than 0.2, it can be assumed that the particle size distribution is bimodal or polymodal. In this case, the mean diameter (z-ave) of the liposomes is not very meaningful. The size distribution should then be checked with a visual method such as AFM or TEM.
19. In principle, the liposomes can interact with the chromatographic material. This can cause the liposomes to burst

and DOX to be released. This can be reduced or prevented by preloading the chromatography column with empty liposomes.

20. It is important to avoid noise and vibration during AFM measurement. Every noise or vibration will have an influential effect on the AFM efficiency. It should also be ensured that the force interaction of the cantilever with the liposome surface is as low as possible. The exact settings depend on the used AFM.
21. The uranyl acetate solution is pipetted onto the dried liposome dispersion. A drop should form. The lipids are negatively contrasted by the uranyl acetate. The remaining drop is then removed. Caution: all uranium compounds are toxic! Observe the disposal regulations!
22. If you will be in the same room with UHF-MRI, you have to remove all metallic objects and jewelry. The presence of any metallic object or jewelry during MRI experiments can be a major problem.
23. It is necessary to prevent hypothermia due to room temperature during UHF-MRI exposure by keeping chamber slides on temperature pads that were contacted with heated water tubes to keep 37 °C as a start temperature.
24. During the MTT assay, be sure to incubate the cells in the dark after adding the MTT reagent. The MTT reagent is highly sensitive to light.

## References

1. Harris L, Batist G, Belt R et al (2002) Liposome-encapsulated doxorubicin compared with conventional doxorubicin in a randomized multicenter trial as first-line therapy of metastatic breast carcinoma. *Cancer* 94:25–36. <https://doi.org/10.1002/cncr.10201>
2. Thorn CF, Oshiro C, Marsh S et al (2011) Doxorubicin pathways: pharmacodynamics and adverse effects. *Pharmacogenet Genomics* 21:440–446. <https://doi.org/10.1097/FPC.0b013e32833fffb56>
3. Tsang W, Chau SP, Kong S et al (2003) Reactive oxygen species mediate doxorubicin induced p53-independent apoptosis. *Life Sci* 73:2047–2058. [https://doi.org/10.1016/S0024-3205\(03\)00566-6](https://doi.org/10.1016/S0024-3205(03)00566-6)
4. Perez AT, Domenech GH, Frankel C et al (2002) Pegylated liposomal doxorubicin (Doxil) for metastatic breast cancer: the Cancer Research Network, Inc., experience. *Cancer Investig* 20(Suppl 2):22–29. <https://doi.org/10.1081/cnv-120014883>
5. Gabizon A, Catane R, Uziely B et al (1994) Prolonged circulation time and enhanced accumulation in malignant exudates of doxorubicin encapsulated in polyethylene-glycol coated liposomes. *Cancer Res* 54:987–992
6. Zhao Y, Alakhova DY, Kim JO et al (2013) A simple way to enhance Doxil® therapy: drug release from liposomes at the tumor site by amphiphilic block copolymer. *J Control Release* 168:61–69. <https://doi.org/10.1016/j.jconrel.2013.02.026>
7. Kong G, Braun RD, Dewhirst MW (2001) Characterization of the effect of hyperthermia on nanoparticle extravasation from tumor vasculature. *Cancer Res* 61:3027–3032
8. Greish K (2010) Enhanced permeability and retention (EPR) effect for anticancer nanomedicine drug targeting. *Methods Mol Biol* 624: 25–37. [https://doi.org/10.1007/978-1-60761-609-2\\_3](https://doi.org/10.1007/978-1-60761-609-2_3)
9. Lindner LH, Eichhorn ME, Eibl H et al (2004) Novel temperature-sensitive liposomes with

- prolonged circulation time. *Clin Cancer Res* 10:2168–2178. <https://doi.org/10.1158/1078-0432.ccr-03-0035>
10. Gaber MH, Wu NZ, Hong K et al (1996) Thermosensitive liposomes: extravasation and release of contents in tumor microvascular networks. *Int J Radiat Oncol Biol Phys* 36:1177–1187. [https://doi.org/10.1016/s0360-3016\(96\)00389-6](https://doi.org/10.1016/s0360-3016(96)00389-6)
  11. Kneidl B, Peller M, Winter G et al (2014) Thermosensitive liposomal drug delivery systems: state of the art review. *Int J Nanomedicine* 9:4387–4398. <https://doi.org/10.2147/IJN.S49297>
  12. Henkelman RM, Stanisz GJ, Graham SJ (2001) Magnetization transfer in MRI: a review. *NMR Biomed* 14:57–64. <https://doi.org/10.1002/nbm.683>
  13. Kim MS (2016) Investigation of factors affecting body temperature changes during routine clinical head magnetic resonance imaging. *Iran J Radiol* 13:e34016. <https://doi.org/10.5812/iranjradiol.34016>
  14. Alawak M, Mahmoud G, Dayyih AA et al (2020) Magnetic resonance activatable thermosensitive liposomes for controlled doxorubicin delivery. *Mater Sci Eng C Mater Biol Appl* 115:111116. <https://doi.org/10.1016/j.msec.2020.111116>
  15. Marxer EEJ, Brüssler J, Becker A et al (2011) Development and characterization of new nanoscaled ultrasound active lipid dispersions as contrast agents. *Eur J Pharm Biopharm* 77: 430–437. <https://doi.org/10.1016/j.ejpb.2010.12.007>
  16. Levacheva I, Samsonova O, Tazina E et al (2014) Optimized thermosensitive liposomes for selective doxorubicin delivery: formulation development, quality analysis and bioactivity proof. *Colloids Surf B Biointerfaces* 121:248–256. <https://doi.org/10.1016/j.colsurfb.2014.02.028>
  17. Sitterberg J, Ozcetin A, Ehrhardt C et al (2010) Utilising atomic force microscopy for the characterisation of nanoscale drug delivery systems. *Eur J Pharm Biopharm* 74:2–13. <https://doi.org/10.1016/j.ejpb.2009.09.005>
  18. Duse L, Pinnapireddy SR, Strehlow B et al (2018) Low level LED photodynamic therapy using curcumin loaded tetraether liposomes. *Eur J Pharm Biopharm* 126:233–241. <https://doi.org/10.1016/j.ejpb.2017.10.005>
  19. Lee GR, Wintrobe MM (1993) Wintrobe's clinical hematology, 9th edn. Lea & Febiger, Philadelphia/London
  20. Abraham SA, Waterhouse DN, Mayer LD et al (2005) The liposomal formulation of doxorubicin. *Methods Enzymol* 391:71–97. [https://doi.org/10.1016/S0076-6879\(05\)91004-5](https://doi.org/10.1016/S0076-6879(05)91004-5)
  21. Nwe K, Xu H, Regino CAS et al (2009) A new approach in the preparation of dendrimer-based bifunctional diethylenetriaminepentacetic acid MR contrast agent derivatives. *Bioconjug Chem* 20:1412–1418. <https://doi.org/10.1021/bc900057z>
  22. Fritze A, Hens F, Kimpfler A et al (2006) Remote loading of doxorubicin into liposomes driven by a transmembrane phosphate gradient. *Biochim Biophys Acta* 1758:1633–1640. <https://doi.org/10.1016/j.bbamem.2006.05.028>
  23. Negussie AH, Yarmolenko PS, Partanen A et al (2011) Formulation and characterisation of magnetic resonance imageable thermally sensitive liposomes for use with magnetic resonance-guided high intensity focused ultrasound. *Int J Hyperth* 27:140–155. <https://doi.org/10.3109/02656736.2010.528140>
  24. Hansen CB, Kao GY, Moase EH et al (1995) Attachment of antibodies to sterically stabilized liposomes: evaluation, comparison and optimization of coupling procedures. *Biochim Biophys Acta* 1239:133–144. [https://doi.org/10.1016/0005-2736\(95\)00138-s](https://doi.org/10.1016/0005-2736(95)00138-s)
  25. Plenagl N, Duse L, Seitz BS et al (2019) Photodynamic therapy - hypericin tetraether liposome conjugates and their antitumor and antiangiogenic activity. *Drug Deliv* 26:23–33. <https://doi.org/10.1080/10717544.2018.1531954>
  26. Mahmoud G, Jedelská J, Strehlow B et al (2015) Bipolar tetraether lipids derived from thermoacidophilic archaeon Sulfolobus acidocaldarius for membrane stabilization of chlorin e6 based liposomes for photodynamic therapy. *Eur J Pharm Biopharm* 95:88–98. <https://doi.org/10.1016/j.ejpb.2015.04.009>
  27. Schmid M, Wölk C, Giselbrecht J et al (2018) A combined FTIR and DSC study on the bilayer-stabilising effect of electrostatic interactions in ion paired lipids. *Colloids Surf B Biointerfaces* 169:298–304. <https://doi.org/10.1016/j.colsurfb.2018.05.031>
  28. Mosmann T (1983) Rapid colorimetric assay for cellular growth and survival: application to proliferation and cytotoxicity assays. *J Immunol Methods* 65:55–63. [https://doi.org/10.1016/0022-1759\(83\)90303-4](https://doi.org/10.1016/0022-1759(83)90303-4)
  29. Tariq I, Pinnapireddy SR, Duse L et al (2019) Lipodendriplexes: a promising nanocarrier for enhanced gene delivery with minimal cytotoxicity. *Eur J Pharm Biopharm* 135:72–82. <https://doi.org/10.1016/j.ejpb.2018.12.013>

30. Pétriat F, Roux E, Leroux JC et al (2004) Study of molecular interactions between a phospholipidic layer and a pH-sensitive polymer using the Langmuir balance technique. *Langmuir* 20:1393–1400. <https://doi.org/10.1021/la035583f>
31. Barenholz Y (2012) Doxil®--the first FDA-approved nano-drug: lessons learned. *J Control Release* 160:117–134. <https://doi.org/10.1016/j.jconrel.2012.03.020>
32. Shi C, Thum C, Zhang Q et al (2016) Inhibition of the cancer-associated TASK 3 channels by magnetically induced thermal release of Tetrrandrine from a polymeric drug carrier. *J Control Release* 237:50–60. <https://doi.org/10.1016/j.jconrel.2016.06.044>



# Chapter 10

## Preparation and Physical Characterization of DNA Binding Cationic Liposomes

Vaibhav Saxena

### Abstract

Cationic liposomes are routinely employed as one of the major nonviral transfecting agents for intracellular delivery of hydrophilic molecules such as nucleic acids, peptides, and proteins. Cationic liposomes when complexed with DNA form a strong positively charged cationic liposome–DNA complex or lipoplex. The chapter discusses, primarily, the major preparation technique for cationic liposomes and its physical characterization, with a focus on SYBR Green I dye exclusion assay and DNA encapsulation enhancement by freeze–thaw technique. SYBR Green I dye exclusion assay is a technique to determine the total amount of liposomal lipids required to bind a unit weight of DNA, which is critical for transfection experiments. Freeze–thaw technique on the other hand is one of the major techniques to improve DNA encapsulation efficiency in liposomes.

**Key words** Cationic liposomes, Lipoplex, Transfection, DNA, Fluorescence, Freeze–thaw, Dye exclusion, Extrusion, Encapsulation

---

### 1 Introduction

The cationic lipids are amphiphilic molecules, containing a positively charged polar head group (usually amino groups), a hydrophobic domain (comprising alkyl chains or cholesterol), and a linker connecting the polar head group with the non-polar tail, e.g., DOTAP, DODAB, DOTMA, etc. [1, 2]. Liposomes prepared by these cationic lipids and in combination with a neutral helper lipid are utilized as the primary choice nonviral transfection agents to deliver DNA and other genes inside the cells [3, 4]. Cationic liposomes make a strong electrostatic complex when bound to negatively charged DNA, resulting in the formation of cationic liposome–DNA complex or lipoplex, which has an overall positive charge [5–7]. Upon transfection, the positively charged lipoplex binds to the negatively charged cell membrane and enters cells through endocytosis, and then the cargo from the complex gets

released into the cytoplasm upon the escape from endo-lysosomal barrier. The escape is believed to be the results of destabilization effect of cationic liposomes on endosomes membrane [8–10].

SYBR Green I dye exclusion assay is being utilized as one of the extensive techniques for physical characterization of DNA binding cationic liposomes [11, 12]. SYBR Green I (SGI) is a highly sensitive, fluorescent nucleic acid dye that binds preferentially to dsDNA over ssDNA and RNA with little fluorescence emitted from unbound SGI molecules [13]. When DNA is mixed with SYBR Green I dye, it forms a DNA-SYBR dye complex, which when excited at 497 nM, emits the light at 520 nM. The dye exclusion assay works on the principle of determining the loss of fluorescence due to the displacement of SYBR Green I dye from the DNA-SYBR dye complex, upon the introduction of cationic liposomes [14, 15]. The binding of DNA with cationic liposomes results in the formation of strong DNA-liposomal complex. This technique is being successfully utilized to determine the total amount of liposomal lipids required to bind a unit weight of DNA. The assay finds its application in transfection experiments where it determines the total amount of liposomal formulation required to complex the DNA.

Freeze-thawing technique is one of the major techniques alongside dehydration-rehydration and reverse phase evaporation techniques to improve DNA encapsulation in liposomes [16]. For DNA binding cationic liposomes, the freeze-thawing technique further facilitates the enhanced interaction of electrostatically bound DNA with liposomal lipid membranes, thus promoting enhanced encapsulation efficiency [17–19]. In many cases, the lipoplex after the freeze-thaw cycles is further passed through the extruder membrane with a defined pore size and then gets evaluated for encapsulation efficiency [20].

---

## 2 Materials (Reagents and Equipments)

- *Reagents.*

Lipids: L-alpha phosphatidylcholine (egg phosphatidylcholine) (PC), 1,2-dioleoyl-3-trimethylammonium-propane (DOTAP) (Avanti Polar Lipids, Alabaster, AL, USA). Storage –20 °C. SYBR Green I dye and Lambda dsDNA. Storage –20 °C (Invitrogen). Buffer media: Phosphate buffer saline (PBS, pH 7.4) or Trisaminomethane (Tris) buffer, pH 7.4, HEPES buffer (N-2-hydroxyethylpiperazine-N-2-ethane sulfonic acid) pH 7.4 and nuclease free water (Fisher Scientific, Pittsburgh, PA, USA). Storage +25 °C.

- *Equipment.*

Rotary evaporator, round-bottom flasks and tubes and probe sonicator (Fisher Scientific Model 120 Sonic Dismembrator), fluorescence spectrophotometer (Hitachi), cuvettes (clear on four sides), vortex mixer, mini-extruder (Avanti®), micro-pipettes, and micropipette tips.

---

### 3 Methods-A

#### A. Preparation of DNA binding cationic liposomes.

1. A standard thin-film hydration method will be utilized to prepare DNA binding cationic (DOTAP) liposomes.
2. In a round-bottom flask, take an appropriate amount of PC and DOTAP lipids (e.g., 90:10 molar ratio) from chloroform stock solutions to give the desired mole fraction of individual lipid with a total lipid concentration of 5 mg/mL in the hydrated form (*see Note 1*).
3. Remove chloroform under vacuum at 40 °C for 30 min using a rotary evaporator to generate a thin dried lipid film (*see Note 2*).
4. Hydrate the dried lipid film using either phosphate buffer saline (PBS, pH 7.4) or 10 mM Tris buffer (pH 7.4) (*see Note 3*).
5. Sonicate the resulting crude liposomal suspension of multilamellar vesicles (MLVs) using a probe sonicator for two 5 min periods with an interval of 1 min, in an ice-water bath to generate small unilamellar vesicles (SUVs) liposomes (*see Note 4*).
6. Transfer the prepared DOTAP liposomes (SUVs) to fresh round-bottom flask or tubes and proceed to physical characterization studies (*see Note 5*).

---

### 4 Notes-A

1. Cover the round-bottom flask and stock lipid tubes with parafilm all the time to prevent chloroform evaporation. Perform the step in laboratory fume hood to prevent inhalation of chloroform.
2. Fill the level of water bath in rotary evaporator sufficient to ensure partial submersion of round-bottom flask.
3. Shake the round bottom flask to ensure complete hydration of lipid film.

4. Fill sufficient amount of ice in water bath of probe sonicator to prevent the fall in water temperature. Align the sonicator by submerging the probe in the hydrated suspension, placed just sufficiently above the base of the tube/flask.
5. Cover the liposome tube/flask with parafilm or aluminum foil.

## 5 Methods-B

### B. SYBR dye exclusion assay for DNA titration.

1. Prepare a 1:5000 working stock solution of SYBR Green I dye by diluting 2  $\mu$ L of the dye with 10,000  $\mu$ L of 5 mM HEPES buffer, pH 7.4 (*see Note 1*).
2. Prepare a mix of 2.5 mL of HEPES buffer, pH 7.4, and 0.5 mL SYBR Green I dye solution (1:5000 diluted with HEPES buffer) in a 3 mL disposable cuvette (*see Note 2*).
3. Using micropipettes, add a known amount of unlabeled DNA (~0.5–2  $\mu$ g) to the premix from **step 2**.
4. Measure and record the fluorescence emission from the solution at 520 nM with a Hitachi Fluorescence spectrophotometer set at an excitation wavelength of 497 nM, 2.5 mM excitation, and emission slits (*see Note 3*).
5. Vortex the premade cationic liposomes (*see Subheading 3, Method-A*) briefly for 30 s and then add the liposomes to the cuvette mix in 5–10  $\mu$ L increments until the fluorescence of SYBR dye–DNA complex was completely lost. Perform the measurements in triplicate (*see Note 4*).
6. The final DNA binding capacity of cationic liposomes was then determined in terms of total  $\mu$ g of liposomal lipids/ $\mu$ g of DNA (*see Note 5*).

## 6 Notes-B

1. Prepare the stock solution in dark, protected from light due to light sensitivity of SYBR Green I dye. Keep the stock solution tubes covered with aluminum foil all the time.
2. Mix the stock solution well with HEPES buffer in a disposable cuvette.
3. Add DNA and allow the fluorescence reading from DNA-SYBR dye complex to stabilize before recording.
4. Add the liposomes slowly to the cuvette and carefully record the decrease in fluorescence readings.
5. Convert the volume of liposomes added in  $\mu$ L to the amount of liposomal lipids in  $\mu$ g.

---

## 7 Methods-C

- C. *Improving DNA encapsulation in lipoplex by freeze-thaw technique.*
1. A standard thin-film hydration method was utilized to prepare DOTAP-based cationic liposomes (*see Subheading 3, Method-A*).
  2. Make a stock solution in (mg/mL) of the known amount of DNA in nuclease free water (*see Note 1*).
  3. Determine the amount of liposomal lipids required to bind a unit weight of DNA as per SYBR Green I dye exclusion assay (*see Subheading 5, Method-B*).
  4. To prepare DNA-cationic liposome complex (lipoplex), combine a known amount of DNA to the pre-determined quantity of cationic liposomal formulation as determined by SYBR assay from step 3 (*see Note 2*).
  5. Vortex the mix and keep the tube containing the lipoplex at room temperature for 15–20 min.
  6. Transfer the freshly prepared lipoplex in cryogenic vial to perform freeze-thaw cycles. For freezing cycle, dip the vial in liquid nitrogen (−196 °C) for 5 min, followed by a thaw cycle in water bath at 40 °C for 5 min. Repeat the freeze-thaw cycles 10 times (*see Note 3*).
  7. Transfer the contents from cryogenic vial to fresh round-bottom flask or tubes.
  8. Keep the freshly prepared lipoplex by freeze-thaw technique at room temperature for at least 15–20 min before proceeding for lipoplex characterization studies (*see Note 4*).
  9. Additionally, depending upon the size of nucleic acid and nature of the experimental study, a handheld mini-extruder is utilized to pass the lipoplex after freeze-thaw cycles, through the extruder membrane of specific pore size (e.g., 0.1 µM, 0.2 µM) for defined number of cycles (*see Note 5 and 6*).

---

## 8 Notes-C

1. Use fresh nuclease free water to reconstitute the lyophilized DNA.
2. Mix the DNA and liposomes in a fresh mini-centrifuge tube.
3. Minimum of ten freeze-thaw cycles are required for enhanced DNA encapsulation.

4. Cover the lipoplex tube/flask with parafilm or aluminum foil.
5. Use fresh extruder membrane prior to each usage.
6. Refer to mini-extruder instrument manual for detailed operation understanding.

## References

1. Lonez C, Vandenbranden M, Ruysschaert JM (2008) Cationic liposomal lipids: from gene carriers to cell signaling. *Prog Lipid Res* 47: 340–347
2. Martin B, Sainlos M, Aissaoui A, Oudrhiri N, Hauchecorne M, Vigneron JP et al (2005) The design of cationic lipids for gene delivery. *Curr Pharm Des* 11:375–394
3. Felgner PL, Gadek TR, Holm M, Roman R, Chan HW, Wenz M, Northrop JP, Ringold GM, Danielsen M (1987) Lipofection: a highly efficient, lipid-mediated DNA-transfection procedure. *Proc Natl Acad Sci U S A* 84: 7413–7417
4. Simões S, Pires P, Düzgünes N, Pedroso de Lima MC (1999) Cationic liposomes as gene transfer vectors: barriers to successful application in gene therapy. *Curr Opin Mol Ther* 1: 147–157
5. Lasic DD, Strey HH, Stuart MCA, Podgornik R, Frederik PM (1997) The structure of DNA-liposome complexes. *J Am Chem Soc* 119:832–833
6. Radler JO, Koltover I, Salditt T, Safinya CR (1997) Structure of DNA-cationic liposome complexes. DNA intercalation in multilamellar membranes in distinct interhelical packing regimes. *Science* 275:810–814
7. Simberg D, Weisman S, Talmon Y, Barenholz Y (2004) DOTAP (and other cationic lipids): chemistry, biophysics, and transfection. *Crit Rev Ther Drug Carrier Syst* 21(4):257–317
8. Ewert K, Evans HM, Ahmad A, Slack NL, Lin AJ, Martin-Herranz A et al (2005) Lipoplex structures and their distinct cellular pathways. *Adv Genet* 53:119–155
9. Zuhorn IS, Engberts JB, Hoekstra D (2007) Gene delivery by cationic lipid vectors: overcoming cellular barriers. *Eur Biophys J* 36: 349–362
10. Elouahabi A, Ruysschaert JM (2005) Formation and intracellular trafficking of lipoplexes and polyplexes. *Mol Ther* 11:336–347
11. Xu Y, Szoka FC (1996) Mechanism of DNA release from cationic liposome/DNA complexes used in cell transfection. *Biochemistry* 35:5616–5623
12. Weissig V, Lizano C, Torchilin VP (2000) Selective DNA release from DQAsome / DNA complexes at mitochondria-like membranes. *Drug Deliv* 7:1–5
13. Briggs C, Jones M (2005) SYBR green I-induced fluorescence in cultured immune cells: a comparison with Acridine Orange. *Acta Histochem* 107:301–312
14. Weissig V, D’Souza GGM, Torchilin VP (2001) DQAsomes/ DNA complexes release DNA upon contact with isolated mouse liver mitochondria. *J Control Release* 75:401–408
15. Wagle M, Martinville LE, D’Souza GGM (2011) The utility of an isolated mitochondrial fraction in the preparation of liposomes for the specific delivery of bioactives to mitochondria in live mammalian cells. *Pharm Res* 28:2790–2796
16. Pierre-Alain M, Oberholzer T, Luisi P (1997) Entrapment of nucleic acids in liposomes. *Biochim Biophys Acta* 1329:39–50
17. Pick U (1981) Liposomes with a large trapping capacity prepared by freezing and thawing of sonicated phospholipid mixtures. *Arch Biochem Biophys* 212(1):186–194
18. Schoen P, Bijl L, Wilschut J (1998) Efficient encapsulation of plasmid DNA in anionic liposomes by a freeze/thaw extrusion procedure. *J Liposome Res* 8(4):485–497
19. Zhou X, Klibanov AL, Huang L (1992) Improved encapsulation of DNA in pH-sensitive liposomes for transfection. *J Liposome Res* 2(1):125–139
20. Chapman CJ, Erdahl WL, Taylor RW, Pfeiffer DR (1990) Factors affecting solute entrapment in phospholipid vesicles prepared by the freeze-thaw extrusion method: a possible general method for improving the efficiency of entrapment. *Chemistry of Physics and Lipids* 55(2): 73–83



# Chapter 11

## Tunable pH Sensitive Lipoplexes

Hélène Dhotel, Michel Bessodes, and Nathalie Mignet

### Abstract

To provide long circulating nanoparticles able to carry a gene to tumor cells, we have designed anionic pegylated lipoplexes which are pH sensitive. The reduction of positive charges in nucleic acid carriers allows reducing the elimination rate, increasing circulation time in the blood, leading to improved tumor accumulation of lipid nanoparticles. Anionic pegylated lipoplexes have been prepared from the combined formulation of cationic lipoplexes and pegylated anionic liposomes. The neutralization of the particle surface charge as a function of the pH was monitored by dynamic light scattering in order to determine the ratio between anionic and cationic lipids that would give pH-sensitive complexes. This ratio has been optimized to form particles sensitive to pH change in the range 5.5–6.5. Compaction of DNA into these newly formed anionic complexes was checked by DNA accessibility to Picogreen. The transfection efficiency and pH-sensitive property of these formulations were shown in vitro using baflomycin, a vacuolar H<sup>+</sup>-ATPase inhibitor.

**Key words** Anionic lipoplexes, Pegylated lipoplexes, pH-sensitive lipoplexes, Gene delivery to tumor, Anionic cholesterol

---

### 1 Introduction

Nonviral nucleic acid delivery has made tremendous progresses these last 4 years thanks to the FDA approval of siRNA and mRNA both delivered by lipid nanoparticles [1–4]. Despite these advances, systemic delivery of nucleic acid, in particular DNA, still suffers from limited endosomal escape and low circulation time resulting in low efficacy in delivering the gene at the target. Works on DNA delivery have involved different types of cationic lipids [5, 6] or polymers [7, 8], degradable cationic lipid/DNA complexes [9, 10], or polymer/DNA complexes [11, 12] and more recently ionizable lipids [13, 14] which made the difference, as regard to the previously studied nanocarriers, and became part of the recently accepted siRNA and mRNA drugs [15].

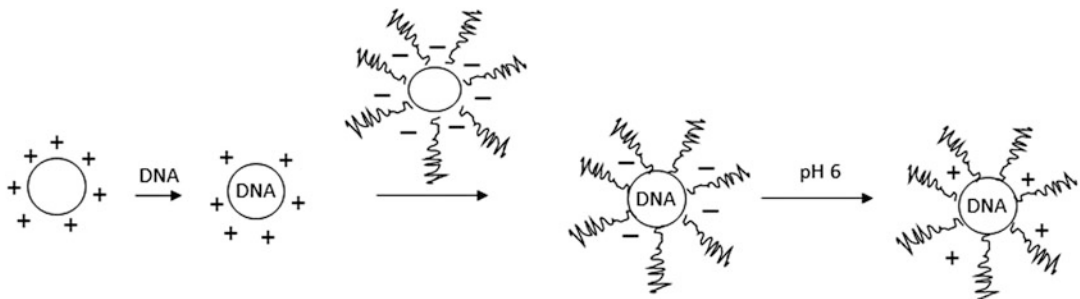
To improve nucleic acid delivery from endosomes, various strategies might be used, upon them triggered release by physical

means [16], but also chemical triggers such as pH changes. In the present work, we have focused our studies on the pH-sensitive strategy. This might involve the use of pH labile components into the formulation such as pH degradable lipid [17–19] or polymer [20]. The pH sensitivity might also be provided by a relevant mixture of titrable anionic and cationic lipids in the formulation. Numerous works have been reported on such pH-sensitive lipoplexes, mostly to increase gene delivery into the cells upon endosome pH drop [21–23]. These are mostly cationic lipoplexes, as they allow a high nucleic acid compaction and an efficient cell uptake. For instance, in the LPDII particles, DNA/polylysine complexes were mixed with acid-sensitive CHEMS/DOPE/DOPE-Peg-folate liposomes to form acid-sensitive lipoplexes [24]. The pH sensitivity is given by the CHEMS and DOPE lipids which are able to form a hexagonal phase at acidic pH, leading to a lipoplex destabilization in the endosomal compartment [25, 26]. This destabilization might also be brought by fusogenic peptides [27]. In our case, the idea is different. The concept is to form tunable pH-sensitive lipoplexes [28], meaning that only the ratio between the anionic and the cationic lipid would be responsible for the pH sensitivity, whatever the anionic and cationic lipid chosen.

Delivering nucleic acid to tumor using nonviral vectors involves two main requirements:

- A long circulation time to obtain the highest possible vector accumulation in the tumor vascularization; since this requires poorly charged lipoplexes, in particular a limited amount of cationic charges [29], we have chosen to develop anionic lipoplexes
- A reversal of these anionic charges or an amplification of the cationic charges in the tumor environment upon pH drop, in order to obtain cationic lipoplexes that will efficiently enter the cells by binding to the anionic plasma membrane and deliver its DNA content.
- For this last step, acid-sensitive PEG had been developed [30–32].
- A fusogenic lipid might also be incorporated into the lipoplex.

To reach these goals, we have designed tunable anionic pH-sensitive lipoplexes. These complexes are anionic at physiological pH and pegylated to improve their circulation time, as compared to cationic lipoplexes [33]. Moreover, they become cationic at pH under 6, in order to promote efficient tumor cell internalization, since it is widely recognized that extracellular pH is acidic in ischemic tumor tissue (see Scheme 1).



**Scheme 1** Schematized representation of the sequential process used for the formation of anionic lipoplexes and charge reversibility upon reduction of the pH. It does not take into account the structure of the complexes neither the position of DNA into the particle lipidic bilayer

## 2 Materials

### 2.1 Abbreviations of the Lipids Used

PEG, polyethylene glycol; DOPE, dioleoylphosphatidylethanolamine; CHEMS, cholestryl hemisuccinate; DPPC, dipalmytoyl-phosphatidylcholine. The names of the different lipids were generated with AutoNom 2000 software which is based on IUPAC rules. The cationic lipid whose name according to the nomenclature is 2-{3-[Bis-(3-amino-propyl)-amino]-propylamino}-N-ditetradecylcarbamoyl methyl-acetamide or RPR209120 that we called DMAPAP was previously described in the supporting information of Thompson et al. [34]. We can provide this lipid. The tetracarboxylated derivative, [(2-{Cholesteryloxycarbonyl-[2-(bis-carboxymethyl-carbamoyloxy)-ethyl]-amino}-ethoxycarbonyl)-carboxymethyl-amino]-acetic acid, that we named CCTC is described in Mignet et al. [35].

### 2.2 Chemicals and DNA Provided or Synthesized

L- $\alpha$ -Dioleoyl phosphatidylethanolamine (DOPE) and 1,2-dipalmitoyl-*sn*-glycero-3-phosphocholine (DPPC) were purchased from Avanti Polar Lipids. The chol-PEG<sub>110</sub> was obtained in one step from the reaction of cholestryl chloroformate and  $\alpha$ -amino- $\omega$ -methoxy-PEG. The luciferase encoding gene was obtained as reported [33]. Picogreen® was purchased from Molecular Probes, USA; baflomycin from Sigma, France; the BCA kit from Pierce; and the luciferase kit from Promega.

### 2.3 Equipment

Anionic liposome was prepared by the film method on a rotary evaporator Heidolph, VWR, equipped with a Vacuubrand CVC2 to control the pressure. Sonication was performed on sonicator branson 1210. Size and zeta potentials measurements were performed on a Zetasizer NanoSeries from Malvern Instruments equipped with a MPT2 autotitrator. Fluorescence was measured on a multi-label plate reader Wallac Victor2 1420 Multilabel Counter, Perkin Elmer, France, equipped with excitation and emission filters ( $350 \pm 10$  nM,  $450 \pm 10$  nM).

## 2.4 Buffer Preparation

1. Prepare the tris(hydroxymethyl)aminolethane-maleate 50 mM, pH 7:  
Prepare a solution of Tris-HCl acid maleate 50 mM by mixing 6 g of tris(hydroxymethyl) aminomethane and 5.8 g of maleic acid in 1 L H<sub>2</sub>O. Prepare a 50 mM NaOH solution. Mix the 50 mL of the Tris-HCl acid maleate solution and 48 mL of NaOH solution. Verify and adjust the pH by adding one of the Tris-HCl acid maleate or NaOH solutions.
2. Prepare the solution of 5% glucose by mixing 5 g in 100 mL H<sub>2</sub>O.
3. Prepare the Tris-maleate/glucose buffer: Mix the Tris-maleate, and the glucose solutions volume to volume to obtain the tris-maleate 25 mM, glucose 2.5%.
4. Prepare the Hépès 40 mM and a solution of 20% glucose (20 g in 100 mL H<sub>2</sub>O). Mix the Hépès and the glucose solutions volume to volume to obtain the Hépès 20 mM, glucose 10%.

## 3 Methods

Obtaining anionic self-associated lipoplexes is not obvious, since a competition occurs between the anionic charge of the particles and the anionic charges of the nucleic acid. The easiest way to proceed is to obtain cationic lipoplexes core by mixing cationic lipid and DNA or mRNA. Then an anionic pegylated liposome is added to the mixture to form an anionic pegylated lipoplex (Scheme 1). The PEG lipid was used to avoid aggregation that would occur by mixing the cationic lipoplexes and the anionic liposome and will also be useful to limit protein interaction upon systemic injection [35]. The cationic lipid [34] we used bears two primary amines, one secondary and one tertiary amine; we designed original negatively charged cholesterol bearing four carboxylate moieties [33] in order to limit the amount of cholesterol in the liposomes.

Thanks to the presence of the carboxylate moieties, the anionic particle charge should be reversed to a cationic one at a determined appropriate pH. To reach this goal, the ratio between the two lipids has to be optimized, taking into accounts the DNA negative charges. The optimal ratio was determined by zeta potential measurements combined with titration experiments, as will be described (Data obtained represented Fig. 1). Light scattering was also used to ensure that the particle size remained in the right size range (around 100–200 nm), which is fundamental to maintain the particle circulating into the bloodstream [6]. To evaluate if plasmid DNA was well confined into the structure formed, Picogreen™ was used, and the fluorescence associated with free DNA or compacted DNA was measured. Compacted DNA does not allow Picogreen™ to intercalate into the DNA base pair and gives

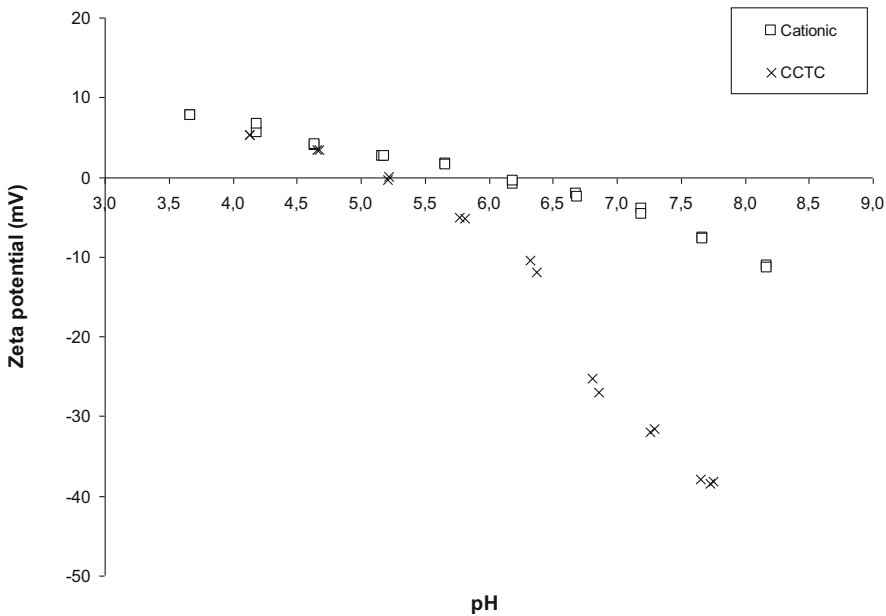


**Fig. 1** Zeta potential of the particles as a function of the pH. The pH was initially measured at pH 8.25 and decreased by addition of a solution of HCl at 0.1 M, in order to obtain steps with a pH decrease of 0.5. A measure of the electrophoretic mobility and dynamic diameter was measured every variation of 0.5 in pH after the pH was stabilized. The measurements were taken at room temperature

a low fluorescence level. The intracellular pH sensitivity of the anionic pegylated lipoplexes was shown in vitro using baflomycin, an ATPase inhibitor, which reduces endosome acidification (Fig. 2).

### 3.1 Preparation of Cationic Liposomes

1. Dissolve separately the lipids DMAPAP (10 µmol, 10 mg) and DOPE (10 µmol, 7.3 mg) in chloroform (500 µL each). Take care that the lipids are well dissolved separately before mixing them (*see Note 1*).
2. Mix them into a round-bottom flask (10 mL) (*see Note 2*).
3. Put the flask at the evaporary evaporator to remove the solvent in a pressure controlled manner. First reduce the pressure from 1000 to 200 mbar in approximately 15 min with a middle rotation speed. When the drop forms, increase the rotation speed at its maximum level to drag the drop into the film. Then, reduce the pressure from 200 to 5 mbar in 30 minutes and leave the film under reduced pressure for an additional hour (*see Note 3*).
4. The film being dry, add 1 mL (to afford a final concentration of 20 mM) milliQ filtered (0.22 µm) H<sub>2</sub>O, and leave the flask under gentle rotation overnight at room temperature (*see Note 4*).

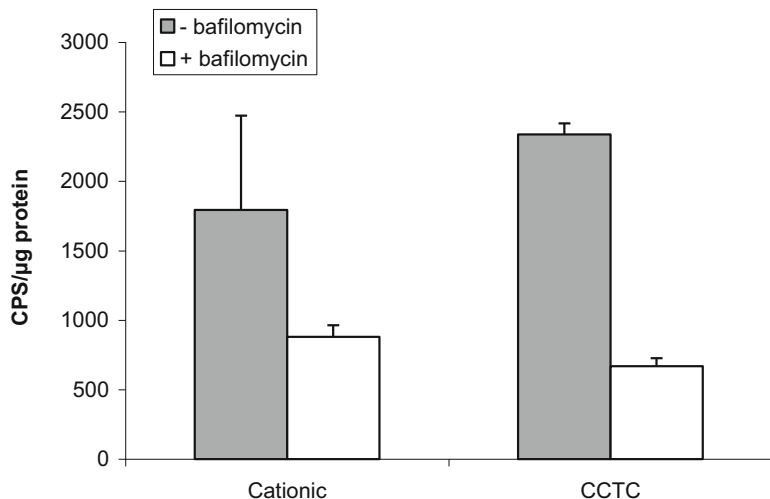


**Fig. 2** Transfection of the cationic and anionic formulations using a plasmid encoding for the luciferase reporter gene in presence and absence of baflomycin. The Y axis represents the level of luciferase expression per protein ( $\mu\text{g}$ ), mean values + SD. The background level of the untreated cells was removed for each samples

5. Mix gently the mixture on a vortex if the film is not fully detached from the wall. Sonicate the particles during 5 min to afford a rather homogeneous size distribution of approximately 150–200 nM.
6. Control the size by dynamic light scattering (*see Note 5*). For measurements on a nanoZS (Malvern Instruments), dilute 5  $\mu\text{L}$  of the particles obtained in a 500  $\mu\text{L}$  cuvette; start the measurement in the automatic mode.

### 3.2 Preparation of Cationic Lipoplexes

Lipoplexes were prepared in Tris-maleate 25 mM, glucose 2.5% with a charge ratio cationic lipid/anionic lipid = 6, which corresponds to a ratio total lipid to DNA = 12.

1. Dilute the DMAPAP/DOPE suspension initially at 20 mM to 5 mM in  $\text{H}_2\text{O}$ .
2. Dilute 6  $\mu\text{g}$  pDNA in 100  $\mu\text{L}$  Tris-maleate 25 mM, glucose 2.5%.
3. Dilute 15  $\mu\text{L}$  of the 5 mM DMAPAP/DOPE suspension in 100  $\mu\text{L}$  Tris-maleate 25 mM, glucose 2.5%.
4. Add the plasmid DNA to the cationic liposome dropwise in few seconds with constant vortexing (*see Note 6*).
5. Leave the sample 1 h at room temperature to incubate before using it or adding it to the anionic liposomes.

### **3.3 Preparation of Anionic PEGylated Liposomes**

The anionic liposomes were prepared by the film method as described for the cationic liposome in Subheading 3.1.

1. Dissolve separately the lipids DPPC (5 µmol, 3.7 mg), CCTC (15 µmol, 7.4 mg), and Chol-PEG<sub>110</sub> (0.5 µmol, 2.5 mg) in chloroform (200 µL, 600 µL, and 200 µL, respectively). Take care that the lipids are well dissolved separately before mixing them (*see Note 1*).
2. Mix them into a round-bottom flask (10 mL) and evaporate the chloroform under reduced pressure as described in Subheading 3.1, step 3 (*see Notes 2 and 3*).
3. The film being dry, add 1 mL (to afford a final concentration of 20.5 mM) milliQ filtered (0.22 µm) H<sub>2</sub>O, and leave the flask under gentle rotation overnight at room temperature.
4. Mix gently the mixture on a vortex if the film is not fully detached from the wall.
5. Filter the particles successively on 0.45 and 0.22 µm polyethyl-sulfonate filters.
6. Control the size by dynamic light scattering (*see Note 5*). For measurements on a nanoZS (Malvern Instruments), dilute 5 µL of the particles obtained in a 500 µL cuvette, start the measure in the automatic mode.

### **3.4 Preparation of Anionic PEGylated Lipoplexes**

The preformed cationic lipoplexes were added to the anionic liposomes according to the charge lipid ratio DMAPAP/CCTC (±) = 1.3.

### **3.5 Titration Experiments**

1. Prepare a suspension of the anionic liposomes at 0.55 mM from the 20.5 mM suspension prepared in Subheading 3.3.
2. Dilute 100 µL of this anionic liposome suspension in Hepes 20 mM, glucose 10%.
3. Add the preformed lipoplexes described in Subheading 3.2 to the suspension of the anionic liposomes.
4. Prepare the HCl 0.1 M buffer and fix it to the titrator (*see Note 7*).
5. Rinse the autotitrator cables with H<sub>2</sub>O. Prime the HCl buffer and rinse again.
6. Dilute the anionic pegylated lipoplexes prepared in 3.4 in 10 mL H<sub>2</sub>O and fix the flask at the autotitrator, including the pH electrode.
7. Enter the protocol: zeta potential measurements with an initial pH point taken at the pH of the solution, in this case pH 8.25 and points taken every 0.5 pH change until pH 3.7 is reached. Stir between each measure to ensure the solution is homogeneous. Electrophoretic mobility is converted automatically to the ζ potential according to the Smoluchowski equation by the system.

**3.6 DNA  
Complexation Checked  
by Fluorescence**

1. Prepare the Picogreen® solution as described by the provider (1/200 in Tris-EDTA buffer).
2. Load into a 96-well plate free DNA or complexed DNA (40 ng) in tripliquets.
3. Add 200 µL of the Picogreen solution (Subheading 3.6, step 1) to each well filled with DNA and three more to obtain the Picogreen background level.
4. Read the emission at 450 nM under an excitation at 350 nM on a multiplate reader able to measure fluorescence.
5. For the calculation, calculate the mean and the standard error on each tripliquets. Remove the Picogreen background from the sample data. Calculate the percentage of fluorescence of each sample by dividing the sample data by the value of the free DNA taken as 100% fluorescence.

**3.7 In Vitro  
Experiments**

1. B16 murine cells were grown into DMEM supplemented with L-glutamine (29.2 mg/mL), penicillin (50 units/mL), streptomycin (50 units/mL), and 10% fetal bovine serum.
2. The day before the experiment, seed B16 cells into 24-well culture plates at a density of 50,000 cells per well and incubate at 37 °C, under 5% CO<sub>2</sub> for 24 h.
3. One hour before transfection, wash the cells with fresh medium with or without baflomycin.
4. Add 100 µL of cationic or anionic lipoplexes containing 0.5 µg DNA onto each well in tripliquet, and incubate the plates at 37 °C for 6 h in the presence of 5% CO<sub>2</sub>, and then replace by fresh medium for 18 h.
5. Wash the cells twice with PBS and treat with 200 µL of a passive lysis buffer (Promega). After 15 min, centrifuge the cells for 5 min at 12,000 tr/min.
6. Add 10 µL of the supernatant and 10 µL of iodoacetamide to a 96-well plate, and incubate at 37 °C for 1 h. Quantify the protein content with the BCA protein assay KIT (PIERCE), and report to BSA taken as a reference curve (*see Note 8*).
7. Quantify the luciferase activity using a commercial kit Luciferase assay system (PROMEGA): Load 10 µL of the lysed cells into a 96-well plate, and place it into the lecture plate reader. Load the luciferase substrate to the injector. 50 µL of the luciferase substrate is injected via an injector, and the absorbance is read immediately at 563 nM on a Wallac Victor2 1420 Multilabel Counter (Perkin Elmer).

8. For the calculation, background of the untreated cells, taken as negative controls, was removed from the sample data. The relative counts obtained for luciferase quantification were divided by the protein content in each well to normalize the results per  $\mu\text{g}$  of protein. The cationic formulation was taken as the positive reference formulation.

---

## 4 Notes

1. Solubility of the lipids should be checked with intensive care since presence of unsoluble entities will appear in the film and reduce particle homogeneity after hydration.
2. The ratio between the volume to be reduced (or the amount of lipids) and the round-bottom flask is important since the film should occupy as much flask wall as possible. From the surface of the flask occupied by the film will depend on the number of layers in the liposomes.
3. Make sure that the film is not crackled by a too rapid pressure reduction. If so, dissolve again the lipids in 1 mL CHCl<sub>3</sub> and start again part 3. It is always preferable to obtain a homogeneous film along the flask wall; it will provide more homogeneous liposome size after the hydration step.
4. Evaporation and hydration time are usually reported as shorter, but we have found that taking time to do these steps is required to form homogeneous liposome sizes.
5. All buffers and water used should be filtered on 0.22  $\mu\text{m}$  filters since any dust might interfere with light scattering experiments.
6. In order to maintain an excess of cationic charges and hence avoid precipitation by going through a charge ratio (+/-) equal to 1, we add DNA on the cationic lipid and not the opposite order.
7. All buffers should be degassed prior titration to avoid any volume error.
8. The concentration range of BSA should be done for each experiment since the values are fully dependent on the incubation time. It should be performed in the same buffer as the buffer used for the cells, in this case passive lysis buffer.

---

## Acknowledgments

The author would like to thank Caroline Richard for her dedicated work during her fellowship.

## References

1. Kulkarni JA, Witzigmann D, Chen S, Cullis PR, Van der Meel R (2019) Lipid nanoparticle Technology for Clinical Translation of siRNA therapeutics. *Acc Chem Res* 52:2435–2444
2. Kulkarni JA, Witzigmann D, Thomson SB, Chen S, Leavitt BR, Cullis PR, Van der Meel R (2021) The current landscape of nucleic acid therapeutics. *Nat Nanotechnol* 16(630–6):43
3. Buschmann MD, Carrasco MJ, Alishetty S, Paige P, Alameh MG, Weissman D (2021) Nanomaterial delivery systems for mRNA vaccines. *Vaccine* 9:65–95
4. Ftouh M, Kalboussi N, Abid N, Sfar S, Mignet N, Bahoul B (2021) Contribution of nanotechnologies to vaccine development and drug delivery against respiratory viruses. *PPAR Res*:6741290
5. Bessodes M, Dhotel H, Mignet N (2019) Lipids for nucleic acid delivery: cationic or neutral Lipoplexes, synthesis, and particle formation. In: Ogris M, Sami H (eds) Nanotechnology for nucleic acid delivery, Methods in molecular biology, vol 1943. Humana Press, New York
6. Tranchant I, Thompson B, Nicolazzi C, Mignet N, Scherman D (2004) Physicochemical optimization of plasmid delivery by cationic lipids. *J Gene Med* 1:S24–S35
7. Drean M, Debuigne A, Goncalves C, Jérôme C, Midoux P, Rieger J, Guégan P (2017) Use of primary and secondary polyvinylamines for efficient gene transfection. *Biomacromolecules* 18:440–451
8. Nguyen DN, Green JJ, Chan JM, Langer R, Anderson DG (2009) Polymeric materials for gene delivery and DNA vaccination. *Adv Mater* 21:847–867
9. Byk G, Wetzer B, Frederic M, Dubertret C, Pitard B, Jaslin G, Scherman D (2000) Reduction-sensitive lipopolymamines as a novel nonviral gene delivery system for modulated release of DNA with improved transgene expression. *J Med Chem* 43:4377–4387
10. Mignet N, Byk G, Wetzer B, Scherman D (2003) DNA complexes with reducible cationic lipid for gene transfer. In: Methods in enzymology, vol 373. Academic Press, pp 357–369
11. Lutten J, Van Nostrum C, De Smedt S, Hennink W (2008) Biodegradable polymers as non-viral carriers for plasmid DNA delivery. *J Control Release* 126:97–110
12. Heller P, Hobenrik D, Lächelt U, Schinnerer M, Weber B, Schmidt M, Wagner E, Bros M, Barz M (2017) Combining reactive triblock copolymers with functional cross-linkers: a versatile pathway to disulfide stabilized-polyplex libraries and their application as pDNA vaccines. *J Control Release* 258:146–160
13. Semple SC et al (2010) Rational design of cationic lipids for siRNA delivery. *Nat Biotechnol* 28:172–176
14. Han X, Zhang H, Butowska K, Swingle KL, Alameh MG, Weissman D, Mitchell MJ (2021) An ionizable lipid toolbox for RNA delivery. *Nat Commun* 12:7233
15. Suzuki Y, Ishihara H (2021) Difference in the lipid nanoparticle technology employed in three approved siRNA(Patisiran), and mRNA (COVID-19 vaccine) drugs. *Drugs Metabol Pharmacokinet* 41:100424
16. Do HD, Martin B, Doan BT, Corvis Y, Mignet N (2019) Advances on non-invasive physically triggered nucleic acid delivery from nanocarriers. *Adv Drug Deliv Rev* 138:3–17
17. Garinot M, Masson C, Mignet N, Bessodes M, Scherman D (2007) Chapter 8: synthesis and advantages of acid-labile formulations for lipoplexes. In: Gregoriadis G (ed) Liposome technology, vol 1, 3rd edn, pp 139–163
18. Martin B, Sainlos M, Aissaoui A, Oudrhiri N, Hauchecorne M, Vigneron JP, Lehn JM, Lehn P (2005) The design of cationic lipids for gene delivery. *Curr Pharm Des* 3:375–394
19. Roux E, Stomp R, Giasson S, Pezolet M, Moreau P, Leroux JC (2002) Steric stabilization of liposomes by pH-responsive *N*-isopropylacrylamide copolymer. *J Pharm Sci* 91: 1795–1802
20. Kim Y, Park J, Lee M, Kim Y, Park T, Kim S (2005) Polyethylenimine with acid-labile linkages as a biodegradable gene carrier. *J Control Release* 103:209–219
21. Shi G, Guo W, Stephenson S, Lee R (2002) Efficient intracellular drug and gene delivery using folate receptor-targeted pH-sensitive liposomes composed of cationic/anionic lipid combinations. *J Control Release* 80:309–319
22. Guo X, Szoka FC (2003) Chemical approaches to triggerable lipid vesicles for drug and gene delivery. *Acc Chem Res* 36:335–341
23. Sato Y (2021) Development of lipid nanoparticles for the delivery of macromolecules based on the molecular design of pH-sensitive cationic lipids. *Chem Pharm Bull* 69:1141–1159
24. Lee R, Huang L (1996) Folate-targeted, anionic liposome-entrapped polylysine-condensed DNA for tumor cell-specific gene transfer. *J Biol Chem* 271:8481–8487

25. Hafez I, Cullis P (2000) Cholesteryl hemisuccinate exhibits pH sensitive polymorphic phase behavior. *Biochim Biophys Acta* 1463:107–114
26. Koynova R, Wang L, Tarahovsky Y, MacDonald R (2005) Lipid phase control of DNA delivery. *Bioconjug Chem* 16:1335–1339
27. Hafez I, Ansell S, Cullis P (2000) Tunable pH-sensitive liposomes composed of mixtures of cationic and anionic lipids. *Biophys J* 79: 1438–1446
28. Simões S, Slepushkin V, Gaspar R, de Lima M, Düzgüneş N (1998) Gene delivery by negatively charged ternary complexes of DNA, cationic liposomes and transferrin or fusogenic peptides. *Gene Ther* 7:955–964
29. Zalipsky S, Brandeis E, Newman MS, Woodle MC (1994) Long circulating, cationic liposomes containing amino-PEG-phosphatidyl-ethanolamine. *FEBS Lett* 353:71–74
30. Masson C, Garinot M, Mignet N, Wetzer B, Mailhe P, Scherman D, Bessodes M (2004) pH sensitive PEG lipids containing orthoester linkers: new potential tools for nonviral gene delivery. *J Control Release* 99:423–434
31. Choi J, MacKay J, Szoka F (2003) Low-pH-sensitive PEG-stabilized plasmid-lipid nanoparticles: preparation and characterization. *Bioconjug Chem* 14:420
32. Kale A, Torchilin V (2007) Enhanced transfection of tumor cells *in vivo* using “smart” pH-sensitive TAT-modified pegylated liposomes. *J Drug Target* 15:537–548
33. Mignet N, Richard C, Seguin J, Largeau C, Bessodes M, Scherman D (2008) Anionic pH-sensitive pegylated lipoplexes to deliver DNA to the tumors. *Int J Pharm* 361:194–201
34. Thompson B, Mignet N, Hofland H, Lamons D, Seguin J, Nicolazzi C, de la Figuera N, Kuen R, Meng Y, Scherman D, Bessodes M (2005) Neutral post-grafted colloidal particles for gene delivery. *Bioconjug Chem* 16:608–614
35. Mignet N, Cadet M, Bessodes M, Scherman D (2007) Chapter 16: incorporation of PEG lipid into Lipoplexes: on-line incorporation assessment, and pharmacokinetics advantages. In: Gregoriadis G (ed) *Liposome technology*, vol 2, 3rd edn, pp 273–292



# Chapter 12

## Solid Lipid Nanoparticles for Drug Delivery

Wei-Chung Luo and Xiuling Lu

### Abstract

Solid lipid nanoparticles are promising carriers that allow for the delivery of poorly water-soluble drugs and have the potential to achieve sustained drug release or targeted delivery to the site of interest. Here we describe the preparation of solid lipid nanoparticles by forming a microemulsion at an elevated temperature which, upon cooling, yields a suspension of solid nanoparticles. This nanotemplate engineering method is inexpensive, reproducible, and easy to scale up.

**Key words** Solid lipid nanoparticles, Sustained release, Cancer treatment, Microemulsion, Dexamethasone palmitate

---

### 1 Introduction

Solid lipid nanoparticles (SLNs) emerged in 1991 as a substitute drug delivery system to liposomes, emulsions, and polymeric nanoparticles [1]. They are colloidal carriers with a diameter ranging from 50 to 1000 nm, consisting of a lipid core that is in the solid state at or lower than physiological temperature and an outer layer comprised of surfactants that stabilize the lipid matrix (Fig. 1). In SLNs, drug is either encapsulated in the lipid core or attached to the surface. The drug adhered to the surface will disperse from the particles first and result in a burst release. The lipid matrix subsequently erodes or degrades, depending on the properties of the lipid composition, and sustainably releases the drug from the core [1].

SLNs have various advantages including biocompatible and biodegradable compositional ingredients, the avoidance of organic solvents during preparation, ease in large-scale production and sterilization, and good chemical stability of encapsulated drugs due to immobilization of drug molecules in the solid lipid [1–3]. Compared with liposomes, the ingredients and manufacturing process of SLNs are also relatively cheaper [4]. Therefore, SLNs

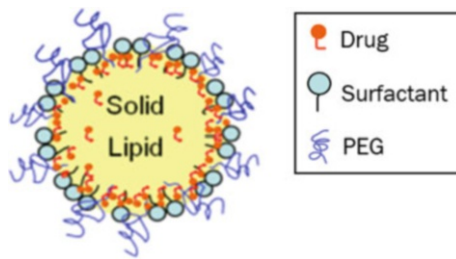


**Fig. 1** The structure of a PEGylated drug-loaded solid lipid nanoparticle

have been increasingly employed as a drug delivery system for various therapeutic applications, including anti-microbials, treatments for central nervous system diseases, skin disorders, hypertension, osteoporosis, and so on [4]. Cancer treatment represents the most relevant field of SLN applications (42%) from 2013 to 2020 [4]. Besides the fact that cancer remains as the second leading cause of death in the United States and requires more effective therapeutic methods to be developed [5], the nano-size of SLNs and the potential of ad hoc modifications make them suitable to pass through several biological barriers and deliver drugs to the sites of interest with lower toxicity [6]. Moreover, SLNs have been reported to overcome multidrug resistance through co-delivery of molecules that inhibit multidrug resistance mechanisms and avoid the efflux transporters such as P-glycoprotein [6]. In addition to intravenous administration, SLNs have been exploited for other routes of administration including cutaneous, transdermal, nasal, ocular, and oral, allowing patients to benefit from less frequent and painful therapeutic options [4, 6].

However, the drug loading capacity of SLNs is limited because of the crystalline structure of solid lipids and potential polymorphic transitions of the lipid such as triglycerides during storage. This is sometimes induced by exposure to light and temperature or shear force and may result in SLN gelation or drug expulsion [2, 7, 8]. In addition to these stability issues, drug molecules on the surface may also hydrolyze in aqueous dispersions, affecting the clinical outcome of the treatment. Therefore, drying techniques including spray drying and freeze-drying have been commonly applied to improve their long-term stability [9–12].

The lipids used to prepare SLNs include fatty acids, fatty alcohols, fatty esters, steroids, waxes, monoglycerides, diglycerides, and triglycerides [7, 8]. Ionic and non-ionic polymers such as Pluronic® F-68, Tween® 60 or Tween® 80, surfactants, and organic salts can be used as emulsifiers [7, 8]. Both hydrophilic and hydrophobic drugs have been reported to be encapsulated in SLNs by different preparation methods such as hot and cold high-pressure homogenization (HPH), solvent emulsification–evaporation, solvent emulsification–diffusion, emulsification–sonification, solvent

injection, and double emulsion method (specifically for hydrophilic drugs) [13].

While large-scale production of SLNs is mainly obtained by the HPH technique [2, 13], where a high-pressure homogenizer is employed to reduce the oil droplet size to nano dimensions [14], the “nanotemplate engineering” method developed is suitable for small-scale production in the laboratory and can be easily adjusted for a larger scale [15]. This method is similar to the hot HPH method and emulsification–sonification, but without the need of sophisticated instruments such as a high-pressure homogenizer or a probe sonicator, and does not produce a large volume of dispersion that requires further concentration. In this chapter, we describe how to prepare SLNs using the nanotemplate engineering method [16–18]. Dexamethasone palmitate is an anti-inflammatory agent with poor water solubility but dissolves in melted lipid stearyl alcohol, so no organic solvents are added, avoiding the need to remove residual solvents and associated toxicity issues. In cases where the drug intended to be encapsulated does not dissolve in the melted lipid(s), depending on the organic solvent’s miscibility with water, solvent emulsification–evaporation or solvent emulsification–diffusion methods can instead be employed for preparing SLNs.

---

## 2 Materials

1. 1-Octadecanol (stearyl alcohol) as the solid lipid core. Store at room temperature.
2. Brij™ S20 (polyethylene glycol octadecyl ether) as the main surfactant. Store at room temperature.
3. Tween® 60 as the co-surfactant. Store at room temperature.
4. Dexamethasone palmitate powder. Store at room temperature.
5. Ultrapure water (18.2 MΩ·cm at 25 °C).
6. 20 mL glass vial.
7. Magnetic stir bar.
8. Hot plate with magnetic stirrer.

---

## 3 Methods

The preparation method is illustrated in Fig. 2. The following procedure is for preparation of a 5 mL SLN suspension. For scaling up or down, multiply the weight of ingredients and the volume of ultrapure water by the appropriate factor to obtain the desired volume of nanosuspension.

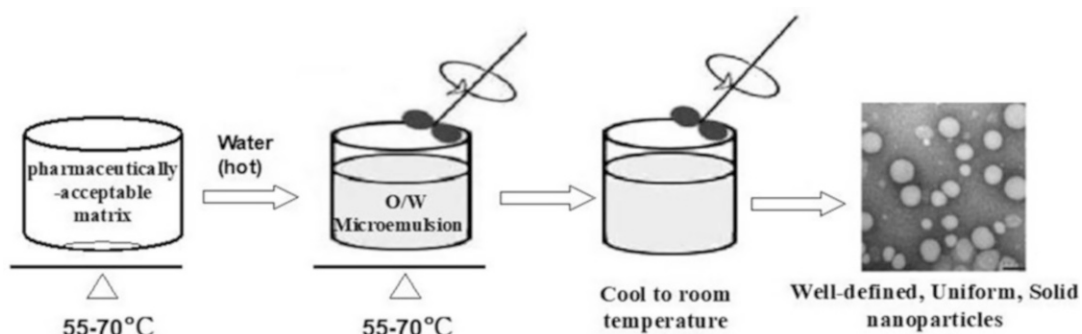


**Fig. 2** Preparation of solid lipid nanoparticles



**Fig. 3** The appearance of placebo solid lipid nanoparticles

### 3.1 Preparation of Placebo SLNs without Drugs

1. Weigh out 2 mg of Tween® 60 in a 20 mL glass vial (*see Note 1*).
2. Weigh out 8 mg of stearyl alcohol and 17.5 mg of Brij™ S20 on weighing papers and transfer to the glass vial.
3. The glass vial is heated in a water bath at 75 °C (*see Note 2*) for 10 min to fully melt the lipid and surfactants. Meanwhile, heat a beaker with 20 mL (*see Note 3*) of ultrapure water at the same temperature.
4. Place a stir bar into the vial. Use a pipet or a graduated cylinder to measure 5 mL (*see Note 4*) of heated water from the beaker and add into the vial. Maintain the mixture at 75 °C, and stir at 400 rpm for 30 min to make a warm o/w microemulsion.
5. Transfer the vial into a water bath at room temperature. Keep stirring at 400 rpm for another 30 min to wait for the lipid and surfactants to solidify (Fig. 3) (*see Note 5*).

### **3.2 Preparation of Dexamethasone Palmitate-Loaded SLNs**

1. Weigh out 2 mg of Tween® 60 in a 20 mL glass vial (*see Note 1*).
2. Weigh out 8 mg of stearyl alcohol and 17.5 mg of Brij™ S20 on weighing papers and transfer to the glass vial.
3. Weigh out 2.4 mg of dexamethasone palmitate powder (*see Note 6*) and transfer to the glass vial.
4. The glass vial is heated in a water bath at 75 °C (*see Note 2*) for 10 min to fully melt the lipid and surfactants and dissolve dexamethasone palmitate. Meanwhile, heat a beaker with 20 mL (*see Note 3*) of ultrapure water at the same temperature.
5. Place a stir bar into the vial (*see Note 7*). Use a pipet or a graduated cylinder to measure 5 mL (*see Note 8*) of heated water from the beaker and add into the vial. Maintain the mixture at 75 °C and stir at 400 rpm for 30 min (*see Note 9*) to make a warm o/w microemulsion.
6. Transfer the vial into a water bath at room temperature. Keep stirring at 400 rpm for another 30 min to wait for the lipid and surfactants to solidify (*see Note 10*).

### **3.3 Purification of Dexamethasone Palmitate-Loaded SLNs**

1. Transfer the nanosuspension to a 15 mL centrifuge tube and centrifuge at 3000 rpm for 15 min at 4 °C to remove unentrapped drug. Collect the supernatant.
2. Transfer the supernatant to a 15 mL ultra-filtration tube (100 K MWCO) and centrifuge at  $5000 \times g$  at 4 °C for an hour (*see Note 11*) to remove free drug. Discard the filtrate.
3. Wash the retentate by adding 10–15 mL of ultrapure water and centrifuge again at  $5000 \times g$  at 4 °C for an hour. Discard the filtrate. Repeat this step for two additional times.
4. Add a small amount of ultrapure water to the viscous concentrated retentate to help transfer the retentate to a 15 mL centrifuge tube (*see Note 12*). Resuspend the retentate by adding ultrapure water to make a 5 mL SLN suspension (*see Note 13*). Vortex to disperse SLNs homogeneously.

### **3.4 SLN Characterization**

1. Dynamic light scattering (DLS) can be used to assess the particle size distribution by collecting 100 µL of the SLN suspension and diluting to 1 mL using ultrapure water. The mean particle size of placebo SLNs is usually around 100 nm, and the polydispersity index is below 0.2. The particle size of drug-loaded SLNs tends to be slightly greater.
2. Laser Doppler velocimetry (LDV) can be used to measure the zeta potential by collecting 100 µL of the suspension and diluting to 1 mL using 900 µL of 10 mM sodium chloride solution. The zeta potential of placebo SLNs is usually around

–5 mV, while that of drug-loaded SLNs is affected by the charge of the drug molecule.

3. High-performance liquid chromatography (HPLC) can be used to evaluate the drug loading of SLNs. The nanosuspension is ultra-filtered as in Subheading 3.3, step 2. The retentate is collected and dissolved in methanol. The concentration of dexamethasone palmitate in the filtrate and in the dissolved nanoparticles is determined by HPLC, and encapsulation efficiency can thus be calculated (*see Note 14*).

---

## 4 Notes

1. Tween® 60 is a pale-to-yellow waxy paste at room temperature; thus it is easier to directly weigh out the desired amount of Tween® 60 in the container used for preparing the SLN suspension to avoid the loss during transferring from a weighing paper or a weighing pan. Tween® 60 is also recommended to be added into the container before other ingredients, so it will not be contaminated by other ingredients if excessive Tween® 60 is to be removed. Depending on the desired volume of the nanosuspension, the 20 mL glass vial can be substituted with other containers, such as a 125 mL Erlenmeyer flask.
2. The melting points of stearyl alcohol, Brij™ S20, and Tween® 60 are 59.8 °C, 44–46 °C, and 45–50 °C, respectively. The temperature of the water bath should be kept higher than 65 °C to ensure the melted states of the lipid and surfactants.
3. The volume of the heated water should be more than the desired volume of the nanosuspension to ensure that a sufficient amount of water is added to the organic phase later. The temperature of the water should also be kept higher than 65 °C to make an o/w microemulsion at the next step.
4. The volume of the water added can be adjusted to the targeted volume of the final nanosuspension.
5. When SLNs are formed, the originally turbid microemulsion should turn into a translucent nanosuspension.
6. A solubility test for the drug in melted stearyl alcohol above 60 °C should be conducted first. If the drug to be encapsulated does not dissolve in stearyl alcohol, a drug solution should be prepared with an organic solvent that also dissolves in stearyl alcohol, such as chloroform, ether, or methanol. The weight of the drug can be adjusted according to the targeted drug loading.
7. If the drug to be encapsulated does not dissolve in stearyl alcohol, add the drug solution to the melted lipid and

surfactants at this step prior to the addition of water to make a homogeneous organic phase containing drug.

8. The volume of the water added can be adjusted to the targeted volume of the final nanosuspension. If a drug solution has been added to the organic phase, a volume ratio of at least 1:10 (organic phase/aqueous phase) is recommended to achieve SLNs of size relatively close to the size of placebo SLNs.
9. If a drug solution has been added to the organic phase, depending on the boiling point of the organic solvent, the stirring time may need to be extended to fully evaporate the solvent.
10. When SLNs are formed, the originally turbid microemulsion should turn into a translucent (may have some color depending on the drug) nanosuspension. Some unentrapped drug may precipitate to the bottom and can be visually observed. If a drug solution has been added to the organic phase and a turbid solution is obtained after cooling, this indicates that the organic solvent has not been fully removed by evaporation.
11. Multiple tubes may be needed if the volume of the nanosuspension is large.
12. Combine the retentate when multiple tubes are used.
13. The final volume can be customized to make SLN suspensions of other concentrations.
14. When dexamethasone palmitate was added at 10–30% (w/w) of stearyl alcohol, > 90% of encapsulation efficiencies were achieved.

## References

1. Mishra V, Bansal KK, Verma A et al (2018) Solid lipid nanoparticles: emerging colloidal nano drug delivery systems. *Pharmaceutics* 10:191
2. Ghasemiyeh P, Mohammadi-Samani S (2018) Solid lipid nanoparticles and nanostructured lipid carriers as novel drug delivery systems: applications, advantages and disadvantages. *Res Pharm Sci* 13:288
3. Martins S, Sarmento B, Ferreira DC, Souto EB (2007) Lipid-based colloidal carriers for peptide and protein delivery – liposomes versus lipid nanoparticles. *Int J Nanomedicine* 2:595
4. Sciol Montoto S, Muraca G, Ruiz ME (2020) Solid lipid nanoparticles for drug delivery: pharmacological and biopharmaceutical aspects. *Front Mol Biosci* 7:319
5. Kochanek K, Xu J, Arias E (2020) Mortality in the United States, 2019. Hyattsville, MD
6. Bayón-Cordero L, Alkorta I, Arana L (2019) Application of solid lipid nanoparticles to improve the efficiency of anticancer drugs. *Nano* 9:474
7. Duan Y, Dhar A, Patel C et al (2020) A brief review on solid lipid nanoparticles: part and parcel of contemporary drug delivery systems. *RSC Adv* 10:26777–26791
8. Naseri N, Valizadeh H, Zakeri-Milani P (2015) Solid lipid nanoparticles and nanostructured lipid carriers: structure, preparation and application. *Adv Pharm Bull* 5:305
9. Malamatari M, Charisi A, Malamatari S et al (2020) Spray drying for the preparation of nanoparticle-based drug formulations as dry powders for inhalation. *Processes* 8:788
10. Freitas C, Müller RH (1998) Spray-drying of solid lipid nanoparticles (SLNTM). *Eur J Pharm Biopharm* 46:145–151
11. Luo W-C, O'Reilly Berings A, Kim R et al (2021) Impact of formulation on the quality and stability of freeze-dried nanoparticles. *Eur J Pharm Biopharm* 169:256–267

12. Howard MD, Lu X, Jay M, Dziubla TD (2012) Optimization of the lyophilization process for long-term stability of solid-lipid nanoparticles. *Drug Dev Ind Pharm* 38:1270–1279
13. Das S, Chaudhury A (2011) Recent advances in lipid nanoparticle formulations with solid matrix for oral drug delivery. *AAPS PharmSciTech* 12:62–76
14. Duong VA, Nguyen TTL, Maeng HJ (2020) Preparation of solid lipid nanoparticles and nanostructured lipid carriers for drug delivery and the effects of preparation parameters of solvent injection method. *Molecules* 25:4781
15. Lu X, Howard MD, Mazik M et al (2008) Nanoparticles containing anti-inflammatory agents as chemotherapy adjuvants: optimization and in vitro characterization. *AAPS J* 10: 133–140
16. Mumper RJ, Jay M (2006) Microemulsions as precursors to solid nanoparticles. US Patent 7,153,525, 26 Dec 2006
17. Kim JK, Howard MD, Dziubla TD et al (2011) Uniformity of drug payload and its effect on stability of solid lipid nanoparticles containing an ester prodrug. *ACS Nano* 5:209–216
18. Mumper RJ, Cui Z, Oyewumi MO (2007) Nanotemplate engineering of cell specific nanoparticles. *J Dispers Sci Technol* 24:569–588



# Chapter 13

## Stable Discoidal Bicelles: Formulation, Characterization, and Functions

**Ying Liu, Yan Xia, Armin Tahmasbi Rad, Wafa Aresh, Justin M. Fang, and Mu-Ping Nieh**

### Abstract

Bicellar mixtures have been used as alignable membrane substrates under a magnetic field applicable for the structural characterization of membrane-associated proteins. Recently, it has shown that bicelles can serve as nanocarriers to effectively deliver hydrophobic therapeutic molecules to cancer cells with a three- to ten-fold enhancement compared to that of liposomes of a chemically identical composition. In this chapter, detailed preparation protocol, common structural characterization methods, the structural stability, the cellular uptake and a few unique functions of bicellar nanodiscs are discussed.

**Key words** Phospholipids bicelles, Drug delivery carrier, Small-angle X-ray scattering (SAXS), Small-angle neutron scattering (SANS), Dynamic light scattering (DLS), Transmission electron microscopy (TEM), PEGylated lipid, Cellular uptake

---

### 1 Introduction

The term, “bicelle” (**bilayered micelle**) was initiated by Sanders and Landis in 1995 [1]. Since then, bicelles have been extensively applied as model supporting biomembranes for the structural characterization of membrane-associated proteins [2–5] because of their preferred orientation in moderate magnetic fields and their planar domain that provides more natural (low-curvature) environment for the proteins than most of the surfactant micelles do. Bicelles are phospholipid mixtures composed of a long-chain lipid (with  $\geq 12$  carbons in each acyl chain) and a short-chain lipid (with 6 ~ 8 carbons in each acyl chain). They have several advantages such as attainable high lipid concentration, uniform size, robust formation, and easy integration with amphiphilic/lipophilic molecules, allowing them to be used for other important applications such as crystallization of membrane proteins [6–8], biomolecular separation [9], and carriers for skin care applications

[10–12]. A most recent study has also shown that the discoidal shape of bicelles greatly benefits the cellular uptake compared to spherical shape of vesicles by a factor of 3 and above [13], providing a new opportunity to be employed as nanocarriers for theranostic delivery in the biomedical context.

Spontaneous morphology of bicelles as a function of temperature ( $T$ ) and concentration ( $C_{lp}$ ) has also been investigated using a variety of techniques, e.g., solid-state nuclear magnetic resonance (NMR), small-angle neutron scattering (SANS), and cryogenic transmission electron microscopy (cryo-TEM) summarized in a review article [14], which reveals detailed spontaneous structural information. In addition to  $T$  and  $C_{lp}$ , two other important parameters dictating the spontaneous morphology are the molar ratios of long-chain to short-chain lipid,  $Q$ , and charged long-chain to total long-chain lipid,  $R$ . Generally speaking, for samples with lower  $Q$  (i.e.,  $\leq 2$ ), fast tumbling bicelles are expected throughout most of the  $T$  range [15–18], while higher- $Q$  samples (i.e.,  $2 < Q < 6$ ) have a more complicated spontaneous structural diagram as described below. At high temperature, multilamellar vesicles are found in the absence of charged long-chain lipid [14, 19–21]. Magnetically alignable ribbons or perforated lamellae take place in the window of high  $C_{lp}$  ( $> 2.5$  wt.%) at the moderate  $T$  range (slightly above the melting transition temperature,  $T_M$  of the long-chain lipid) [20, 22, 23]. As  $T \ll T_M$ , bicelles are expected over a wide range of  $C_{lp}$  [14, 20, 24]. These bicelles are more stable at high  $C_{lp}$  and  $R$  values.

## 2 Materials

### 2.1 Phospholipids

#### 2.1.1 Long-Chain Phosphatidylcholines

The most common long-chain lipids used for bicellar formulation (but not limited to) are 1, 2-dipalmitoyl-*sn*-glycero-3-phosphocholine (DPPC, di-16:0) and 1,2-dimyristoyl-*sn*-glycero-3-phosphocholine (DMPC, di-14:0).

#### 2.1.2 Short-Chain Phosphatidylcholines or Detergents

Short-chain lipids can be 1, 2-dihexanoyl-*sn*-glycero-3-phosphocholine (DHPC, di-6:0), 3-[*(3*-Cholamidopropyl)dimethylammonio]-2-hydroxy-1-propanesulfonate (CHAPSO) or bile salts.

#### 2.1.3 Charged Long-Chain Phospholipid

The charged lipid is normally chosen to have the same acyl chain length as the long-chain lipid. They can be phosphatidylglycerol (PG), phosphatidic acid (PA), and phosphatidylserine (PS). Generally speaking, the molar ratio of charged long-chain lipid to zwitterionic long-chain lipid is kept between 0.01 and 0.2. Lower charge density leads to instability of the discoidal morphology, and higher charge density may affect the efficacy of cellular uptake.

**2.1.4 Polyethylene Oxide Conjugated (PEGylated) Phospholipid**

1,2-Distearoyl-*sn*-glycero-3-phosphoethanolamine-N-[methoxy (polyethylene glycol)-2000] (ammonium salt) (PEG2000-DSPE) is also used for stabilize the bicelles. Normally the molar ratio of PEG2000-DSPE to total long chain lipids is less than 0.1.

All the phospholipids listed above can be purchased from Avanti Polar Lipids and used without further purification.

**2.1.5 Lipophilic or Amphiphilic Molecules**

The bicellar platform can be used for encapsulation of lipophilic or amphiphilic compounds such as Nile red, pyrene, cholesterol, hydrophobic Au-clusters, etc.

**2.2 Solvent**

Bicelle can be prepared in a variety of aqueous solutions, e.g., water, phosphate-buffered saline (PBS), and Tris buffers, etc. Any amphiphilic compound in the solution may associate with the bicelles.

### 3 Methods

**3.1 Calculation of the Required Lipid Quantities**

The two parameters  $Q$  and  $R$  mentioned in the introduction can be defined as  $Q = \frac{[DPPC] + [DPPG] + [PEG2000 - DSPE]}{[DHPC]}$  and  $R = \frac{[DPPG]}{[DPPC] + [DPPG] + [PEG2000 - DSPE]}$  for a DPPC/DPPG/DHPC/PEG2000-DSPE bicellar system (here, we consider PEG2000-DSPE as a long-chain lipid). Note that [X] represents the molar number of species X.

**3.2 Dissolving Lipids in Organic Solvent**

The correct quantities of all dry lipids are first weighed and then homogeneously dispersed in appropriate amount of organic solvent (e.g., methanol, chloroform, or benzene). Complete dissolution will result in a transparent solution. Sometime vortexing and mild heating are required to assist the dissolution.

**3.3 Evaporation of the Solvent**

After all the species are homogenized, the majority of the solvent should be evaporated by heating the sample at  $T \sim 50$  °C with gentle blow of nitrogen. As the solution turns into honey-like high-viscosity liquid, the sample should be completely dried by vacuum for overnight. For less volatile solvent, higher  $T(50 \sim 60$  °C) can be applied in combination of vacuum.

**3.4 Sample Hydration**

The aqueous bicellar solution is obtained by redispersing the dried sample in desired solvent (i.e., water or buffer), yielding a high  $C_{lp}$  stock (> 10 wt.%), followed by 5–10 times of  $T$ -cycle between above and below  $T_M$  with additional vortexing. The solution should be viscous and translucent (or opaque) at  $T > T_M$ , while it becomes water-like and transparent at  $T < T_M$  as shown in Fig. 1. After temperature cycling, the stock solution should be stored at 4 °C. Bicellar samples can be obtained from the stock solution diluted to the desired  $C_{lp}$  at a  $T < T_M$ .

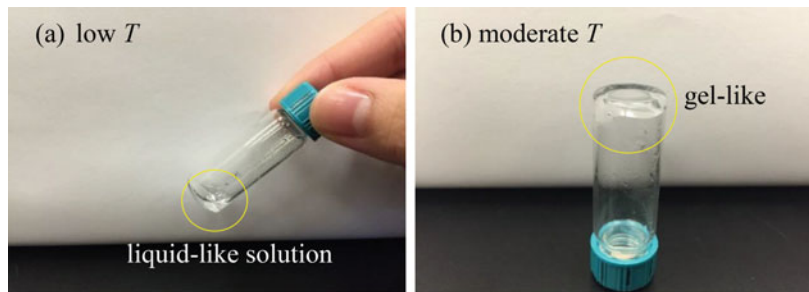


**Fig. 1** DMPC/DMPG/DHPC bicelle ( $Q = 3$  and  $R = 0.02$ ) with a concentration of 10 wt.% at low  $T$  (a) and moderate  $T$  (b), which shows a transparent and liquid-like at low  $T$  but gel-like at moderate  $T$

## 4 Structural Characterization

After sample preparation, the bicelles can be characterized using the techniques described below.

### 4.1 Dynamic Light Scattering (DLS)

The easiest and most accessible method to probe the formation of bicelles is DLS, which renders the hydrodynamic radius,  $R_H$ , of the nanoparticles in a solution based on Stokes–Einstein relationship. It should be noted that the obtained  $R_H$  is calculated under the assumption of spheres, which would yield an equivalent diffusivity of the nanoparticles. However, the true morphology and detailed internal structure of nanoparticles cannot be revealed. Moreover, high- $C_{lp}$  and high charge density on the bicelles may affect the mutual diffusion coefficient of the nanoparticles. In general, DLS measurements should be taken at  $C_{lp} < 1.0$  wt.% (depending on the  $R$  value) to avoid strong interparticle interaction. It should also be noted that the higher- $R$  samples may result in a peak revealing a smaller size because of the rapid diffusion as shown in Fig. 2. This can be overcome by further diluting the solution to a lower  $C_{lp}$ . However, in some cases bicelles may be not stable if  $R$  is low (e.g.,  $< 0.01$ ) and in the absence of PEGylated lipid as they might form vesicles [19, 25]. The obtained  $R_H$  for bicelles normally ranges around 6 ~ 15 nm [26]. If the measured  $R_H$  is larger than 20 nm, it implies that the unstable bicelles may have already transformed into vesicles. However, exceptionally large discs with radius  $> 50$  nm have been found as hydrophobic quantum dots (QDs) (with radii  $> 4$  nm) are entrapped [27].

### 4.2 Negatively Stained (ns-) and Cryo-TEM

TEM is the most direct method to visualize morphology of the nanoparticles. Either ns-TEM or cryo-TEM can be applied to investigate the bicellar structure. Uranium acetate salt can be used for staining the background to enhance the contrast. Since the structure of bicelles mostly remains intact under vacuum (occasionally fusion of bicelles may take place), the micrograph is able to

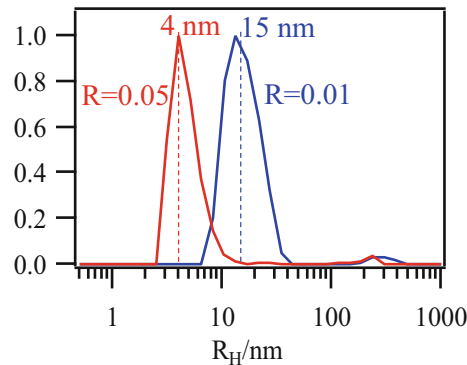


**Fig. 2** The intensity-weighted DLS result of a DPPC/DPPG/DHPC bicellar solution ( $C_{lp} = 0.1$  wt.% and  $Q = 3$ ), with two different charge densities  $R = 0.01$  (blue) and  $0.05$  (red) at  $T = 25$  °C. Two distinct distribution functions with a peak located at 15 nm and 4 nm, respectively, are found, indicative a strong interparticle interaction for the highly charged sample

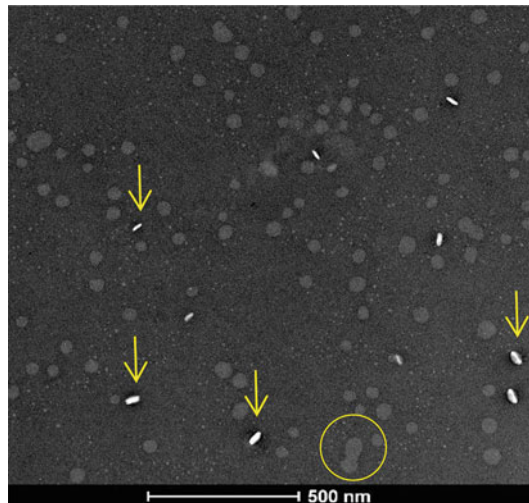


**Fig. 3** The ns-TEM micrograph of a DPPC/DPPG/DHPC/PEG2000-DSPE bicellar solution ( $C_{lp} = 0.01$  wt.%,  $Q = 3$ ,  $R = 0.05$ ). The image reveals the discoidal plane for most of the nanodiscs and occasionally the rim of the nanodiscs (arrows). The fusion between two discs during drying process is also captured (in the circle) in the micrograph

reveal the nanoscale morphology faithfully. Since both vesicles (i.e., liposomes) and discoidal bicelles are possible structures in a bicellar system, the projected 2-D TEM images of discs may resemble those of intact vesicles. Nevertheless, under the ns-TEM setting, they are distinguishable. In the case of vesicles, broken edges of the burst spheres are commonly observed due to the vacuum, while the 2-D projection of 3-D bicelles may vary from line (rim of the disc), ellipse (titled discs), to circle (discoidal plane). Fig. 3 shows a

ns-TEM of 0.01 wt.% DPPC/DHPC/DPPG/PEG2000-DSPE bicolles after being dried under vacuum. The image indicates relatively uniform size of bicolles and discoidal plane, rim, and fusion in process are also observed.

Cryo-TEM will provide similar information as ns-TEM does except that all structures will be frozen and thus remain intact (including vesicles), and the object will be darker than the background. In spite of the abovementioned advantages in determining shape, the structural information obtained from TEM is local, mostly in the  $\mu\text{m}^2$  range. To ensure the structures are uniform throughout the sample, multiple micrographs have to be taken in order to assume the observed structure. Moreover, it is difficult to conduct the *in situ* study at the same condition as in solution using TEM. An alternative method, which overcomes both challenges, would be small-angle scattering technique as described below.

#### **4.3 Small-Angle X-Ray Scattering (SAXS) and Small-Angle Neutron Scattering (SANS)**

Like DLS, SAXS and SANS techniques are indirect methods to provide structural information. The result heavily relies on interpretation of the scattering patterns. However, scattering allows us to investigate the global structures in stringent *in situ* environments, thus complementary to TEM measurement. The amplitude of scattering intensity as a function of scattering vector is basically the Fourier transform (from the real to the reciprocal space) of the density fluctuation in the system. Therefore, square of the Fourier transform (multiplication of the Fourier transform with its conjugate) describes the scattering intensity. If the structures of nanoparticles are uniform (i.e., low polydispersity) with unimodal distribution, we can assume the specific structure with detailed dimensions and certain polydispersity in the real space and then take a spatial Fourier transform of the density function into the scattering vector,  $q$  (reciprocal space) domain. The square of the transform, after being convoluted with the instrumental resolution function, is proportional to the scattering intensity,  $I(q)$ . Figure 4 shows the SANS result of the DPPC/DHPC/DPPG bicolles (in  $\text{D}_2\text{O}$ ) and the best fit for the data using a core-shell discoidal model [28], where the core and the shell represent the hydrophobic acyl chains and hydrophilic headgroup layer, respectively. The best-fitting structural parameters are discoidal core radius ( $R_{\text{core}} = 18.6 \text{ nm}$ ), shell thickness ( $t_{\text{shell}} = 1.3 \text{ nm}$ ), and discoidal core thickness ( $t_{\text{core}} = 2.5 \text{ nm}$ ), indicating that the small-angle scattering method can not only resolve the shape but also detailed internal structure of the nanoparticles with sufficient contrast. The NIST (National Institute of Standards and Technology) Center for Neutron Research (NCNR) has developed a variety of available scattering models for SANS data fitting coded in IGOR-PRO program [28]. SAXS provides the similar structural information as SANS does. The main difference between SANS and SAXS is the origin of contrast: the former being neutron scattering length

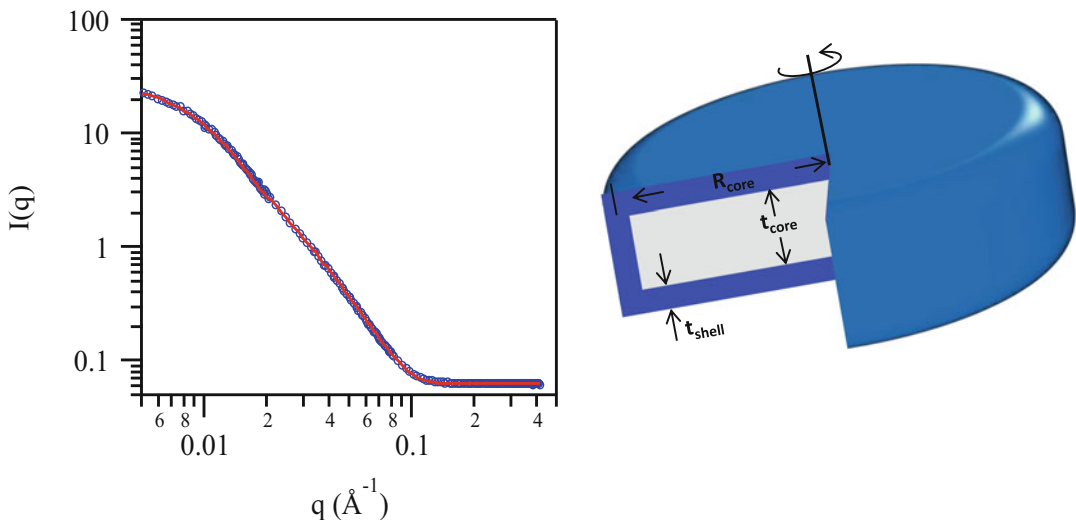


**Fig. 4** The SANS data (blue circles) of a DPPC/DPPG/DHPC bicellar solution ( $C_{lp} = 0.1$  wt.%,  $Q = 3$ ,  $R = 0.01$ ). The core-shell discoidal model as shown in the sketch applied to fit the SANS data (red solid curve) to obtain structural parameters of the bicelles

density and the latter electron density. For this reason, the SANS and SAXS patterns differs drastically and the core-shell discoidal model is no longer appropriate for fitting the SAXS data of bicelles at a high scattering vector range ( $> 0.6 \text{ \AA}^{-1}$ ). Cheu et al. developed a new SAXS model (five-layer core-shell discoidal model) to describe the scattering data of bicelles [29]. The five layers represent phosphate-ordered methylene-disordered middle region-ordered methylene-phosphate, respectively, to resolve the internal structure of the bilayer of the discs if SAXS were collected over an extended scattering vector range ( $> 0.6 \text{ \AA}^{-1}$ ) [29].

## 5 Stability and Cellular Uptake

The instability of bicelles can presumably be triggered by either insufficient amount of short-chain lipid (i.e., DHPC) associated with bicelles, insufficient Coulombic repulsive force, or weak steric interaction. It is known that the high-curvature discoidal rim is stabilized by the short-chain DHPC which has a high spontaneous curvature. However, DHPC and long-chain lipid have distinct water solubility. Therefore, as the bicellar sample is diluted, more DHPC is drawn from the bicelles into aqueous phase compared to the long-chain lipid, which increases the instability of the bicelles, resulting in fusion of bicelles and eventually the formation of vesicles. The lipid dissociation from bicelles was also observed for charged long-chain lipid, which is more soluble than zwitterionic long-chain lipid, upon dilution of the bicelles. It has been reported

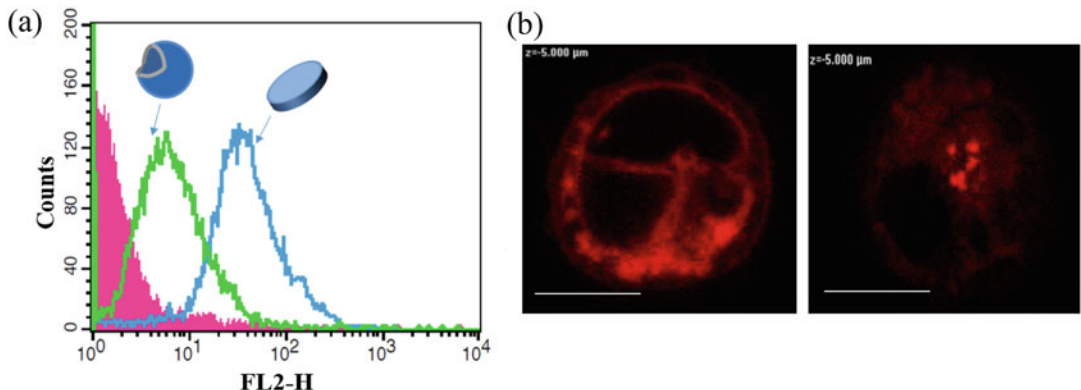


**Fig. 5** (a) The cellular flow cytometric histograms of CCRF-CEM cells alone (pink), liposomes (green), and bicellar nanodiscs (blue). The uptake peak of bicellar nanodiscs indicates 6 ~ 7 times of fluorescence in comparison with that of liposomes. (b) The fluorescence confocal micrograph of CCRF-CEM cells after being incubated with Nile red containing bicelles (left) and liposomes (right). The bar is 10  $\mu$ m

that the size of bicelles would reach to a new equilibrium size after dilution due to the enhanced line tension and that the kinetics can be described by a transport-limited process as a function of surface charge potential associated with the bicelles [26]. Bicelles can be further stabilized by PEG2000-DSPE through steric interaction. The PEG2000-DSPE containing bicelles were found stable for weeks [30]. Most recently, the structure of such bicelles was found stable in buffer and serum at  $T < T_M$ , and their cellular uptake was found three to tenfold of that of the similar-sized liposomes [13]. Figure 5(a) shows a comparison of in vitro cellular uptake by  $1.8 \times 10^5$  CCRF-CEM cells between chemically identical bicelles and liposomes via a flow cytometric study. Both are of the same  $C_{lp}$  (0.1 wt.%) and contain the same molar ratio of Nile red fluorescence dye to lipids (1:100). The only difference between the two is morphology. The two kinds of Nile red containing nanoparticles (bicelles and vesicles) were incubated with the cells at 37 °C for 2 h individually and washed with buffer prior to the flow cytometric measurements. The result shows that the peak fluorescence in the case of bicelles is 6 ~ 7 times of that for liposomes. The disc-enhanced cellular uptake was also observed in fluorescence confocal micrograph as shown in Fig. 5b, which confirmed the internalization of the nanoparticles as well. Bicelles can also be used to entrap amphiphilic molecules to shuttle them across cell membranes. Most recently, an in vitro study indicates high efficacy in targeting microRNA through peptide nucleic acid-loaded bicelles [31]. In vitro and in vivo studies of using bicelles as carriers to deliver meta-Tetra(hydroxyphenyl) chlorin, an agent for targeting photodynamic treatment [32] and co-deliver paclitaxel and parthenolide [33] on tumors, also show significant improvement on the efficacy compared with other types of delivery mechanisms.

## 6 Hydrophobic Confinement

It has been reported that ligand-protected Au nanoclusters (Au-NCs) [34], hydrophobic QDs [27], and organo-metallic supramolecules [35] can be successfully entrapped in the bicelles. The term “NANO<sup>2</sup>” representing nanoparticles (NPs) in nanodiscs is used to describe such nanocomplex. At low NP-to-lipid compositions, bicelles accommodate most of the NPs at the rim region made of fluid DHPC [Fig. 6a–c]. The Au-NCs with 25 Au atoms in core, whose surface was conjugated with different hydrocarbons, have little or no photoluminescence when dispersed in organic solvents. Intriguingly, photoluminescence and photoacoustic signal enhance significantly in NANO<sup>2</sup>-Au-NCs [Fig. 6d]. Similar enhancement in fluorescence was also found for NANO<sup>2</sup>-QD [Fig. 6e]. It is hypothesized that the restricted motion of the surface ligand of the QD under encapsulation could change the pathway of energy dissipation from non-radiative to emissive mechanisms [27]. In order to fully understand the mechanism,

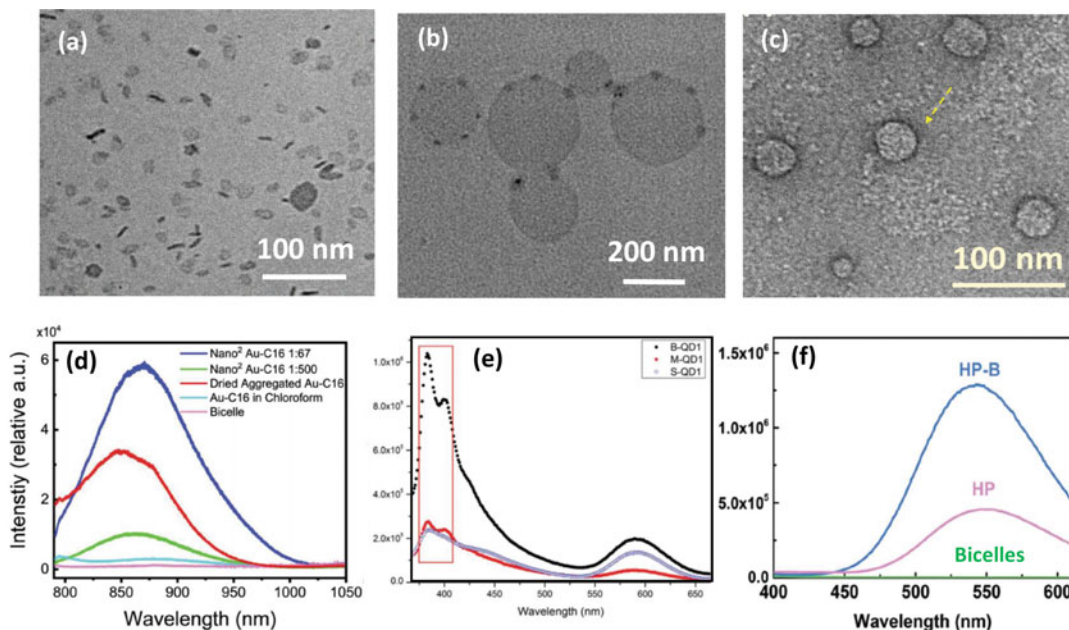


**Fig. 6** The negatively staining TEM images of NANO<sup>2</sup>: (a) NANO<sup>2</sup>-AuNC [34], (b) NANO<sup>2</sup>-QD [27], and (c) NANO<sup>2</sup>-supramolecule [35]. Darker circumferences representing a higher electron density were found in (a) and (c), while QDs aggregated into several globules at the rim of discs in (b). The enhanced photoluminescence (fluorescence) of (a), (b), and (c) are compared against their dispersions in the organic solvent in (d), (e), and (f), respectively. In (d), the photoluminescence includes samples with two molar ratios of Au-NC to lipids (1:67 and 1:500), the dry Au-NC, the Au-NC in chloroform and bicelles [34]. In (e), the photoluminescence includes NANO<sup>2</sup>-QD (B-QD), QD entrapped in DHPC micelles (M-QD), and QD in chloroform (S-QD) [27]. In (f), the fluorescence spectra of NANO<sup>2</sup>-Supramolecule (HP-B; HP representing the supramolecular morphology being Hexagonal Prism), the supramolecules in chloroform (HP), and bicelles (B) are shown [35]

further study on other similar  $\text{NANO}^2$ -semiconductor systems is required. Another type of  $\text{NANO}^2$  containing drum-like self-assemblies from organo-metallic supramolecules also demonstrates enhanced fluorescence in comparison with its free form [Fig. 6f]. The enhancement is rationalized by the dissociation of  $\pi\text{-}\pi$  stacking between the drum-like assemblies upon encapsulation due to limited space in the  $\text{NANO}^2$  [35]. These outcomes suggest a new capability to control the degree of hydrophobic confinement and the rigidity of hydrophobic environment for the entrapped species.

---

## Acknowledgments

The authors would like to acknowledge the funding support from NSF-CMMI 1131587, CBET 1433903, and 1605971.

## References

1. Sanders CR, Landis GC (1995) Reconstitution of membrane proteins into lipid-rich bilayered mixed micelles for NMR studies. *Biochemistry* 34(12):4030–4040
2. Diller A, Loudet C, Aussénac F et al (2009) Bicelles: a natural ‘molecular goniometer’ for structural, dynamical and topological studies of molecules in membranes. *Biochimie* 91(6):744–751
3. Naito A (2009) Structure elucidation of membrane-associated peptides and proteins in oriented bilayers by solid-state NMR spectroscopy. *Solid State Nucl Magn Reson* 36(2):67–76
4. Poget SF, Girvin ME (2007) Solution NMR of membrane proteins in bilayer mimics: small is beautiful, but sometimes bigger is better. *Biochim Biophys Acta* 1768(12):3098–3106
5. Prosser RS, Evanics F, Kitevski JL et al (2006) Current applications of bicelles in NMR studies of membrane-associated amphiphiles and proteins. *Biochemistry* 45(28):8453–8465
6. Johansson LC, Wohri AB, Katona G et al (2009) Membrane protein crystallization from lipidic phases. *Curr Opin Struct Biol* 19(4):372–378
7. Kimble-Hill AC (2013) A review of factors affecting the success of membrane protein crystallization using bicelles. *Front Biol* 8(3):261–272
8. Poulos S, Morgan JL, Zimmer J et al (2015) Bicelles coming of age: an empirical approach to bicelle crystallization. *Methods Enzymol* 557:393–416
9. Mills JO, Holland LA (2004) Membrane-mediated capillary electrophoresis: interaction of cationic peptides with bicelles. *Electrophoresis* 25(9):1237–1242
10. Barbosa-Barros L, Barba C, Rodriguez G et al (2009) Lipid nanostructures: self-assembly and effect on skin properties. *Mol Pharm* 6(4):1237–1245
11. Rodriguez G, Barbosa-Barros L, Rubio L et al (2009) Conformational changes in stratum corneum lipids by effect of bicellar systems. *Langmuir* 25(18):10595–10603
12. Rodriguez G, Barbosa-Barros L, Rubio L et al (2015) Bicelles: new lipid Nanosystems for dermatological applications. *J Biomed Nanotechnol* 11(2):282–290
13. Aresh W, Liu Y, Sine J et al (2016) The morphology of self-assembled lipid-based nanoparticles affects their uptake by cancer cells. *J Biomed Nanotechnol* 12(10):1852–1863
14. Katsaras J, Harroun TA, Pencer J et al (2005) “Bicellar” lipid mixtures as used in biochemical and biophysical studies. *Naturwissenschaften* 92(8):355–366
15. Andersson A, Maler L (2006) Size and shape of fast-tumbling bicelles as determined by translational diffusion. *Langmuir* 22(6):2447–2449
16. Beaugrand M, Arnold AA, Henin J et al (2014) Lipid concentration and molar ratio boundaries for the use of isotropic bicelles. *Langmuir* 30(21):6162–6170
17. Lind J, Nordin J, Maler L (2008) Lipid dynamics in fast-tumbling bicelles with varying bilayer thickness: effect of model transmembrane

- peptides. *Biochim Biophys Acta* 1778(11): 2526–2534
18. Ye W, Lind J, Eriksson J et al (2014) Characterization of the morphology of fast-tumbling bicelles with varying composition. *Langmuir* 30(19):5488–5496
19. Nieh M-P, Dolinar P, Kučerka N et al (2011) Formation of kinetically trapped nanoscopic unilamellar vesicles from metastable nanodiscs. *Langmuir* 27(23):14308–14316
20. Soong R, Nieh M-P, Nicholson E et al (2010) Bicellar mixtures containing pluronic F68: morphology and lateral diffusion from combined SANS and PFG NMR studies. *Langmuir* 26(4):2630–2638
21. Yang P-W, Liu T-L, Hu Y et al (2012) Small-angle X-ray scattering studies on the structure of mixed DPPC/diC7PC micelles in aqueous solutions. *Chin J Phys* 50(2):349–356
22. Li M, Morales HH, Katsaras J et al (2013) Morphological characterization of DMPC/CHAPSO bicellar mixtures: a combined SANS and NMR study. *Langmuir* 29(51): 15943–15957
23. Nieh M-P, Raghunathan VA, Kline SR et al (2005) Spontaneously formed unilamellar vesicles with path-dependent size distribution. *Langmuir* 21(15):6656–6661
24. Nieh M-P, Raghunathan VA, Pabst G et al (2011) Temperature driven annealing of perforations in bicellar model membranes. *Langmuir* 27(8):4838–4847
25. Mahabir S, Wan W, Katsaras J et al (2010) Effects of charge density and thermal history on the morphologies of spontaneously formed unilamellar vesicles. *J Phys Chem B* 114(17): 5729–5735
26. Hu A, Fan T-H, Katsaras J et al (2014) Lipid-based nanodiscs as models for studying meso-scale coalescence – a transport limited case. *Soft Matter* 10(28):5055–5060
27. Fang JM, Basu S, Li M et al (2022) Restriction-in-motion of surface ligands enhances photoluminescence of quantum dots – experiment and theory. *Adv Mater Interfaces* 9:2102079
28. Kline SR (2006) Reduction and analysis of SANS and USANS data using IGOR Pro. *J Appl Crystallogr* 39(6):895–900
29. Cheu C, Yang L, Nieh M-P (2020) Refining internal bilayer structure of bicelles resolved by extended-q small angle X-ray scattering. *Chem Phys Lipids* 231:104945
30. Liu Y, Li M, Yang Y et al (2014) The effects of temperature, salinity, concentration and PEGylated lipid on the spontaneous nanostructures of bicellar mixtures. *Biochim Biophys Acta* 1838(7):1871–1880
31. Rad AT, Malik S, Yang L et al (2019) A universal discoidal nanoplatform for the intracellular delivery of PNAs. *Nanoscale* 11:12517
32. Tahmasbi Rad A, Chen C-W, Aresh W et al (2019) Combinational effects of active targeting, shape, and enhanced permeability and retention for cancer Theranostic Nanocarriers. *ACS Appl Mater Interfaces* 11(11): 10505–10519
33. Rad AT, Hargrove D, Daneshmandi L et al (2022) Codelivery of paclitaxel and Parthenolide in discoidal Bicelles for a synergistic anti-cancer effect: structure matters. *Adv NanoBiomed Res* 2:2100080
34. Tahmasbi Rad A, Bao Y, Jang H-S et al (2021) Aggregation-enhanced photoluminescence and photoacoustics of atomically precise gold nanoclusters in lipid nanodiscs (NANO<sup>2</sup>). *Adv Func Mater* 31(10):2009750
35. Liu C-H, Wang H, Yang L et al (2021) Nano-complex made up of antimicrobial metallo-supramolecules and model biomembranes—characterization and enhanced fluorescence. *Nanoscale* 13(35):14973–14979



# Chapter 14

## The Post-insertion Method for the Preparation of PEGylated Liposomes

Sherif E. Emam, Nehal E. Elsadek, Taro Shimizu, and Tatsuhiko Ishida

### Abstract

PEGylation is a crucial process for decorating the surface of liposomes with polyethylene glycol (PEG) for clinical use. This process endows the liposomes extended circulation time and improved stability *in vivo*. The post-insertion method is one of the well-established techniques for PEGylation. This method requires only one-step incubation to accomplish the transfer of PEGylated lipids from PEGylated lipid-based micelles into the membranes of preformed liposomes.

**Key words** Post-insertion method, Liposomes, Micelles, Polyethylene glycol (PEG), Long-circulating

---

### 1 Introduction

Since Alec D Bangham's evolutionary discovery of liposomes in the 1960s, the utility of these spherical vesicles has steadily expanded and now encompasses a wide variety of applications that have garnered widespread acceptance. Liposomes are vesicles with a self-assembled bilayer of amphiphilic lipids (phospholipids) surrounding an aqueous core. Liposomes can carry a variety of active molecules (hydrophilic, lipophilic, amphipathic) for purposes that are highly valued by the medical (therapeutic and diagnostic agents), cosmetic, and food (additives, antimicrobials, preservatives, etc.) industries. Integral to the utility of liposomes are prominent characteristics such as biocompatibility, biodegradability, ease of preparation, and a high level of stability. Therefore, the uses of liposomes as drug delivery systems have been robustly investigated [1].

For medical applications, however, when conventional liposomes are intravenously injected, they are immediately associated with opsonins such as immunoglobulins and complement components that form immune complexes, which results in enhanced

clearance of the liposomes from blood circulation via increased uptake by the cells of the mononuclear phagocyte (reticuloendothelial) system [2]. To reduce liposome opsonization and extend their circulation time, the surface of liposomes is coated with polysaccharides or glycolipids. Also, hydrophilic synthesized polymers such as polyethylene glycol (PEG)-lipid derivatives have been extensively tested since the late 1980s and early 1990s [3, 4]. The latter approach is referred to as PEGylation, which has become the most successful. Due to their properties of long circulation, PEGylated liposomes are also known as Stealth liposomes®, long circulating liposomes, or sterically stabilized liposomes. This ability allows them to passively accumulate in solid tumors or inflamed tissues with increased vascular permeability, which translates to an enhanced permeability and retention (EPR) effect [5]. Some PEGylated liposomal formulations such as Doxil®, Caelyx®, Onivyde®, and Lipodox® have been approved for clinical use [6–8]. PEGylation is generally achieved via the insertion of a synthesized PEGylated lipid such as 1,2-distearoylsn-glycero-3-phosphoethanolamine-n-[methoxy (polyethyleneglycol)-2000] (PEG<sub>2000</sub>-DSPE) into a liposomal lipid membrane. In addition, PEGylated liposomes can be employed to target specific disease sites by grafting the terminus of PEG with a variety of targeting moieties such as protein ligands, peptides, antibodies, and oligosaccharides [5, 9, 10]. Therefore, in this chapter, we focus on a technique that is used to graft the outer layer of liposomes with PEG<sub>2000</sub>-DSPE or a targeting moiety.

PEGylated liposomes are generally created by adding PEGylated lipids either during liposome preparation via mixing with other lipid components (pre-insertion) or after liposome preparation (post-insertion) (Fig. 1). Post-insertion techniques are effective for obtaining PEGylated liposomes with pharmacokinetic properties similar to those of the PEGylated liposomes created by pre-insertion techniques [11–13]. Moreover, post-insertion techniques possess several advantages over pre-insertion techniques, particularly in terms of cost and flexibility. In the pre-insertion techniques, the targeting ligands must be grafted to the terminus of the PEG coating on the preformed PEGylated liposomes in a separate step and under conditions that could destabilize the liposomes. In the post-insertion method, on the other hand, the targeting ligands are covalently grafted to the terminus of the PEG portion of PEGylated lipid-based micelles, which then are inserted into the preformed liposomes forming ligand-modified PEGylated liposomes (Fig. 2). In addition, modification of the exterior surface of liposomes during the post-insertion method creates inner space for the encapsulation of larger amounts of drugs than what is available when using conventional PEGylated liposomes (pre-insertion). Post-insertion can be simply applied to a variety of preformed drug-containing liposomes in a single step [11, 12, 14].

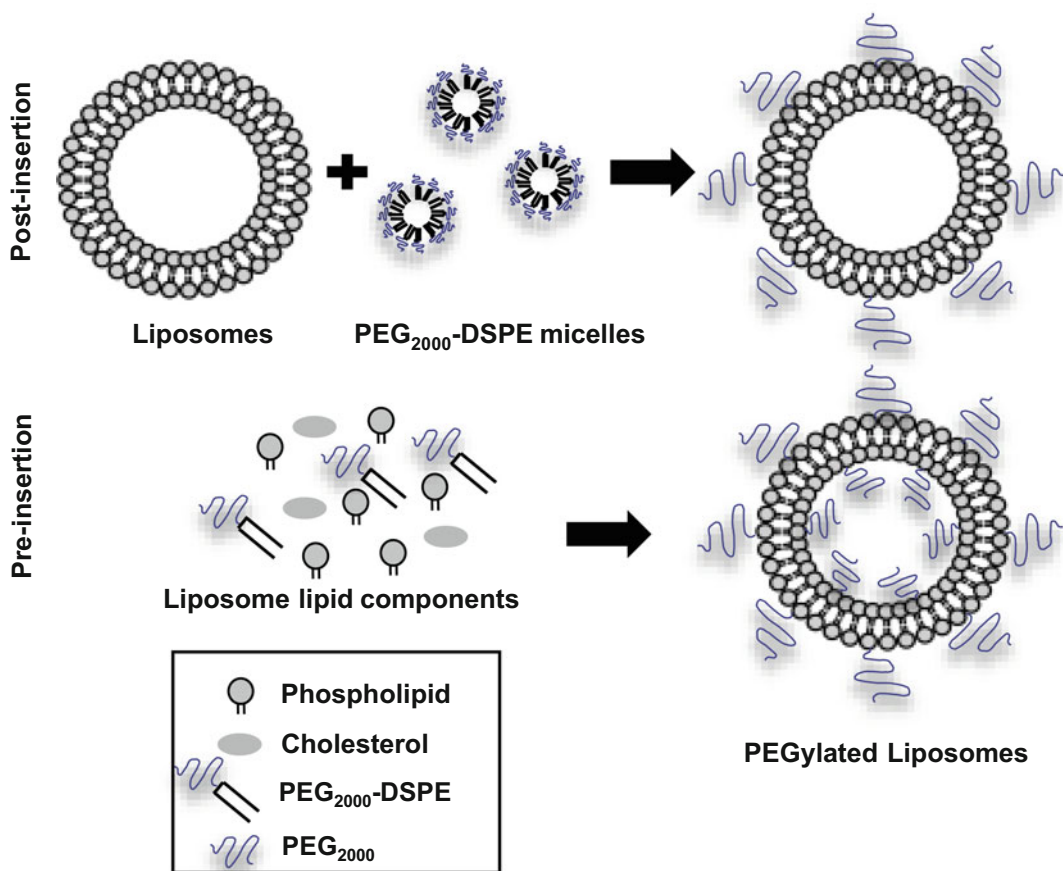


**Fig. 1** Methods of PEGylation for liposomes. PEGylation for liposomes is accomplished by one of two methods: pre-insertion or post-insertion. In the pre-insertion method, PEGylated lipid derivatives ( $\text{PEG}_{2000}$ -DSPE) are mixed with liposome lipid components during liposome preparation, which results in  $\text{PEG}_{2000}$ -DSPE being embedded into both the inner and outer layers of liposomes. In the post-insertion method,  $\text{PEG}_{2000}$ -DSPE-based micelles are mixed with preformed liposomes, which results in the embedding of  $\text{PEG}_{2000}$ -DSPE in only the outer layer of liposomes

The protocol for the post-insertion technique provides researchers with a precise guideline that includes technical precautions for successfully preparing PEGylated liposomes.

## 2 Materials

1. Pear-shaped flask (10 mL).
2. Glass syringe.
3. Incubator.
4. Sterile Milli-Q water.

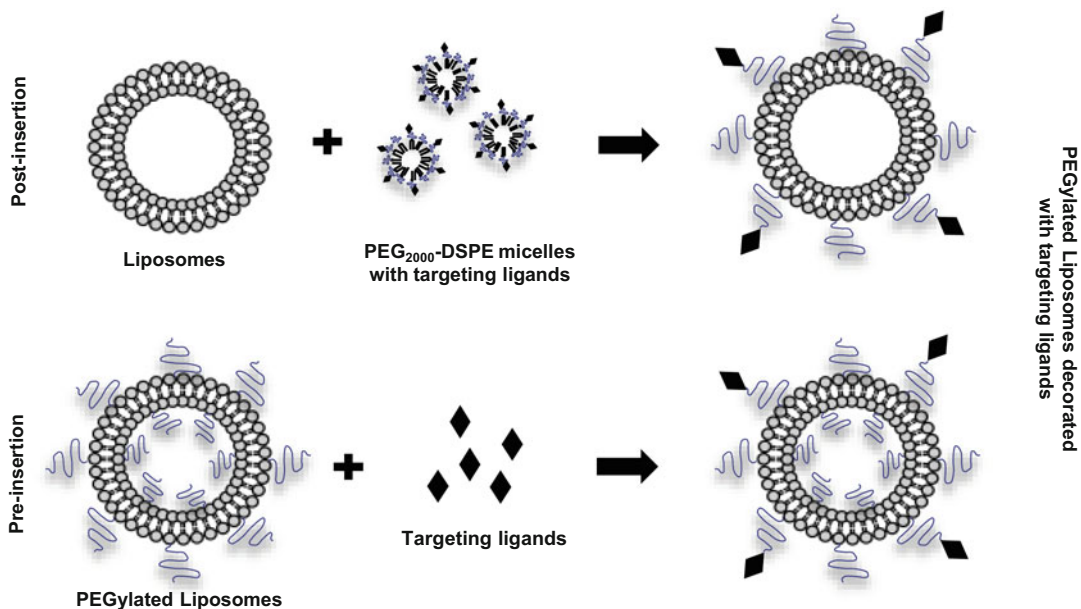


**Fig. 2** Grafting targeting ligands into PEGylated liposomes. Modifying PEGylated liposomes with targeting ligands differs between pre-insertion and post-insertion techniques. In the pre insertion method, targeting ligands are grafted to the terminus of the PEGylated lipids that have already been incorporated in the preformed PEGylated liposomes. In the post-insertion method, targeting ligands are covalently grafted to the terminus of the PEG portion of PEGylated lipid-based micelles, which then are inserted into preformed liposomes

5. HEPES (4-(2-hydroxyethyl)-1-piperazineethanesulfonic acid) buffer (pH 7.4): Dissolve 5.95 g HEPES and 8.18 g of NaCl in 950 mL Milli-Q water; adjust the pH to 7.4 with 2 M NaOH; and adjust the volume to 1 L with Milli-Q water. Sterilize HEPES buffer by autoclaving.
6. 50 mM hydrogenated soy 1- $\alpha$ -phosphatidylcholine (HSPC) stock: Dissolve 392.5 mg HSPC in 10 mL chloroform.
7. 50 mM cholesterol (CHOL) stock: Dissolve 193.33 mg cholesterol in 10 mL chloroform.
8. 5 mM 1,2-distearoylsn-glycero-3-phosphoethanolamine-n-[methoxy (polyethyleneglycol)-2000] (PEG<sub>2000</sub>-DSPE) stock: Dissolve 141.7 mg PEG<sub>2000</sub>-DSPE in 10 mL chloroform.
9. Chloroform.
10. Vortex mixer.
11. Rotary evaporator.
12. Vacuum desiccator.
13. Water-bath sonicator.
14. Lipex extruder (Lipex Biomembranes Inc., VC, Canada).

15. Polycarbonate membranes with pore sizes of 400, 200, and 100 nm.
16. Malvern Zetasizer Nano ZS (Malvern Instruments Ltd., WR, UK).
17. Nitrogen gas tank.

---

### 3 Methods

#### 3.1 Preparation of Preformed Liposomes

1. Make sure that all equipment is clean and dry (*see Note 1*).
2. Rinse the 10 mL pear-shaped flask thoroughly with 1 mL chloroform. You can use the flask directly after the rinsing step; no need to wait for it to dry.
3. Ensure that each lipid is well dissolved before mixing them (*see Note 2*).
4. Mix phospholipid (HSPC) and CHOL (2:1 molar ratio) (other lipids and molar ratios can be used) into the evaporating pear-shaped glass flask; add 1.2 mL of 50 mM HSPC stock solution and 0.6 mL of 50 mM CHOL stock solution. Vortex to mix the components together. Assemble the flask with the rotary evaporator (*see Notes 3–8*).
5. Evaporate the chloroform slowly by spinning and heating (40 °C) under reduced pressure using a rotary evaporator equipped with a vacuum pump until a dry lipid film forms; about 2 h is required (*see Notes 9–15*).
6. Store the dried lipid films overnight in a vacuum desiccator to remove the residual traces of chloroform (*see Note 16*).
7. Hydrate the dried lipid films by adding 3 mL HEPES buffer, pH 7.4, with agitation at 60 °C for 2 h (vortex every 30 min) to produce multilamellar vesicles (MLVs) (*see Notes 9, 17, and 18*).
8. Reduce the size of the MLVs by sequentially passing them through polycarbonate membrane filters with pore sizes of 400, 200, and 100 nm using an extruder heated to 60 °C. The extrusion must be carried out at low pressure to avoid rupturing the polycarbonate membranes. The extrusion step must be repeated 3–5 times for each pore size (*see Notes 9, 19–22*).

#### 3.2 Characterization of Preformed Liposomes

1. Determine the particle sizes of the liposomes using dynamic light scattering equipment such as the Zetasizer nano series. The prepared liposomes should be homogeneous in size. The average size should be approximately 100 nm with a polydispersity index (PDI) below 0.2 (*see Note 23*).

- Determine the phospholipid concentration of liposomes via colorimetric Bartlett phospholipid assay [15] with KH<sub>2</sub>PO<sub>4</sub> (monopotassium phosphate) as a standard (theoretical concentration should be about 20 mM) (*see Notes 24 and 25*). In Bartlett phospholipid assay, convert phospholipids (5 µL) to inorganic phosphates by heating them with perchloric acid (500 µL) at 300 °C for 5 min inside a chemical fume hood, then cooling with air. Add ammonium molybdate (4.5 mL) to further convert inorganic phosphates to phospho-molybdic acid. The final step is the reduction of the formed compound by heating it with 4-amino-2-naphthyl-4-sulfonic acid (200 µL) at 80 °C for 15 min to produce a blue colored complex that can be determined at 830 nm.

#### **4 Preparation of PEGylated Lipid (PEG<sub>2000</sub>-DSPE)-Based Micelles**

- Add 2 mL of 5 mM PEG<sub>2000</sub>-DSPE to the evaporating pear-shaped glass flask. Attach the flask to a rotary evaporator (*see Notes 1–8 and 26*).
- Evaporate the chloroform by spinning and heating (40 °C) under reduced pressure using a rotary evaporator equipped with a vacuum pump until a dry lipid film forms (*see Notes 9–15*).
- Keep the dried lipid films overnight in a vacuum desiccator to remove the residual traces of chloroform (*see Note 16*).
- Hydrate the dried lipid films by adding 2 mL HEPES buffer, pH 7.4, with gentle agitation at 60 °C to produce PEG<sub>2000</sub>-DSPE-based micelles (about 5 mM) (*see Notes 9, 17, 18, and 27–29*).
- Determine the particle size of the resultant micelles. The mean particle size should be between 30 and 50 nm. When using PEG<sub>2000</sub>-DSPE in combination with another ligand to create micelles, the size of the micelles produced can be larger (*see Note 23*).
- Determine the phospholipid content of the micelles with the colorimetric Bartlett phospholipid assay (theoretical concentration should be about 5 mM) (*see Notes 24 and 25*).

##### **4.1 Transfer of PEG<sub>2000</sub>-DSPE from the Micelles to the Preformed Liposomes**

- Incubate the preformed liposomes with aliquots of PEG<sub>2000</sub>-DSPE-based micelles (fluorescence- or radio-labeled PEG<sub>2000</sub>-DSPE can be used for further characterization of the PEGylated liposomes created by the post-insertion method) at a molar ratio of 4 mol% PEG<sub>2000</sub>-DSPE to the phospholipid concentration of preformed liposomes for 1 h at 60 °C with gentle shaking (*see Notes 30–40*).

2. Remove the excess contaminating PEG<sub>2000</sub>-DSPE-based micelles from the prepared PEGylated liposomes using chromatography on Sepharose CL-4B columns eluted with HEPES buffer pH 7.4 (*see Notes 41–48*).

#### **4.2 Characterization of the Prepared PEGylated Liposomes**

1. Determine the particle size and zeta potential of the resultant PEGylated liposomes. When compared with the preformed (plain) liposomes, the size of the resultant PEGylated liposomes is expected to increase by 10–30 nm, while their surface charge is expected to decrease (*see Notes 23 and 49–50*) due to the PEGylation.
2. Determine the amount of PEG<sub>2000</sub>-DSPE (fluorescence or radio-labeled PEG<sub>2000</sub>-DSPE) that is incorporated into the resultant PEGylated liposomes after purification. Typical modification efficiency will be 100% of the added PEGylated lipids (*see Notes 39 and 51*).

---

## **5 Notes**

1. Glassware should be completely dry (with no trace of water), because water hinders the solvent evaporation and the production of uniform lipid films.
2. The solubility of each lipid should be thoroughly checked before they are mixed, because the presence of any insoluble particles will appear in the film and a homogeneous liposome size will not be achieved after the hydration step.
3. For evaporation of the organic solvent, ordinary round-bottom flasks and glass conical tubes with round bottoms can also be utilized.
4. Lipids (powder or dissolved in chloroform) should be stored at –20 °C, or lower, and brought to room temperature for 20 min before use. To maintain lipid stability and avoid lipid oxidation, the air inside the lipid powder package should be replaced with nitrogen gas before storage. To avoid the loss of chloroform, which is highly volatile, containers containing the dissolved lipids should be firmly closed and wrapped with plastic tape or parafilm. Fresh lipid solutions are preferred for accurate molar ratios due to the vaporization of chloroform during the repeated use of dissolved lipid stocks.
5. Lipids should be handled under a chemical fume hood to avoid inhaling any vapor that could escape. It is preferable to weigh lipids with a disposable plastic spatula rather than a metal spatula, which may negatively interact with the lipids.

6. Chloroform has a high vapor pressure at room temperature. Therefore, chloroform should be handled under a chemical fume hood.
7. Glassware should be used instead of plasticware while working with chloroform.
8. Glass syringes should be rinsed with chloroform several times before use and between different lipids.
9. Heating is a critical step in accelerating the solvent evaporation (in rotary evaporator), the lipid film hydration, the extrusion of MLVs, and the post-insertion process. The stability of the encapsulated drug and the phase transition temperatures of the selected lipids are the controlling factors in selecting the temperatures for heating.
10. The volume of the sample (lipid solution) to be evaporated should not exceed half of the flask; otherwise, sample loss could occur. To guarantee appropriate evaporation and no sample loss, large samples (volumes exceeding half of the flask) should be divided before being placed in the rotary evaporator. Also, the sample volume should not be too small in proportion to the flask bottom because the formed film should occupy as much of the flask walls as possible.
11. Heat the bath to enhance the evaporation process. The heating should be adjusted to a moderate temperature (mostly 40 °C). Excessive temperature, or a temperature above the boiling point of the solvent, will cause the evaporation rate to surpass the capacity of the condenser, which could cause the evaporation process to fail.
12. Rotation of the flask is important to increase the surface area of the sample for better evaporation and to protect the samples from overheating. A moderate rotation speed should be maintained (about 60 rpm), particularly at the beginning of the process to avoid sample loss.
13. A vacuum pump should be used to lower the pressure, which lowers the boiling point of the solvent being utilized and eases the evaporation process. To begin the evaporation process, the pressure is decreased from 1000 to 100 mbar. After the solvent has evaporated and the film has formed, the pressure is set to auto mode to eliminate the solvent completely, and the film is held under decreased pressure for an additional hour. When the pressure falls to zero, the evaporation process is finished.
14. A condenser with a cooling coil or a dry ice condenser is used to easily remove chloroform vapor in order to avoid the machine becoming saturated with solvent vapor, which can stop the evaporation of the remaining solvents from the lipid film.

15. Both the size and size distribution of the liposome particles following hydration are influenced by the quality of the dry lipid film. If the dry lipid film on the flask walls is non-homogeneous or crackled, redissolve the lipid film in 2 mL of chloroform and repeat the evaporation step.
16. Before placing the films in the desiccator, the flask should be sealed with a parafilm. Punch pores in the parafilm to allow the remaining solvent to evaporate. Keep the lipid film away from any moisture prior to the hydration step.
17. During the hydration step, the temperature of the lipid film should exceed the phase-transition temperature of the most rigid lipid in the selected lipids to ensure the fluidity of the lipids and the formation of MLVs or PEGylated lipid-based micelles. Hydration at lower temperatures makes it difficult to detach the lipid film from the flask, resulting in irregular lipid aggregates and preventing the formation of MLVs or uniform PEGylated lipid-based micelles.
18. A water bath sonicator could be used for the hydration of lipid films to produce a suspension of MLVs or PEGylated lipid-based micelles.
19. The extrusion temperature should exceed the phase-transition temperature of the selected lipids to create softer MLVs that could more easily pass through the pores of the polycarbonate filter membranes. Extrusion at lower temperatures could prevent the MLVs from passing smoothly through the filter pores, which could cause blockage.
20. Failure of the liposomes to spill out of the extruder could be caused by one of the following developments: (a) the temperature of the water bath used in the extrusion step is lower than that recommended for liposomes (raise the temperature used); (b) filter clogging (increase the pressure and temperature used. If there is no response, use a Pasteur pipette to remove the lipid suspension from the extruder and replace the filters).
21. To avoid cross-contamination between various formulations, the extruder should be washed with detergent and then boiling water to eliminate any residual lipids inside the extruder cavities.
22. Sonication can be used as an alternative method to reduce the size of the MLVs. To avoid the destruction of liposome components and encapsulated drugs, be cautious of the heat generated during multiple sonication cycles.
23. A Zetasizer nano series could also provide the zeta potentials for the samples being tested. All measurements are done at 25 °C. For accurate readings, highly concentrated samples should be diluted; concentrations of 100–400 µM are usually appropriate.

For particle size measurement, liposomes or PEGylated lipid-micelles are diluted in 500 µl of the selected buffer and transferred to the measuring cuvettes (polystyrene, glass, or quartz). For zeta potential measurement, dilute liposomes are diluted in 1000 µl of the selected buffer and transferred to the measuring cuvettes (polystyrene). All buffers used in measurements must be filtered through a 0.22 µm filter membrane.

24. The maximum phospholipid concentration for the Bartlett assay should be considered, and the added liposome samples should be adjusted accordingly to fall within the assay detection limits (25–100 nmoles/test tube). However, this assay is incompatible with buffers containing inorganic phosphates such as PBS, and in such a case the Stewart phospholipid assay should be used instead.
25. The final concentration of phospholipids may be significantly lower than the theoretical value. Possible causes include the following: (a) inadequate temperature in the extrusion step (make sure that you used the correct temperature for the lipids and that the extruder reaches the required temperature before starting the extrusion process) and (b) incorrect lipid stock solutions.
26. Fluorescence- or radio-labeled PEG<sub>2000</sub>-DSPE can be added to easily track the added PEGylated lipid.
27. During the hydration of lipid films of PEG<sub>2000</sub>-DSPE and/or other PEGylated lipid derivatives, the final lipid concentration should be higher than their critical micelle concentrations in order to form micelles.
28. As an alternative to the thin-lipid film-hydration method for micelle formation, micelles can be directly produced by dissolving PEG<sub>2000</sub>-DSPE lipid powder in HEPES buffer (at concentrations higher than the critical micelle concentrations) with gentle shaking, and this can also be used for the post-insertion technique.
29. Micelle formation can be confirmed either by determining the turbidity at 240 nm or by tracking the micelle particle size change using a Zetasizer.
30. The drug-loading step should be completed before beginning the post-insertion process.
31. To complete and/or facilitate the transfer of PEG<sub>2000</sub>-DSPE to the outer layer of liposomes, the post-insertion process should be carried out at a temperature higher than the phase transition temperature of the selected lipids. Using temperatures lower than the phase transition temperature of liposomal lipids reduces the amount of transferred PEG<sub>2000</sub>-DSPE into the liposomes.

32. The saturation level (fluidity) of phospholipids used in liposome preparation should be optimized. Liposomes prepared from highly unsaturated (fluid) phospholipids with very low phase transition temperatures will accept a large amount of PEG<sub>2000</sub>-DSPE. The release of transferred PEG<sub>2000</sub>-DSPE from the lipid bilayers of liposomes, however, could result in a low incorporation ratio of PEG<sub>2000</sub>-DSPE into liposomes. Therefore, highly fluid phospholipids are not recommended for the post-insertion method. In addition, a high CHOL content in the preformed liposomes is also important. For example, in the preformed liposomes composed of saturated phospholipids, high CHOL content increases fluidity and therefore increases the insertion of PEG<sub>2000</sub>-DSPE to the preformed liposomes. Accordingly, a low phospholipid/CHOL molar ratio is essential for the efficient integration of PEG<sub>2000</sub>-DSPE into the preformed liposomes.
33. The ligand transfer to liposome surfaces using PEG<sub>2000</sub>-DSPE-based micelles should be controlled. A high density of ligands on PEGylated liposomes could lead to a loss of the stealth properties of PEGylated liposomes, which could result in their rapid clearance from blood circulation.
34. Sufficient incubation time is a determining factor for the effective transfer of PEG<sub>2000</sub>-DSPE to the preformed liposomes due to the increase in the contact time between the liposomes and the micelles. Extended incubation times at high temperatures, on the other hand, can compromise the stability of the lipids and encapsulated drugs.
35. DSPE is the best lipid anchor for the retention of a PEG coating on liposome surfaces. At 37 °C, DSPE will keep the PEG coat for up to 70 h *in vitro* [16]. Other lipid anchors, such as cholesterol, can also be employed.
36. Different PEGylated lipid derivatives with different PEG molecular weights can be post-inserted to transfer specific targeting moieties grafted at the terminus of the PEG portion of a PEGylated lipid to the preformed liposomes. PEG<sub>2000</sub> lipid derivatives are the best coupling lipids for this method and can be tailored with functional groups such as a methyl group or maleimide to carry a variety of targeting ligands.
37. When coupling PEGylated lipid derivatives with specific ligands, mPEG<sub>2000</sub>-DSPE lipids (80 mol% of total PEGylated lipids) are added during micelle preparation as stabilizers to prevent the intermicellar crosslinking of added ligands.
38. If the post-insertion technique is applied to PEGylated liposomes, pre-existing PEG in the bilayer of PEGylated liposomes hinders the further insertion of PEG<sub>2000</sub>-DSPE and reduces the incorporation ratio of PEG<sub>2000</sub>-DSPE into the outer

monolayer because the upper limit of the final portion of PEG<sub>2000</sub>-DSPE in the liposomal bilayers after insertion should not exceed 5–6 mol%. Furthermore, excess PEG coating interferes with the interaction of liposomes with target cells.

39. Conventional liposomes such as HSPC:CHOL (2:1, molar ratio) are the optimal formulae for a post-insertion method that will yield a modification efficiency of 100% of the added PEGylated lipids due to the absence of pre-existing PEG in this formulation. PEGylated liposomes containing up to 2 mol% PEG<sub>2000</sub>-DSPE such as HSPC:CHOL:PEG<sub>2000</sub>-DSPE (2:1:0.04, molar ratio) also allow sufficient transfer of PEG<sub>2000</sub>-DSPE and ligands grafted to PEGylated lipids to the outer surface of PEGylated liposomes [12].
40. Increasing the concentration of PEG<sub>2000</sub>-DSPE-based micelles improves the amount of PEG<sub>2000</sub>-DSPE transferred into the preformed liposomes. Actually, 4 mol% PEG<sub>2000</sub>-DSPE micelles achieved better PEG<sub>2000</sub>-DSPE and ligand transfer into the preformed liposomes than 2 mol% PEG<sub>2000</sub>-DSPE-based micelles [12].
41. Prepare a slurry of Sepharose CL-4B in the HEPES buffer, pH 7.4 (eluent), in a ratio of 3:1 (resin: buffer). De-gas the slurry before packing in the column. Pour resin slurry on the inner wall of the column to avoid the trapping of air bubbles (any trapped air should be removed before use). For higher separation efficiency, the height of the final resin bed inside the column should be 20–25 cm.
42. Store the packed column in the presence of 20% ethanol at room temperature if it will not be used immediately.
43. Keep the column, resin, eluent, and sample at the same temperature to avoid the formation of air bubbles in the column (e.g., room temperature).
44. Equilibrate the column by elution three times with the selected eluent such as HEPES buffer (this step is also required for eluent change).
45. Adjust the sample volume to be about 2–5% of the total resin bed.
46. To clean the column of residual ligand proteins or lipids, elute the column once with 0.5 M NaOH or nonionic detergent solution, and then elute three times with the selected eluent (e.g., HEPES buffer).
47. Gradient centrifugation can be used as an alternative to gel chromatography to remove excess PEG<sub>2000</sub>-DSPE-based micelles after post-insertion into the preformed liposomes.
48. The purification of the resulting liposomes after post-insertion can also be carried out through dialysis of the liposomes against

HEPES buffer in the dialysis cassette overnight at room temperature. Ultracentrifugation and centrifugal filtration can also be applied.

49. The type of PEGylated lipids used for micelle preparation is the determinant for the increase in the particle size and for the decrease in the zeta potential of the prepared PEGylated liposomes compared with the preformed conventional liposomes.
50. Zeta potential measurement is used as an indicator of technique success.
51. Apart from using fluorescent or radio-labeled PEGylated lipids to prepare micelles, other techniques can be used to determine the amount of PEG that is incorporated into the prepared PEGylated liposomes:
  - (a) Measuring the phospholipid concentration can be used to indirectly calculate the amount of incorporated PEGylated lipids where phospholipid concentration is measured for the fractions containing the non-bound PEG. The amount of incorporated PEG will be the difference between the amount of PEGylated lipids initially added and the amount of non-incorporated PEG. To create the calibration curve, the phospholipid concentration of known concentrations of PEGylated lipids is measured.
  - (b) I<sub>2</sub> assay, which is based on the spectrophotometric analysis of the complex formed between PEG and barium iodide, can be used for either direct or indirect calculation of the amount of PEGylated lipids incorporated. In the case of direct measurement, disruption of the prepared PEGylated liposomes using methanol is required before starting the assay. Liposome samples may require dilution with distilled water to fall within the detection limits of the assay (1.25–7.5 µg/mL of PEGylated lipids). Two aqueous solutions are used to treat the samples: 250 µL of 5% barium chloride (w/v in 1 M hydrochloric acid) and 250 µL of iodine (1.27 g dissolved in 100 mL of 2% potassium iodide (w/v)). Incubate this mixture for 15 min at room temperature and then quantify the complex formed at a wavelength of 535 nM using a spectrophotometer. Conventional bare liposomes should be used as a negative control.

## References

1. Torchilin VP (2005) Recent advances with liposomes as pharmaceutical carriers. *Nat Rev Drug Discov* 4(2):145–160. <https://doi.org/10.1038/nrd1632>
2. Ishida T, Maeda R, Ichihara M et al (2003) Accelerated clearance of PEGylated liposomes in rats after repeated injections. *J Control Release* 88(1):35–42. [https://doi.org/10.1016/S0168-3659\(02\)00462-5](https://doi.org/10.1016/S0168-3659(02)00462-5)

3. Woodle MC, Lasic DD (1992) Sterically stabilized liposomes. *Biochim Biophys Acta Rev Biomembr* 1113(2):171–199. [https://doi.org/10.1016/0304-4157\(92\)90038-C](https://doi.org/10.1016/0304-4157(92)90038-C)
4. Allen TM (1994) The use of glycolipids and hydrophilic polymers in avoiding rapid uptake of liposomes by the mononuclear phagocyte system. *Adv Drug Deliv Rev* 13(3):285–309. [https://doi.org/10.1016/0169-409X\(94\)90016-7](https://doi.org/10.1016/0169-409X(94)90016-7)
5. Maeda H (2021) The 35th anniversary of the discovery of EPR effect: a new wave of Nanomedicines for tumor-targeted drug delivery – personal remarks and future prospects. *J Pers Med* 11:3. <https://doi.org/10.3390/jpm11030229>
6. Duggan ST, Keating GM (2011) Pegylated liposomal doxorubicin. *Drugs* 71(18):2531–2558. <https://doi.org/10.2165/11207510-000000000-00000>
7. Burade V, Bhowmick S, Maiti K et al (2017) Lipodox® (generic doxorubicin hydrochloride liposome injection): in vivo efficacy and bioequivalence versus Caelyx® (doxorubicin hydrochloride liposome injection) in human mammary carcinoma (MX-1) xenograft and syngeneic fibrosarcoma (WEHI 164) mouse models. *BMC Cancer* 17(1):405. <https://doi.org/10.1186/s12885-017-3377-3>
8. Frampton JE (2020) Liposomal Irinotecan: a review in metastatic pancreatic adenocarcinoma. *Drugs* 80(10):1007–1018. <https://doi.org/10.1007/s40265-020-01336-6>
9. Zalipsky S, Hansen CB, Lopes de Menezes DE et al (1996) Long-circulating, polyethylene glycol-grafted immunoliposomes. *J Control Release* 39(2):153–161. [https://doi.org/10.1016/0168-3659\(95\)00149-2](https://doi.org/10.1016/0168-3659(95)00149-2)
10. Moreira JN, Ishida T, Gaspar R et al (2002) Use of the post-insertion technique to insert peptide ligands into pre-formed stealth liposomes with retention of binding activity and cytotoxicity. *Pharm Res* 19(3):265–269. <https://doi.org/10.1023/A:1014434732752>
11. Zalipsky S, Mullah N, Harding JA et al (1997) Poly(ethylene glycol)-grafted liposomes with oligopeptide or oligosaccharide ligands appended to the termini of the polymer chains. *Bioconjug Chem* 8(2):111–118. <https://doi.org/10.1021/bc9600832>
12. Ishida T, Iden DL, Allen TM (1999) A combinatorial approach to producing sterically stabilized (stealth) immunoliposomal drugs. *FEBS Lett* 460(1):129–133. [https://doi.org/10.1016/S0014-5793\(99\)01320-4](https://doi.org/10.1016/S0014-5793(99)01320-4)
13. Mare R, Paolino D, Celia C et al (2018) Post-insertion parameters of PEG-derivatives in phosphocholine-liposomes. *Int J Pharm* 552(1–2):414–421. <https://doi.org/10.1016/j.ijpharm.2018.10.028>
14. Allen TM, Brandeis E, Hansen CB et al (1995) A new strategy for attachment of antibodies to sterically stabilized liposomes resulting in efficient targeting to cancer cells. *Biochim Biophys Acta Biomembr* 1237(2):99–108. [https://doi.org/10.1016/0005-2736\(95\)00085-H](https://doi.org/10.1016/0005-2736(95)00085-H)
15. Bartlett GR (1959) Colorimetric assay methods for free and phosphorylated glyceric acids. *J Biol Chem* 234(3):469–471
16. Silvius JR, Zuckermann MJ (1993) Interbilayer transfer of phospholipid-anchored macromolecules via monomer diffusion. *Biochemist* 32(12):3153–3161. <https://doi.org/10.1021/bi00063a030>



# Chapter 15

## Click Chemistry for Liposome Surface Modification

**Maria Vittoria Spanedda, Marcella De Giorgi, Béatrice Heurtault, Antoine Kichler, Line Bourel-Bonnet, and Benoît Frisch**

### Abstract

Click chemistry, and particularly azide–alkyne cycloaddition, represents one of the principal bioconjugation strategies that can be used to conveniently attach various ligands to the surface of preformed liposomes. This efficient and chemoselective reaction involves a Cu(I)-catalyzed azide–alkyne cycloaddition which can be performed under mild experimental conditions in aqueous media. Here we describe the application of a model click reaction to the conjugation, in a single step, of unprotected  $\alpha$ -L-thiomannosyl ligands, functionalized with an azide group, to liposomes containing a terminal alkyne-functionalized lipid anchor. Excellent coupling yields were obtained in the presence of bathophenanthrolinedisulphonate, a water-soluble copper-ion chelator, acting as catalyst. No vesicle leakage was triggered by this conjugation reaction, and the coupled mannose ligands were exposed at the surface of the liposomes. The major limitation of Cu(I)-catalyzed click reactions is that this type of conjugation is restricted to liposomes made of saturated (phospho)lipids. To circumvent this constraint, an example of alternate copper-free azide–alkyne click reaction has been developed, and it was applied to the anchoring of a biotin moiety that was fully functional and could be therefore quantified. Molecular tools and results are presented here.

**Key words** Liposomes, Azide–alkyne cycloaddition, Bioconjugation, Click chemistry, Mannose, Copper-free click chemistry

---

### 1 Introduction

Liposomes have attracted considerable interest because of their potential applications in various fields such as membrane models, diagnostics, and drug and gene delivery. Due to their structure—closed vesicles with an aqueous core surrounded by phospholipid bilayer(s)—they can incorporate hydrophilic as well as hydrophobic compounds. Furthermore, conventional liposomes are biocompatible, biodegradable, non-toxic, and non-immunogenic. In the field of nanomedicine, liposomes are probably the most successful drug delivery system, with at least 14 drugs in clinical use for a range of indications such as cancer therapy, fungal diseases, analgesics, viral vaccines, photodynamic therapy [1].

A strategy that could further help to the use of those nanoparticles in medicine is the development of actively targeted vesicles. There are two major approaches to achieve this: firstly, through non-covalent adsorption onto the surface of liposomes [2–4] and secondly through covalent modification of the vesicles. In the present chapter, we will focus on the second strategy using click chemistry.

Liposomes can be surface-modified with a variety of molecules that carry out number of functions such as promoting the selective targeting of the vesicles to specific tissues or cell types and/or modulate their biodistribution and pharmacokinetic properties [5]. Targeting, which represents a major issue to increase the selectivity and efficiency of bioactive molecules (e.g., drugs, genes, etc.), involves, in most cases, the use of ligands that are recognized by receptors (over)expressed at the surface of target cells [6–8]. These ligands are either relatively small molecules, such as folic acid, peptides, or carbohydrate clusters which trigger receptor-mediated endocytosis, or proteins such as monoclonal antibodies and their fragments that are directed against specific antigens. The design of targeting liposomes is much dependent on the development of well-controlled bioconjugation reactions, and numerous methods have been developed to attach ligands to the surface of liposomes; for reviews, see [6, 9–13]. Those reactions fall into two major categories: (i) conjugation of ligands to hydrophobic anchors and subsequent incorporation of the lipidated ligands into liposomes either during the preparation of the vesicles or by post-insertion into preformed vesicles (reviewed in [12]), or (ii) covalent coupling of ligands to the surface of preformed vesicles that carry functionalized (phospho)lipid anchors [13]. In the case of phospholipids, phosphatidylethanolamine (PE) is the most used for chemical modification, due to its reactive amino group, and its chemistry has been extensively studied [13]. However, using totally synthetic lipids as anchors has the advantage to fully control the physicochemical properties and the reactivity of the expected final lipid. The most popular conjugations involve the reaction of thiol-containing ligands with anchors carrying thiol-reactive functions such as maleimide, bromoacetyl, or 2-pyridylidithio linkages, generating thioether or disulfide bonds, respectively [14–16]. Amide and carbamate bonds were also used, and more recently peptide ligands were coupled to the surface of liposomes via hydrazone and  $\alpha$ -oxo hydrazone linkages [17]. With the inception of sterically stabilized liposomes [18], ligands were also coupled at the distal end of a PEG spacer arm linked to a hydrophobic anchor [5, 19, 20]. Chemically controlled conjugation between preformed liposomes and ligands should ideally combine several features such as mild reaction conditions in aqueous media, high yields, chemoselectivity, and bioorthogonality. In this respect, the application of the “click chemistry” concept, and particularly the copper(I)-

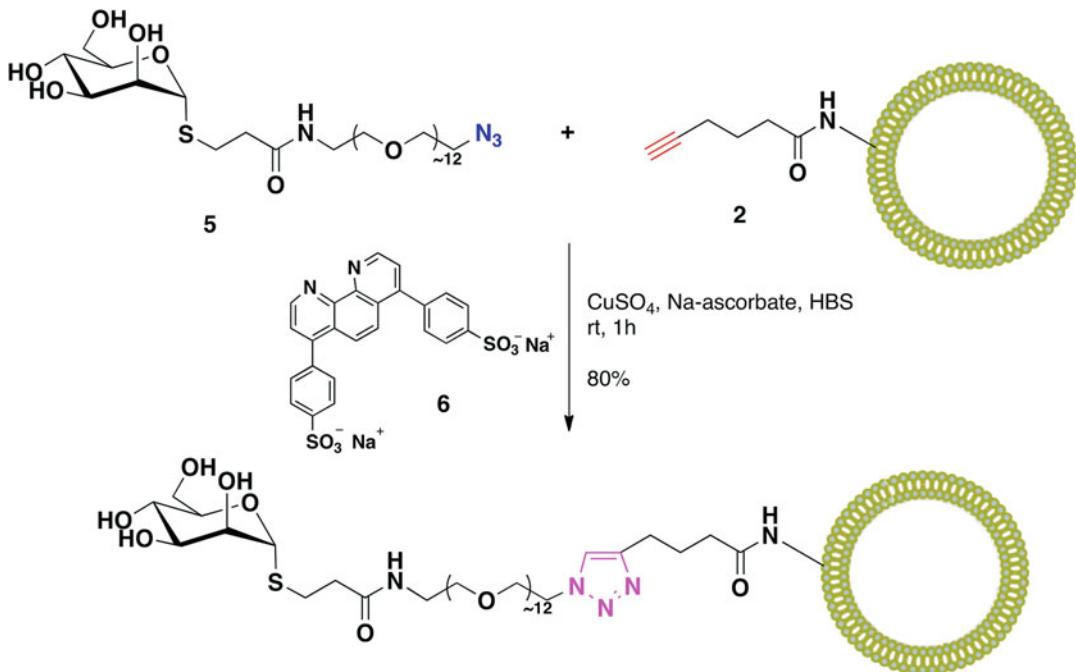
catalyzed 1,3-dipolar cycloaddition reaction of azides and alkynes yielding 1,4-disubstituted 1,2,3-triazole linked conjugates [21], is very attractive for the development of new bioconjugation strategies. This reaction, which has attracted considerable interest over the last years (for significant reviews, see [22–24]), is particularly appealing because of its high regiospecificity, chemoselectivity, and tolerance to a wide variety of other functional groups.

Most examples of the use of click chemistry are related to the targeting of cells (often tumor cells) or organs through the conjugation of peptides and proteins to the surface of liposomes. The target depends on the chosen peptides/proteins. As recent example, Hood et al. (2018) performed a vascular targeting through the ligation of monoclonal antibodies or their single chain variable fragments directed to platelet–endothelial cell adhesion molecule and intracellular adhesion molecule proteins [25]. In the same way, Grimsley et al. (2021) demonstrated the possibility to visualize and treat dysfunctional vascular remodeling by targeting fluorescently labeled liposomes functionalized with a collagen-specific peptide [26]. Surface azide functionalized liposomes were developed to target tumor cells and achieved improved drug delivery for the treatment of cancer. Based on this strategy, Liang and coworkers grafted photosensitizer-modified cetuzimab (benzoporphyrin derivative of the antibody) onto a liposome encapsulating the anti-tumor molecule irinotecan enabling synergistic targeting of cancer cells [27], while Xiao et al. developed a liposomal platform incorporating antitumoral drug nanocrystals such as ciprofloxacin for tumor cell targeting [28]. To target and destroy tumor cells, a multimeric approach was also developed by Ringhieri et al. in 2017 allowing the coupling of several peptides (functionalized by a propargyl function) targeting HER2 using a hydrophobic anchor modified by 1, 2, or 4 azide functions [29].

In addition to the coupling of targeting moieties onto liposomes, other approaches using the surface modification of the vesicles by click chemistry have been recently described. In the work of Qin et al. [30], for example, it is the surface of the targeted cells (lymphatic endothelial cells) that is labeled with an azide-functionalized PEGylated lipid. The click chemistry reaction with antigen-loaded liposomes takes place *in situ* in the mouse body, allowing the development of a highly effective antitumor vaccine [30]. In the work of Shen et al. (2020, 2019), the liposome serves as a conveyor for a mannosylated lipid functionalized by an azide incorporated in the phospholipid bilayer [31, 32]. Once in the cell, the mannosylated lipid and the mannose obtained after enzymatic degradation are re-expressed at the cell surface exposing the azide residue and allowing specific labeling with an alcyne-functionalized fluorophore. Silk-coated polystyrene fiber scaffolds have also been used to create a biomimetic coating of the cell membrane by fusing liposomes to their surface, making the membrane much more

biocompatible in order to mitigate the foreign-body reaction. The strategy used consisted in the modification of the fibers with azide groups that then can react with the alkynes present on the surface of the liposomes, allowing them to be coated around the fibers [33]. Indeed, liposomes modified to allow click chemistry are also interesting tools to understand biological mechanisms. Considering that lipid exchange among biological membranes has important repercussions on the applications of liposomes, Gleue and colleagues described the lipid escape from liposomal membranes and their insertion into other membranes using fluorescent dyes covalently attached to the liposomes through click chemistry [34]. Desai et al. developed a liposome click membrane permeability assay of individual peptides and peptide mixtures. Encapsulation of membrane impermeant DBCO–biotin in the lumen of the liposomes enabled the monitoring and differential identification of membrane permeable azido-modified peptides exhibiting high or low translocation into the luminal space based on copper-free click biotin conjugation [35]. This assay can inform on structure transport relationships to orientate peptide drug discovery.

In the present chapter, we describe the application of click chemistry to the conjugation, in a single step, of an unprotected  $\alpha$ -D-mannosyl derivative carrying a spacer arm functionalized with an azide group, to the surface of liposomes that incorporate a synthetic lipid carrying a terminal triple bond (Scheme 1). Reaction conditions were optimized for this model reaction, and mannosylated vesicles were obtained in excellent yield. As assessed by agglutination experiments with Concanavalin A, the mannose residues were perfectly accessible on the surface of the vesicles and could engage into multivalent interactions. Thus, click chemistry can be added to the toolbox of reactions available to the conjugation of ligands at the surface of carriers such as liposomes [36, 37] or nanoparticles [38, 39]. However, copper catalyzed click chemistry reactions onto liposomes have some major limitations, as the impossibility to use unsaturated lipid-containing liposomes and the toxicity of residual copper in living systems. Therefore, we have studied a copper-free click reaction, so-called strain-promoted azide–alkyne cycloaddition (SPAAC), in order to circumvent those problems [40]. Thereafter, a biotin was grafted onto liposomes via the reaction of a constrained cyclooctyne with an azide. These supplementary data implement and reinforce the interest of bioorthogonal copper-free “click chemistry” onto liposomes. Even if new click chemistry reactions like inverse electron-demand Diels–Alder cycloaddition (iEDDA) can now be applied to the surface of liposomes [41], SPAAC is still a valuable tool for the simplicity of synthesis and the availability of the corresponding reagents.



**Scheme 1** Coupling by click reaction of an azido-functionalized mannosyl ligand to preformed liposomes that incorporate a terminal alkyne-functionalized lipid anchor

## 2 Materials

### 2.1 Synthesis

1. Dicyclohexylcarbodiimide (DCC), *N*-(3-dimethylaminopropyl)-*N'*-ethylcarbodiimide hydrochloride (EDCI), *N*-hydroxysuccinimide (NHS), 5-hexynoic acid, and di-isopropylethylamine (DIEA) were purchased from Sigma-Aldrich (Saint-Quentin-Fallavier, France).
2. Dipalmitoylglycero-ethoxy-ethoxy-ethoxy-ethylamine (**1**) was synthesized as described previously [42].
3. Compound (**3**) was synthesized as outlined in [43].
4. Compound (**4**) was synthesized according to [44].
5. 1-Fluorocyclooct-2-yne carboxylic acid (**8**) was synthesized as described in [45].
6. DOG-PEG<sub>4</sub>-NH<sub>2</sub> (**7**) and BiotinOSuc (**10**) were synthesized according to [46].
7. 11-Azido-3,6,9-trioxaundecan-1-amine ( $\text{H}_2\text{N-PEG}_3\text{-N}_3$ ) was synthesized according to [47].

## 2.2 Liposome Preparation

- 1,2-Dipalmitoyl-*sn*-glycero-3-phosphocholine (DPPC) and 1,2-dipalmitoyl-*rac*-glycero-3-phospho-*rac*-(1-glycerol) sodium salt (DPPG) (from Sigma-Aldrich) were stored at -20 °C as solutions in chloroform/methanol (9/1 v/v). The purity of the phospholipids (over 99%) was assessed by TLC (*see Note 1*).
- Cholesterol (Sigma-Aldrich) was recrystallized in methanol.
- HBS: 10 mM HEPES, 145 mM NaCl, pH 6.5.
- HBS-CF: 10 mM HEPES, 40 mM 5(6)-carboxyfluorescein, 100 mM NaCl, pH 6.5 stored at 4 °C.
- Sonicator equipped with a 3-mM-diameter titanium probe (Vibra Cell, Sonics and Materials Inc., Danbury, CT).
- The size of the liposomes was determined by dynamic light scattering using a Sub-micron Particle Analyzer (Coulter, Hialeah, FL).

## 2.3 Azide-Alkyne Coupling Reaction by Click Chemistry

- L-Ascorbic acid sodium salt (Acros-Organics (Noisy-le-Grand, France)).
- Bathophenanthrolinedisulphonic acid disodium salt (**6**) (Alfa Aesar, Strasbourg- Bischheim, France).
- Sol. A: 8 mM CuSO<sub>4</sub>.5H<sub>2</sub>O in HBS (prepared freshly, stored at 4 °C).
- Sol. B: 145 mM sodium ascorbate in HBS (prepared freshly, stored at 4 °C).
- Sol. C: 28 mM compound **6** in HBS (prepared freshly, stored at 4 °C).
- Quant-Tag Biotin kit was purchased from Vector Laboratories, Inc., cat No. BDK-2000.

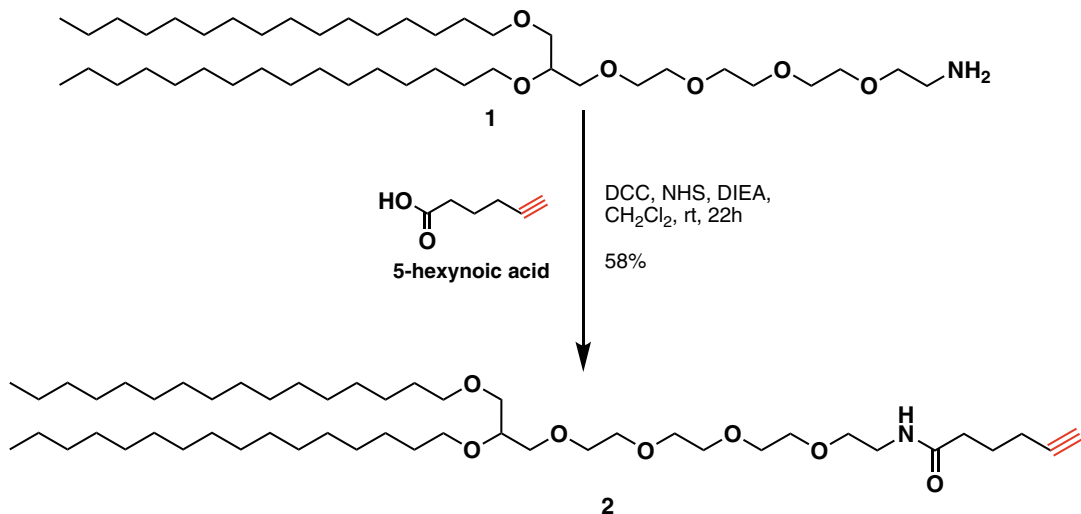
## 3 Methods

All the methods concerning copper-catalyzed click reaction are presented in Subheading 3.1; all the methods concerning copper-free reaction are displayed in Subheading 3.2.

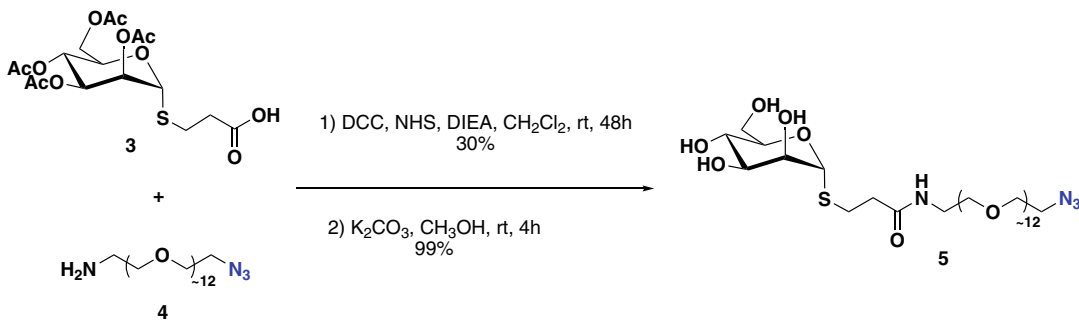
### 3.1 Copper-Catalyzed Click Reaction

#### 3.1.1 Synthesis of the Terminal Alkyne-Functionalized Lipid Anchor (2) (Scheme 2)

- DCC (52 mg, 0.25 mmol) and NHS (12 mg, 0.105 mmol) were added to a solution of 5-hexynoic acid (23 mg, 0.21 mmol) in CH<sub>2</sub>Cl<sub>2</sub> (4 mL).
- 1** (150 mg, 0.21 mmol) and DIEA (43 µL, 0.25 mmol) were then added to the mixture.
- After 22 h of reaction at room temperature under stirring and under argon, the formed precipitate was removed by filtration, and the organic phase was washed with 2 × 10 mL of a citric



**Scheme 2** Synthesis of the terminal alkyne-functionalized lipid anchor (**2**)



**Scheme 3** Synthesis of the azido-functionalized 1-thiomannose derivative (**5**)

acid solution (5%, w/v) followed by 2 × 10 mL of brine. After passage over MgSO<sub>4</sub>, the solvent was evaporated to dryness. The reaction product was obtained (98 mg; yield 58%) after purification by chromatography on silica gel eluted with CH<sub>2</sub>Cl<sub>2</sub>: EtOAc (9:1 to 7:3).

### 3.1.2 Synthesis of the Azido-Functionalized Mannosyl Ligand (**5**) (Scheme 3)

- To a solution of **3** (149 mg, 0.342 mmol) in 3 mL of CH<sub>2</sub>Cl<sub>2</sub> were added DCC (85 mg, 0.41 mmol) and NHS (47 mg, 0.41 mmol).
- After 45 min of stirring at room temperature under argon, the amine **4** (210 mg, 0.342 mmole) in 1 mL of CH<sub>2</sub>Cl<sub>2</sub> containing DIEA (47.5 µL, 0.273 mol) was added to the reaction mixture. After 18 h, 20 µL of DIEA and 0.2 eq. of amine **4** were again added. The stirring was continued during 48 h.
- The precipitate was then removed by filtration, and the organic phase was washed with 2 × 10 mL of a citric acid solution

(5%, w/v) then by water. After passage over MgSO<sub>4</sub>, the solvent was evaporated to dryness.

4. The reaction product **5** (129 mg; yield 30%, yellow oil) was obtained after purification by chromatography on silica gel eluted with CH<sub>2</sub>Cl<sub>2</sub>: MeOH (30:1). (*see Note 2*).

### *3.1.3 Liposome Preparation*

1. Small unilamellar vesicles (SUV) were prepared by sonication. Briefly, phospholipids (DPPC, DPPG) and cholesterol (70/20/50 molar ratio) dissolved in chloroform/methanol (9:1, v/v) were mixed in a round-bottom flask.
2. For functionalized vesicles, **2** dissolved in chloroform/methanol (9:1, v/v) was added at given concentrations (between 5 and 10 mol %).
3. After solvent evaporation under high vacuum, the dried lipid film was hydrated by addition of 1 mL HBS to obtain a final concentration of 10 µmol lipid/mL.
4. The mixture was vortexed, and the resulting suspension was sonicated for 1 h at 60 °C, i.e., above the Tm of the lipids, using a 3-mM-diameter probe sonicator.
5. The liposome preparations were then centrifuged at 10,000  $\times$  g for 10 min to remove the titanium particles originating from the probe.

### *3.1.4 Liposome Characterization*

1. The size of the liposomes was determined by dynamic light scattering. The different vesicle preparations were homogeneous in size and exhibited an average diameter between 90 and 130 nM.
2. The phospholipid content of liposomes was determined according to Rouser [48] with sodium phosphate as standard.

### *3.1.5 Conjugation of the Azido-Functionalized Ligand to Liposomes by Click Reaction (Scheme 1)*

1. To a 200 µL suspension in HBS of liposomes containing the alkyne-functionalized lipid anchor **2** that was adjusted to 1 mM of alkyne group (i.e., ~ 0.5 mM surface available alkyne group) were added in that precise order: sol. A (286 µL) and sol. B (355 µL) followed by 164 µL of sol. C. Finally, 15 µL of a 13.9 mM solution of **5** in water were added to the reaction mixture. (*See Notes 3, 4, and 5.*)
2. The reaction mixture was gently stirred under argon at room temperature for 1 h.
3. After the conjugation step, liposomes were purified by exclusion chromatography on a 1 × 18 cm Sephadex G-75 (Amersham Biosciences) column equilibrated in HBS.

### 3.1.6 Quantification of the Conjugation Reaction

1. The mannose residues coupled to the liposomes were quantified by the resorcinol–sulfuric acid method [47]. The standard curve was established as follows: to a  $12.2 \times 100$  mM glass tube containing 2–12 µg of D-mannose in 200 µL water were added successively 20 µL of 0.1% (w/v) Triton X-100, 200 µL of a 6 mg/mL aqueous solution of resorcinol, and 1 mL of 75% (v/v)  $\text{H}_2\text{SO}_4$ .
2. The tubes were vortexed and covered with aluminum foil before heating in a boiling water bath for 12 min and then cooled to room temperature. The optical density was then recorded at 430 nM.
3. Aliquots of conjugated liposomes (about 0.4 µmol lipid) were dried under vacuum using a Speed Vac.
4. HBS (200 µL) was added to the tubes, and the mixtures, after vortex mixing, were treated as indicated above for the standards. Before optical density reading, the samples were filtered through a 0.45 µm PTFE filter. (See Note 7.)

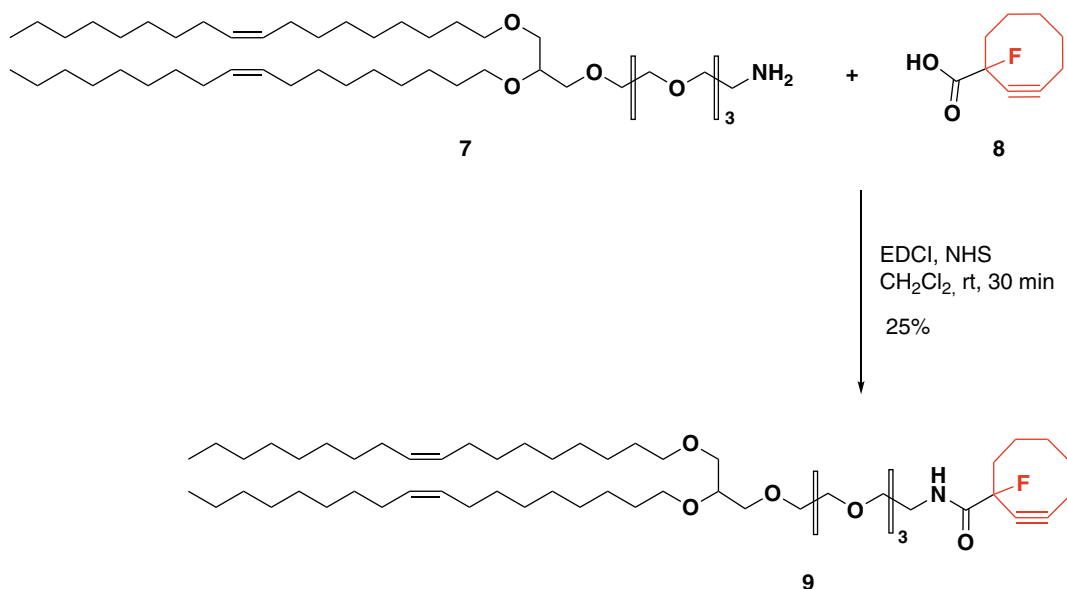
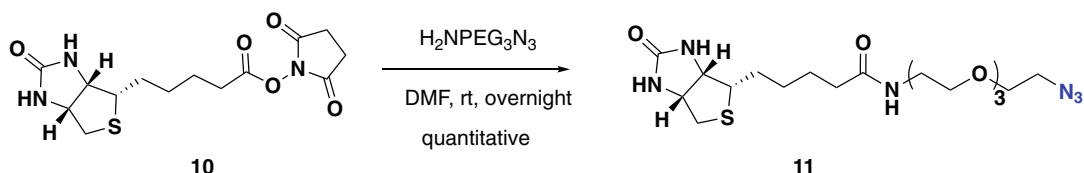
### 3.1.7 Liposome Stability under Coupling Conditions

1. Liposomes were prepared as above in HEPES-CF.
2. Non-encapsulated dye was eliminated by gel filtration (see above).
3. The dye-loaded liposomal suspensions were treated as above for the click chemistry coupling step.
4. The leakage of 5(6)-carboxyfluorescein was assessed by determining the increase of fluorescence ( $\lambda_{\text{ex}}$  490 nM;  $\lambda_{\text{em}}$  520 nM) observed in the presence of excess detergent. To measure the total fluorescence intensity corresponding to 100% dye release, Triton X-100 (0. 1% w/v final) was added to the vesicles.
5. The percentage of dye release caused by the coupling conditions was calculated using the eq.  $(F - F_0) \times 100 / (F_t - F_0)$ , where  $F$  is the fluorescence intensity measured after exposing the vesicles to the coupling conditions and  $F_0$ ,  $F_t$  the intensities obtained before the coupling conditions and after Triton X-100 treatment, respectively [14].  $F_t$  values were corrected for dilutions caused by the Triton X-100 addition. (See Notes 6, 8, and 9.)

## 3.2 Copper-Free Reaction

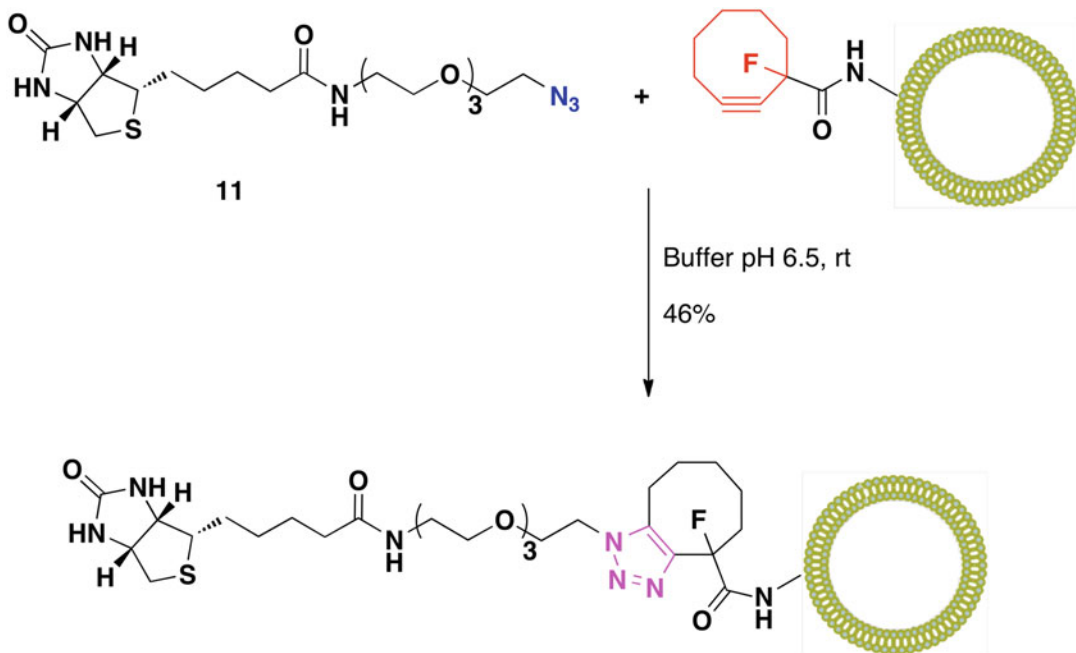
### 3.2.1 Synthesis of Fluorocyclooctyne-Functionalized Lipid Anchor (9) (Scheme 4)

1. To a solution of 1-fluorocyclooct-2-ynecarboxylic acid **8** (51 mg, 0.30 mmol) in  $\text{CH}_2\text{Cl}_2$  (1 mL) were added EDCI (58 mg, 0.30 mmol) and NHS (1 mg, 0.03 mmol). The solution was allowed to react for 30 min at room temperature.
2. DOG-PEG<sub>4</sub>-NH<sub>2</sub> **7** (120 mg, 0.15 mmol) in  $\text{CH}_2\text{Cl}_2$  (1 mL) was added.

**Scheme 4** Synthesis of the terminal cyclooctyne-functionalized lipid anchor (**9**)**Scheme 5** Synthesis of the azido-functionalized biotin derivative (**11**)

### 3.2.2 Synthesis of the Azido-Functionalized Biotin Ligand (**11**) (Scheme 5)

3. After 16 h of stirring at room temperature, CH<sub>2</sub>Cl<sub>2</sub> was removed under vacuum, and the product **9** (7 mg, yield 25%) was obtained after purification by chromatography on silica gel eluted with cyclohexane/EtOAc (7:3 to 0:10).
1. Biotin-O-Suc **10** (187 mg, 0.55 mmol) was solubilized in DMF (5 mL) by gently warming.
2. The solution was slowly cooled to room temperature avoiding precipitation.
3. 11-Azido-3,6,9-trioxaundecan-1-amine (H<sub>2</sub>N-PEG<sub>3</sub>-N<sub>3</sub>) [46] (109 mg, 0.50 mmol) was added, and the reaction was kept at room temperature overnight.
4. After concentration under vacuum, the crude reaction solid was purified by trituration in a solution of CH<sub>2</sub>Cl<sub>2</sub>:Et<sub>2</sub>O (3:7) affording, after filtration, the product as a white solid **11** (219 mg; quant.).



**Scheme 6** Coupling by copper free click reaction of an azido-functionalized biotinyl ligand to preformed liposomes that incorporate a terminal cycloalkyne-functionalized lipid anchor

### 3.2.3 Conjugation of the Azido-Functionalized Ligand to Liposomes by Click Reaction (Scheme 6)

1. Biotin-N<sub>3</sub> **11** (10 mM in water, 5% mol/mol) was added to a suspension of fluorocyclooctyne-functionalized liposomes in buffer (*see Note 10*).
2. The mixture was incubated during 1, 6, 24, and 48 h at 25 °C under argon.
3. Exclusion chromatography was performed in order to remove unbound probe. 1 × 20 cm Sephadex G-100 column was used to this aim, and it was equilibrated with the same buffer as the coupling step.
4. Fractions were combined and freeze-dried.

### 3.2.4 Biotin Quantification

- Biotin quantification was realized using the Quant-Tag Biotin kit.
1. Suspensions of liposomes (5 µL) were placed in triplicate in a 96-well microplates.
  2. 100 µL of reagent solution was added.
  3. After an incubation at 25 °C for 30 min appearance of a yellow-orange coloration indicates the presence of biotin.
  4. The absorbance at  $\lambda = 535$  nM was realized in a microplate reader (Bio-Rad, model 550, Marnes-la-Coquette, France).

---

**4 Notes**

1. The purity of DPPC and DPPG was determined by TLC on silica gel plates (Merck 0.25 mm, Kieselgel 60F<sub>254</sub>, 40–60 µm) eluted with, respectively, CHCl<sub>3</sub>:MeOH:H<sub>2</sub>O (65:25:4, v/v) and CHCl<sub>3</sub>:MeOH:CH<sub>3</sub>COOH:H<sub>2</sub>O (25:15:4:2, v/v). Both phospholipids showed a single spot revealed either by a fluorescamine spray reagent, UV (254 nM), or by I<sub>2</sub> vapors.
2. Compound **5** was built with a relatively long PEG spacer arm of defined length (12 ethylene glycol units) [44]. The purpose was to provide an optimal accessibility of the liposomal mannose ligands to their receptors [49]. However, the PEG spacer arm length can be changed if needed, e.g., for stealth vesicles.
3. In contrast to the nearly quantitative click reactions observed between small molecular weight molecules carrying alkyne and azide functions in the presence of catalytic amounts of the ascorbate/CuSO<sub>4</sub> couple, in the present case, where the terminal alkyne was exposed at the surface of vesicles of ~100 nM diameter, much higher ascorbate/CuSO<sub>4</sub> concentrations were needed to achieve conjugation reactions. Nevertheless, even under these conditions, the coupling yields remained relatively modest, i.e., about 25% conjugation was observed in the presence of 2.3 mM CuSO<sub>4</sub> and 51.5 mM sodium ascorbate. This observation is in agreement with other works in literature which showed that for bioconjugation reactions involving, for example, large molecular complexes, catalytic quantities of the ascorbate/CuSO<sub>4</sub> system are not enough to drive click reactions to completion [50].
4. To increase the yield of the click reaction, we have added a ligand of copper ions. Indeed, stabilization of Cu(I) oxidation state by specific heterocyclic ligands was shown to largely accelerate the 1,3-dipolar cycloaddition reaction between azides and alkynes [51]. In our case, bathophenanthrolinedisulfonate (**6**) provided a highly water-soluble and potent chelate catalyst for the click reaction [51]. When used in a twofold molar excess over copper, **6** allowed to reduce the agglutination of the vesicles, to largely increase the yield of mannosylation, and to decrease the reaction time. For example, under standard conditions (24 h), the coupling yield increased from 23%, in the absence of **6**, to nearly completion in its presence. Moreover, reaction times could also be decreased because within 1 h in the presence of **6**, the observed conjugation of **5** was already about 80%. Altogether, we have routinely conjugated—in high yield—ligands such as **5** (using a twofold molar excess over surface exposed alkyne groups) to the surface of preformed liposomes carrying alkyne functions in the presence of

CuSO<sub>4</sub>/Na-ascorbate/**6** (2.3, 50, and 4.6 mM) in an aqueous buffer (pH 6.5) at room temperature for 6 h (standard conditions).

5. In the liposome field, it is of importance to verify the integrity of the vesicles after the coupling steps. To that end, using a dynamic light scattering technique, we have first verified whether the reaction conditions described above altered the size of the vesicles. Some changes were noticeable using our standard conditions, i.e., about 50% diameter increases were noted even under control conditions in the absence of **6**. However, we found that this effect could be efficiently limited just by changing the order of reactants added to the liposome suspensions. Thus, when ligand **6** was added before the CuSO<sub>4</sub>/ascorbate mixture followed by the mannosyl ligand **5**, no significant increase in size of the vesicles could be observed, and, importantly, an identical yield of conjugation was measured.
6. The experimental conditions used for the click reaction could, in principle, provoke some leakage of the vesicles. To test this point, we have exposed to our standard coupling conditions the same type of liposomes having encapsulated self-quenching concentrations of 5(6)-carboxyfluorescein. Using well-established methods based on fluorescence quenching determinations [14], we could demonstrate that no leakage was triggered by the conjugation reaction.
7. To determine whether the conjugated mannose residues were easily accessible at the surface of the liposomes, we have incubated suspensions of targeted vesicles that contained 10 mol % of mannosyl residues exposed at their surface, in the presence of concanavalin A. Addition of the lectin resulted in a gradual increase of turbidity, as assessed by an increase of the OD at 360 nM which reached a plateau after about 15 min. In contrast, no absorbance change was observed with control liposomes. The subsequent addition of an excess of free D-mannose (5.0 mM) triggered a prompt decrease in turbidity confirming that the aggregation was due to a specific recognition of the mannose residues on the surface of the vesicles by the lectin that resulted in an aggregation due to multivalent interactions.
8. The use of copper catalysts in click chemistry could represent a limitation; indeed, vesicles made of unsaturated phospholipids are known to be readily (per)oxidized by copper ions in the presence of oxygen (i.e., via formation of reactive oxygen species) and to become leaky [51, 52]. This restricts the application of the conjugation technique discussed in this chapter to liposomes made of saturated phospholipids. Alternative means of promoting catalyst-free ligation reactions between azides

and alkynes have been described recently. They involve an activation of the alkyne partner either in strain-promoted activation of cycloalkynes in [3 + 2] cycloaddition reactions with azides [53, 54] or 1,3-dipolar cycloadditions of azides with electron-deficient alkynes [55]. Recently, a “traceless Staudinger ligation” based on the reduction of azides by phosphines via iminophosphorane intermediates has also emerged as a new ligation strategy [56]. This bioconjugation reaction, which has been used, for example, for the chemical synthesis of proteins, could constitute an attractive extension of the click reactions to biological systems that are sensitive to the action of copper ions.

9. Another potential problem is “Cu(I) saturation” [23]. In order for the click reaction to take place, the Cu(I)-acetylide complex intermediate must have physical contact with the azide. If this complex is however closely surrounded by other terminal alkynes, the possibility exists that these alkynes will also chelate with the complex, thereby “saturating” it. This effectively prevents any azide group from reaching the complex and performing the displacement reaction. One example came from the work of Ryu and Zhao [57] which described a substrate containing four terminal alkynes in close proximity and that was unable to undergo a click reaction. However, when the alkynes were replaced by azide functional groups, the substrate readily reacted. In our case Cu(I) saturation could also be invoked to explain vesicle aggregation under certain reaction conditions.
10. Liposomes were prepared and characterized as in the previous Subheadings (3.1.3 and 3.1.4).

The functionalized liposomes **9** were ligated to biotin-based reagent **11**, and the experimental conditions were finely tuned to optimize the conversion (up to 46%). The biotinyl liposomes were demonstrated functional and totally accessible in an affinity test based on biotin scaffold quantification. It was checked by DLS that the size of the SUVs remained unchanged after chemical ligation and after gel filtration purification steps ( $\varnothing$  70–100 nM). Thus, the coupling reaction and the purification steps do not alter the size of the liposomes. In another work, we demonstrated that the fluorocyclooctyne derivatives are inert toward thiols [40]. This last observation allowed us to perform a one-pot double ligation onto liposomes by using two anchors of the type cyclooctyne and dibromomaleimide without any cross-coupling reaction. These techniques could be of great interest for the incorporation of epitopes or immunoadjuvants on lipid particles as ingredients for synthetic vaccines. More widely, those methodologies can be applied to peptide, protein, and carbohydrate ligation onto liposomes. These results implement the amount of bioorthogonal chemical bonds available for liposome chemical modifications.

## References

1. Guimaraes D, Cavaco-Paulo A, Nogueira E (2021) Design of liposomes as drug delivery system for therapeutic applications. *Int J Pharm* 601:120571
2. Caracciolo G (2015) Liposome-protein corona in a physiological environment: challenges and opportunities for targeted delivery of nanomedicines. *Nanomedicine* 11:543–557
3. Pistone S, Rykke M, Smistad G, Hiorth M (2017) Polysaccharide-coated liposomal formulations for dental targeting. *Int J Pharm* 516:106–115
4. Sato H, Miyashita Y, Sasaki K, Kishimura A, Mori T, Katayama Y (2018) Non-covalent coating of liposome surface with IgG through Its constant region. *Chem Lett* 47:770–772
5. Torchilin VP (2006) Multifunctional nanocarriers. *Adv Drug Deliv Rev* 58:1532–1555
6. Forssen E, Willis M (1998) Ligand-targeted liposomes. *Adv Drug Deliv Rev* 29:249–271
7. Allen TM (2002) Ligand-targeted therapeutics in anticancer therapy. *Nat Rev Cancer* 2:750–763
8. Sapra P, Allen TM (2003) Ligand-targeted liposomal anticancer drugs. *Prog Lipid Res* 42:439–462
9. Schuber F (1995) Chemistry of ligand-coupling to liposomes. In: Philippot JR, Schuber F (eds) *Liposomes as tools in basic research and industry*. CRC Press, Boca Raton, pp 21–39
10. Nobs L, Buchegger F, Gurny R, Allemann E (2004) Current methods for attaching targeting ligands to liposomes and nanoparticles. *J Pharm Sci* 93:1980–1992
11. Torchilin VP (2005) Recent advances with liposomes as pharmaceutical carriers. *Nat Rev Drug Discov* 4:145–160
12. Schuber F, Said Hassane F, Frisch B (2007) Coupling of peptides to the surface of liposomes - application to liposome-based synthetic vaccines. In: Gregoriadis G (ed) *Liposome technology*, 3rd edn. Informa Healthcare, New York, pp 111–130
13. Lima PHC, Butera AP, Cabeca LF, Ribeiro-Viana RM (2021) Liposome surface modification by phospholipid chemical reactions. *Chem Phys Lipids* 237:105084
14. Barbet J, Machy P, Leserman LD (1981) Monoclonal antibody covalently coupled to liposomes: specific targeting to cells. *J Supramol Struct Cell Biochem* 16:243–258
15. Martin FJ, Papahadjopoulos D (1982) Irreversible coupling of immunoglobulin fragments to preformed vesicles. *J Biol Chem* 257:286–288
16. Schelté P, Boeckler C, Frisch B, Schuber F (2000) Differential reactivity of maleimide and bromoacetyl functions with thiols: application to the preparation of liposomal diepitope constructs. *Bioconjug Chem* 11:118–128
17. Bourel-Bonnet L, Pecheur EI, Grandjean C, Blanpain A, Baust T, Melnyk O, Hoflack B, Gras-Masse H (2005) Anchorage of synthetic peptides onto liposomes via hydrazone and alpha-oxo hydrazone bonds. Preliminary functional investigations. *Bioconjug Chem* 16: 450–457
18. Immordino ML, Dosio F, Cattel L (2006) Stealth liposomes: review of the basic science, rationale, and clinical applications, existing and potential. *Int J Nanomed* 1:297–315
19. Zalipsky S, Mullah N, Harding JA, Gittelman J, Guo L, DeFrees SA (1997) Poly(ethylene glycol)-grafted liposomes with oligopeptide or oligosaccharide ligands appended to the termini of the polymer chains. *Bioconjug Chem* 8:111–118
20. Sudimack J, Lee RJ (2000) Targeted drug delivery via the folate receptor. *Adv Drug Deliv Rev* 41:147–162
21. Kolb HC, Sharpless KB (2003) The growing impact of click chemistry on drug discovery. *Drug Discov Today* 8:1128–1137
22. Lutz JF, Zarafshani Z (2008) Efficient construction of therapeutics, bioconjugates, biomaterials and bioactive surfaces using azide-alkyne “click” chemistry. *Adv Drug Deliv Rev* 60:958–970
23. Hein CD, Liu XM, Wang D (2008) Click chemistry, a powerful tool for pharmaceutical sciences. *Pharm Res* 25:2216–2230
24. Moorhouse AD, Moses JE (2008) Click chemistry and medicinal chemistry: a case of "cyclo-addiction". *ChemMedChem* 3:715–723
25. Hood ED, Greineder CF, Shuvaeva T, Walsh L, Villa CH, Muzykantov VR (2018) Vascular targeting of radiolabeled liposomes with bio-orthogonally conjugated ligands: single chain fragments provide higher specificity than antibodies. *Bioconjug Chem* 29:3626–3637
26. Grimsley LB, West PC, McAdams CD, Bush CA, Kirkpatrick SS, Arnold JD, Buckley MR, Dieter RA, Freeman MB, McNally MM, Stevens SL, Grandas OH, Mountain DJH (2021) Liposomal nanocarriers designed for sub-endothelial matrix targeting under vascular flow conditions. *Pharmaceutics* 13:1816

27. Liang BJ, Pigula M, Baglo Y, Najafali D, Hasan T, Huang HC (2020) Breaking the selectivity-uptake trade-off of photoimmunoconjugates with nanoliposomal irinotecan for synergistic multi-tier cancer targeting. *J Nanobiotechnol* 18:1
28. Xiao Y, Liu Q, Clulow AJ, Li T, Manohar M, Gilbert EP, de Campo L, Hawley A, Boyd BJ (2019) PEGylation and surface functionalization of liposomes containing drug nanocrystals for cell-targeted delivery. *Colloids Surf B Biointerfaces* 182:110362
29. Ringhieri P, Mannucci S, Conti G, Nicolato E, Fracasso G, Marzola P, Morelli G, Accardo A (2017) Liposomes derivatized with multimeric copies of KCCYSL peptide as targeting agents for HER-2-overexpressing tumor cells. *Int J Nanomed* 12:501–514
30. Qin H, Zhao R, Qin Y, Zhu J, Chen L, Di C, Han X, Cheng K, Zhang Y, Zhao Y, Shi J, Anderson GJ, Zhao Y, Nie G (2021) Development of a cancer vaccine using *in vivo* click-chemistry-mediated active lymph node accumulation for improved immunotherapy. *Adv Mater* 33:e2006007
31. Shen L, Cai K, Yu J, Cheng J (2019) Novel liposomal azido Mannosamine lipids on metabolic cell Labeling and imaging via Cu-free click chemistry. *Bioconjug Chem* 30:2317–2322
32. Shen L, Cai K, Yu J, Cheng J (2020) Facile click-mediated cell imaging strategy of liposomal azido Mannosamine lipids via metabolic or nonmetabolic Glycoengineering. *ACS Omega* 5:14111–14115
33. Yang L, Lin X, Zhou J, Hou S, Fang Y, Bi X, Yang L, Li L, Fan Y (2021) Cell membrane-biomimetic coating via click-mediated liposome fusion for mitigating the foreign-body reaction. *Biomaterials* 271:120768
34. Gleue L, Schupp J, Zimmer N, Becker E, Frey H, Tuettenberg A, Helm M (2020) Stability of Alkyl chain-mediated lipid anchoring in liposomal membranes. *Cell* 9:2213
35. Desai TJ, Habulihaz B, Cannon JR, Chandramohan A, Kaan HYK, Sadruddin A, Yuen TY, Johannes C, Thean D, Brown CJ, Lane DP, Partridge AW, Evers R, Sawyer TK, Hochman J (2021) Liposome click membrane permeability assay for identifying permeable peptides. *Pharm Res* 38:843–850
36. Hassane FS, Frisch B, Schuber F (2006) Targeted liposomes: convenient coupling of ligands to preformed vesicles using “click chemistry”. *Bioconjug Chem* 17:849–854
37. Cavalli S, Tipton AR, Overhand M, Kros A (2006) The chemical modification of liposome surfaces via a copper-mediated [3 + 2] azide-alkyne cycloaddition monitored by a colorimetric assay. *Chem Commun (Camb)* 14: 3193–3195
38. Sun EY, Josephson L, Weissleder R (2006) “Clickable” nanoparticles for targeted imaging. *Mol Imaging* 5:122–128
39. Nieto C, Vega MA, Martin Del Valle EM (2020) Trastuzumab: more than a guide in HER2-positive cancer Nanomedicine. *Nanomaterials (Basel)* 10:1674
40. Salome C, Spanedda MV, Hilbold B, Berner E, Heurtault B, Fournel S, Frisch B, Bourel-Bonnet L (2015) Smart tools and orthogonal click-like reactions onto small unilamellar vesicles. *Chem Phys Lipids* 188:27–36
41. Fritz T, Voigt M, Worm M, Negwer I, Muller SS, Kettenbach K, Ross TL, Roesch F, Koynov K, Frey H, Helm M (2016) Orthogonal click conjugation to the liposomal surface reveals the stability of the lipid anchorage as crucial for targeting. *Chemistry* 22:11578–11582
42. Espuelas S, Haller P, Schuber F, Frisch B (2003) Synthesis of an amphiphilic tetraantennary mannosyl conjugate and incorporation into liposome carriers. *Bioorg Med Chem Lett* 13:2557–2560
43. Ponpipom MM, Bugianesi RL, Robbins JC, Doepper TW, Shen TY (1981) Cell-specific ligands for selective drug delivery to tissues and organs. *J Med Chem* 24:1388–1395
44. Iyer S, Anderson A, Reed S, Swanson B, Schmidt J (2004) Synthesis of orthogonal end functionalized oligoethylene glycols of defined lengths. *Tetrahedron Lett* 45:4285–4288
45. Schultz MK, Parameswarappa SG, Pigge FC (2010) Synthesis of a DOTA—biotin conjugate for radionuclide chelation via Cu-free click chemistry. *Org Lett* 12:2398–2401
46. Spanedda MV, Salome C, Hilbold B, Berner E, Heurtault B, Fournel S, Frisch B, Bourel-Bonnet L (2015) Smart tools and orthogonal click-like reactions onto small unilamellar vesicles: additional molecular data. *Data Brief* 5: 145–154
47. Borcard F, Godinat A, Staedler D, Blanco HC, Dumont AL, Chapuis-Bernasconi C, Scaletta C, Applegate LA, Juillerat FK, Gonzenbach UT, Gerber-Lemaire S, Juillerat-Jeanneret L (2011) Covalent cell surface functionalization of human fetal osteoblasts for tissue engineering. *Bioconjug Chem* 22:1422–1432
48. Rouser G, Fkeischer S, Yamamoto A (1970) Two dimensional thin layer chromatographic separation of polar lipids and determination of

- phospholipids by phosphorus analysis of spots. *Lipids* 5:494–496
49. Monsigny M, Petit C, Roche AC (1988) Colorimetric determination of neutral sugars by a resorcinol sulfuric acid micromethod. *Anal Biochem* 175:525–530
50. Engel A, Chatterjee SK, Al-arifi A, Riemann D, Langner J, Nuhn P (2003) Influence of spacer length on interaction of mannosylated liposomes with human phagocytic cells. *Pharm Res* 20:51–57
51. Lewis WG, Magallon FG, Fokin VV, Finn MG (2004) Discovery and characterization of catalysts for azide-alkyne cycloaddition by fluorescence quenching. *J Am Chem Soc* 126:9152–9153
52. Gal S, Pinchuk I, Lichtenberg D (2003) Peroxidation of liposomal palmitoylinoleoyl-phosphatidylcholine (PLPC), effects of surface charge on the oxidizability and on the potency of antioxidants. *Chem Phys Lipids* 126:95–110
53. Baskin JM, Prescher JA, Laughlin ST, Agard NJ, Chang PV, Miller IA, Lo A, Codelli JA, Bertozzi CR (2007) Copper-free click chemistry for dynamic *in vivo* imaging. *Proc Natl Acad Sci USA* 104:16793–16797
54. Ning X, Guo J, Wolfert MA, Boons GJ (2008) Visualizing metabolically labeled glycoconjugates of living cells by copper-free and fast huisgen cycloadditions. *Angew Chem Int Ed Engl* 47:2253–2255
55. Li Z, Seo TS, Ju J (2004) 1,3-Dipolar cycloaddition of azides with electron-deficient alkynes under mild condition in water. *Tetrahedron Lett* 45:3143–3146
56. Tam A, Soellner MB, Raines RT (2007) Water-soluble phosphinothiols for traceless staudinger ligation and integration with expressed protein ligation. *J Am Chem Soc* 129:11421–11430
57. Ryu EH, Zhao Y (2005) Efficient synthesis of water-soluble calixarenes using click chemistry. *Org Lett* 7:1035–1037



# Chapter 16

## Surface Modification of Liposomes Using Folic Acid

Mengran Guo, Zhongshan He, Xi He, and Xiangrong Song

### Abstract

Liposomes are usually defined as spherically shaped microscopic vesicles that consist of one or more phospholipid bilayer membranes. They are widely used in drug delivery due to their biocompatibility, biodegradability, and stability. In recent years, a growing body of research shows that folic acid (FA)-modified liposomes can be targeted to deliver therapeutics to tumor and inflammation sites via receptor-mediated endocytosis between FA and folate receptor (FR). Taking this advantage, FA-modified liposomes are usually used in the targeted treatment of cancer, atherosclerosis, and arthrosis. In this chapter, we provided a classical thin-film hydration method to prepare FA-modified liposomes. We expect that our strategies would provide new opportunities for the development of FA-modified liposomes for research and clinical uses.

**Key words** Liposomes, Surface modification, Folic acid, FA-modified liposomes, Thin-film hydration method, Targeted drug delivery

---

### 1 Introduction

Liposomes consisting of phospholipid bilayer membranes have been extensively researched as potential drug carriers for the therapy of several diseases, such as cancer, arthritis, and atherosclerosis [1–4], due to their biocompatibility and easily modified superiority. It is well known that the folate receptor (FR) is overexpressed in many cancers, such as colon cancer, non-small cell lung cancer, ovarian cancer, breast cancer, etc. It is also highly expressed on inflammatory cell surfaces, such as pro-inflammatory macrophages existing in atherosclerotic plaques. Folic acid (FA) is a hydrophilic B vitamin and can be targeted to bind with FR on tumor cells, which facilitates specific cellular internalization of nanoparticles modified with FA via receptor-mediated endocytosis [5]. As a targeted molecular, FA has several advantages, such as nontoxicity, stable storage, low price, and easy modification [6]. Therefore, liposomes modified with FA are promising to improve the precision of drug delivery during cancer or inflammatory disease therapy [7].

Generally, the modification of liposomes with FA can be achieved via a reaction between FA and any components of liposomes (e.g., lipids, cholesterol, and proteins). In this method, we chose poly(ethylene glycol)-cholesterol (PEG-Chol) conjugated with FA as the targeting ligand to prepare FA-modified liposomes through thin-film hydration. A detailed introduction of the materials and methods is presented as follows. We hope that our work can provide a reference for researchers working on liposomes.

## 2 Materials

All reagents are prepared and stored at room temperature before use (unless indicated otherwise).

1. 1-palmitoyl-2-stearoyl-sn-glycero-3-phosphatidylcholine (HSPC), 1,2-distearoyl-sn-glycero-3-phosphoethanolamine-N-[Methoxy(polyethylene glycol)-2000] (DSPE-PEG<sub>2000</sub>), cholesterol (Chol), and folic acid-PEG-succinyl-cholesterol conjugate (FA-PEG-Chol) (Fig. 1) are dividedly dissolved in ethanol to prepare a stock solution with a concentration of 10 mg/mL. These stock solutions are also stored at -20 °C and returned to room temperature before use.
2. Ethanol is an analytical reagent, and ultrapure water is obtained using the Milli-Q integral water purification system.
3. Phosphate-buffered saline (PBS) is prepared by dissolving 8 g of NaCl, 0.2 g of KCl, 1.44 g of Na<sub>2</sub>HPO<sub>4</sub>, and 0.24 g of KH<sub>2</sub>PO<sub>4</sub> in 800 mL ultrapure water. Then its volume is diluted

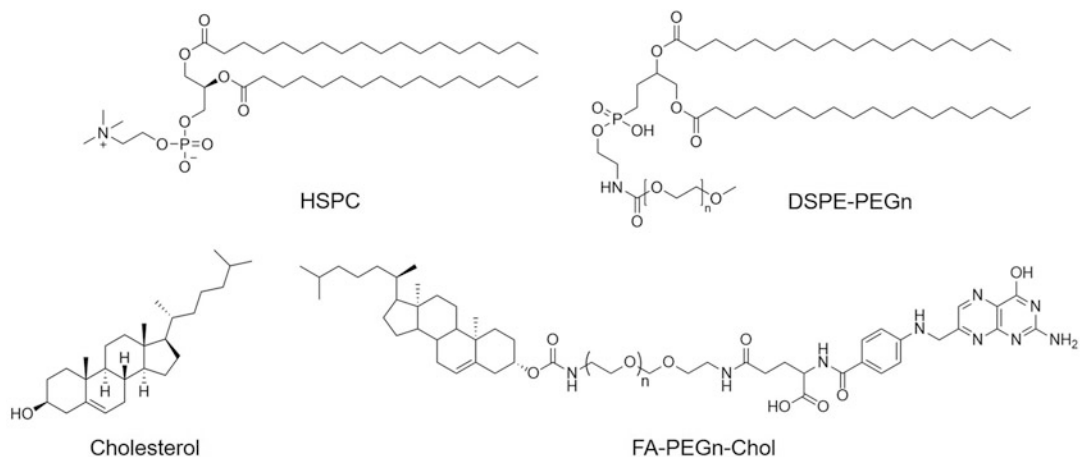


**Fig. 1** Chemical structures of 1-palmitoyl-2-stearoyl-sn-glycero-3-phosphatidylcholine (HSPC); 1,2-distearoyl-sn-glycero-3-phosphoethanolamine-N-[carboxy (polyethylene glycol)-2000] (DSPE-PEG<sub>2000</sub>); cholesterol (Chol); and folate-modified PEGn-succinyl-cholesterol conjugate (FA-PEGn-Chol)

into 1 L of ultrapure water, and pH is adjusted to 7.4 with hydrogen chloride (HCl).

4. 50 mL eggplant-shaped bottles.
5. Polycarbonate membranes with pore sizes 400 nm, 200 nm, 100 nm, and 50 nm.
6. Rotary evaporator (Büchi AG, Flawil, Switzerland).
7. Ultrasonic homogenizer (SCIENTZ, Ningbo, China).
8. Malvern Zetasizer Nano ZS instrument (ZEN3600, Malvern Instruments).
9. Transmission electron microscopy (TEM, HITACHI, HT7700, 100 kV, Japan).

### 3 Methods

The FA-modified liposomes are prepared through a classical thin-film hydration method (Fig. 2). And all procedures are carried out at room temperature unless otherwise specified.

#### 3.1 Preparation of the Thin Lipid Film

1. The HSPC, Chol, DSPE-PEG<sub>2000</sub> (*see Note 1*), and FA-PEGn-Chol stock solutions are separately added into a 50 mL eggplant-shaped bottle with a mole ratio of 40:15:3:2. The total concentration of the lipids is recommended not to exceed 1 mM (*see Note 2*). The mixture is diluted into 2 mL of ethanol and mixed briefly.
2. The mixed solution is evaporated on a rotary evaporator with a water bath of 37–45 °C (*see Note 3*) for 60 min. The rotary speed is 30–60 rpm, and the angle of the eggplant-shaped bottle is 30–45 °C. When the organic solvent is removed, a transparent thin film forms on the inner face of the eggplant-shaped bottle.

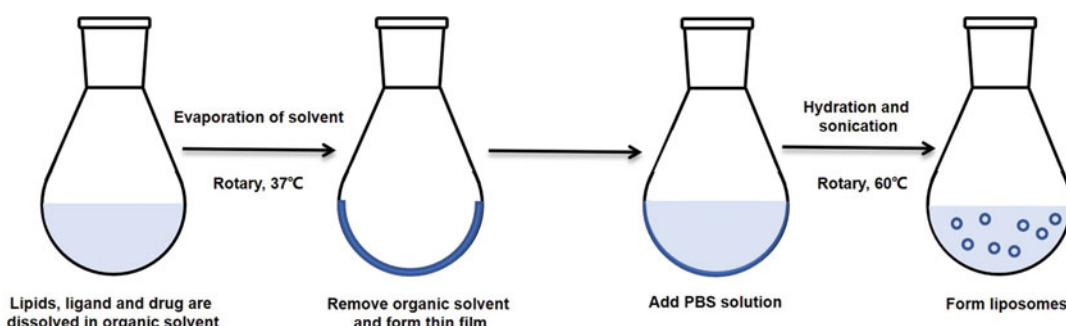


**Fig. 2** Preparation procedure of FA-modified liposomes

### **3.2 Hydration of the Dry Lipid Film**

1. Four milliliters of PBS (pH 7.4) (*see Note 4*) is added to the dry lipid film in the eggplant-shaped bottle.
2. The mixture is maintained in a water bath of 60–65 °C with a rotary rate of 60–100 rpm (*see Note 5*) for 45 min to hydrate the dry lipid film. The rotatory angle is the same as described in Subheading 3.1 (*see Note 4*). If some lipids stay on the inside surface of the flask, the solution can be put in a water bath sonicator for 15 s to help the lipids suspend in the solution.
3. The solution is transferred to a 10 mL glass round bottom ultrasonic tube with an inner diameter of 1.5 cm. The solution is homogenized using an ultrasonic homogenizer under an ice bath to obtain translucent liposome suspension (100 W, on/off cycle: 3/3 s, 3–5 min).
4. The suspension is sterilized by filtering through a Millipore 0.20 µm membrane filter (*see Note 6*) and stored at 4 °C before use.

### **3.3 Preparation of FA-Modified Liposomes Loading with Lipophilic Drugs**

1. To prepare the drug-loading FA-modified liposomes, the drug is first dissolved in ethanol with a concentration of 1–10 mg/mL (*see Note 7*).
2. The drug solution is mixed with the lipid stock solutions initially in a 50 mL eggplant-shaped bottle.
3. The following procedures are the same as in Subheadings 3.1 and 3.2.

### **3.4 Characterization of the FA-Modified Liposomes**

1. The concentration of FA-modified liposomes is 0.5 mg/mL.
2. The zeta potential, particle size, and polydispersity index (PDI) are determined by a Malvern Zetasizer Nano ZS instrument.
3. The morphology of FA-modified liposomes is characterized by transmission electron microscopy (Fig. 3). Briefly, the samples are placed on a copper grid and then stained with a 2% (w/v) phosphotungstic acid solution for 2 min at room temperature.

## **4 Notes**

1. The purpose of the addition of DSPE-PEG<sub>2000</sub> is to overcome plasma protein adsorption and increase the long circulation capacity. And the density of FA is closely associated with the targeting properties of the liposomes in different cells. As previously reported [8], the increasing amount of FA-PEG-Chol improves the binding ability between the ligands and receptors, which further promotes the internalization of FA-modified liposomes. However, when the amount of FA-PEG-Chol exceeds 1%, the uptake of FA-modified liposomes

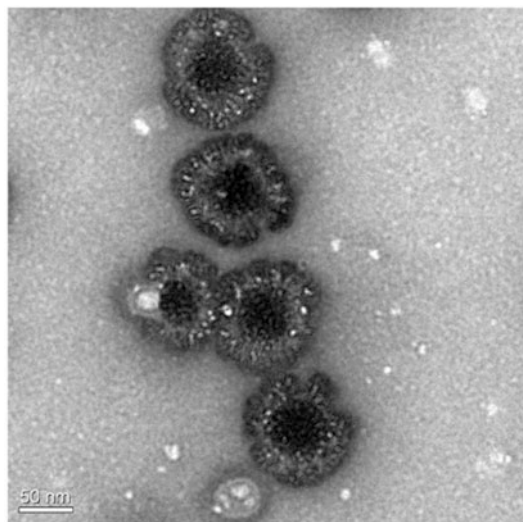


**Fig. 3** TEM image of FA-modified liposomes

by macrophages almost achieves saturation. Thus, a proper percentage of FA should be optimized for different cells.

2. The total concentration of the lipids is suggested to be not more than 1 mM as the more lipids are added, the thicker the film becomes. In addition, the lipids may gather at the bottom of the bottle, which is not conducive to hydration and dispersion.
3. In the evaporation procedure, it is necessary to adjust the temperature of the water bath to match the boiling point of the organic solvent. This can be observed from the condition of the liquid in the reflux pipe, which is best when the reflux liquid is dripping rather than flowing. This is conducive to the formation of a uniform film.
4. In the hydration procedure, the volume of added PBS should be equivalent to or more than that of the initial organic solvent. What's more, the angle of the eggplant bottle should be the same as that in the evaporation procedure. This will ensure that the thin film is hydrated completely.
5. The hydration temperature is suggested to range from 60 °C to 65 °C because the phase transition temperature of phospholipids is around 60 °C. Hydrated at the phase transition temperature, the phospholipid is easy to form liposomes.
6. To obtain the desired particle size, the FA-modified liposomes can be extruded through different sizes of polycarbonate membranes, such as 400 nm, 200 nm, 100 nm, or 50 nm.
7. When loading with a lipophilic drug, the particle size and encapsulation efficiency of FA-modified liposomes are

significantly affected by the amount of the drug. An excessive drug will result in an increase in particle size, a reduction in encapsulation efficiency, as well as drug leakage. While an inadequate drug may not be able to meet the dosing requirement. Thus, the amount of drug should be optimized to achieve proper particle size and higher drug loading.

## Acknowledgments

This study was supported by the National Key S&T Special Projects (2018ZX09201018-024) and 1.3.5 project for disciplines of excellence, West China Hospital, Sichuan University (ZYGD18020/ZYJC18006).

## References

- Duan S, Yu Y, Lai C, Wang D, Wang Y, Xue D, Hu Z, Lu X (2018) Vincristine-loaded and sgc8-modified liposome as a potential targeted drug delivery system for treating acute lymphoblastic Leukemia. *J Biomed Nanotechnol* 14:910–921. <https://doi.org/10.1166/jbn.2018.2530>
- Yang M, Feng X, Ding J, Chang F, Chen X (2017) Nanotherapeutics relieve rheumatoid arthritis. *J Control Release* 252:108–124. <https://doi.org/10.1016/j.jconrel.2017.02.032>
- Yang M, Ding J, Feng X, Chang F, Wang Y, Gao Z, Zhuang X, Chen X (2017) Scavenger receptor-mediated targeted treatment of collagen-induced arthritis by dextran sulfate-methotrexate prodrug. *Theranostics* 7:97–105. <https://doi.org/10.7150/thno.16844>
- Karagkiozaki V, Logothetidis S, Pappa AM (2015) Nanomedicine for atherosclerosis: molecular imaging and treatment. *J Biomed Nanotechnol* 11:191–210. <https://doi.org/10.1166/jbn.2015.1943>
- Kumar P, Huo P, Liu B (2019) Formulation strategies for folate-targeted liposomes and their biomedical applications. *Pharmaceutics* 11. <https://doi.org/10.3390/pharmaceutics11080381>
- Moghimpour E, Rezaei M, Ramezani Z, Kouchak M, Amini M, Angali KA, Dorkoosh FA, Handali S (2018) Folic acid-modified liposomal drug delivery strategy for tumor targeting of 5-fluorouracil. *Eur J Pharm Sci* 114:166–174. <https://doi.org/10.1016/j.ejps.2017.12.011>
- Xu Q, Guo M, Jin X, Jin Q, He Z, Xiao W, Zou W, Xu R, Cheng L, He S et al (2021) Interferon regulatory factor 5 siRNA-loaded folate-modified cationic liposomes for acute lung injury therapy. *J Biomed Nanotechnol* 17: 466–476. <https://doi.org/10.1166/jbn.2021.3046>
- Fang D, Jin Q, Jin Z, Wang F, Huang L, Yang Y, He Z, Liu Y, Jiang C, Wu J et al (2019) Folate-modified liposomes loaded with Telmisartan enhance anti-atherosclerotic potency for advanced atherosclerosis in ApoE(−/−) mice. *J Biomed Nanotechnol* 15:42–61. <https://doi.org/10.1166/jbn.2019.2676>



# Chapter 17

## Preparation and Characterization of Trastuzumab Fab-Conjugated Liposomes (Immunoliposomes)

ShanShan Jin, Huimin Li, and Yuhong Xu

### Abstract

Immunoliposomes are made by conjugating antibodies or antibody fragments on liposome surfaces. Antibody fragments Fab', single-chain Fv fragments (scFv), or new constructs such as nanobodies are commonly used instead of whole IgGs for reduced risk immunogenicity. Here we described the preparation and characterization of immunoliposome-containing trastuzumab Fabs on the surface. The targeting ligand Fab-PEG-DSPE was synthesized by site-specific coupling between the C-terminal cysteine of the Fab and the maleimide group at the distal end of a DSPE-PEG. It was incorporated into preformed liposomes at 60 °C above the lipid bilayer phase transition temperature. The binding avidity of the immunoliposomes containing different Fab valencies was characterized using biolayer interferometry.

**Key words** Trastuzumab Fab fragment, Immunoliposomes, PEG-DSPE, Avidity

---

### 1 Introduction

Immunoliposomes are liposomes containing antibodies or antibody fragments on the surface. In the pioneering study by Gregoriadis et al., liposomes mixed with purified antisera raised against cancer cells were taken up by the respective cell, leading to improved drug delivery [1]. Leserman et al. developed a method for the covalent coupling of monoclonal antibodies to liposomes [2]. They used the heterobifunctional cross-linking agent N-hydroxy-succinimidyl 3-(2-pyridyldithio) propionate (SPDP) for reaction with the lysine residues on the antibody surface. However, in order to minimize disturbances to the antibody complementarity-determining region (CDR) binding structures, conjugations through the cysteine residues in the hinge region are considered preferable [3, 4]. Furthermore, Maruyama and coworkers showed that the antibody needs to be added at the distal end of a polyethylene glycol (PEG) linker to avoid steric hindrance [5, 6].

In this study, we used DSPE-PEG2K-maleimide with a 2 kD PEG linker to react with the cysteine residue specifically added at the C-terminal end of the antibody Fab sequence. The Fab sequence is selected from the anti-Her2 IgG trastuzumab, and cysteine was added at the C-terminal end. It has a molecular weight of about 48 kD with higher than 98% purity. Alternatively, it is also possible to use cysteine at the end of a Fab' fragment obtained by enzymatic digestion of a full-length IgG Mab.

The attachment of antibodies on the liposome surface can be achieved by carrying out the coupling reaction either before or after the formation of liposomes. We describe the Fab-PEG-DSPE coupling reaction, followed by purification and incorporation into liposomes, in this chapter. It is also called the postinsertion method in the literature. The average numbers of Fab-PEG-DSPE molecules on each liposomes are estimated and used to correlate with the liposome binding avidity toward target cells.

---

## 2 Materials

All solutions are prepared using deionized water and sterile filtered before use. The antibody-containing solution should be kept refrigerated unless otherwise specified.

### 2.1 **Fab Conjugation and Purification**

1. Trastuzumab Fab: provided by Hangzhou HighField Biopharmaceuticals Corp. at 1–5 mg/mL stock concentration and > 98% purity (*see Note 1*).
2. Ethylenediaminetetraacetic acid (EDTA) stock solution: 100 mM.
3. Tris–HCl buffer stock solution: 1.0 M, pH 10.4.
4. Reducing agent: 50 mM β-Mercaptoethylamine hydrochloride (β-MEA-HCl) (Sigma-Aldrich, St. Louis, USA).
5. HiTrap desalting columns prepacked with Sephadex G-25 superfine resin (Cytiva, Boston, USA).
6. 10× phosphate-buffered saline (PBS): NaCl 1.37 M, KCl 26.83 mM, Na<sub>2</sub>HPO<sub>4</sub> 81 mM, KH<sub>2</sub>PO<sub>4</sub> 17.6 mM, pH 7.4.
7. 1,2-distearoyl-sn-glycero-3-phosphoethanolamine-N-[maleimide (polyethylene glycol)-2000] (ammonium salt) (DSPE-PEG2K-maleimide) (NOF Corporation, Tokyo, Japan).
8. 1,2-distearoyl-sn-glycero-3-phosphoethanolamine-N-[methoxy (polyethylene glycol)-2000] (mPEG<sub>2000</sub>-DSPE) (Lipoid, Ludwigshafen, Germany).
9. L-cysteine stop solution: 0.1 M L-cysteine, 2 mM EDTA, pH 5.0.
10. HEPES buffer: 30 mM, 2 mM EDTA, pH 6.8.

11. HiPrep 26/60 Sephadex S-100 HR (Cytiva, Boston, USA).
12. Amicon® Ultra-4 (Merck, Darmstadt, Germany), 10 kD MWCO.

## **2.2 Liposome and Immunoliposome Preparation**

1. HSPC: hydrogenated soybean phosphatidylcholine (Lipoid, Ludwigshafen, Germany).
2. Chol: cholesterol (A.V.T., Shanghai, China).
3. Ethanol (Nanjing Reagent, Nanjing, China).
4. Ammonium sulfate solution: 250 mM, pH 5.0.
5. HEPES buffer: 10 mM, pH 7.0.
6. Polycarbonate membrane: 200, 100, 80, and 50 nM pore size (Whatman, Maidstone, UK).
7. Sepharose® CL-4B cross-linked (Merck, Darmstadt, Germany).

## **2.3 Immunoliposome Characterizations**

1. MAbPac™ reversed-phase liquid chromatography (RPLC) column (Thermo Fisher Scientific, Waltham, USA).
2. 96-well solid black flat bottom polystyrene tissue culture (TC)-treated microplates (Corning, NY, USA).
3. 96-well MAX plate (Probe Life, Palo Alto, CA).
4. HFC (anti-HigG Fc) probes (Probe Life, Palo Alto, CA).
5. Her2/ErbB2 (23–450) protein with Fc tag: purity >95% (Acro Biosystems, Beijing, China).
6. 10× K buffer: 0.2% bovine serum albumin (BSA) + 0.05% sodium azide +0.02% Tween 20 in 1000 mL PBS.

## **3 Methods**

### **3.1 Fab Coupling and Purification**

1. Bring the trastuzumab Fab stock to room temperature (20 ~ 25 °C). Add EDTA stock solution and Tris–HCl buffer stock to an antibody concentration of 1.0 mg/mL with 2.5 mM EDTA, pH 6.5.
2. Add 8.4 µL of 50 mM β-MEA·HCl to 1 mg of the Fab solution and place the reaction tube on an orbital shaker set at 100 rpm for 60 min at room temperature. The Fab to β-MEA·HCl molar ratio in the solution should be about 1:20 (*see Note 2*).
3. Load the mixture onto a prepacked HiTrap desalting column equilibrated with 1× PBS, 2.0 mM EDTA, pH 7.0. Collect the protein fraction and store refrigerated at 2–8 °C.
4. Weigh 3.57 mg of DSPE-PEG2K-maleimide and 14.28 mg of mPEG<sub>2000</sub>-DSPE. Dissolve in 1 mL of 30 mM HEPES buffer

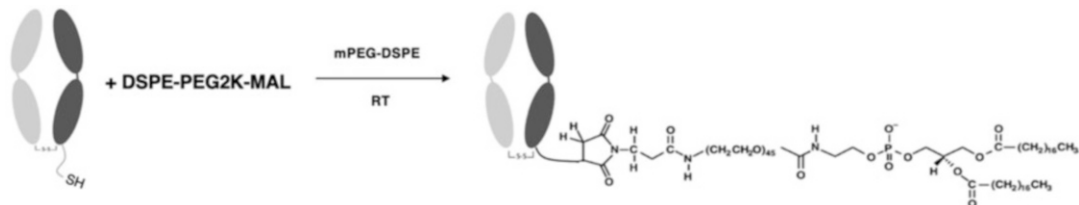


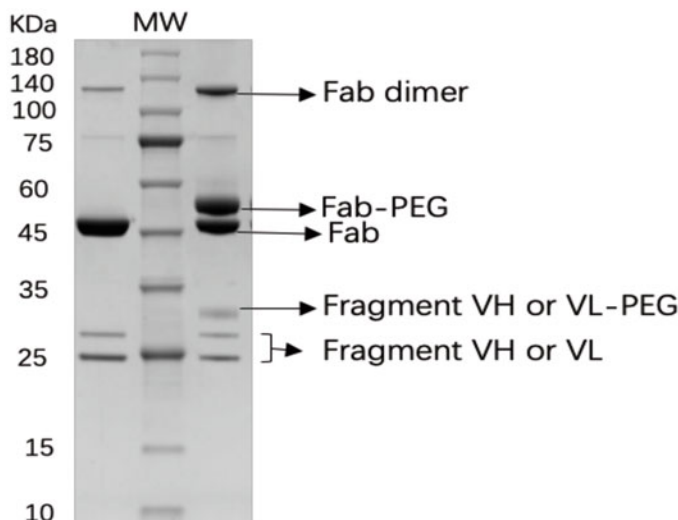
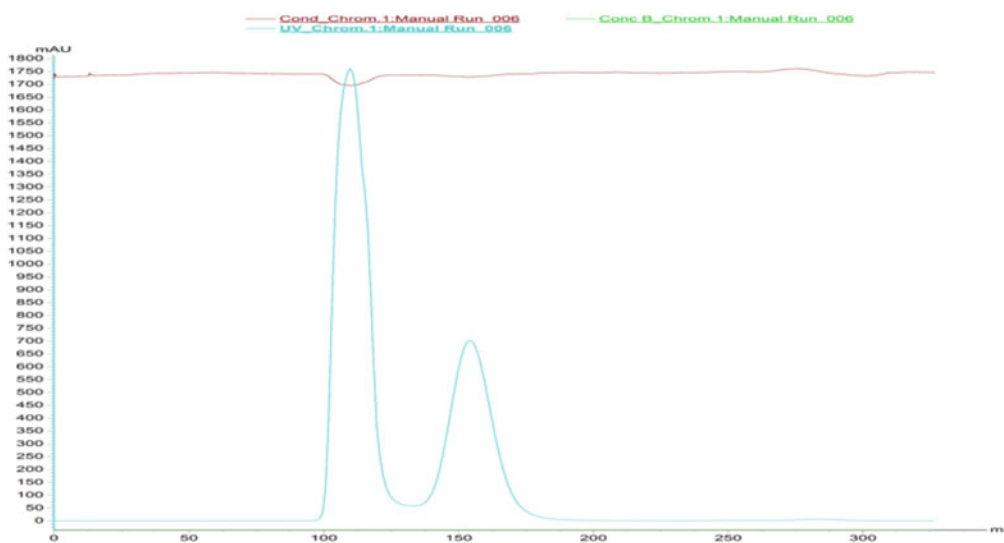
**Fig. 1** The coupling reaction between the trastuzumab Fab and DSPE-PEG-mal

(pH 6.8) containing 2 mM EDTA. Vortex or occasionally sonicate until fully dissolved (*see Note 3*).

5. Cool the DSPE-PEG2K-maleimide and mPEG<sub>2000</sub>-DSPE mixed micelle solution at 2–8 °C. Add into the reduced Fab solution until there are equal molar concentrations of DSPE-PEG2K-maleimide and Fab. The reaction scheme is shown in Fig. 1 (*see Note 4*).
6. At the end of the reaction, add the L-cysteine stop solution to quench the reactant. The L-cysteine concentration should be about 1 mM (*see Note 5*).
7. The reactants before or after the coupling reaction are analyzed through sodium dodecyl-sulfate polyacrylamide gel electrophoresis (SDS-PAGE), as shown in Fig. 2a. The bands from the top down are Fab dimer, Fab-PEG-DSPE, Fab, and VH–VL.
8. Load the products onto a HiPrep 26/60 Sephadex S-100 HR (Cytiva, Boston, USA). Elute with 1–2 CV of 1× PBS buffer (pH 7.0) at the flow rate of 29.4 cm/h. Fab-PEG-DSPE should elute first, followed by the unreacted Fab. A representative chromatograph is shown in Fig. 2b.
9. Collect the Fab-PEG-DSPE fraction and concentrate the purified Fab-PEG-DSPE using an Amicon® Ultra-4 tube to about 2 mg/mL protein concentration. Freeze and store in a –70 °C freezer.
10. The Fab-PEG-DSPE binding affinity is characterized by biolayer interferometry (BI) using a GatorPrime (Gator Bio, Palo Alto, CA, USA). Measurements are repeated three times and, the binding curves are analyzed using Gatorone (Version 1.7.2, Probelife).

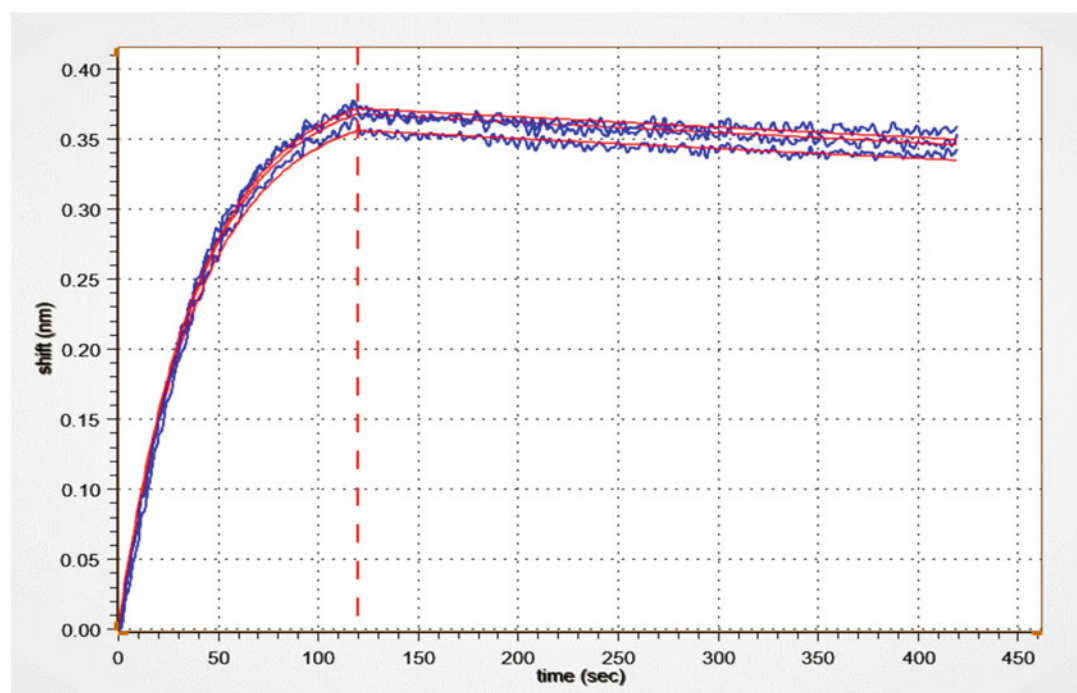
### 3.2 Immunoliposome Preparation

1. Dissolve all the lipids in ethanol to about 30 mg/mL lipid concentration. Place the glass bottle in a water bath at 60 °C and stir until completely dissolved (*see Note 6*).
2. Inject the lipid ethanol solution into a 250 mM ammonium sulfate solution prewarmed at 60 °C. The mixture is kept with constant stirring at 60 °C for 45 min (*see Note 7*).

**A****B**

**Fig. 2** Analysis of Fab-PEG-DSPE. (a) NR SDS-PAGE (4–20%) of the coupling reaction products. (b) Size-exclusion chromatography for the purification of Fab-PEG-DSPE. (c) Biolayer interferometry analysis of the Fab-PEG-DSPE affinity toward target cells

C

**Fig. 2** (continued)

3. The lipid suspension is then extruded sequentially through polycarbonate membranes with pore sizes of 200, 100, 80, and 50 nM, using a custom-made extruder (AITESEN, Suzhou, China).
  4. Adjust or replace the liposome suspension buffer to contain 10 mM HEPES pH 7.0 (*see Note 8*).
  5. Place the liposome suspension in a 60 °C water bath. Add the purified Fab-PEG-DSPE and incubate for 10–30 min. The Fab-PEG-DSPE to lipid molar ratio may be adjusted in order to make liposomes with different Fab valencies (*see Note 9*).
  6. The incubation at 60 °C should not last longer than 30 min. Chill the solution on ice immediately afterward (*see Note 10*).
  7. The immunoliposomes may be further purified using a Sepharose CL-4B column (10 cm × 0.8 cm). The fractions collected can be analyzed for Fab-PEG-DSPE concentration (Fig. 3). The liposome-encapsulated doxorubicin concentration is also analyzed for comparison (*see Note 11*).
- 3.3 Characterization of Immunoliposomes**
1. The immunoliposomes were characterized for Z-average particle size and polydispersity (PDI) using Zetasizer Nano ZS90 (Malvern Instruments, Herrenberg, Germany).

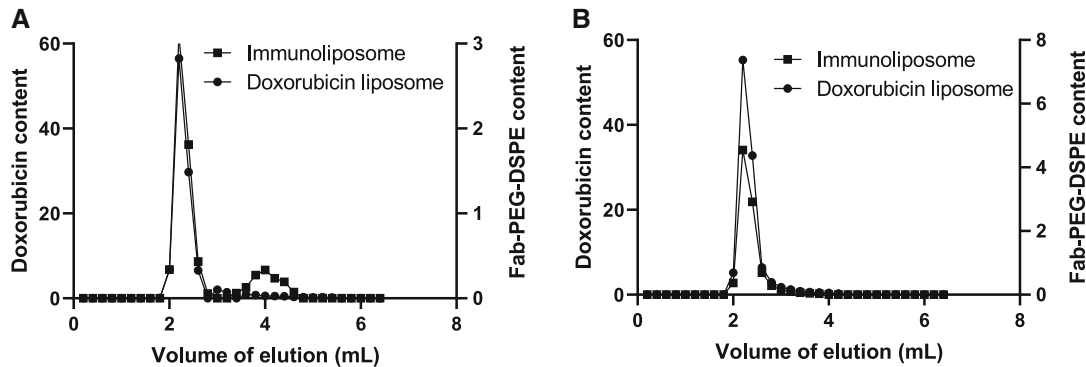


**Fig. 3** Analysis of immunoliposome prepared under two conditions. Sepharose CL-4B size exclusion chromatograph was used and both (a) 37 °C for 1 h, (b) 60 °C for 30 min

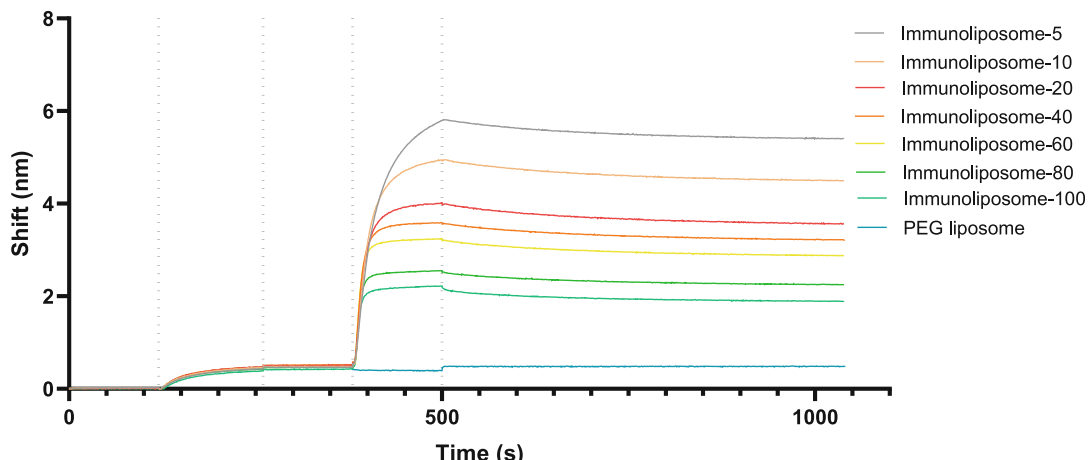


**Fig. 4** Real-time binding curves of immunoliposomes with Fab valencies of 5, 10, 20, 40, 60, 80, and 100

2. The amount of Fab-PEG-DSPE in the liposome suspension is quantified through reversed-phase high-performance liquid chromatography (RP-HPLC) using a MAbPac RP column. The average Fab-PEG-DSPE valency on liposomes may be estimated by quantifying the amount of Fab-PEG-DSPE of the total lipid concentrations (*see Note 12*).
3. Immunoliposome avidity is determined through biolayer interferometry using GatorPrime. Figure 4 shows the BLI binding curves of immunoliposomes containing different Fab-PEG-DSPE valencies.

---

## 4 Notes

1. The trastuzumab Fab consists of the trastuzumab light chain and part of the heavy chain linked by disulfide bonds. The detailed sequences are as follows:

*>Heavy-chain.*

EVQLVESGGGLVQPGGSLRLSCAASGFNIKD-TYIHWVRQAPGKGLEWVARIYPTNGYTRYADSVKGRFTISADTSKNTAYLQMNSLRAEDTAVYYCSRWGGDG-FYAMDYWGQGTLTVSSASTKGPSVFPLAPSKSTSGG-TAALGCLVKDVFPEPVTWSWNSGALTSGVHTF-PAVLQSSGLYSLSSVVTVPSSSLGTQ-

TYICNVNHKPSNTKVDKKVEPKSCDKTHTCAA

*>Light-chain.*

DIQMTQSPSSLSASVGDRVTITCRASQDVNTAVA-WYQQKPGKAPKLLIYSASFYSGVPSRFSGSRSGTDFTLTISLQPEDFATYYCQQHYTTPPTFGQGTKVEIKRT-VAAPSVFIFPPSDEQLKSGTASVVCLNNFY-PREAKVQWKVDNALQSGNSQESVTEQDSKD-STYSLSSLTLSKADYEHKVYA-CEVTHHQGLSSPVTKSFNRGEC.

2. The Fab to  $\beta$ -Mercaptoethylamine ratio as well as the reaction temperature are critical for exposing the C-terminal free thiol on the Fab.  $\beta$ -Mercaptoethylamine hydrochloride has relatively mild activities. Agents such as dithiothreitol DTT and tris (2-carboxyethyl)phosphine (TCEP) were found to have the propensity of disrupting the interchain disulfide bonds.
3. The DSPE-PEG2K-maleimide concentration in the mixed micelle solution is about 1.5 mM. The addition of mPEG<sub>2000</sub>-DSPE helps to maintain antibody stability during conjugation and improve coupling efficiency.
4. The molar ratio of DSPE-PEG2K-maleimide to Fab, the reaction temperature, and the duration are all critical for the coupling reaction. They all need to be optimized for different antibody fragments. In this study, equal molar of DSPE-PEG2K-maleimide to Fab was reacted at 2–8 °C for 1.5 h.
5. L-cysteine is used to inactivate the unreacted DSPE-PEG2k-maleimide. It should be removed during the Fab-PEG-DSPE purification step. It may affect the Fab-PEG-DSPE stability if not promptly removed.
6. Liposomes or lipid nanoparticles (LNPs) can be made with different lipid compositions and different cargo capacities. For example, small interfering RNA (siRNA) or messenger RNA (mRNA) may be loaded during liposome preparation.

Drugs such as doxorubicin and irinotecan may be loaded after liposome formation.

7. The buffer condition may be adjusted for different application purposes. The ammonium sulfate buffer solution is used to enable doxorubicin loading into the liposomes.
8. The buffer condition needs to be optimized for maximum antibody stability.
9. The Fab valency on immunoliposomes is defined as the average copy number of Fabs on each liposome. It can be estimated based on the Fab-PEG-DSPE to lipid ratio added. For example, one can estimate that there are about 100 K lipids per 80–100 nM unilamellar liposome (SUV). When the Fab-DSPE-PEG to lipid molar ratio is about 1:1000, the estimated Fab valency is 100.
10. The Fab-PEG-DSPE incorporation process is more efficient when the incubation temperature is at 60 °C. But try to limit the incubation time to as short as possible to minimize damaging the structure of the antibody.
11. Since almost all the Fab-PEG-DSPEs were incorporated into the liposomes after incubation for 30 min at 60 °C, this step may be omitted.
12. The total amount of Fab-PEG-DSPE was quantified for the estimation of immunoliposome Fab valency, as described in **Note 9**.

## References

1. Gregoriadis G, Neerunjun ED (1975) Homing of liposomes to target cells. *Biochem Biophys Res Commun* 65(2):537–544
2. Leserman LD, Barbet J, Kourilsky F, Weinstein JN (1980) Targeting to cells of fluorescent liposomes covalently coupled with monoclonal antibody or protein a. *Nature* 288(5791):602–604
3. Alley SC, Okeley NM, Senter PD (2010) Antibody-drug conjugates: targeted drug delivery for cancer. *Curr Opin Chem Biol* 14(4): 529–537
4. Tsuchikama K, An Z (2018) Antibody-drug conjugates: recent advances in conjugation and linker chemistries. *Protein Cell* 9(1):33–46
5. Maruyama K, Takizawa T, Yuda T, Kennel SJ, Huang L, Iwatsuru M (1995) Targetability of novel immunoliposomes modified with amphiphatic poly(ethylene glycol)s conjugated at their distal terminals to monoclonal antibodies. *Biochim Biophys Acta* 1234(1):74–80
6. Maruyama K, Takizawa T, Takahashi N, Tagawa T, Nagaike K, Iwatsuru M (1997) Targeting efficiency of PEG-immunoliposome-conjugated antibodies at PEG terminals. *Adv Drug Deliv Rev* 24(2):235–242



# Chapter 18

## Pyrophosphorylated-Cholesterol-Modified Bone-Targeting Liposome Formulation Procedure

**Yanzhi Liu, Zhenshan Jia, Luoyang Ma, and Dong Wang**

### Abstract

Bone-targeting drug delivery systems have been rapidly developed to increase drug efficacy and safety for musculoskeletal diseases in the past decades. Bone-targeting drug delivery is mainly based on ligands that have hydroxyapatite affinity. We previously reported a pyrophosphorylated cholesterol ligand-based bone-targeting liposome formulation for the treatment of bone fracture delayed union. Different from traditional bone-targeting ligands: bisphosphonates tetracyclines and polyanion peptides. Pyrophosphorylated cholesterol has no intrinsic pharmacological effects and can be naturally degraded into metabolites (both pyrophosphate and cholesterol are substances that naturally exist in the body), leading to minimal safety concerns. Pyrophosphorylated cholesterol is not only biodegradable, but it also provides strong bone affinity, which could target different bone substructures/surfaces, further improving drug delivery efficiency *in vivo*. Here, we describe the synthesis protocol of pyrophosphorylated cholesterol and a reverse-evaporation-based formulation protocol of pyrophosphorylated-cholesterol-modified bone-targeting liposomes for hydrophilic drug encapsulation. We also provide instructions for the bone-targeting property evaluation of the pyrophosphorylated-cholesterol-modified liposome *in vitro* and *in vivo*. Our system has wide applications and has already been used to study drug treatment for fracture delayed union and nonunion. As a promising bone-targeting drug delivery system, our system may be extrapolated to clinical applications of other bone anabolic agents for different bone diseases.

**Key words** Liposomes, Bone targeting, Pyrophosphorylated cholesterol, Drug delivery, Pyrophosphate, Bone

---

### 1 Introduction

As a novel targeting ligand, pyrophosphorylated cholesterol is developed to address the limitations of current bone-targeting liposome (BTL) formulations. Most of the current bone targeting ligands are designed to target the biomineral component of the bone (hydroxyapatite (HA)), which makes up more than 70% of the bone. Different bone-targeting ligands have preferential distribution to the hard tissues *in vivo* due to their strong affinity to HA through calcium chelation [7]. Compared to conventional

bone-targeting ligands, such as bisphosphonates [5, 6], tetracyclines [8], and polyanion peptides [2, 4], which have been used extensively in the past two decades in developing bone-targeting delivery systems, pyrophosphorylated cholesterol is a new targeting ligand with unique advantages. First, different from bisphosphonates (antiresorptive agents for the treatment of osteoporosis) and tetracycline (an antibacterial drug), pyrophosphorylated cholesterol has no intrinsic pharmacological effects. Both pyrophosphate and cholesterol are substances that naturally exist in the body and can be processed into inert metabolites, leading to minimal safety concerns. Second, compared to bone-targeting polyanion peptides, pyrophosphorylated cholesterol is not only biodegradable but also provides stronger bone affinity. In addition, pyrophosphorylated-cholesterol-modified liposomes have proven to be able to target different bone substructures/surfaces, further improving drug delivery efficiency *in vivo* [3, 9]. In the following sections, the synthesis of pyrophosphorylated cholesterol and the formulation of pyrophosphorylated-cholesterol-modified bone-targeting liposomes are described.

---

## 2 Materials

Cholesterol (Sigma Chemical Co, St Louis, USA), lecithin ( $\geq 96\%$ , MP Biomedicals™, LLC, Solon, OH, USA), dichloromethane (Aladdin, Shanghai, China), hydroxyapatite powder (HA, DNA-grade Bio-Gel HTP gel, Bio-Rad, Hercules, CA, USA), OCT compound (Sakura Finetek, CA, USA), Sulfo-Cyanine5.5 NHS ester (Lumiprobe, MD, USA), PD-10 columns (GE Healthcare, Piscataway, NJ, USA), Nuclepore™ Track-Etch Membrane Filtration Products (0.2  $\mu\text{m}$ , diameter 19 mM, GE Healthcare, WI, USA), filter supports (0.45  $\mu\text{m}$ , diameter 10 mM, Avanti® Polar Lipids, AL, USA), and IRDye 800CW carboxylate (LI-COR Biosciences, Lincoln, NE, USA). All other reagents and solvents, if not specified, are purchased from either Fisher Scientific (Pittsburgh, PA, USA) or Acros Organics (Morris Plains, NJ, USA).

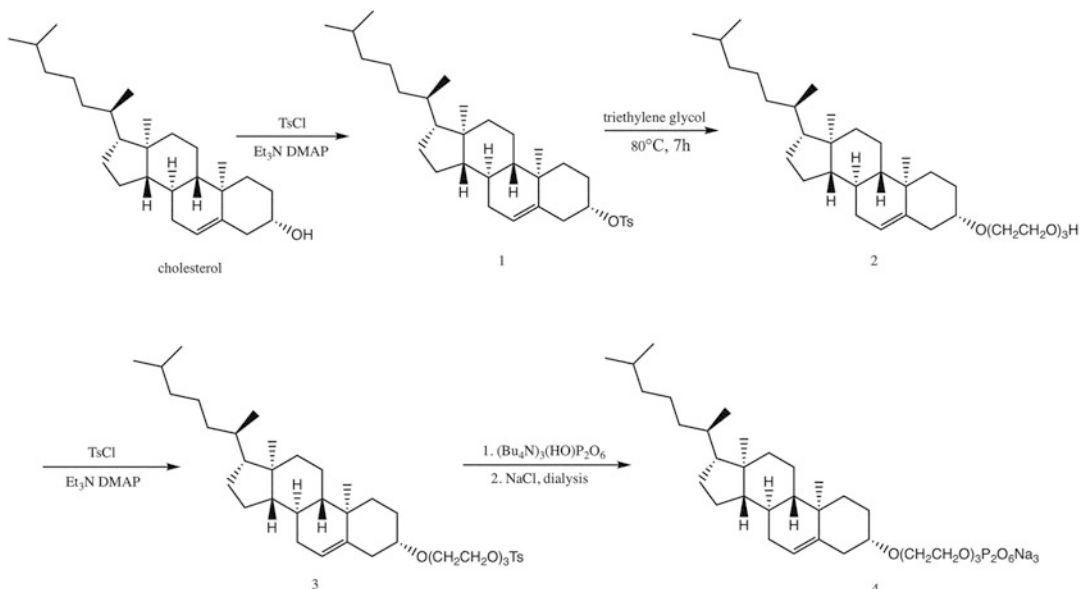
---

## 3 Methods

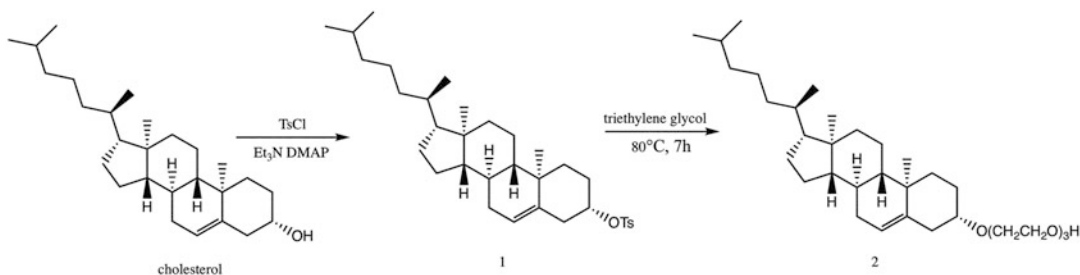
### 3.1 Synthesis of Pyrophosphorylated Cholesterol (Fig. 1)

#### 3.1.1 Synthesis of Triethylene-Glycol-Conjugated Cholesterol Compound 2 (Fig. 2)

1. In a 100 mL dried round-bottom flask, cholesterol (3.86 g, 10 mmol), triethylamine ( $\text{Et}_3\text{N}$ , 2.02 g, 20 mmol), and 4-dimethylaminopyridine (DMAP, 244 mg, 2 mmol) are dissolved in anhydrous dichloromethane (DCM, 20 mL).
2. The solution is cooled at 0 °C by ice bath.
3. 4-toluenesulfonyl chloride (TsCl, 2.85 g, 15 mmol) is added. The solution is allowed to sit at room temperature and stirred for 20 h.

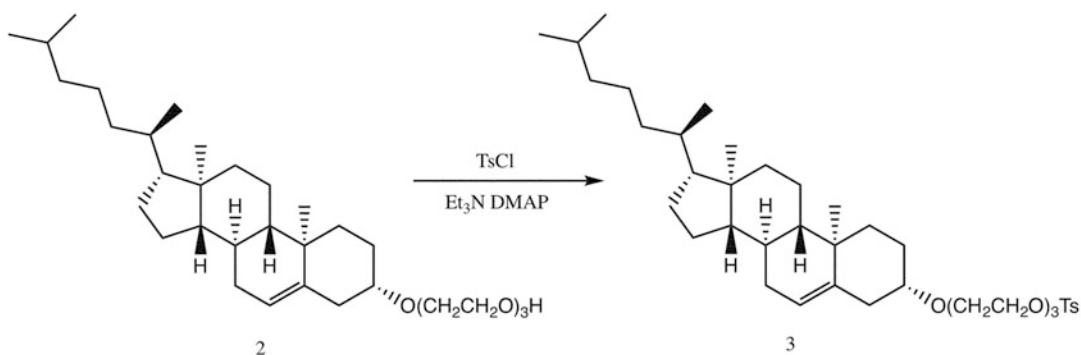


**Fig. 1** The synthetic route of pyrophosphorylated cholesterol (cholesterol-PPi)



**Fig. 2** The synthesis of triethylene-glycol-conjugated cholesterol compound **2**

- Ethyl acetate (100 mL) is added, and the solution is sequentially washed with a hydrogen chloride (HCl) solution (30 mL, 1 M), brine (100 mL, twice), and water (100 mL, twice).
- The organic phase is combined and dried over  $\text{MgSO}_4$ , and then the solvent is removed by rotary evaporation.
- Triethylene glycol (24 g, 160 mmol) and 60 mL of 1,4-dioxane (60 mL) are added. The solution is heated at  $80^\circ\text{C}$  and stirred for 7 h and then allowed to return to room temperature.
- Ethyl acetate (100 mL) is added. The solution is then transferred to a separation funnel and sequentially washed with brine (100 mL, twice) and water (100 mL, twice).

**Fig. 3** The synthesis of compound 3

8. The organic phase is dried over  $\text{MgSO}_4$ , and the solvent is evaporated. The residue is then purified through flash chromatography with ethyl acetate as the mobile phase. After the evaporation of the solvent collected, 3.65 g of compound 2 is obtained with a yield of 70.5%.

### *3.1.2 Synthesis of Compound 3 (Fig. 3)*

- In a 100 mL round-bottom flask, triethylene-glycol-conjugated cholesterol (compound 2, 3.1 g, 6.0 mmol),  $\text{Et}_3\text{N}$  (1.21 g, 12 mmol), and 4-(dimethylamino)pyridine (DMAP) (146 mg, 1.2 mmol) are dissolved in anhydrous DCM (30 mL).
- The solution is cooled at 0 °C.  $\text{TsCl}$  (1.37 g, 7.2 mmol) is then added. The solution is stirred at 0 °C for 1 h, then allowed to warm up, and stirred for 3 h at room temperature.
- Ethyl acetate (100 mL) is added and washed with an HCl solution (1 M, 20 mL), brine (100 mL, twice), and water (100 mL, twice). The organic phase is dried over  $\text{MgSO}_4$  and filtered. The solvent of the filtrate is then removed.
- The residue is purified by flash chromatography. After removal of the solvent from the collection, 3.58 g of product is obtained with a yield of 88.8%.

### *3.1.3 Synthesis of Pyrophosphorylated Cholesterol Compound 4 (Cholesterol-PPi, Fig. 4)*

- In a dried 100 mL round-bottom flask, compound 3 (336 mg, 0.5 mmol) and  $(\text{Bu}_4\text{N})_3(\text{HO})\text{P}_2\text{O}_6$  (902 mg, 1 mmol) are dissolved in  $\text{CH}_3\text{CN}$  (10 mL) and tetrahydrofuran (THF) (3 mL).
- The solution is stirred at room temperature, and the progress of the reaction is monitored by thin-layer chromatography (TLC) until its completion.
- After evaporation of the solvents, the residue is dissolved in water (50 mL) and dialyzed (MWCO = 10 kDa) first against an  $\text{NaCl}$  solution and then distilled water. The solution is then taken out of the dialysis bag and transferred to a separation funnel. Ethyl acetate (40 mL) is added to extract the organic by-product.

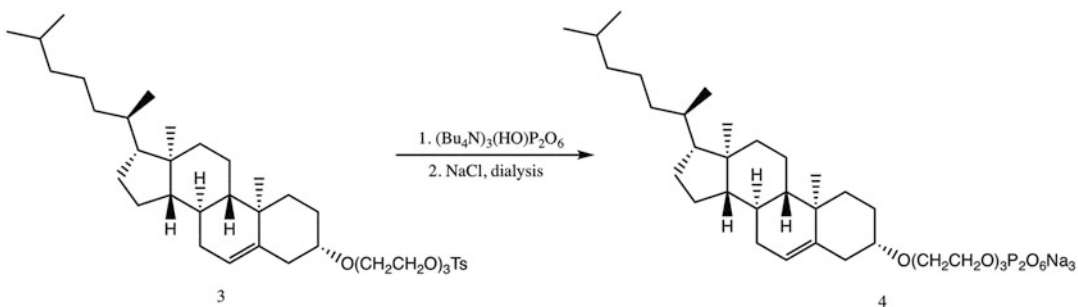


**Fig. 4** Synthesis of pyrophosphorylated cholesterol compound 4 (cholesterol-PPi)

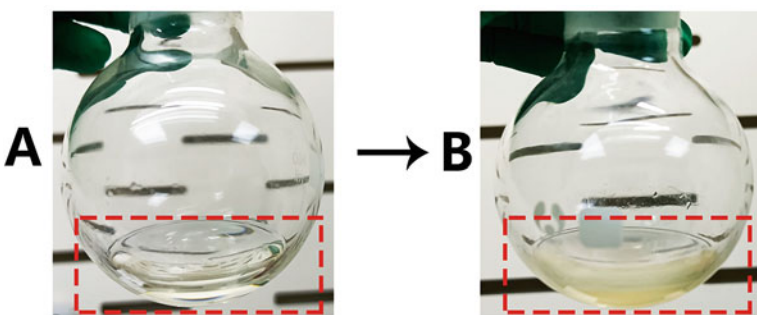


**Fig. 5 (a)** Lecithin dissolved in dichloromethane. **(b)** The drug (e.g., salvianic acid A (SAA)) aqueous solution is added to the dichloromethane (DCM) mixed solution. In order to reduce DCM evaporation, the reagent dissolution and solution transfer need to be swift

4. The aqueous phase is collected from the separation funnel and lyophilized to give 315 mg of white powder as the final product (pyrophosphorylated cholesterol, abbreviation: cholesterol-PPi) with a yield of 84.6%.

### 3.2 Pyrophosphorylated-Cholesterol-Modified Bone-Targeting Liposome Formulation

#### 3.2.1 Liposome Formulation

The reverse phase evaporation method is used for liposome formulation. Lecithin, cholesterol, and cholesterol-PPi are dissolved in DCM in a round-bottom flask. The molar ratio of lecithin:cholesterol:cholesterol-PPi:drug is kept at 38:14:3:30. The ratio of cholesterol-PPi can be increased to completely replace cholesterol in liposomes for better bone-targeting efficiency. However, a high ratio of cholesterol-PPi may decrease drug encapsulation efficacy.

1. Lecithin ( $150\text{ mg}$ ,  $1.9 \times 10^{-4}\text{ mol}$ ), cholesterol ( $27\text{ mg}$ ,  $7 \times 10^{-5}\text{ mol}$ ), and cholesterol-PPi ( $11\text{ mg}$ ,  $1.5 \times 10^{-5}\text{ mol}$ ) are dissolved in DCM ( $6\text{ mL}$ ) in a round-bottom flask (Fig. 5a).
2. A drug solution (e.g. salvianic acid A (SAA),  $30\text{ mg}$ ,  $1.5 \times 10^{-4}\text{ mol}$  in  $2\text{ mL}$  of phosphate-buffered saline (PBS) solution, pH 7.4) is added into the mixed lipid solution (Fig. 5b). The volume ratio of the drug aqueous phase and DCM is kept at 1:3 (see Note 1).

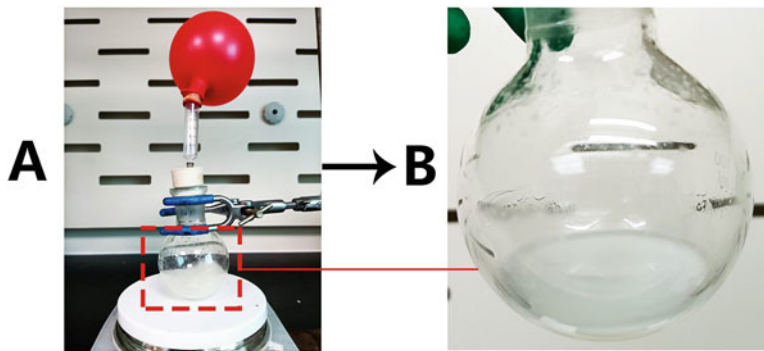


**Fig. 6** (a) Nitrogen protection for the mixed solution during the stirring process. (b). The mixed solution is stirred to form an emulsion. Nitrogen protection is needed in the stirring process to prevent salvianic acid A (SAA) oxidation and dichloromethane (DCM) evaporation

3. The mixture is stirred at 1500 rpm/min for 10 min (*see Note 2*) (Fig. 6a). The mixture became either a clear one-phase dispersion or a homogeneous opalescent dispersion (Fig. 6b).
4. DCM in the resulting emulsion is removed using a rotary evaporator at 500 mbar for 2 h, followed by 200 mbar for 1 h at ambient temperature (Fig. 7).
5. After the evaporation process, the liposome formulation product is extruded back and forth using an Avanti® Mini-Extruder (Avanti Polar Lipids, Alabaster, AL, USA) equipped with a 0.2/0.4 µm membrane (Fig. 8) 11 times to obtain the liposome with desirable size (Figs. 9a and 10) (*see Note 3*).

### 3.3 Liposome Purification

#### 3.3.1 PD-10 Desalting Column Preparation

The formulated liposome is purified with a PD-10 column using a spinning protocol to remove the free drug according to the manufacturer's instruction (GE Healthcare, Little Chalfont, UK) (Fig. 9c).

1. Remove the top cap and pour off the column storage solution.
2. Remove the top filter using forceps.
3. Cut the sealed end of the column at the notch.
4. Put the PD-10 desalting column into a 50 mL collection tube by using a column adapter.
1. Fill up the column with an equilibration buffer and allow the equilibration buffer to enter the packed bed completely.
2. Repeat three times and discard the flow-through (*see Note 4*).

#### 3.3.2 Column Equilibration



**Fig. 7** The thin film formed after dichloromethane (DCM) evaporation. The DCM in the system is gradually removed by rotary evaporation. During the evaporation of the solvent, the mixture foams up continuously. As the majority of the solvent is removed, the mixture first forms a viscous gel in the flask, and subsequently, it becomes an aqueous suspension during the evaporation process. When scaling up the formulation volume, the stirring time should be extended appropriately, and the volume of the flask and the mixer also need to be enlarged accordingly to avoid insufficient mixing

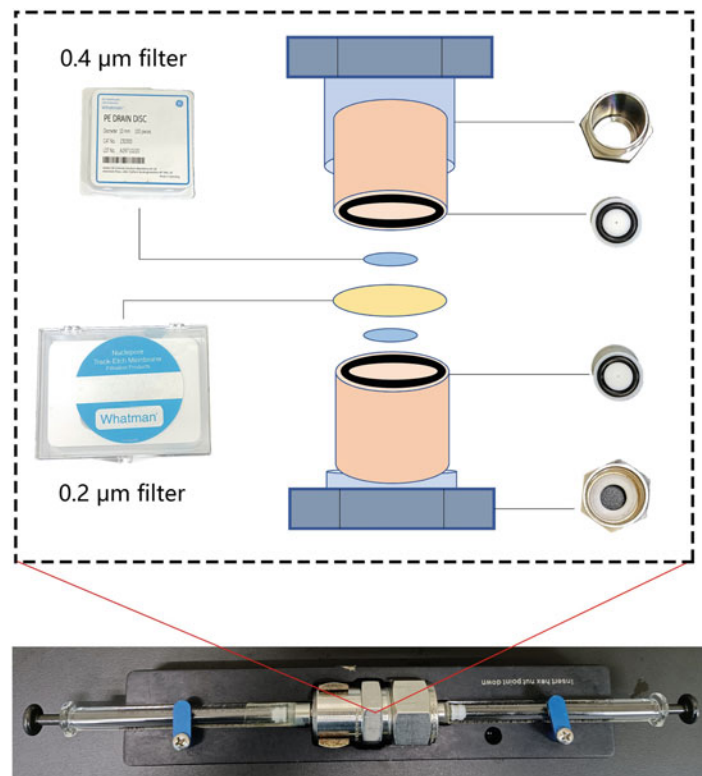


**Fig. 8** Extrusion device for the formulation of liposomes. Note: The emulsion will have greater resistance when extruding through the filter for the first time, and it needs to be extruded slowly to prevent the rupture of the filter membrane in the device

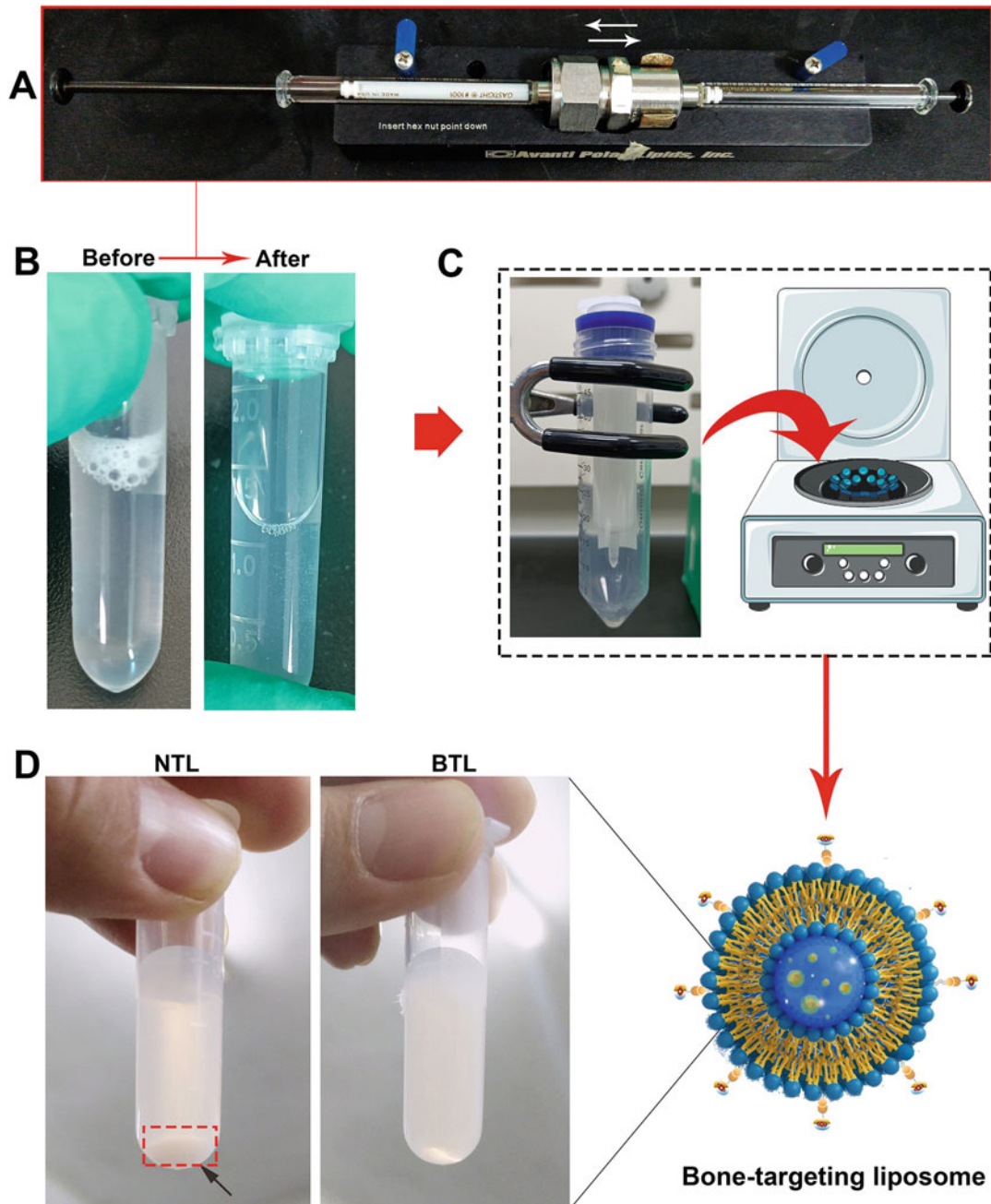


**Fig. 9** (a) Liposome extrusion. (b) The appearance of liposomes before and after extrusion (the liposome is diluted with PBS). The viscosity of the liposome solution decreases, and the solution is more transparent after extrusion. (c) The formulated liposome is purified with a PD-10 column using a spinning protocol to remove the free drug. (d) The appearance of nontargeting liposome (NTL, liposome without pyrophosphorolated cholesterol) and bone-targeting liposome (BTL, liposome with pyrophosphorolated cholesterol) stored 4 °C after 7 days. NTL is found to aggregate with precipitation, while BTL maintains good dispersion

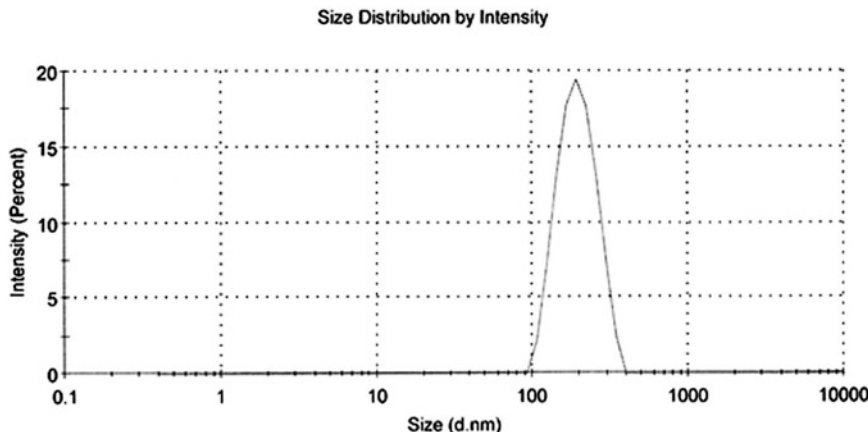


**Fig. 10** Particle size distribution of liposomes after extrusion. After the liposome is extruded through a 0.4  $\mu\text{m}$ /0.2  $\mu\text{m}$  filter, the liposome diameter range can be controlled within 100 ~ 200 nm

3. Fill up the column a fifth time with equilibration buffer and spin down at  $1000 \times g$  for 2 min.
4. Discard the flow-through.

### 3.3.3 Sample Application

1. Add the sample (1.75–2.5 mL) slowly in the middle of the packed bed.

### 3.3.4 Elution

1. Place the PD-10 desalting column into a new 50 mL collection tube.
2. Elute by centrifugation  $1000 \times g$  for 2 min.
3. Collect the eluate.

The purified liposomes are collected for further application.

## 3.4 Characterization of Pyrophosphorylated-Cholesterol-Modified Bone-Targeting Liposomes

### 3.4.1 Liposome Characterization

1. The effective hydrodynamic diameters, the polydispersity index (PDI), and the  $\zeta$ -potential of the formulated liposomes are characterized by Zetasizer Nano ZS90 (Malvern Instruments, Worcestershire, UK).
2. The determination of pyrophosphate content in the pyrophosphorylated-cholesterol-modified liposomes can be determined according to previous publications [1].

## 3.5 Bone-Targeting Property Characterization of the Liposome

### 3.5.1 HA Binding Affinity Test

Bone-targeting properties of pyrophosphorylated-cholesterol-modified liposomes can be evaluated through hyaluronan (HA) binding test *in vitro* and histological analysis *in vivo*.

Different fluorescent dyes can be incorporated into the pyrophosphorylated-cholesterol-modified liposomes. Water-soluble dyes (e.g., Rhodamine B) can be encapsulated in the core

of the liposome, and hydrophobic dyes (e.g., cholesterol-fluorescein-5-isothiocyanate (FITC)) can be inserted into the lipid membrane.

(1) *Rhodamine B-Labeled Pyrophosphorylated-Cholesterol-Modified Liposome Formulation.*

1. Lecithin (40 mg), cholesterol (10 mg), and cholesterol-PPi (7 mg) are dissolved in a 6 mL DCM in a round-bottomed flask to form a mixed lipid solution.
2. Rhodamine B (1.5 mg) is dissolved in 1 mL PBS, and the rhodamine B solution is added to the mixed lipid solution.
3. The mixture is stirred at 1500 rpm/min for 10 min. The following liposome formulation steps are the same as described above.
4. Nontargeting liposomes (NTLs) are prepared using only cholesterol without cholesterol-PPi as a negative control.

(2) *FITC-Labeled Pyrophosphorylated-Cholesterol-Modified Liposome Formulation.*

1. Lecithin (40 mg), cholesterol (10 mg), cholesterol-PPi (7 mg), and cholesterol-FITC (0.5 mg) are dissolved in a 6 mL DCM in a round-bottomed flask to form a mixed lipid solution.
2. One milliliter of PBS solution is added to the mixed lipid solution.
3. The mixture is stirred at 1500 rpm/min for 10 min. The following liposome formulation steps are the same as described above.
4. Nontargeting liposomes are prepared using only cholesterol without cholesterol-PPi as a negative control.

(3) *HA Binding Test.*

1. Fluorescent-labeled liposomes (rhodamine B/FITC-labeled liposome, 5 mL), including liposomes with/without pyrophosphorylated cholesterol, are transferred into 50 mL centrifugation tubes.
2. HA powders (12.5 mg) are added to each sample respectively. The mixtures are then gently shaken for 2 h at 37 °C.
3. After centrifugation at 1000 rpm for 3 min, HA powders are washed at least three times with double distilled (DD) water.
4. The HA powder suspensions are dropped on a slice and evaluated through a fluorescent imaging system (for example, IVIS system or fluorescent microscope or other fluorescent imaging systems) (Fig. 11).

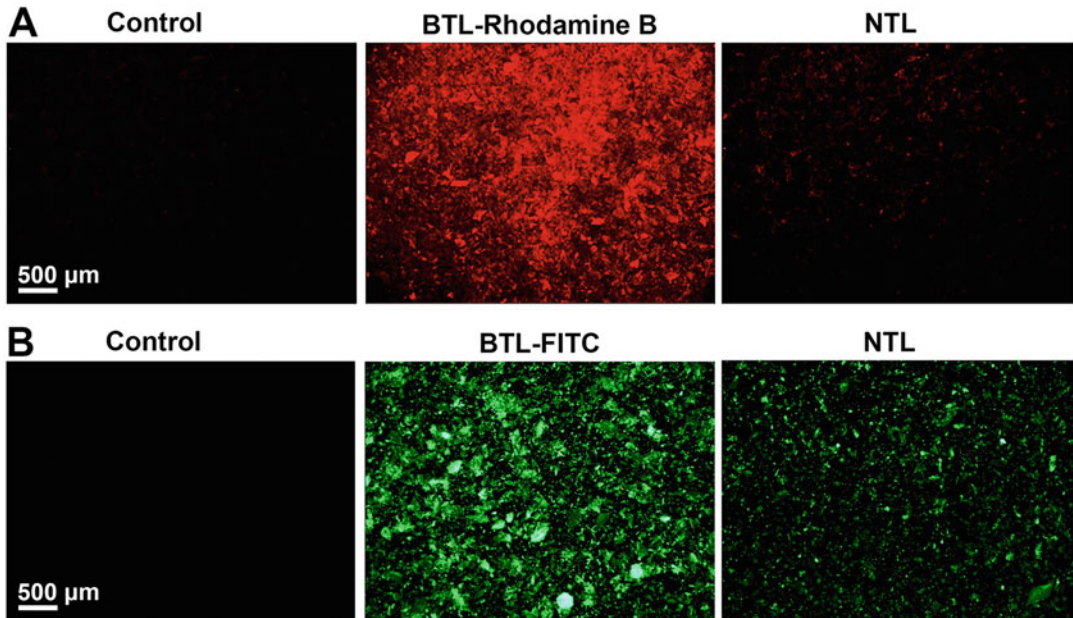


**Fig. 11** (a) Rhodamine B is encapsulated in the core of BTL liposomes and incubated with HA powders for HA binding affinity test. (b). The hydrophobic dyes (cholesterol-FITC) are inserted into the lipid membrane of the liposome and incubated with HA powders for HA binding affinity test. The nontargeting liposome (NTL, liposome without pyrophosphorylated cholesterol) demonstrated weak HA binding affinity, while the bone-targeting liposome (BTL, liposome with pyrophosphorylated cholesterol) revealed strong HA binding affinity. Rhodamine B and FITC solutions are used as control

### 3.5.2 Bone-Targeting Test In Vivo

#### (1) Fluorescent-Labeled Liposome Formulation.

Different fluorescent dyes can be incorporated into the pyrophosphorylated-cholesterol-modified liposomes. The water-soluble near-infrared fluorescent dyes (e.g., IRDye 800CW or Cy5.5) can be encapsulated in the core of the liposome to prepare fluorescent liposomes.

1. Lecithin (60 mg), cholesterol (15 mg), and cholesterol-PPI (10.5 mg) are dissolved in a 9 mL DCM in a round-bottomed flask to form a mixed lipid solution.
2. Cy5.5 (0.15 mg)/IRDye 800CW (0.3 mg) dissolved in a 1 mL PBS and the Cy5.5/IRDye 800CW solution are added to the mixed lipid solution.
3. The mixture is stirred at 1500 rpm/min for 10 min. The following liposome formulation steps are the same as described above.

#### (2) Liposome Distribution Test.

1. To evaluate the potential binding of pyrophosphorylated-cholesterol-modified liposomes to the hard tissue in vivo, fluorescent-labeled liposomes, including BTL and NTL

(Cy5.5 0.15 mg/mL or IRDye 800CW 0.3 mg/mL), are intravenously injected in 12-week-old CD-1 mice (1 uL/g mouse body weight) for in vivo bone-targeting evaluation.

2. Twenty-four/forty-eight/seventy-two hours after injection, the major organs (including, tibia, femur, lung, liver, kidney, and spleen) are collected for evaluating liposome accumulation through a fluorescent imaging system (for example, IVIS system or other fluorescent imaging systems).

**(3) Liposome Bone-Targeting Test.**

1. To evaluate the potential binding of pyrophosphorylated-cholesterol-modified liposomes to the hard tissue in vivo, a fluorescent-labeled liposome (rhodamine B 1.5 mg/mL or cholesterol-FITC 0.5 mg/mL) is locally injected to fracture the femur/intact femur of young CD-1 mice (1 uL/g mouse body weight) for in vivo bone-targeting evaluation. Calcein (10 mg/kg mouse body weight) or xylenol orange (XO, 30 mg/kg mouse body weight) is administered subcutaneously in the mice 1 day prior to liposome injection. It is better to use young mice aged <3 weeks because the bones of young mice are easy to perform cryosections (10 µm) on.
2. Twenty-four hours after injection, femur samples were collected for cryosections (10 µm). The cryosections of the distal femur and fracture femur region are imaged using a fluorescent microscope or confocal microscopy (Figs. 12 and 13).

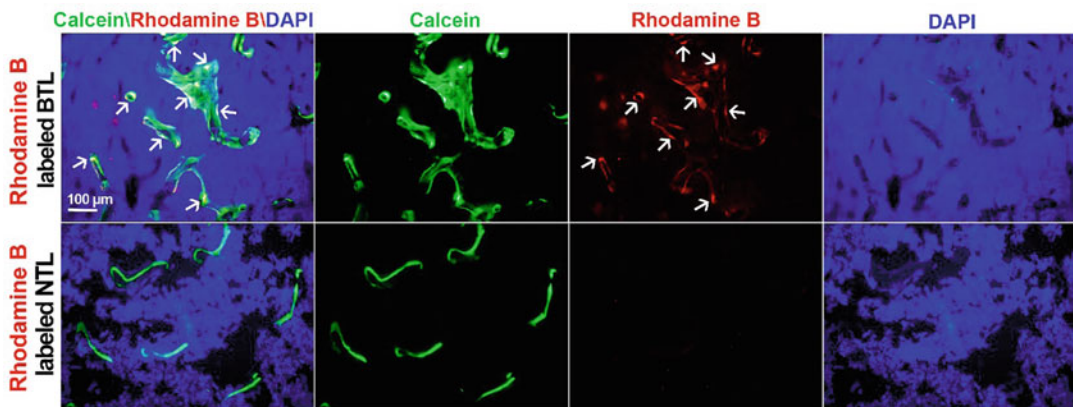


**Fig. 12** Rhodamine B-labeled BTL/NTL liposomes are locally injected into the femur of mice (rhodamine B dye is encapsulated in the core of the BTL liposomes). Cryosection images demonstrate that rhodamine B-labeled BTL binds significantly to the bone surface. Calcein is used to label bone formation surfaces

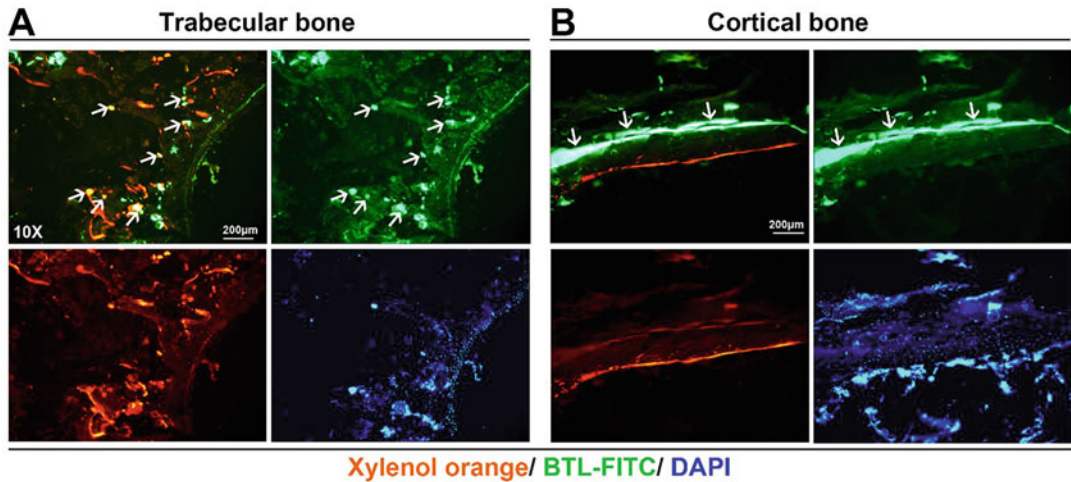


**Fig. 13** FITC-labeled BTL liposomes are locally injected into the femur of mice (liposome surface modified with fluorescent FITC). Cryosection images demonstrate that FITC-labeled BTL binds significantly to the bone surface. Xylenol orange is used to label bone formation surfaces

#### (4) Liposome Retention Test.

1. To further monitor the retention of pyrophosphorylated-cholesterol-modified liposomes, fluorescent-labeled liposomes, including BTL and NTL (Cy5.5 0.15 mg/mL or IRDye 800CW 0.3 mg/mL), are locally injected into the fractured femur/intact femur of 12-week-old CD-1 mice (1  $\mu$ L/g mouse body weight) for in vivo bone-targeting evaluation.
2. After liposome formulation, a live animal fluorescent imaging system is used to monitor the retention and distribution of the liposomes in mice to evaluate liposome accumulation (for example, IVIS system or other fluorescent imaging systems).

---

## 4 Prospects of Application

Previous research demonstrated that pyrophosphorylated-cholesterol-modified bone-targeting liposomes are capable of loading hydrophilic drugs. Salvianic acid A loaded pyrophosphorylated-cholesterol-modified bone-targeting liposomes can accelerate the healing of delayed fracture union in mice [3] and promote the bone healing of nonunion in rabbits [9]. The results support pyrophosphorylated cholesterol modified bone-targeting liposome formulation as a promising drug delivery system. It may be further extrapolated to the utility of other bone anabolic agents for clinical management of different bone diseases.

## 5 Notes

1. A further increase in DCM may help improve liposome extrusion.
2. Increasing the stirring time does not help improve drug encapsulation efficacy. And oxidable drugs need to be protected with inert gas during the stirring process.
3. In order to reduce the extrusion resistance of liposome formulation, sonication can be used to induce large-size liposomes and reduce extrusion resistance. After a rotary evaporation process, liposomes will lose a part of their liquid volume. PBS can be added to liposomes to supplement the liquid volume for extrusion.
4. In the column equilibration step of liposome purification with a PD-10 column, about 25 mL equilibration buffer should be used in total for all three steps. LabMate PD-10 Buffer Reservoir can be used for more convenient equilibration (allows the loading of a total of 25 mL buffer at the same time).

## References

1. Chen F, Jia Z, Rice KC et al (2013) The development of dentotropic micelles with biodegradable tooth-binding moieties. *Pharm Res* 30: 2808–2817
2. Huang L, Wang X, Cao H et al (2018) A bone-targeting delivery system carrying osteogenic phytomolecule icaritin prevents osteoporosis in mice. *Biomaterials* 182:58–71
3. Liu Y, Jia Z, Akhter MP et al (2018) Bone-targeting liposome formulation of Salvianic acid a accelerates the healing of delayed fracture Union in Mice. *Nanomedicine* 14:2271–2282
4. Rotman SG, Grijpma DW, Richards RG et al (2018) Drug delivery systems functionalized with bone mineral seeking agents for bone targeted therapeutics. *J Control Release* 269:88–99
5. Sun S, Tao J, Sedghizadeh PP et al (2021) Bisphosphonates for delivering drugs to bone. *Br J Pharmacol* 178:2008–2025
6. Wang D, Miller S, Sima M et al (2003) Synthesis and evaluation of water-soluble polymeric bone-targeted drug delivery systems. *Bioconjug Chem* 14:853–859
7. Wang D, Miller SC, Kopeckova P et al (2005) Bone-targeting macromolecular therapeutics. *Adv Drug Deliv Rev* 57:1049–1076
8. Xie Y, Liu C, Huang H et al (2018) Bone-targeted delivery of simvastatin-loaded PEG-PLGA micelles conjugated with tetracycline for osteoporosis treatment. *Drug Deliv Transl Res* 8:1090–1102
9. Zhou L, Wu H, Gao X et al (2020) Bone-targeting liposome-encapsulated Salvianic acid a improves nonunion healing through the regulation of HDAC3-mediated endochondral ossification. *Drug Des Devel Ther* 14:3519–3533



# Chapter 19

## Method of Simultaneous Analysis of Liposome Components Using HPTLC/FID

Sophia Hatziantoniou and Costas Demetzos

### Abstract

Liposomes are composed of different kinds of lipids or lipophilic substances and are used as carriers of bioactive molecules. The characterization of the prepared liposomes consists of the calculation of the drug-to-lipid-molar ratio by measuring the lipids and the encapsulated molecule.

The present work describes an analytical methodology for the simultaneous determination of all the lipid ingredients of liposome formulation using thin-layer chromatography coupled with a flame ionization detector (TLC/FID), employing the least possible sample quantity. The method consists of the chromatographic separation of the liposomal ingredients on silica gel scintillated on quartz rods and the subsequent detection of the ingredients by scanning the rods through hydrogen flame. The produced ions are detected by a flame ionization detector, and the signal is converted to a chromatogram.

This method may be applied at every step of the liposome preparation for examining the quality of the raw materials, tracking possible errors in the preparation procedure, and finally analyzing the content of the final liposomal composition.

**Key words** Liposome, Lipid analysis, Drug/lipid ratio, Drug loading, HPTLC/FID

---

### 1 Introduction

Liposome technology is widely applied to both pharmaceutical and cosmetic formulations. Liposomes are used as a suitable vehicle for bioactive molecules in order to overcome their poor water solubility or their possible undesired side effects on normal cells [1, 2]. The main component of the lipid bilayers of the liposomes are acyl-phosphatidylcholines of natural or synthetic origin. Other lipid substances, such as cholesterol or charged lipids, may be used in order to give the desired performance to the liposomal formulation [3].

The characterization of liposomes requires the calculation of drug-to-lipid ratio, measuring the amount of the encapsulated active ingredient as well as all the used components [4].

In the present work, we describe a method of simultaneous determination of all the liposomal ingredients using thin-layer chromatography coupled with a flame ionization detector (TLC/FID) [2, 5, 6]. The sample ingredients are separated on reusable silica-coated quartz rods using the classical thin-layer chromatography techniques and subsequently analyzed by passing through a flame ionization detector. The flame of the burner is generated by an external hydrogen supply and atmospheric oxygen, which is supplied by the air pump that is incorporated into the instrument. The procedure requires only one measurement per sample, and it can be applied even in very small or much-diluted samples. The speed of analysis and the ability to assess many samples at the same time make this method suitable for routine. This method may find application to the assessment of liposomal formulations, the quality control of raw materials, and the preparation procedure.

---

## 2 Materials

### 2.1 *Liposomal Sample Lyophilization*

Screwed cup glass vials of 5 mL capacity.  
Parafilm.

### 2.2 *Sample Preparation*

Pasteur pipettes.  
Cotton wool.

### 2.3 *Sample Spotting*

Chromarods-III.  
Glass syringe of 1  $\mu$ L capacity.

### 2.4 *Sample Development*

Development tank.

The following solvent mixture of analytical grade have been used for liposome component separation:

- Chloroform/methanol/d-Water 45:25:5 (v/v) [7, 8] (*see Note 1*).
- Iatroskan<sup>new</sup>MK-5 (Iatron Laboratories, INC. Tokyo, Japan).
- Lipids and bioactive components of analytical grade for the preparation of standard solutions at concentrations similar to that of the samples.

---

### 3 Methods

#### 3.1 Liposomal Sample Lyophilization

1. Prepare 500 µL aliquots of each liposome sample in screwed cup glass vials of 5 mL capacity.
2. Cover the vials with parafilm and pierce it with a needle to create thin holes.
3. Freeze the samples (*see Note 2*) and place them in the freeze-drier overnight [9].
4. Place the cups on the vials and store at 4 °C until use.

#### 3.2 Sample Preparation

1. Dilute the freeze-dried residue in chloroform or other suitable solvent mixtures.
2. Filter the samples through cotton filters in order to remove the sugars used as cryoprotectants or the salts of the buffers used [1] (*see Note 3*).
3. Wash the residue on the cotton filter with 1 mL chloroform twice and add the filtrates.
4. Remove the chloroform under nitrogen stream.
5. Weigh the residue and add a proper volume of chloroform (*see Note 4*) to a final concentration of about 20 mg/mL.

#### 3.3 Sample Spotting

1. Run a blank scan to ensure that the Chromarods-III are clean.
2. Using a glass syringe of 1 µL capacity, spot 1 µL of the sample solutions on the zero point of the Chromarods-III (*see Note 5*). Apply the sample on two to three Chromarods-III to calculate the mean area of three measurements.
3. Use the last Chromarod-III for corresponding standards at concentrations similar to the samples.

#### 3.4 Sample Development

1. Line the rear side of the development tank with a piece of filter paper.
2. Pour the mobile phase (60–70 mL of solvent mixture) into the development tank and cover it with its glass lid (*see Note 1*).
3. Gently move the tank to wet the filter paper lining and allow the tank to saturate with solvent vapor (*see Note 6*).
4. Place the rod holder in the development tank and leave it until the solvent mixture front reaches the desired height (*see Note 7*).
5. Remove the rod holder from the development tank and allow the excessive solvent to drain.
6. Hold the rod holder under a stream of hot air for 1 min to completely remove the solvent residue (*see Note 8*).

**3.5 Sample Scanning**

1. Place the rod holder in the scanning frame.
2. Scan the Chromarods-III at the following conditions: scanning speed 30 s/scan, airflow 2000 L/h, and hydrogen flow 160 mL/min.

**3.6 Calibration Curve**

1. Prepare standard solutions for each component of the sample at a concentration that is about 2-fold higher from the theoretical.
2. Spot gradually increasing volumes of the standard solution from 0.2 to 1  $\mu$ L using two rods per volume.
3. Place the rod holder into the development chamber and follow steps 4–6 of “Sample Development” (see Subheading 3.4).
4. Scan the rods and obtain the chromatogram.
5. Calculate the calibration curve, plotting the area under the peak against the ingredient’s quantity.

**3.7 Qualitative and Quantitative Analysis**

1. After obtaining the chromatogram of the sample, identify each peak, comparing the retention time to that of the corresponding standard. An example of the chromatogram is shown in Fig. 1.
2. Calculate the content of each component using the peak area (area under the curve (AUC)) of the unknown and the corresponding calibration curve.

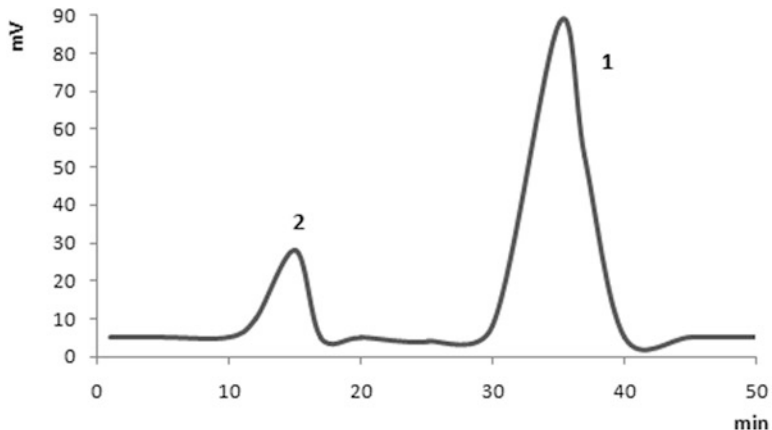


**Fig. 1** Chromatogram of a liposomal formulation containing phosphatidylcholine (1) and bioactive molecule (2). The separation of the liposomal ingredients was achieved using the multiple development technique. The two subsequent mobile phases were (a)  $\text{CHCl}_3/\text{CH}_3\text{OH}/\text{d-H}_2\text{O}$  45:25:5 (v/v) up to 5 cm (50% of the Chromarod-III) and (b) hexane/diethyl ether 40:60 (v/v) up to 10 cm (100% of the Chromarod-III). After the separation of the ingredients and the elimination of the solvent vapor, the Chromarods-III were scanned at the following conditions: scanning speed 30 s/scan, airflow 2000 L/h, and hydrogen flow 160 mL/min

---

## 4 Notes

1. For the enhancement of the component separation, several solvent mixtures should be tried. The best technique suggested is the multiple development method, in which two successive mobile phases are used: at first, the samples are allowed to develop until 5 cm from zero point (50% of the rods) in chloroform/methanol/d-Water 45:25:5 (v/v) in order to separate the phospholipids [2, 5, 6]. Subsequently, the solvent is removed under a hot air stream, and the samples are placed in the second development tank containing either hexane/diethyl ether/glacial acetic acid 80:20:2 (v/v) or hexane/diethyl ether 40:60 (v/v) until 10 cm (100% of the rods) for the separation of nonpolar components from the phospholipids.
2. Place the samples in a deep freezer for 20 min or immerse them in a dry ice/isobutanol bath until frozen.
3. Place cotton wool in Pasteur pipettes, creating cotton filters of 1 cm height. Wash them with 1 mL chloroform twice.
4. The appropriate solvent selection is based on the sufficient solubility of the sample components. The solvent with the lowest boiling point and polarity is preferred in order to produce narrow spots.
5. Hold the syringe in such a way as to avoid scratching the silica surface, allowing the sample drop to touch the surface of the Chromarod-III. The sample volume should be placed in small aliquots to produce a narrow spot. The sample spot should be as narrow as possible (less than 3 mm) to ensure good separation performance.
6. Wet the filter paper with solvent immediately before starting the development in order to ensure complete solvent vapor saturation.
7. Do not allow the solvent front to exceed 100 cm from zero point because some separated components may be out of the scanning area.
8. If the solvent is not completely removed, the signal will have noise and the results will not be reproducible.

## References

1. Hatziantoniou S, Dimas K, Georgopoulos A, Sotiriadou N, Demetzos C (2006) Cytotoxic and antitumor activity of liposome-incorporated sclareol against cancer cell lines and human colon cancer xenografts. *Pharmacol Res* 53(1): 80–87
2. Goniotaki M, Hatziantoniou S, Dimas K, Wagner M, Demetzos C (2004) Encapsulation of naturally occurring flavonoids into liposomes: physicochemical properties and biological activity against human cancer cell lines. *J Pharm Pharmacol* 56(10):1217–1224

3. Gabizon A, Papahadjopoulos D (1988) Liposomes formulations with prolonged circulation time in blood and enhanced uptake by tumors. *Proc Natl Acad Sci USA* 85:6949–6953
4. Fan Y, Marioli M, Zhang K (2021) Analytical characterization of liposomes and other lipid nanoparticles for drug delivery. *J Pharm Biomed Anal* 192:113642. <https://doi.org/10.1016/j.jpba.2020.113642>
5. Hatziantoniou S, Demetzos C (2006) Qualitative and quantitative one step analysis of lipids and encapsulated bioactive molecules in liposome preparations by HPTLC/FID (Iatroskan). *J Liposome Res* 16(4):321–330
6. Kaourma E, Hatziantoniou S, Georgopoulos A, Kolocouris A, Demetzos C (2005) Development of simple thiol-reactive liposome formulations, one-step analysis and physico-chemical characterization. *J Pharm Pharmacol* 57(4):527–531
7. Henderson JR, Tocher DR (1992) Thin-layer chromatography. In: Hamilton RJ, Hamilton S (eds) *Lipid analysis: a practical approach*. Oxford University Press, Oxford, pp 100–108
8. De Schrijver R, Vermeulen D (1991) Separation and quantitation of phospholipids in animal tissues Iatroskan TLC/FID. *Lipids* 26(1):74–76
9. Madden TD, Boman N (1999) Lyophilization of liposomes in liposomes rational design (ed. Janoff S). Marcel Dekker, New York, pp 261–282



# Chapter 20

## High-Performance Liquid Chromatography Coupled with Tandem Mass Spectrometry Method for the Identification and Quantification of Lipids in Liposomes

Yujie Shi and Xiaona Li

### Abstract

Liposomes are spherical, closed vesicles consisting of at least one lipid bilayer with a water chamber and are widely used to encapsulate bioactive molecules. Lipid membranes, composed of different types of lipids or lipophilic components, determine whether liposomes can achieve the desired purpose and determine the overall quality of liposomes. Thus, the quantification of lipid components and encapsulated molecules is essential to characterize and control the quality of liposomes. Moreover, multicomponent simultaneous determination is the preferred method for lipid component analysis in liposomes. Therefore, the present work describes an analytical methodology for the simultaneous determination of commonly used lipids in liposome formulations, using high-performance liquid chromatography coupled with a tandem mass spectrometry (MS) detector (HPLC-MS/MS). HPLC-MS/MS consists of a rapid and highly efficient chromatographic separation of the liposomal components with a C18 column and the subsequent detection of the ingredients through an MS detector, along with an accurate mass fragmentation pattern. The analytical process mainly includes lipid extraction, solution preparation, the optimization of chromatographic conditions, and method validation. We hope this analytical methodology is valuable and efficient and can be applied to the analysis of multiple types of lipids in liposomes, such as raw material quality analysis, formulation study, overall quality control, etc.

**Key words** Liposome, Lipid analysis, HPLC-MS/MS

---

### 1 Introduction

Liposomes (LPs) are closed spherical vesicles consisting of at least one lipid bilayer with an aqueous inner compartment [1]. Liposomes can encapsulate hydrophobic and hydrophilic compounds in between lipid membranes and the core [2]. At present, liposome technology is widely used to simulate membranes, control drug release, achieve drug-targeted delivery, make skin and cosmetics matrices, transport biological macromolecules such as genes into cells, etc. Usually, liposome formulations contain four main chemical components: drugs or other active ingredients, lipids,

polyethylene glycol (PEG)-lipids, and nonlipid inactive components (such as buffer components) [3]. Among them, lipids are very important for liposomes. Lipids constitute lipid membranes of liposomes, which determine whether liposomes can achieve the desired purpose and the overall quality of liposomes.

A common component of the liposome lipid bilayer is acylphosphatidylcholine of natural or synthetic origin, which can be incorporated into other lipids, such as cholesterol or charged lipids, to give the liposome preparation the required properties. Phosphatidylcholine (PC) is the most common neutral phospholipid and the main component of liposomes. Synthetic PCs include dipalmitoylphosphatidylcholine (DPPC), distearoylphosphatidylcholine (DSPC), and dimyristoylphosphatidylcholine (DMPC), as well as other common neutral phospholipids. Phosphatidylethanolamine (PE) is also widely used in liposomes [4–6]. In addition, phosphatidylglycerol (PG), phosphatidic acid (PA), phosphatidylinositol (PI), phosphatidylserine (PS), etc. belong to anionic lipids commonly used in drug delivery formulations [7, 8]. Furthermore, cationic lipids, such as 1,2-dioleoyl-3-trimethylammonium-propane (DOTAP), 1,2-di-O-octadecenyl-3-trimethylammonium-propane (DOTMA), 2,3-dioleyloxy-N-[2-(sperminecarboxamido)ethyl]-N,N-dimethyl-1-propanaminium trifluoroacetate (DOSPA), and cholesterol derivatives, have attracted more and more attention for their usage in encapsulating nucleic acids and peptides [9]. Different from these lipids, cholesterol, a neutral lipid, plays a strategic role in liposomes and could influence membrane stability and regulate the fluidity and permeability of liposome membranes [10, 11]. Furthermore, lipid characteristics have an impact on delivery efficiency, loading capacity, pharmacological and toxicological properties, overall quality of liposomes, etc. [12]. The composition of the lipid membrane of liposomes also determines the liposome's particle size distribution, zeta potential, physical stability, and drug release mechanism [4, 13]. Thus, the molar ratio of drug to lipid is usually calculated to characterize the prepared liposomes. In addition, the lipid content of commercially available liposomes needs to be evaluated for approval by the Food and Drug Administration (FDA) [14]. Therefore, the quantification of lipids in liposomes is of great significance.

Chromatographic methods are preferred for lipid analysis because they can simultaneously separate and quantify a number of lipids. Initially, thin-layer chromatography coupled with a flame ionization detector (HPTLC/FID) was widely used for the simultaneous analysis of almost all the liposomal ingredients [15–17]. But due to its unsatisfactory resolution, reproducibility, and sensitivity, it has been gradually replaced by **high-performance liquid chromatography** (HPLC) in recent years. HPLC coupled with an ultraviolet-visible (UV-vis) detector or diode array detector (DAD) can be used to analyze unsaturated lipids [18, 19]. But these lipids usually absorb at the terminal absorption wavelength,

such as 200–210 nM, which limits the choice of solvents to minimize spectral interference. Furthermore, most lipids lack chromophores [20]. Therefore, this method is not universal in lipid analysis. Excitingly, methods of HPLC coupled with universal detectors, such as evaporative light scattering detectors (ELSDs), charged aerosol detectors (CADs), and mass spectrometry (MS), are preferred for multiple lipid component analysis, especially for the simultaneous detection of phospholipids and degradation products. HPLC-CAD is suitable for the quantitation of most common lipids, except for some volatile lipids, such as short-chain free fatty acids. No complex lipid extraction or derivatization is required in this method. But as a new detection method, HPLC-CAD is not used much at present. HPLC-ELSD is a rapid, economical, and sensitive method for the simultaneous quantification of the lipids of liposome formulations, with or without the need for lipid extraction processes. Although various HPLC-ELSD methods have been used for lipid quantitation in liposomal formulations, the use of lipid content as part of routine characterization studies of liposomes is not common [21]. Notably, HPLC-MS/MS is very powerful for obtaining the structure information of liposome formulations, the quantitative determination of phospholipid degradation products or cholesterol oxidation products, etc. [22–25], and its application in lipid analysis is gradually increasing.

In the present work, we take the most used lipid components in liposome formulations as examples and describe a method of measuring multiple liposomal ingredients simultaneously using HPLC-MS/MS. The lipids are separated with a C18 column and subsequently analyzed by an MS detector. As shown in Fig. 1, the method mainly includes stock solution and working solution preparation, lipid extraction, the optimization of MS and LC conditions, method validation, and sample analysis. The ability to assess many samples simultaneously makes this method suitable for the analysis of the lipid composition of lab-prepared liposomes, the interbatch variance analysis of liposomes, etc.

---

## 2 Materials

All solvents and additives are of LC-MS grade. Water is prepared using an ultrapure water system (resistivity of 18 MΩ·cm at –25 °C). All standards of lipids (including distearoylphosphatidyl-choline (DSPC), cholesterol, and 1,2-dimyristoyl-rac-glycero-3-methoxypolyethylene glycol-2000 (DMG-PEG2000), etc.) in liposomes are of LC grade or reference grade (purity≥98%). Pharmaceutics formulations (PFs) are obtained from the laboratory or vendors. All products are stored at appropriate temperatures.

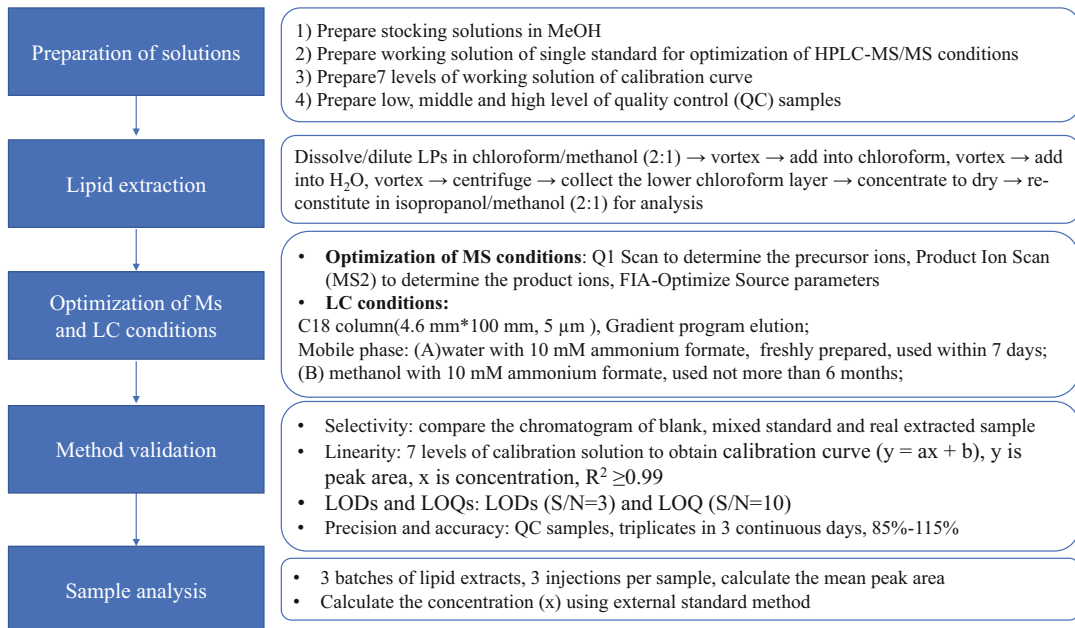


**Fig. 1** Overview scheme of lipid analysis using the HPLC-MS/MS system

## 2.1 Lipid Extraction

1. Chloroform (CHCl<sub>3</sub>), methanol (MeOH), and isopropanol, LC-MS grade.
2. Water (H<sub>2</sub>O), LC-MS grade.
3. Centrifuge tube, 15 mL.
4. Vortexer.
5. Centrifuge.
6. Vacuum concentrator.
7. Pipettes (Eppendorf).

## 2.2 Preparation of Stock and Working Solution

1. MeOH, LC grade.
2. H<sub>2</sub>O, LC grade.
3. Electronic balance.
4. Volumetric flasks, 5 mL and 10 mL.
5. 1.0 mg/mL stock solutions of each lipid ingredient standard in methanol [26]: distearoylphosphatidylcholine (DSPC), cholesterol, DMG-PEG2000, etc. (see Note 1).

Add 10.0 mg DSPC, cholesterol, DMG-PEG2000, or other lipid into a 10 mL volumetric flask, dissolve and dilute with methanol to volume to prepare standard stock solution with a concentration of 1.0 mg/mL, respectively.

6. 1.0 μg/mL standard solutions (for precursor ion optimization): prepared by dilution 1000 times of each 1.0 mg/mL stock solution, respectively. Pipette 1.0 mg/mL stock solution 50 μL to a 5 mL volumetric flask and make up to volume

with methanol to obtain a 10.0 µg/mL standard solution; then pipette 200 µL of the obtained 10.0 µg/mL standard solution into a 2 mL volumetric flask, dilute to volume with methanol to obtain 1.0 µg/mL standard solution, respectively.

7. A series of mixed standard calibration solutions (including 7 levels): Diluted from all standard stock solutions with the initial mobile phase to a series of volumetric flasks. Taking DSPC as an example, the final concentration of DSPC standard in each mixed calibration solution is 2, 10, 25, 50, 100, 250, and 500 ng/mL, respectively. The final concentration of each lipid ingredient is different (*see Notes 2 and 3*).
8. Quality control (QC) samples are prepared at low, middle, and high concentrations of the calibration standard mixture (triplicates of each concentration). Taking DSPC as an example, 5, 125, and 400 ng/mL are the low, middle, and high concentrations. The final concentration of each lipid ingredient is different (*see Note 4*).

All solutions are stored at room temperature.

### **2.3 HPLC-MS/MS Analysis**

1. MeOH, LC-MS grade.
2. Water, LC-MS grade.
3. Ammonium formate, LC-MS grade.
4. Mobile phase A: 10 mM ammonium formate in 100% water.
5. Mobile phase B: 10 mM ammonium formate in 100% methanol (*see Note 5*).
6. Filter membrane, 0.45 µm (*see Note 5*).
7. C18 column (100 mM length \* 4.6 mM i.d., particle size 3 µm) (*see Note 6*).
8. An ultra-high-performance liquid chromatography (UHPLC) system (Shimadzu LC-20A Prominence UFC system, SPD-20A, LC-20 AD, CBM-20A): a binary or quaternary pump, degasser, column oven, and autosampler.
9. AB Sciex API 4000 LC-MS/MS Triple Quad Mass Spectrometer (Applied Biosystems Sciex, CA, USA).

### **2.4 Data Acquisition and Analysis**

1. Analyst® 1.5.1 software.

---

## **3 Methods**

### **3.1 Lipid Extraction**

1. Liposomes (~50 µL or ~ 10 mg) are dissolved or diluted in 0.75 mL of chloroform/methanol (v/v, 2:1) and vortexed using a vortex mixer for 10 min.

2. The mixture is added to 0.2 mL of chloroform and vortexed for 2 min, and then add 0.25 mL of water and vortex for 5 min.
3. After centrifugation at 14,000 rpm for 10 min, three clear layers are obtained, the MeOH and aqueous layer on the top, a thin solid layer at the interface between the water and chloroform, and the lower chloroform layer.
4. Collect the lower chloroform layer, then evaporate it using a vacuum concentrator or high purity of nitrogen gas flow at room temperature.
5. The residues (lipid film) are reconstituted in 1.0 mL of isopropanol/methanol (v/v, 2:1).
6. Sonicate the reconstitution solution for 10 min and centrifuge for 10 min at 15,000 rpm under 4 °C.
7. Transfer the resulting supernatant to a fresh vial and store at 4 °C.
8. Prior to injection, the sample solution was diluted 1000 times with methanol, and 1.0 mL of the diluent was transferred to an HPLC glass vial for subsequent HPLC-MS/MS analysis (*see Note 7*).

### **3.2 Optimization of MS Conditions**

MS analyses were performed in a positive electrospray ionization mode (ESI). Data acquisition and processing were performed using AB SCIEX Analyst 1.5.1 software.

#### **3.2.1 Q1 Scan to Determine the Mass-to-Charge Ratio of Precursor Ions**

1. After entering the Analyst software, click “Hardware Configuration” to enter the system, select “MS-only”, and click the “Activate Profile” to enter the mass spectrometry operation interface.
2. Click “Manual Tuning” under the “Tune and Calibrate.” Then select the “Q1 MS (Q1)” scan type, recommend setting the scan range start from 100 Da to (MW + 30) Da,  $t = 1\text{--}2\text{ s}$ , and set “Center Width” at MW  $\pm 5\text{ Da}$ ,  $t = 0.5\text{ s}$ .
3. Perform Q1 scan via the flow injection of 1.0  $\mu\text{g}/\text{mL}$  standard solution in positive and negative ion modes separately to determine the mass-to-charge ratio of precursor ions. The flow rate is 0.01 mL/min.
4. Ionization polarity is determined by comparing the precursor ion intensities detected in the positive and negative ion modes, and the condition with higher precursor ion intensity is selected for subsequent detection. Ultimately, the positive ion mode is chosen for the analysis of DSPC, cholesterol, DMG-PEG2000, etc. (*see Note 8*).
5. The precursor ions of DSPC, cholesterol, and DMG-PEG2000 are 790.5, 402.4, and 642.7, respectively, corresponding to their  $M + H$ ,  $M_{(\text{isotope})} + H$ , and  $M_{(\text{Structural Fragments})} + H$  ions (*see Notes 9 and 10*).

### *3.2.2 Product Ion Scan (MS2) to Determine the Mass-to-Charge Ratio of Product Ions*

1. Select “Product Ion(MS2)” scan type, recommend setting the scan range start from 50 Da to (MW+10) Da,  $t = 1\sim 2$  s. Product ion scan is performed according to the precursor ions determined in the previous step (*see Note 10*).
2. A high-quality MS2 image is obtained. After smoothing, the mass-to-charge ratio of the product ion is selected and determined to be one decimal place. The product ions of the precursor ions of DSPC, cholesterol, and DMG-PEG2000 are 183.9, 240.2, and 607.3, respectively (*see Note 11*).
3. According to the precursor and product ions selected above, by clicking “Edit Ramp”, optimize the parameters, including the declustering potential (DP) and collision energy (CE) under “Compound”. The optimization results for the ion pairs of DSPC, cholesterol, and DMG-PEG2000 are 790.5 → 183.9 with DP 70 and CE 40, 402.4 → 340.2 with DP 90 and CE 35, and 642.7 → 607.3 with DP 90 and CE 35, respectively (*see Note 12*).

### **3.3 FIA-Optimize Source Parameters**

1. Close all MS interfaces, deactivate the existing mass spectrometry system by clicking “Deactivate Profile”, then select “MS +LC,” click “Activate Profile,” and activate the liquid chromatography and mass spectrometry equipment.
2. Click “Build Acquire Method” in Acquire, open the MS method saved above, and add the equipment: chromatography pump, autosampler, etc.
3. Set chromatographic synchronization.
4. Set the chromatographic parameters. The analysis time is generally 0.6 ~ 1 min, and the composition and flow of the mobile phase are the same as the actual sample analysis. Modify the mass spectrometry analysis time to be consistent with the chromatographic parameters. Save the method, for example, Lipids in LPs FIA-Opt.dam.
5. Under “Tune,” double-click “Quantitative Optimization,” then select FIA analysis and perform automatic optimization according to the wizard. Then MS parameters are optimized at FIA injection mode using direct injection of 1.0  $\mu\text{g}/\text{mL}$  mixed standard solution (without column for lipids separation). The optimized results are collision gas (CAD) 10, curtain gas (CUR) 20 psi, ion spray voltage (IS) 5500, temperature (TEM) 500 °C, ion source gas1 50 psi, ion source gas2 55 psi, and interface heater on (*see Note 13*).

### **3.4 Optimization of Liquid Chromatographic Conditions**

1. Connect and equilibrate the chromatographic column and inject each lipid standard solution (i.e., 500 ng/mL) into the HPLC-MS/MS system.

2. The retention time (RT) of each lipid standard is obtained using a C18 column and the program gradient in “Subheading 3.4.” In this step, the peak shape can be observed through monitoring, and column efficiency (including peak asymmetry factor, tailing factor, and resolution) also can be obtained using equipped instrumental software (*see Note 14*).
3. Based on the chromatographic separation, adjust the LC program gradient and flow rate to acquire a good resolution and good sensitivity in a relatively short running time according to the RTs of different lipids (*see Note 15*).
4. Check the separation of lipids with a mixed standard sample (500 ng/mL). RT is used for the identification of lipid analysis.

### **3.5 The Optimized HPLC Conditions for Lipid Analysis (See Note 15)**

The analysis of lipids is performed using the HPLC system. The separation of analytes is performed using a reversed-phase C18 column (4.6 \* 100 mM, 5 μm).

Mobile phase A: 10 mM ammonium formate in 100% water.

Mobile phase B: 10 mM ammonium formate in 100% methanol.

The gradient program is recommended as follows: 0 min, 50% B, 4 min, 85% B, 16 min, 100% B, 30 min, 100% B, 32 min, 50% B, and 40 min, 50% B.

The flow rate is 0.25 mL/min, column temperature 30 °C, sampler temperature 20 °C, and injection volume 10 μL.

Wash the injection needle before and after injection with the needle-washing solvent MeOH–H<sub>2</sub>O (1:1, v/v).

### **3.6 Analytical Method Validation**

Method validation is carried out according to a series of guidelines, such as the USP 40–NF < 1225 > validation compendial procedures (USP, 2015), the ICH (International Conference on Harmonisation of Technical Requirements for Registration of Pharmaceuticals for Human Use) guidance for the method validation of analytical procedures (ICH, 1996), and FDA’s Guidance for Industry on Bioanalytical Method Validation (FDA, 2018a) [25, 26].

Under each of the following method validation indicators, the operation of the instrument includes the following three steps:

1. Edit the batch files to arrange the injection sequence with the method embedded by Analyst® 1.5.1 software using the LC gradient as described in Subheading 3.4.
  2. Equilibrate the MS ion source and column.
  3. Run batch sequence to acquire LC-MS/MS data.
1. A blank sample and the real sample are prepared by extraction from the pharmaceutic adjuvant without lipids and with lipids according to Subheading 3.2.

#### **3.6.1 Selectivity**

2. The blank sample, mixed standard sample, and real sample (lipid extraction solution) are injected into the HPLC-MS/MS system.

3. According to the chromatograms of blank sample, standard samples and real liposome extraction samples, there should be no interference in chromatogram of blank sample at the same RT of each analyte.

### 3.6.2 Linearity and Range

1. Six or seven levels of calibration solutions are injected into the HPLC system to get integrated peak areas. For DSPC, 2, 10, 25, 50, 100, 250, and 500 ng/mL of standard sample working solutions are selected.
2. Linearity is characterized by a calibrated regression line through a weighted linear regression model. The calibration curve is plotted on the peak area of the analyte against the concentration of the analyte. Concentration ( $x$ ) and peak area ( $y$ ) are used to fit the calibration curve ( $y = ax + b$ ).
3. The linearity range of each analyte covers the sample concentration, with correlation coefficient values ( $R^2$ ) greater than 0.99.

### 3.6.3 The Limit of Detection (LOD) and the Limit of Quantitation (LOQ)

1. The lowest level of calibration solution is diluted into the LOD solution ( $S/N = 3$ ) and/or LOQ solution ( $S/N = 10$ ) with the initial mobile phase and then injected into the HPLC-ELSD system.
2. The sensitivity of the established method is evaluated by the limit of detection (LOD) with a signal-noise ratio ( $S/N \geq 3$ ) and the limit of quantitation (LOQ) with a signal-noise ratio ( $S/N \geq 10$ ).

### 3.6.4 Precision and Accuracy

1. Low, middle, and high concentrations of QC samples ( $n = 3$ ) are injected for analysis over three continuous days. Taking DSPC as an example, 5, 125, and 400 ng/mL are the low, middle, and high concentrations, respectively.
2. Intraday precision and interday precision are calculated as the percentage relative standard deviation (RSD%) of the measured values.
3. Accuracy, defined as recovery, is calculated as the ratio of the measured value (low, middle, and high QC samples, duplicates) of the theoretical value at each concentration.
4. The acceptable precision and accuracy are from 85 to 115% or from 80 to 120% for low concentration.

### 3.6.5 Carryover

Carryover is assessed in a blank sample, which is injected after calibration standard at the upper limit of quantification (ULOQ) (for DSPC, ULOQ is 500 ng/mL). The measurement needs to be repeated at least three times. The response at the retention time of

the lipid in the blank sample should not be greater than 20% of the response in a lower limit of quantification (LLOQ) sample (ULOQ) (for DSPC, LLOQ is 2 ng/mL) (*see Note 16*).

### 3.7 HPLC Analysis of Lipids

1. Lipids of LPs are extracted according to Subheading 3.1.
2. Three batches of extracted lipid samples are prepared from each liposome formulation. The extracted samples are diluted 1000-fold in methanol and used for the injection. Each sample is injected three times to quantify the content of lipids.
3. Obtain the peak areas ( $y$ ) of each lipid using the equipped Analyst<sup>®</sup> 1.5.1 software and calculate the concentration of each lipid ( $x$ ) according to the obtained calibration curve ( $y = ax + b$ ).

---

## 4 Notes

1. Solvents such as ethanol, isopropanol, chloroform-MeOH/isopropanol mixture (1/1, v/v) can be selected to prepare lipid standard stock solutions [27–30].
2. The mixed standard samples should contain all the targeted lipids in the liposomes to be analyzed. These samples are measured together with the liposome extract samples and are also used for peak alignment. Each ingredient's concentration in the mixed standard sample is comprehensively optimized.
3. The standard working solution is prepared and used immediately, especially the lower concentration, which may be reduced due to adsorption and decomposition after a long time.
4. The QC samples also should contain all the targeted lipids in the liposomes to be analyzed. Each ingredient's concentration in the QC sample of low, middle, and high concentrations is determined by the linear range and its concentration in the lipid extract sample. The concentration of the low QC is two- to threefold of that of the lowest concentration of the standard curve; the middle QC is the middle concentration of the standard range, which is about the sample concentration; and the high QC is 70–80% of the highest concentration of the standard curve.
5. Mobile phase A should be freshly prepared and is recommended to be used within 7 days. Mobile phase B is recommended to be used within 6 months. The buffer of 10 mM ammonium formate is recommended to be diluted from a high-concentration solution and filtered by a 0.45 µm nylon filter membrane.

6. Since the main components of liposomes are phospholipids, a reversed-phase column (esp. C18 column) is most frequently used for lipid separation [22].
7. For the quantitation of lipids (such as cholesterol), high-fold dilution (i.e., 1000-fold) is performed using organic solvents, while less-fold dilution (i.e., tenfold) is done for the quantitation of lipid products [25].
8. When using mass spectrometry to detect lipid degradation products, different ionization modes are required for lipids of different properties [24, 25].
9. By changing the DP, observe the increase or decrease in the ions. In the positive mode, focus on searching for  $M + 1$ ,  $M + 18$ ,  $M + 23$ , etc. and preliminarily judge the molecular ions. If they cannot be found, the concentration may be too low or the ionization method is not suitable or the selected solvent system is not suitable.
10. The mass-to-charge ratio of the precursor ion should be accurate to one decimal place.
11. The intensity of the precursor ion is preferably 1/3 to 1/4 of the intensity of the base peak in the spectrum. Make sure that all fragment ions come from the analyte compound, not impurities in the solution, and look for stronger fragment ion information.
12. Each ion is correspondingly set separately. Generally, two optimizations are required to obtain more accurate results. By optimizing the instrument parameters, both parent and product ions reach a certain intensity level so that multireaction monitor (MRM) sensitivity is the highest.
13. Separate optional values that need to be optimized with a semicolon (;).
14. The length of the chromatographic column can be determined according to the requirements of the separation; the qualitative can be longer, and the quantitative can be as short as possible under the condition that the interference can be effectively eliminated so as to improve efficiency; the inner diameter is preferably a small diameter column, such as 2 mM or 1 mM.
15. To optimize HPLC analysis, the components, composition, and gradient program of the mobile phase are optimized for suitable RT and better resolution.
  1. To obtain suitable RT and better resolution, the organic phase ratio, flow rate, or column temperature can be optimized.

2. To avoid or diminish the carryover effect of lipids sticking to the valve groove, the needle of the injector should be washed with sufficient organic solvents (i.e., isopropanol).
16. Carryover should be addressed and minimized during method development.

## References

1. Mehdi Hasan MH, Mondal JC, Al Hasan M, Talukder S, Rashid HA (2017) Liposomes: an advance tools for novel drug delivery system. *Pharma Innov J* 6:304–311
2. Petros RA, DeSimone JM (2010) Strategies in the design of nanoparticles for therapeutic applications. *Nat Rev Drug Discov* 9:615–627
3. Akbarzadeh A, Rezaei-Sababdy R, Davaran S, Joo SW, Zarghami N, Hanifehpour Y et al (2013) Liposome: classification, preparation, and applications. *Nanoscale Res Lett* 8(1):102
4. Soema PC, Willems GJ, Jiskoot W, Amorij JP, Kersten GF (2015) Predicting the influence of liposomal lipid composition on liposome size, zeta potential and liposome-induced dendritic cell maturation using a design of experiments approach. *Eur J Pharm Biopharm* 94:427–435
5. Anderson M, Omri A (2004) The effect of different lipid components on the in vitro stability and release kinetics of liposome formulations. *Drug Deliv* 11:33–39
6. He H, Lu Y, Qi J, Zhu Q, Chen Z, Wu W (2019) Adapting liposomes for oral drug delivery. *Acta Pharm Sin B* 9:36–48
7. Yandrapati RK (2012) Effect of lipid composition on the physical properties of liposomes: a light scattering study. Masters Theses 6864
8. Poelma DL, Ju MR, Bakker SC, Zimmermann LJ, Lachmann BF, van Iwaarden JF (2004) A common pathway for the uptake of surfactant lipids by alveolar cells. *Am J Respir Cell Mol Biol* 30:751–758
9. Ciani L, Casini A, Gabbiani C, Ristori S, Messori L, Martini G (2007) DOTAP/DOPE and DC-Chol/DOPE lipoplexes for gene delivery studied by circular dichroism and other biophysical techniques. *Biophys Chem* 127:213–220
10. Briuglia ML, Rotella C, McFarlane A, Lamprou DA (2015) Influence of cholesterol on liposome stability and on in vitro drug release. *Drug Deliv Transl Res* 5:231–242
11. Kaddah S, Khreich N, Kaddah F, Charcosset C, Greige-Gerges H (2018) Cholesterol modulates the liposome membrane fluidity and permeability for a hydrophilic molecule. *Food Chem Toxicol* 113:40–48
12. Haeri A, Alinaghian B, Daeihamed M, Dadashzadeh S (2014) Preparation and characterization of stable nanoliposomal formulation of fluoxetine as a potential adjuvant therapy for drug-resistant tumors. *Iran J Pharm Res* 13:3–14
13. Caracciolo G, Pozzi D, Capriotti AL, Cavaliere C, Piovesana S, Amenitsch H et al (2015) Lipid composition: a “key factor” for the rational manipulation of the liposome–protein corona by liposome design. *RSC Adv* 5: 5967–5975
14. Liposome drug products – chemistry, manufacturing, and controls; Human pharmacokinetics and bioavailability; and labeling documentation – guidance for industry. 2015
15. Sophia Hatziantoniou CD (2010) Method of simultaneous analysis of liposome components using HPTLC/FID. *Methods Mol Biol* 606: 363–368
16. Sophia Hatziantoniou CD (2017) Method of simultaneous analysis of liposome components using HPTLC/FID. *Methods Mol Biol* 1522: 49–54
17. Hatziantoniou S, Demetzos C (2006) Qualitative and quantitative one-step analysis of lipids and encapsulated bioactive molecules in liposome preparations by HPTLC/FID (IATROS-CAN). *J Liposome Res* 16:321–330
18. Suchocka Z, Gronostajska D, Suchocki P, Pachecka J (2003) New HPLC method for separation of blood plasma phospholipids. *J Pharm Biomed Anal* 32:859–865
19. Singh R, Ajagbe M, Bhamidipati S, Ahmad Z, Ahmad I (2005) A rapid isocratic high-performance liquid chromatography method for determination of cholesterol and 1,2-dioleoyl-sn-glycero-3-phosphocholine in liposome-based drug formulations. *J Chromatogr A* 1073:347–353
20. Hvattum E, Uran S, Sandbaek AG, Karlsson AA, Skotland T (2006) Quantification of phosphatidylserine, phosphatidic acid and free fatty acids in an ultrasound contrast agent by normal-phase high-performance liquid chromatography with evaporative light scattering detection. *J Pharm Biomed Anal* 42:506–512

21. Alsaadi MM, Christine Carter K, Mullen AB (2013) High performance liquid chromatography with evaporative light scattering detection for the characterisation of a vesicular delivery system during stability studies. *J Chromatogr A* 1320:80–85
22. Kothalawala N, Mudalige TK, Sisco P, Linder SW (2018) Novel analytical methods to assess the chemical and physical properties of liposomes. *J Chromatogr B* 1091:14–20
23. Lesnfsky EJ, Stoll MS, Minkler PE, Hoppel CL (2000) Separation and quantitation of phospholipids and lysophospholipids by high-performance liquid chromatography. *Anal Biochem* 285:246–254
24. Siriwardane DA, Wang C, Jiang W, Mudalige T (2020) Quantification of phospholipid degradation products in liposomal pharmaceutical formulations by ultra performance liquid chromatography-mass spectrometry (UPLC-MS). *Int J Pharm* 578:119077
25. Wang C, Siriwardane DA, Jiang W, Mudalige T (2019) Quantitative analysis of cholesterol oxidation products and desmosterol in parenteral liposomal pharmaceutical formulations. *Int J Pharm* 569:118576
26. Jeschek D, Lhota G, Wallner J, Vorauer-Uhl K (2016) A versatile, quantitative analytical method for pharmaceutical relevant lipids in drug delivery systems. *J Pharm Biomed Anal* 119:37–44
27. Meyer O, Roch O, Elmlinger D, Kolbe HVJ (2000) Direct lipid quantitation of cationic liposomes by reversed-phase HPLC in lipoplex preparation process. *Eur J Pharm Biopharm* 50:353–356
28. Simonzadeh N (2009) An isocratic HPLC method for the simultaneous determination of cholesterol, Cardiolipin, and DOPC in lyophilized lipids and liposomal formulations. *J Chromatogr Sci* 47:304–308
29. Oswald M, Platscher M, Geissler S, Goepferich A (2016) HPLC analysis as a tool for assessing targeted liposome composition. *Int J Pharm* 497:293–300
30. Zhou Q, Liu L, Zhang D, Fan X (2012) Analysis of gemcitabine liposome injection by HPLC with evaporative light scattering detection. *J Liposome Res* 22:263–269



# Chapter 21

## DPH Probe Method for Liposome-Membrane Fluidity Determination

Wei He

### Abstract

A liposome is a sealing vesicle composed of a biofilm-like phospholipid bilayer. Continuous phospholipid exchange across the membrane causes spontaneous accumulation and deposition of liposome ions, resulting in the instability of the phospholipid membrane. Effective and reliable techniques to evaluate the stability of liposomes are necessary. Specifically, 1,6-diphenyl-1,3,5-hexatriene (DPH) is a fluorescent probe commonly utilized to assess the fluidity of membranes. Membrane fluidity is inversely proportional to the fluorescence characteristic of DPH; the higher the anisotropy of DPH is, the lower is the membrane fluidity. Here, we described the DPH method for liposome-membrane fluidity determination.

**Key words** 1,6-diphenyl-1,3,5-hexatriene, Liposome, Fluidity, Fluorescence anisotropy

---

### 1 Introduction

The membrane's fluidity is an actual physical property of a liposome, mainly referring to the motion state of the membrane fatty acid chain and membrane protein [1], and the membrane's fluidity directly affects the stability of the liposome. When the temperature is higher than the phase transition temperature, the membrane's fluidity increases, demonstrating an alteration in lateral diffusion, rotation, left-right swing, telescopic oscillation, turnover, and alienation movement. The drug encapsulated in liposomes has a maximum release rate in this state [2]. In addition, some drugs can also affect the fluidity of lipid membranes [3]. DPH is a commonly used fluorescent probe to determine membrane fluidity, which DPH fluorescence anisotropy is a parameter interpreted as a membrane fluidity or microviscosity (viscosity in the bilayer interior) [4]. The dye presents a cis configuration and emits no fluorescence in the solution. However, when inserted into the phospholipid structure, its conformation changes and fluorescence occurs. Membrane fluidity is inversely proportional to the fluorescence

characteristic of DPH. The larger the fluorescence anisotropy is, the lower is the membrane's fluidity. Fluorescent anisotropy provides information about the kinetics and orientation of probes in lipid bilayers [5]. This protocol describes the DPH method for determining liposome-membrane fluidity.

---

## 2 Materials

1,6-diphenyl-1,3,5-hexatriene (DPH, for fluorescence,  $\geq 97.5\%$ ), tetrahydrofuran, dipalmitoylphosphatidylcholine (DPPC), distearoylphosphatidylethanolamine-poly(ethylene glycol) 2000 (DPSE-PEG 2000), 1-StePC, and phosphate buffer (pH 7.4).

---

## 3 Methods

### 3.1 Preparation of Liposomes

1. Film formation: add the lipids, DPPC/1-StePc/DSPE-PEG2000, to a 250 mL eggplant-shaped bottle with a mass ratio of DPPC/1-StePc/DSPE-PEG2000 = 86:10:4 (w/w), followed by adding 12 mL of chloroform/methanol mixed solution (3:1, v/v), dissolving the lipids under water-bath ultrasound condition for 30 s, and drying at 45 °C under vacuum. Finally, a thin film is formed on the eggplant-shaped bottle wall.
2. Film hydration: the film is hydrated in pH 6.5 of phosphate-buffered saline (PBS) at 45 °C for 40 min. A milky white solution is prepared after hydration.
3. Perform ultrasonic treatment for 10 min at 180 W using an ultrasonic probe machine.
4. The liposome is filtered through a 0.22  $\mu\text{m}$  filter.

### 3.2 Incubation of DPH with Liposomes

1. Dissolve the DPH in tetrahydrofuran to form a solution of 1 mM concentration (*see Notes 1 and 2*).
2. Suspend the liposome in phosphate buffer (pH 7.4) to form a 0.05 mM lipid concentration suspension. Mix with DPH solution at the fixed lipid/DPH ratio of 500:1 (v:v), shake for 90 min at room temperature, and leave overnight.

### 3.3 Fluorescence Measure

1. Place the samples into a 96-well plate to measure fluorescence intensity (LS-55 spectrofluorometer) when the polarizer is parallel or perpendicular to the excitation light at 25 °C, 37 °C, 42 °C, and 60 °C.
2. Measure DPH fluorescence anisotropy at the excitation wavelength of 360 nM and the emission wavelength of 425 nM and determine the value of the *G*-factor (ratio of the sensitivities of

the detection system for vertically and horizontally polarized light) for each sample. Anisotropy  $A$  can be calculated from intensities collected in parallel ( $I_{VV}$ ) and perpendicular ( $I_{VH}$ ) directions to the excitation plane. Fluorescence anisotropy for DPH is calculated using the formula [6]:

$$A = \frac{I_{VV} - G * I_{VH}}{I_{VV} + 2G * I_{VH}}$$

$I_{VV}$ : fluorescence intensity is measured when the optical axis of the polarizer and the analyzer are in the same vertical direction.

$I_{VH}$ : fluorescence intensity is measured when the polarizer and analyzer optical axes are vertical and horizontal.

The increase of the anisotropy index ( $A$ ) demonstrated reduced mobilization of the fluorescence probe (DPH) encapsulated inside the lipid bilayer as well as membrane fluidity decrease.

---

#### 4 Notes

1. Pure reagents should be used in the experiment because many impurities are highly fluorescent. It is not recommended to store reagents in plastic containers as the plasticizers (themselves highly fluorescent) present tend to be immersed in aqueous media. Rinse the glass containers with neutralizing ethylenediaminetetraacetic acid (EDTA) to remove trace amounts of heavy metals, which are effective fluorescent quenchers (see ref. [7]).
2. Fluorescent probes for membrane fluidity studies are generally relatively hydrophobic and have low solubility in aqueous media, so organic solvents are used.
3. The probe solution is placed in the dark during the experiment to prevent photochemical decomposition.
4. The excitation and emission wavelengths are fixed at 360 nM and 425 nM.
5. Changes in liposome fluidity at 20–60 °C need to be investigated.
6. Dimethyl sulfoxide (DMSO) should be paid more attention if utilized to dissolve DPH. DMSO is a solid form at room temperature and is easily adhered to the wall of the tube and the tip. Note that it needs to be heated to dissolve, and the tip also requires to be preheated in the incubator; otherwise, it is easy to resolidify on the inner wall of the tip and cause weight losses.
7. The liposome sample must be mixed with the DPH solution for at least 1 h before fluorescence intensity can be detected.

8. To prevent the oxidation of phospholipids, metal utensils should be avoided when weighing lipids [8].
9. The temperature of the water bath should be lower than the boiling point of the organic solvent to not cause the boiling of the organic solvent, which will destroy the film [9].
10. The inside of an eggplant-shaped bottle is very smooth, which is not conducive to the formation of a continuous and uniform film. The eggplant-shaped bottle can be filled with a 1 M NaOH solution and rinsed with distilled water overnight to obtain an eggplant-shaped bottle with a rough inner surface.
11. The liposomes prepared using the film hydration method have a large and nonuniform particle size, and the extrusion method and probe ultrasound are required to control the particle size [10, 11].
12. The ultrasonic probe is immersed in the liposome for dispersion, which releases relatively strong energy and causes local heat generation. Therefore, the container of the ultrasonicated solution is preferably immersed in an ice-water bath. The ultrasonic time should not be too long for fluorescence quenching.

## References

1. Zhao J, Mao S (2021) Tuning the membrane fluidity of liposomes for desirable in vivo fate with enhanced drug delivery. In: Advances in biomembranes and lipid self-assembly. Elsevier, London, pp 67–106
2. Jovanović AA, Balanč BD, Ota A, Ahlin Grabnar P, Djordjević VB, Šavikin KP, Bugarski BM, Nedović VA, Poklar Ulrich N (2018) Comparative effects of cholesterol and  $\beta$ -Sitosterol on the liposome membrane characteristics. Eur J Lipid Sci Technol 120
3. Strugala P, Tronina T, Huszcza E, Gabrielska J (2017) Bioactivity in vitro of quercetin glycoside obtained in *Beauveria bassiana* culture and its interaction with liposome membranes. Molecules 22:1520
4. Poojari C, Wilkosz N, Lira RB, Dimova R, Jurkiewicz P, Petka R, Kepczynski M, Rog T (2019) Behavior of the DPH fluorescence probe in membranes perturbed by drugs. Chem Phys Lipids 223:104784
5. Szabova J, Misik O, Havlikova M, Lizal F, Mravec F (2021) Influence of liposomes composition on their stability during the nebulization process by vibrating mesh nebulizer. Colloids Surf B Biointerfaces 204:111793
6. Xiao Q, Li X, Liu C, Jiang Y, He Y, Zhang W, Azevedo HS, Wu W, Xia Y, He W (2022) Improving cancer immunotherapy via co-delivering checkpoint blockade and thrombospondin-1 downregulator. Acta Pharm Sin B <https://doi.org/10.1016/j.apsb.2022.07.012>
7. Graham JM, Higgins JA (1994) Measurement of membrane fluidity and membrane fusion with fluorescent probes. In: Biomembrane protocols: II. Architecture and function. Springer, New York, pp 177–187
8. Barenholz Y, Lasic DD (2018) An overview of liposome scaled-up production and quality control. In: Handbook of nonmedical applications of liposomes. CRC Press, Boca Raton, pp 23–30
9. Zhang H (2017) Thin-film hydration followed by extrusion method for liposome preparation. In: Liposomes. Springer, Berlin, pp 17–22
10. Awad NS, Haider M, Paul V, AlSawaftah NM, Jagal J, Pasricha R, Husseini GA (2021) Ultrasound-triggered liposomes encapsulating quantum dots as safe fluorescent markers for colorectal cancer. Pharmaceutics 13:2073
11. Xiang B, Cao D-Y (2021) Preparation of drug liposomes by thin-film hydration and homogenization. In: Liposome-based drug delivery systems. Springer, Berlin, pp 25–35



# Chapter 22

## Imaging of Liposomes by Negative Staining Transmission Electron Microscopy and Cryogenic Transmission Electron Microscopy

Anand S. Ubhe

### Abstract

Morphological characteristics of liposomes, such as size and lamellarity directly impact their quality and biological performance of encapsulated drug. Gaining insights into these parameters may also help ensure identification and utilization of most efficient process parameters for liposomes manufacturing. Direct imaging of such self-assembling colloidal structures, although challenging, is feasible through transmission electron microscopy (TEM) which uses nanometer scale wavelength of electrons for illumination, enabling an accurate assessment of the morphological characteristics of liposomes. This chapter will provide background information on the working principle and general sample preparation procedure for the two most commonly used TEM techniques for imaging liposomes, viz. negative staining transmission electron microscopy and cryogenic transmission electron microscopy.

**Key words** Morphology, Particle size, Lamellarity, Liposomes, Negative staining transmission electron microscopy, Cryogenic transmission electron microscopy

---

### 1 Introduction

Superior biopharmaceutical performance of colloidal drug delivery systems over conventional dosage forms can be realized by optimizing their physicochemical parameters, including structural and morphological properties. One of the extensively investigated colloidal drug delivery system in this regard is liposomes [1]. Technological developments in the field of liposomal drug delivery have led to availability of multiple liposome drug products on the market for human use and further continue to be investigated in clinical trials seeking beneficial medical treatments [2]. Liposomes are vesicular structures composed of phospholipid bilayers as their main structural material and are commonly categorized according to their size and/or lamellarity. These categories include small unilamellar vesicles (<100 nm), large unilamellar vesicles (100–800 nm), and

multilamellar vesicles. These specific morphological features can be achieved by using different preparation techniques as well as material compositions [2, 3]. Investigating the size distribution, lamellarity and other structural parameters becomes very valuable as these structural aspects can dictate the *in vivo* biodistribution and/or bioavailability of encapsulated drug [4, 5]. A detailed morphological characterization of liposomes also allows for optimization of their morphological features to improve biological performance of encapsulated drug and hence assure quality of the drug product [6].

For regulatory approval of a generic liposome product, demonstration of its morphological equivalency with the reference listed product is required; since, drug loading, drug retention, as well as drug release rate from liposomes could be affected by liposome morphology and degree of lamellarity. Examples of such parameters include particle morphology, surface potential, size distribution, carrier composition, and the physical form of the encapsulated drug [7, 8].

Electron microscopy is the most direct means of characterizing liposomes to probe their morphological features as magnifications of up to 100,000 $\times$  are possible owing to the shorter wavelength (0.004 nm) of electrons, which also enable spatial resolution at a range between 0.1 and 0.5 nm [9, 10]. Since liposomes are soft matter colloidal systems, transmission electron microscopy (TEM) is most suited for their morphological characterization, as it utilizes illumination beam with lower electron dose for generating sample images [5, 9]. Two of the most commonly used TEM techniques for imaging liposomes are negative staining TEM and cryogenic TEM [5, 11].

---

## 2 Negative Staining Transmission Electron Microscopy

In general, the soft matter components of pharmaceutical colloidal systems, like liposomes, cannot strongly deflect electrons from the incident beam, which would result in TEM images with poor contrast. On the other hand, exposing such samples to high electron doses to improve image contrast may damage native structure of the sample species during imaging. Hence, low incident electron dose needs to be maintained during TEM imaging of these types of samples. To circumvent this, the sample is usually stained with dyes containing elements with high atomic number, such as lead, osmium, wolfram, uranium, molybdenum, and platinum, for characterization by TEM [9]. This enables imaging at a low incident electron dose and significantly improves overall image quality. Based on type of dye used, the technique is classified as negative or positive staining [10].

Selection of an appropriate dye is an important factor in obtaining good-quality TEM images; e.g., for a typical liposome sample that contains phospholipids, it is recommended to cation stain the sample with uranyl ion, which binds to phosphate group of phospholipids. Studies comparing negative staining (using phosphotungstic acid) versus positive staining (using osmium tetroxide) TEM techniques for imaging lipid-based delivery systems have been reported [12].

Although possibly subject to artifacts, negative staining TEM is a faster and simpler technique than cryo-TEM and requires less advanced equipment [11, 13]. It has been used to confirm conjugation of macromolecules, such as transferrin, to DSPC/cholesterol liposomal surfaces, demonstrating its utility as an important imaging tool [14].

---

### 3 Cryogenic Transmission Electron Microscopy (Cryo-TEM)

Compared to conventional TEM in which staining is generally needed for soft matter samples, cryogenic TEM could be a better imaging technique to visualize liposomes in their closest native state. Maintaining a sample in its near-native state during imaging is achieved by plunge freezing the sample, causing vitrification of water. This avoids need for fixing the sample through chemical means which could lead to extraction of lipid components. The frozen sample is then imaged directly using electron microscope under liquid nitrogen temperature conditions. Cryo-TEM imaging is capable of generating high-resolution images and is especially useful for examining size, shape, and lamellarity of liposome preparations [5, 6, 10, 11].

Cryo-TEM has been utilized for structural and morphological characterization of liposome samples as well as for studying effect of drug encapsulation on morphology of liposomes, which could potentially affect biopharmaceutical performance of the overall drug delivery system [6, 9]. The technique is especially useful for biologics, such as proteins or deoxyribonucleic acid (DNA), encapsulated into liposomes or other soft matter delivery systems [4, 10, 15]. Advanced image analysis has been utilized in conjunction with cryo-TEM to demonstrate sphere to ellipsoid/coffee bean shaped deformation of liposomes due to presence of encapsulated single doxorubicin nano rod crystals in the center cavity of the liposomes; being equivalent to the marketed drug product Doxil® [1, 6–8]. Such characterization insights would be very useful in determining optimal drug-loading concentration, vesicular stability, and overall quality of the delivery system [5, 6].

---

## 4 Materials

Commonly used materials for negative staining TEM and cryo-TEM characterization of liposomes are listed below [1, 4, 9, 13, 16, 17].

### 4.1 Sample Preparation

1. Micropipette (2–10 µL).
2. Pipette tips (2–10 µL).
3. Adsorbent pad/filter paper.
4. 200/300 mesh carbon-coated TEM copper grid.
5. 2.5% uranyl acetate solution.

### 4.2 TEM Sample Handling

1. Cryo-TEM sample handler, e.g., Leica EM GP cryo-preparation station or Vitrobot.
  2. Transmission electron microscope with a charge-coupled device (CCD) camera and image analysis software, e.g., JEOL JEM 1010, FEI Tecnai 12G2 with a Gatan workstation.
- 

## 5 Methods

General procedures for performing conventional negative staining TEM and cryo-TEM characterization of liposomes are described below [1, 4, 9, 13, 16, 17].

### 5.1 Negative Staining Transmission Electron Microscopy (TEM)

1. Apply approximately 5–10 µL of liposome sample on a 200 mesh TEM carbon-coated copper grid.
2. Dab the sample grid with an adsorbent pad to remove any excess sample.
3. Place a drop of 2.5% uranyl acetate on the sample grid and allow it to stain the sample for approximately 1 min.
4. Dab the sample grid with an adsorbent pad to remove any excess stain.
5. The sample grid is now ready to be imaged under TEM.
6. Use an acceleration voltage of 80–120 kV to allow low electron dosing for TEM imaging to minimize any radiation damage to liposome sample during imaging.

### 5.2 Cryogenic Transmission Electron Microscopy (Cryo-TEM)

1. Pipette out approximately 3–5 µL of liposome sample on a TEM copper grid coated with a perforated lacey carbon 300 mesh.
2. Dab the sample grid with an adsorbent pad to remove any excessive sample. Achieving a thin film of the sample (20–300 nm) is critical.

3. Transfer the sample grid to a cryo-TEM sample handler, e.g., Leica EM GP cryo-preparation station or Vitrobot.
4. Plunge the sample grid into liquid ethane at just above its freezing point ( $-183^{\circ}\text{C}$ ). This will allow the vitrification of the liposome sample without forming ice crystals.
5. Keep the vitrified sample under liquid nitrogen until transferred to transmission electron microscope for imaging.  
**Steps 4 and 5** should be conducted quickly to avoid formation of crystalline ice and ideally maintain water in a vitrified or glassy state.  
Also, maintain the cryo-sample holder below  $-170^{\circ}\text{C}$  to prevent sublimation of vitreous water.
6. Transfer the sample to transmission electron microscope. Operate the microscope illumination at 80–120 kV in a low electron dose mode to minimize any radiation damage to the sample and with a few micrometers under-focus to enhance phase contrast.

---

## 6 Notes

Sample preparation is a multi-stage process and a very critical element of TEM characterization. Great extent of skillset and diligence is required for TEM sample preparation to avoid generation of possible artifacts and errors in imaging process, which may affect accuracy and reliability of conclusions made from the characterization [9, 10].

Distortion and flattening of a part of liposome sample, could result during sample preparation, as well as dehydration caused by application of vacuum during imaging. This may affect the results of size distribution analysis. The stain used for TEM sample preparation is expected to bind at lipid bilayer surface and is not expected to penetrate it. Hence, data from this type of TEM imaging alone may not be sufficient to verify encapsulation of drug inside liposomes [5].

Dabbing the sample grid using an adsorbent pad to remove excess sample may cause vehicle flow and induce shear stress in the sample, leading to reorientation and/or morphological rearrangement of liposome structures [6].

Staining of liposome structures can result in appearance of light and dark fringes in the images, which could be mistaken for lamellar structures [10].

Although staining improves image quality, it may be non-uniform, resulting in some of the sample species being sufficiently stained while others being not. The unstained sample species would remain invisible in TEM images, creating artifacts [9].

Despite numerous advantages of cryo-TEM, expertise in sample preparation and data analysis is still a prerequisite to avoid possible artifacts in images, generate data with high signal-to-noise ratio, and its accurate interpretation. Key aspects of sample preparation for cryo-TEM are maintaining native sample environment through vitrification, minimizing formation of ice crystals after freezing, and obtaining a glassy ice layer at a fine thickness of 20–300 nm. The vitrified sample layer should be thin enough to be suitable for microscopic analysis but at the same time thick enough to maintain liposome sample structure. Continuous chilling of sample during analysis is critical since temperature and humidity changes may also affect the native sample structure [9].

Generation of water crystals in sample could create artifacts in TEM images appearing in the form of dots [17].

During the process of vitrification, a possibility of liposome shrinkage and shape distortion exists, resulting in artifacts in TEM images and data [18].

Exposure to electron beam during imaging is also a possible source affecting morphology of liposome sample. Hence, it is important to carefully control exposure of sample to the incident electron beam used for illumination [6]. Larger liposome particles tend to cluster together near the grid wire, making them more susceptible to the damaging effects of incident electron beam [9].

## References

- Nordström R, Zhu L, Härmäk J, Levi-Kalisman Y, Koren E, Barenholz Y et al (2021) Quantitative cryo-TEM reveals new structural details of Doxil-like PEGylated liposomal doxorubicin formulation. *Pharmaceutics* 13(1):123
- Bulbake U, Doppalapudi S, Kommineni N, Khan W (2017) Liposomal formulations in clinical use: an updated review. *Pharmaceutics* 9(2):12
- Peretz Damari S, Shamrakov D, Varenik M, Koren E, Nativ-Roth E, Barenholz Y et al (2018) Practical aspects in size and morphology characterization of drug-loaded nano-liposomes. *Int J Pharm* 547(1):648–655
- Objective characterization of liposomal drug delivery platforms: using cryoTEM and designated image analysis software [Internet]. Bio-Process International. 2016 [cited 2022 Apr 30]. Available from: <https://bioprocessintl.com/bpi-white-papers/objective-characterization-of-liposomal-drug-delivery-platforms-using-cryotem-and-designated-image-analysis-software/>
- Peretz DS. Liposome size distribution and morphology analysis by cryogenic transmission electron microscopy [Internet]. Ben-Gurion University of the Negev; 2014. Available from: <http://aranne5.bgu.ac.il/others/Peretz-DamariSivan.pdf>
- Helvig S, Azmi IDM, Moghimi SM, Yaghmur A (2015) Recent advances in cryo-TEM imaging of soft lipid nanoparticles. *AIMS Biophys* 2(2):116–130
- Research Council for DE and FY2016 Regulatory Science Report. Nanotechnology: physicochemical characterization of nano-sized drug products. FDA [Internet]. 2021 Feb 3 [cited 2022 Apr 30]; Available from: <https://www.fda.gov/industry/generic-drug-user-fee-amendments/fy2016-regulatory-science-report-nanotechnology-physicochemical-characterization-nano-sized-drug>
- Wu Y, Petrochenko P, Szoka FC, Manna S, Koo B, Zheng N et al (2017) Cryogenic transmission electron microscopy (cryo-TEM) reveals morphological changes of liposomal doxorubicin during *in vitro* release. *Microsc Microanal* 23(S1):1216–1217
- Placzek M, Kosela M (2016) Microscopic methods in analysis of submicron phospholipid dispersions. *Acta Pharma* 66(1):1–22

10. Robson AL, Dastoor PC, Flynn J, Palmer W, Martin A, Smith DW et al (2018) Advantages and limitations of current imaging techniques for characterizing liposome morphology. *Front Pharmacol* 9:80
11. Baxa U (1982) Imaging of liposomes by transmission electron microscopy. *Methods Mol Biol Clifton NJ* 2018:73–88
12. Bello V, Mattei G, Mazzoldi P, Vivenza N, Gasco P, Idee JM et al (2010 Aug) Transmission electron microscopy of lipid vesicles for drug delivery: comparison between positive and negative staining. *Microsc Microanal* 16(4):456–461
13. Lujan H, Griffin WC, Taube JH, Sayes CM (2019 Jul 11) Synthesis and characterization of nanometer-sized liposomes for encapsulation and microRNA transfer to breast cancer cells. *Int J Nanomedicine* 14:5159–5173
14. Anabousi S, Laue M, Lehr CM, Bakowsky U, Ehrhardt C (2005 Jul 1) Assessing transferrin modification of liposomes by atomic force microscopy and transmission electron microscopy. *Eur J Pharm Biopharm* 60(2):295–303
15. Yao X, Fan X, Yan N (2020 Aug 4) Cryo-EM analysis of a membrane protein embedded in the liposome. *Proc Natl Acad Sci* 117(31): 18497–18503
16. Chetanachan P, Akarachalanon P, Worawirunwong D, Dararutana P, Bangtrakulnonth A, Bunjop M et al (2008) Ultrastructural characterization of liposomes using transmission electron microscope. *Adv Mater Res* 55–57:709–711
17. Mkam Tsengam IK, Omarova M, Shepherd L, Sandoval N, He J, Kelley E et al (2019) Clusters of nanoscale liposomes modulate the release of encapsulated species and mimic the compartmentalization intrinsic in cell structures. *ACS Appl Nano Mater* 2(11): 7134–7143
18. Laouini A, Jaafar-Maalej C, Limayem-Blouza I, Sfar S, Charcosset C, Fessi H (2012) Preparation, characterization and applications of liposomes: state of the art. *J Colloid Sci Biotechnol* 1(2):147–168



# Chapter 23

## Visualization and Characterization of Liposomes by Atomic Force Microscopy

Konrad Engelhardt, Eduard Preis, and Udo Bakowsky

### Abstract

Atomic force microscopy is a high-resolution and nonoptical technique used to visualize and characterize biological samples and surfaces. In pharmaceutical research and development (R&D) and quality control (QC), drug delivery systems, like liposomes with sizes in a nanometer range, are preferred samples to be studied through atomic force microscopy. The instrument can determine the sample's topography (e.g., height), morphology, and material properties (e.g., hardness, adhesiveness). Various measuring modes, e.g., intermittent contact (AC mode), can generate height (measured), lock-in amplitude, and lock-in phase data, revealing interesting details about the drug delivery system.

In this study, empty and drug-loaded liposomes with various lipid compositions and sizes (50–800 nm) were visualized and characterized with state-of-the-art atomic force microscope (AFM). The main focus here was the preparation methods of the samples, instrumental settings, and pitfalls that can occur during the whole imaging process. Moreover, troubleshooting and postdata processing are essential for a high-quality outcome.

**Key words** Atomic force microscope (AFM), Cantilever, Silicon wafer, Roughness, Scanning artifacts, Liposomes, Vesicles, Nanotechnology, Gene vehicle, Drug delivery systems

---

### 1 Introduction

The visualization and characterization of structures and surfaces at a (sub)nanometer range plays an increasingly important role in modern drug development and quality control.

For this purpose, the atomic force microscope (AFM) is the preferred tool with a lateral (X, Y) resolution of 1–5 nm and a vertical resolution of around 1 Å [1, 2] (Fig. 1). It has many advantages compared to electron and optical microscopes, such as the following:

- The possibility of studying sensitive biological samples like, cells, proteins, and nucleic acids in liquids [3]

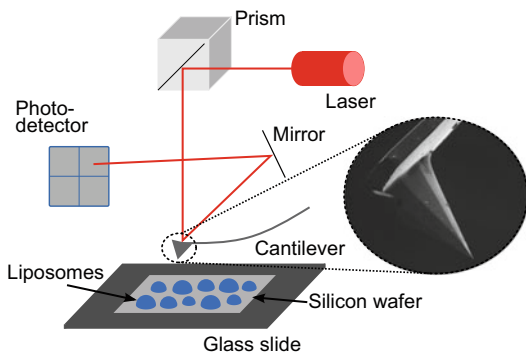


**Fig. 1** Schematic presentation of an atomic force microscope. A laser is directed through a prism and then reflected off by the backside of the cantilever toward an adjustable mirror, which focuses the laser beam onto a photodetector. The measurement is conducted in an intermittent contact mode (AC mode), by which the cantilever oscillates above the sample at a specific frequency and amplitude. Atomic forces between the tip and the sample cause the cantilever to deflect, resulting in a shift of the reflected laser beam

- Relatively simple sample preparation since no fixation or coating is required [4]
- The option to determine the topographical structure of the surfaces and to quantify forces between different specimens [5]

Different measuring modes can be selected depending on the sample's characteristics [6]. The preferred measuring method for soft and fragile samples, like liposomes, is the “intermittent-contact” mode (AC mode), where the needle of the cantilever touches the sample intermittently but does not make permanent contact. The AC mode can protect both the tip and the sample. In the contact mode, the tip is in direct mechanical contact with the surface.

Liposomes, which are soft vesicles consisting of a lipid bilayer enclosing an aqueous core, represent versatile and biocompatible drug delivery systems for a range of drugs, like small molecules [7–10], peptides [11], and genes [12, 13]. Depending on the preparation method, liposomes can have sizes from 50 to 800 nm [14–16], affecting cellular uptake, the ability to cross biological barriers, and elimination [17, 18].

Here, we demonstrate a practical and detailed guide for visualizing and characterizing liposomes with state-of-the-art AFM. Feedback parameters were optimized during the measurement to achieve high-quality output. Using topographical (*height*) data [19] and phase data [20] gives a deep insight into the structural organization of liposomal drug delivery systems. Moreover, we demonstrated how common pitfalls could be avoided and also explained

how to recognize and avoid *artifacts* [21], a common problem, using an indirect imaging method like AFM.

---

## 2 Materials

Please ensure that only ultrapure water with low conductivity ( $0.055\text{ }\mu\text{S}/\text{cm}$ ) and that a resistivity of  $18\text{ }\Omega\cdot\text{m}$  is used to dilute the samples. The experiments should be conducted at room temperature ( $25\text{ }^\circ\text{C}$ ). All buffers need to be filtrated through a  $0.22\text{ }\mu\text{m}$  filter to remove impurities or bacterial contamination.

### 2.1 Atomic Force Microscope

1. JPK NanoWizard® 3 AFM.
2. A cantilever (HS:NSC 14/AlBS) with a pyramidal  $\text{Si}_3\text{N}_4$  tip was used. The cantilever had a length of  $125\text{ }\mu\text{m}$ , a width of  $25\text{ }\mu\text{m}$ , and a thickness of  $2.1\text{ }\mu\text{m}$ . The force constant was  $5\text{ N/m}$ , and the resonance frequency was between  $120$  and  $160\text{ kHz}$  (see Note 1).
3. An acoustic enclosure reduces acoustic noise and maintains a stable temperature during the measurement process.
4. A vibration isolation system stabilizes the AFM.

### 2.2 Silicon Wafer

1. Commercially available silicon wafer.
2. Sharp glass cutter.
3. Ruler.
4. Chloroform/methanol (2/1 v/v) mixture.

### 2.3 Liposomes

1. Liposomes with a total lipid concentration of  $5\text{ mg/mL}$  and different lipid compositions: 1,2-dipalmitoyl-sn-glycero-3-phosphocholine (DPPC); egg phosphatidylcholine (Egg PC); 1,2-dioleoyl-sn-glycero-3-phosphoethanolamine (DOPE); cholesterol, 1,2-dioleoyl-3-trimethylammonium-propane (chloride salt) (DOTAP); 1,2-distearoyl-sn-glycero-3-phosphocholine (DSPC); Solutol HS15 (Kolliphor® HS15); and glycerol dialkyl nonitol tetraether lipid (GDNT) (Fig. 2).
2. HEPES buffer (10 mM, pH 7.4): dissolve  $2.38\text{ g}$  of HEPES in  $900\text{ mL}$  ultrapure water. Adjust the pH with  $1\text{ M NaOH}$  to 7.4 and add ultrapure water to  $1000\text{ mL}$ . Filter the solution through a  $0.22\text{ }\mu\text{m}$  syringe filter and store it at  $4\text{ }^\circ\text{C}$ .
3. PBS buffer: dissolve  $8.00\text{ g}$  of  $\text{NaCl}$ ,  $0.20\text{ g}$   $\text{KCl}$ ,  $0.20\text{ g}$   $\text{KH}_2\text{PO}_4$ , and  $1.15\text{ g}$   $\text{Na}_2\text{HPO}_4$  in  $900\text{ mL}$  ultrapure water. Adjust the pH to 7.4 with  $1\text{ M hydrochloric acid (HCl)}$ . Filter the solution through a  $0.22\text{ }\mu\text{m}$  syringe filter and store it at  $4\text{ }^\circ\text{C}$ .

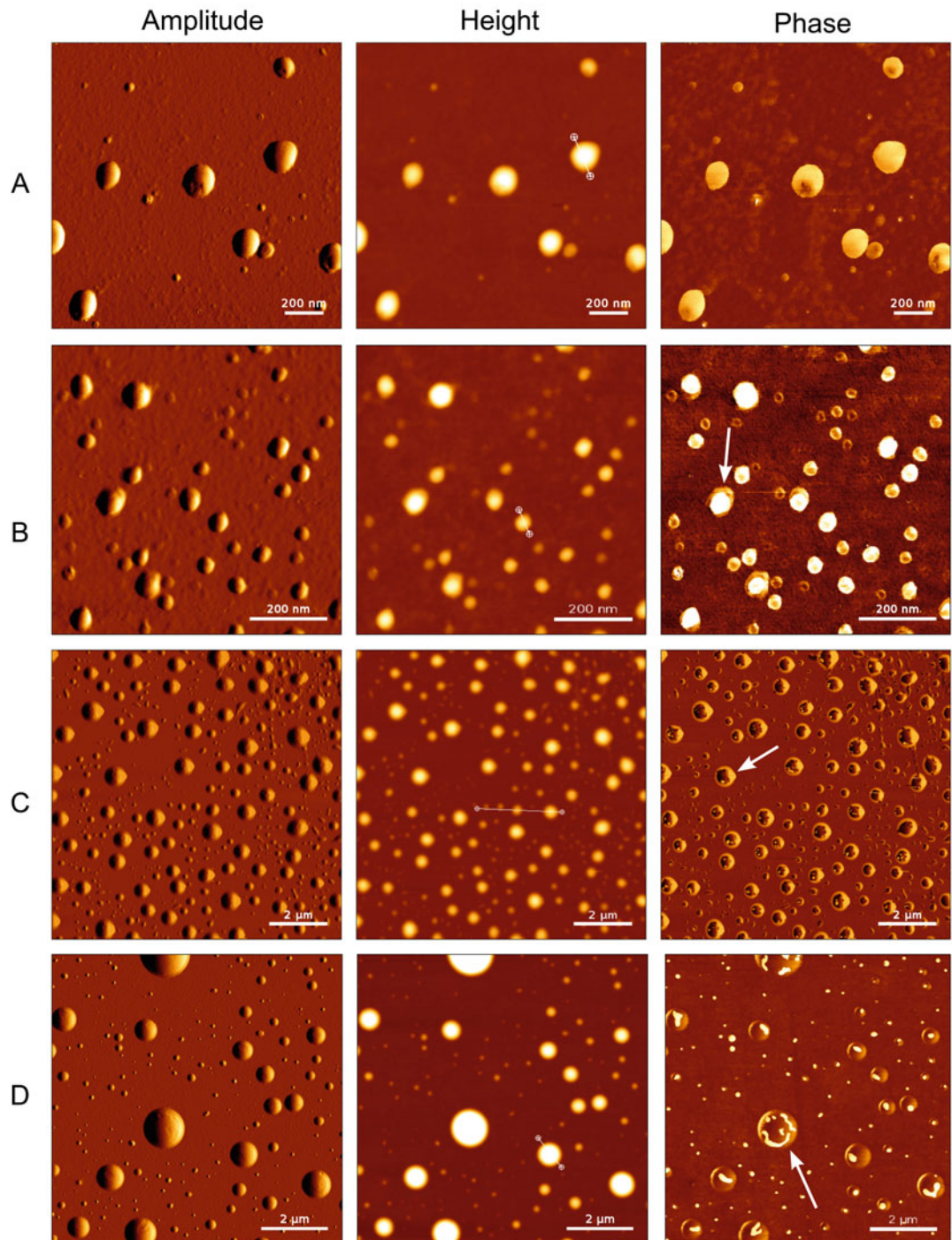


**Fig. 2** Visualization of (a) GDNT/egPC/DOTAP liposomes with a molar ratio of 10/80/10 mol% on a  $1.5\text{ }\mu\text{m} \times 1.5\text{ }\mu\text{m}$  consisting of amplitude, height, and phase image; (b) DOPE/DPPC/cholesterol liposomes with a molar ratio of 70/15/15 mol% on a  $0.75\text{ }\mu\text{m} \times 0.75\text{ }\mu\text{m}$  area consisting of amplitude, height, and phase image, with the latter clearly showing a softer (dark color) region around the liposomes (white arrow); (c) indocyanine green-loaded liposomes with a lipid composition of DSPC/Kolliphor® HS 15 on a  $10\text{ }\mu\text{m} \times 10\text{ }\mu\text{m}$  area consisting of amplitude, height, and phase image, with the latter revealing a bright corona (white arrow) around the vesicles; and (D) indocyanine green-loaded liposomes with a lipid composition of DSPC/Kolliphor® HS 15 on an  $8.5\text{ }\mu\text{m} \times 8.5\text{ }\mu\text{m}$  area consisting of amplitude, height, and phase image, with the latter confirming a different hardness underneath the softer lipid layer (white arrow). Imaging parameters are listed in Table 1

**Table 1**

**The parameters of the JPK NanoWizard® 3 AFM equipped with a cantilever (HS:NSC 14/AIBS) used during the imaging of Fig. 2**

| Parameters      | Figure 2a        | Figure 2b        | Figure 2c        | Figure 2d        |
|-----------------|------------------|------------------|------------------|------------------|
| Line rate       | 0.800 Hz         | 1.500 Hz         | 0.700 Hz         | 0.700 Hz         |
| Overscan time   | 0.062 s          | 0.033 s          | 0.071 s          | 0.071 s          |
| Tip velocity    | 2.7 µm/s         | 3.25 µm/s        | 15.73 µm/s       | 15.73 µm/s       |
| Size            | 1.500 × 1.500 µm | 0.750 × 0.750 µm | 10.00 × 10.00 µm | 8.500 × 8.500 µm |
| Pixels          | 512 × 512        | 512 × 512        | 512 × 512        | 512 × 512        |
| Z range         | 5.0 µm           | 5.0 µm           | 5.0 µm           | 5.0 µm           |
| Mode            | AC mode          | AC mode          | AC mode          | AC mode          |
| IGain           | 120.0 Hz         | 150.0 Hz         | 160.0 Hz         | 160.0 Hz         |
| PGain           | 0.0019           | 0.0024           | 0.0025           | 0.0025           |
| Setpoint        | 896 mV           | 20.4 nm          | 874 mV           | 670 mV           |
| Drive amplitude | 0.017 V          | 0.024 V          | 0.048 V          | 0.115 V          |
| Drive frequency | 147.936 kHz      | 148.452 kHz      | 135.697 kHz      | 135.07 kHz       |
| Phase shift     | -54 deg          | -86 deg          | 88 deg           | 131 deg          |

### 3 Methods

#### 3.1 Preparation and Cleaning of Silicon Wafers

1. Cut 1 cm × 1 cm silicon wafers with a sharp glass cutter and a ruler on a soft pad (*see Note 2*).
2. Clean the silicon wafers in a mixture of chloroform/methanol (2/1 v/v) in a sonication bath for 20 min to remove crude organic contamination (*see Note 3*) (Fig. 3).
3. Rub the silicon wafers with a lint-free wipe soaked in isopropanol.
4. Rinse the silicon wafers with ultrapure water and store them in a clean and closed container until further usage.

#### 3.2 Preparation of Samples

1. Mount a cleaned silicon wafer on a glass slide using double-sided adhesive tape.
2. Dilute the sample 1:100 with ultrapure water, HEPES buffer, or PBS buffer and pipette it onto the silicon wafer.
3. Incubate the sample at room temperature for 15–60 min (*see Note 4*).
4. Remove excess ultrapure water or buffer by aspirating the liquid with a pipette or a lint-free wipe or by simply shaking it off.

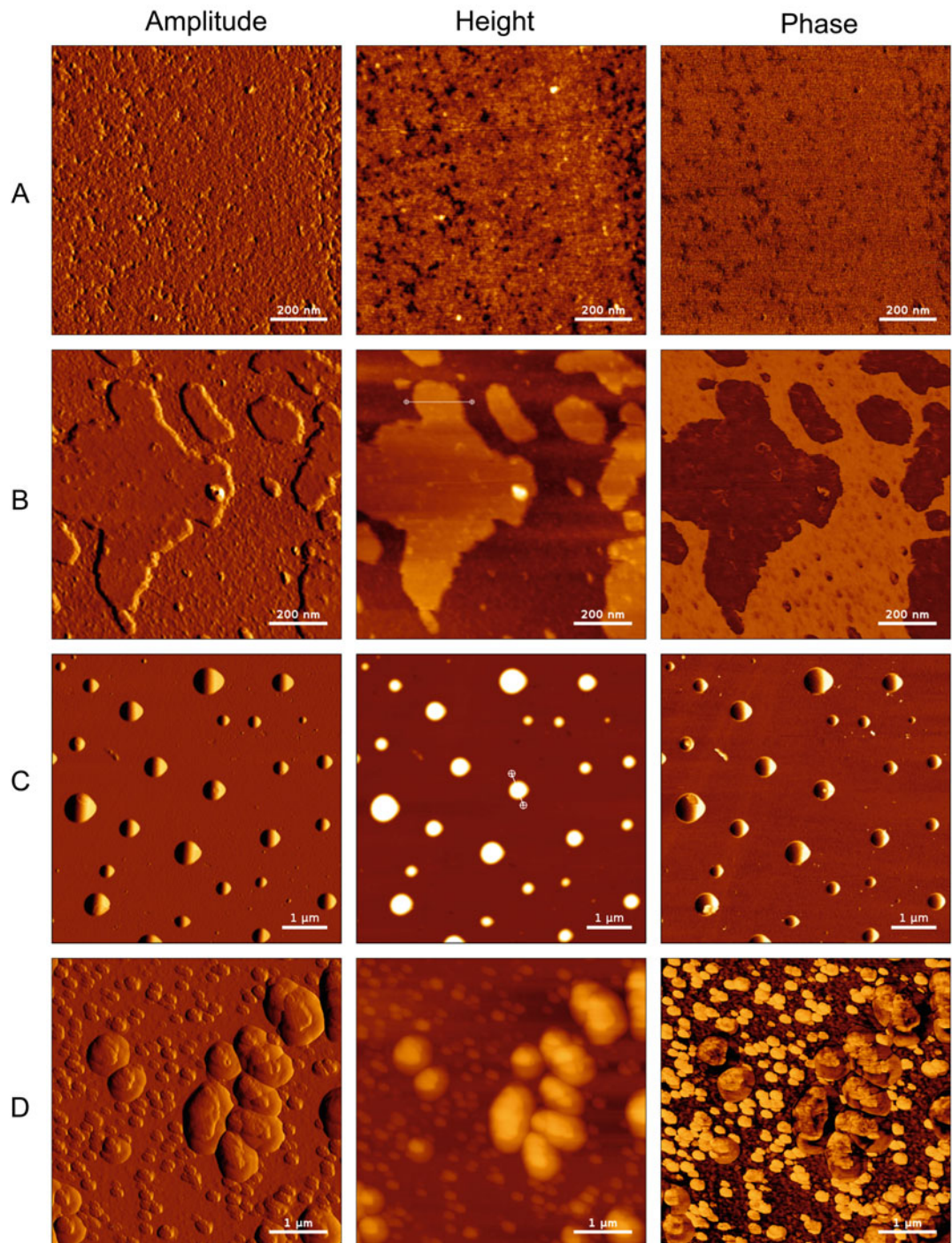


**Fig. 3** Visualization of (a) freshly cut and cleaned silicon wafer with an area of  $1 \mu\text{m} \times 1 \mu\text{m}$  consisting of amplitude, height, and phase image. The average roughness ( $R_a$ ) was 131.7 pm, (b) lipid layer on a  $1 \mu\text{m} \times 1 \mu\text{m}$  area consisting of amplitude, height, and phase image; (c) indocyanine green-loaded liposomes with a lipid composition of DSPC/Kolliphor® HS 15 on a  $6.0 \mu\text{m} \times 6.0 \mu\text{m}$  area consisting of amplitude, height, and phase image; and (d) artifacts of cholesterol-RNA particles on a  $5 \mu\text{m} \times 5 \mu\text{m}$  area consisting of amplitude, height, and phase image. Imaging parameters are listed in Table 2

**Table 2**

**The parameters of the JPK NanoWizard® 3 AFM equipped with a cantilever (HS:NSC 14/AIBS) used during the imaging of Fig. 3**

| Parameters      | Figure 3a                          | Figure 3b                          | Figure 3c                          | Figure 3d                          |
|-----------------|------------------------------------|------------------------------------|------------------------------------|------------------------------------|
| Line rate       | 1.500 Hz                           | 1.500 Hz                           | 0.700 Hz                           | 0.541 Hz                           |
| Overscan time   | 0.033 s                            | 0.033 s                            | 0.071 s                            | 0.083 s                            |
| Tip velocity    | 3.47 $\mu\text{m}/\text{s}$        | 3.42 $\mu\text{m}/\text{s}$        | 15.73 $\mu\text{m}/\text{s}$       | 6 $\mu\text{m}/\text{s}$           |
| Size            | 1.016 $\times$ 1.016 $\mu\text{m}$ | 1.000 $\times$ 1.000 $\mu\text{m}$ | 6.000 $\times$ 6.000 $\mu\text{m}$ | 5.000 $\times$ 5.000 $\mu\text{m}$ |
| Pixels          | 512 $\times$ 512                   | 512 $\times$ 512                   | 512 $\times$ 512                   | 512 $\times$ 512                   |
| Z range         | 5.0 $\mu\text{m}$                  | 5 $\mu\text{m}$                    | 5.0 $\mu\text{m}$                  | 5.0 $\mu\text{m}$                  |
| Mode            | AC mode                            | AC mode                            | AC mode                            | AC mode                            |
| IGain           | 150.0 Hz                           | 150.0 Hz                           | 150.0 Hz                           | 290.0 Hz                           |
| PGain           | 0.0024                             | 0.0024                             | 0.0024                             | 0.0270                             |
| Setpoint        | 813 mV                             | 18.4 nm                            | 871 mV                             | 1.39 V                             |
| Drive amplitude | 0.009 V                            | 0.023 V                            | 0.125 V                            | 0.18 V                             |
| Drive frequency | 149.28 kHz                         | 148.439 kHz                        | 135.75 kHz                         | 165.973 kHz                        |
| Phase shift     | -44 deg                            | -87 deg                            | 90 deg                             | -110 deg                           |

### 3.3 AFM Settings

1. Adjust the laser onto the end of the cantilever so that the reflected laser beam falls onto the photodiode consisting of four segments. A high sum signal (in volts) indicates an optimal alignment of the reflected laser beam (*see Note 5*).
2. Adjust the laser spot onto the center of the detector by moving it using the adjustment screws on the AFM head. The sum must be at its maximum, while vertical and lateral deflection must be close to zero (*see Note 6*).
3. Let the cantilever equilibrate for 10 min in the retracted state.
4. Select intermittent contact mode (AC mode) for oscillating the cantilever in the air.
5. Set the target amplitude to 1.0 V and perform an automatic cantilever tuning where the values of the drive amplitude and gains are automatically chosen to achieve the target amplitude.
6. Perform sweep curves by clicking on the infinity symbol and zooming in around the resonance peak.
7. Choose a setpoint of 85–90% of the lock-in amplitude and select a frequency located slightly left from the amplitude (*see Note 7*).

8. The phase is adjusted automatically during the process but can be optimized by using a fixed offset.
9. Use the stepper motors of the AFM head to make a coarse approach of the cantilever to the sample's surface (*see Note 8*).
10. When the tip is close to the surface, switch to an automatic approach with constant velocity and a dynamic baseline update (the baseline is adjusted automatically) (*see Note 9*).
11. Click the retract button once and open the cantilever tuning window to perform sweep curves to check the cantilever's frequency, lock-in amplitude, and lock-in phase. Readjust the setpoint and frequency.
12. Click run to measure the sample.

### 3.3.1 Imaging

1. For the first image, select a scan size of about  $10 \mu\text{m} \times 10 \mu\text{m}$  to get an overview of the sample. Scan speed needs to be adjusted to 0.6 Hz, so the liposomes are not damaged.
2. Open the oscilloscope window during the scanning process and check if the trace and retrace are almost congruent.
3. Check the quality of the height (measured), lock-in amplitude, and lock-in phase image during the whole imaging process (*see Note 10*).
4. Select a scan region and zoom in to get a more detailed image of the liposomes.

### 3.4 Postprocessing of Images

1. Open the raw images (height (measured), lock-in amplitude, and lock-in phase) with appropriate software, e.g., JPK processing software or Gwyddion.
2. Subtract a polynomial fit from each scan line independently using a limited data range.
3. In the case of punctual bumps, replace outliers with the median of neighboring pixels.
4. In case of linear image errors, interpolate the lines.
5. For a smoother appearance of the particles, it is sometimes helpful to apply a low pass filter that uses Gaussian or Savitzky-Golay smoothing (*see Note 11*).
6. To characterize the liposomes' height or morphology, make a cross-section that gives you valuable details.
7. Generate a three-dimensional (3D) image after applying the previously mentioned procedures.

---

## 4 Notes

1. The cantilever behaves like a spring with a force constant, an amplitude, a frequency, and a phase. Each commercially available cantilever has specific data that must be precisely matched to the sample at hand. For hard samples, e.g., surfaces, one needs a stiff cantilever with a high force constant, while for softer samples, such as liposomes, a softer cantilever with a low force constant must be used. The cantilever must be stored in a dust-free environment, like in a gel pack, to prevent the contamination of the tip.
2. Place the silicon wafer upside down on a soft and clean support to prevent scratches on the glossy side.
3. Chloroform is a carcinogenic organic solvent. Wearing safety goggles and chemical-resistant gloves is recommended during the cleaning step.
4. Depending on the charge and sizes of the liposomes, incubation times can vary. When an unknown sample is measured, several dilutions should be prepared to find the optimal concentration for AFM imaging. An exaggerated incubation time can result in the formation of lipid films since liposomes can undergo fusion processes.
5. A sum signal under 1 V is too low. A readjustment of the system might be required, or a new cantilever has to be inserted into the glass block.
6. Do not overwind the screws since the screws can get blocked or damaged.
7. If the setpoint is too low, it can cause damage to the tip or the sample, whereas a high setpoint fails to interact with the surface correctly.
8. Approach carefully and observe closely to avoid crashing the glass block into the surface.
9. The approach is successful if a blue light on the AFM head is switched on and a red bar is located in the center of the Z-range software panel.
10. If the contrast in the phase image is poor or tails appear on the liposomes, readjust the feedback parameters carefully, e.g., decreasing the setpoint, increasing the gains, or increasing the drive amplitude.
11. Too much smoothing might lead to the disappearance of important surface details. Make sure that the details you want to present are visible even after smoothing (like small attachments on the liposome's surface).

## References

1. Sudarsan V (2017) Chapter 4 – materials for hostile chemical environments. In: Tyagi AK, Banerjee S (eds) Materials under extreme conditions: recent trends and future prospects. Elsevier, Amsterdam/Kidlington/Cambridge, pp 129–158
2. Sitterberg J, Ozcetin A, Ehrhardt C et al (2010) Utilising atomic force microscopy for the characterisation of nanoscale drug delivery systems. *Eur J Pharm Biopharm* 74:2–13. <https://doi.org/10.1016/j.ejpb.2009.09.005>
3. Zylberberg C, Matosevic S (2016) Pharmaceutical liposomal drug delivery: a review of new delivery systems and a look at the regulatory landscape. *Drug Deliv* 23:3319–3329. <https://doi.org/10.1080/10717544.2016.1177136>
4. Last JA, Russell P, Nealey PF et al (2010) The applications of atomic force microscopy to vision science. *Invest Ophthalmol Vis Sci* 51: 6083–6094. <https://doi.org/10.1167/iosv.10-5470>
5. Sebinelli HG, Borin IA, Ciancaglini P et al (2019) Topographical and mechanical properties of liposome surfaces harboring Na,K-ATPase by means of atomic force microscopy. *Soft Matter* 15:2737–2745. <https://doi.org/10.1039/c9sm00040b>
6. Aytekin AA, Tuncay Tanrıverdi S, Aydin Köse F et al (2020) Propolis loaded liposomes: evaluation of antimicrobial and antioxidant activities. *J Liposome Res* 30:107–116. <https://doi.org/10.1080/08982104.2019.1599012>
7. Alawak M, Abu Dayyih A, Mahmoud G et al (2021) ADAM 8 as a novel target for doxorubicin delivery to TNBC cells using magnetic thermosensitive liposomes. *Eur J Pharm Biopharm* 158:390–400. <https://doi.org/10.1016/j.ejpb.2020.12.012>
8. Zheng X, Shao X, Zhang C et al (2015) Intranasal H102 peptide-loaded liposomes for brain delivery to treat Alzheimer's disease. *Pharm Res* 32:3837–3849. <https://doi.org/10.1007/s11095-015-1744-9>
9. Gaspar MM, Radomska A, Gobbo OL et al (2012) Targeted delivery of transferrin-conjugated liposomes to an orthotopic model of lung cancer in nude rats. *J Aerosol Med Pulm Drug Deliv* 25:310–318. <https://doi.org/10.1089/jamp.2011.0928>
10. Duse L, Pinnapireddy SR, Strehlow B et al (2018) Low level LED photodynamic therapy using curcumin loaded tetraether liposomes. *Eur J Pharm Biopharm* 126:233–241. <https://doi.org/10.1016/j.ejpb.2017.10.005>
11. Li L, Hou J, Liu X et al (2014) Nucleolin-targeting liposomes guided by aptamer AS1411 for the delivery of siRNA for the treatment of malignant melanomas. *Biomaterials* 35:3840–3850. <https://doi.org/10.1016/j.biomaterials.2014.01.019>
12. Drabik D, Gavutis M, Valiokas RN et al (2020) Determination of the mechanical properties of model lipid bilayers using atomic force microscopy indentation. *Langmuir* 36:13251–13262. <https://doi.org/10.1021/acs.langmuir.0c02181>
13. Ewe A, Panchal O, Pinnapireddy SR et al (2017) Liposome-polyethylenimine complexes (DPPC-PEI lipopolplexes) for therapeutic siRNA delivery in vivo. *Nanomedicine* 13: 209–218. <https://doi.org/10.1016/j.nano.2016.08.005>
14. Has C, Sunthar P (2020) A comprehensive review on recent preparation techniques of liposomes. *J Liposome Res* 30:336–365. <https://doi.org/10.1080/08982104.2019.1668010>
15. Anabousi S, Kleemann E, Bakowsky U et al (2006) Effect of PEGylation on the stability of liposomes during nebulisation and in lung surfactant. *J Nanosci Nanotechnol* 6:3010–3016. <https://doi.org/10.1166/jnn.2006.461>
16. Marxer EEJ, Brüssler J, Becker A et al (2011) Development and characterization of new nanoscaled ultrasound active lipid dispersions as contrast agents. *Eur J Pharm Biopharm* 77: 430–437. <https://doi.org/10.1016/j.ejpb.2010.12.007>
17. Inoh Y, Nagai M, Matsushita K et al (2017) Gene transfection efficiency into dendritic cells is influenced by the size of cationic liposomes/DNA complexes. *Eur J Pharm Sci* 102:230–236. <https://doi.org/10.1016/j.ejps.2017.03.023>
18. Kolašinac R, Kleusch C, Braun T et al (2018) Deciphering the functional composition of fusogenic liposomes. *Int J Mol Sci* 19. <https://doi.org/10.3390/ijms19020346>
19. Duarte AA, Botelho do Rego AM, Salerno M et al (2015) DPPG liposomes adsorbed on polymer cushions: effect of roughness on amount, surface composition and topography. *J Phys Chem B* 119:8544–8552. <https://doi.org/10.1021/acs.jpcb.5b02384>

20. Ruozzi B, Tosi G, Tonelli M et al (2009) AFM phase imaging of soft-hydrated samples: a versatile tool to complete the chemical-physical study of liposomes. *J Liposome Res* 19:59–67. <https://doi.org/10.1080/08982100802584071>
21. Ricci D, Braga PC (2004) Recognizing and avoiding artifacts in AFM imaging. *Methods Mol Biol* 242:25–37. <https://doi.org/10.1385/1-59259-647-9:25>



# Chapter 24

## Determination of the Subcellular Distribution of Fluorescently Labeled Liposomes Using Confocal Microscopy

Melani A. Solomon

### Abstract

It is being increasingly recognized that therapeutics need to be delivered to specific organelle targets within cells. Liposomes are versatile lipid-based drug delivery vehicles that can be surface modified to deliver the loaded cargo to specific subcellular locations within the cell. Hence, the development of such technology requires a means of measuring subcellular distribution by utilizing imaging techniques that can visualize and quantitate the extent of this subcellular localization. The apparent increase of resolution along the Z-axis offered by confocal microscopy makes this technique suitable for such studies. In this chapter, we will describe the application of confocal laser scanning microscopy (CLSM) to determine the subcellular distribution of fluorescently labeled mitochondriotropic liposomes.

**Key words** Liposomes, Subcellular accumulation, Mitochondria, Confocal microscopy, Z-stacks

---

### 1 Introduction

Most drug delivery approaches are focused on achieving the delivery of the bioactive molecule to specific tissues or specific cells in the tissues. Very recently, there has been an interest in delivering a molecule to its specific subcellular target. Contrary to a prior understanding that delivering a molecule to its target cell is sufficient, it is now recognized that it may be more beneficial to deliver a therapeutic molecule to its intended subcellular target [1]. These subcellular targets may be (a) lysosomes in the case of enzymes for lysosomal storage diseases [2]; (b) mitochondria in the case of mitochondrial deoxyribonucleic acid (DNA) diseases, antioxidants, or the delivery of chemotherapeutic agents that have their site of action in the mitochondria [3]; (c) cytosol for the delivery of small interfering ribonucleic acid (siRNA) and cytotoxic peptides [4]; and (d) nucleus for the delivery of nucleotides, transcription factors, or genome editing strategies, such as the CRISPR-Cas9

system [5]. Liposomes, lipid-based drug delivery systems that consist of an aqueous core and a lipid bilayer membrane, can be surface functionalized with ligands that can enable their delivery to different subcellular targets within the cell [5–10]. The development of potential subcellularly targeted liposomes requires analytical techniques that can track the liposome and/or the delivered cargo in the cell. Fluorescent tracing of the carrier is a technique that has found widespread use in the evaluation of drug delivery platforms. While epifluorescence techniques are useful to determine the overall association of a fluorescently labeled nanocarrier with cells, it lacks the resolution required to discern the location of the particle inside the cell. On the other hand, confocal microscopy offers higher contrast and resolution on the *Z*-axis by utilizing the concept of a spatial pinhole that eliminates the background fluorescence from all surrounding optical planes except the focal plane [11]. With the advent of laser excitation sources, confocal laser scanning microscopy (CLSM) is now a widely used tool to optically section a sample and eventually reconstruct, in 3D, the precise location of the particle in the cell [11]. This technique combined with the use of fluorescent dyes that preferentially accumulate in different organelles of the cell has enabled the study of the subcellular distribution of liposomes. In this chapter, we will describe the preparation of fluorescently labeled liposomes and the determination of the subcellular distribution of liposomes with the mitochondria. We utilize a mitochondriotropic ligand, stearyl triphenylphosphonium (STPP), to prepare mitochondriotropic liposomes and compare the subcellular distribution of these liposomes versus unmodified liposomes. We also verify our results by tracking the cargo of the liposomes, which in this case is Oregon Green®-488 labeled paclitaxel, a fluorescent analog of our intended cargo, paclitaxel. Using similar techniques as described here, the localization of liposomes in different subcellular targets can be studied using dyes specific to the subcellular compartment.

---

## 2 Materials

### 2.1 Liposome Components

1. Lipids: obtain lipids as solutions in chloroform from Avanti Polar lipids (*see Note 1*) and store all lipid solutions at –20 °C until use. Phosphatidylcholine (PC, Mol weight = 760): 25 mg/mL, cholesterol (Chol, Mol weight = 386): 20 mg/mL, and rhodamine (Rh-PE, Mol weight = 1301.7): 1 mg/mL.
2. Stearyl triphenylphosphonium (STPP, Mol weight = 595.6): obtained as a synthesized product as described by Bodappati et al [12].
3. Paclitaxel Oregon Green® 488 conjugate (OG Pxt, Mol wt. 1319.28) obtained as a powder (Molecular Probes,

Eugene, OR, USA). Add 76 µL of methanol to the powder to bring the concentration to 1 mM. Store at –20 °C protected from light and use within 1 month of reconstitution.

4. Sterile phosphate-buffered saline (PBS), 1× (Quality Biological, Gaithersburg, MD, USA).
5. 5 mL glass culture tubes (Fisher Scientific, Pittsburgh, PA, USA).
6. Parafilm.
7. Aluminum foil.

## **2.2 Cell Culture Components**

1. Human breast cancer BT-20 cells (American Type Collection of Cultures, Manassas, VA, USA).
2. Complete cell culture medium (DMEM/10%FBS/1%penicillin-streptomycin): mix 450 mL DMEM media (Corning, NY, USA) with 50 mL of fetal bovine serum (Corning, NY, USA) and 5 mL of penicillin-streptomycin solution (Corning cell-gro®, NY, USA). Sterile filter the mix using a 0.22 µm vacuum filtration system (EMD Millipore, Billerica, MA, USA). Store at 4 °C for up to 6 months.
3. Sterile PBS, 1× (Quality Biological, Gaithersburg, MD, USA).
4. 0.25% trypsin/ethylenediaminetetraacetic acid (EDTA) solution (Corning, NY, USA).
5. Tissue culture plasticware: 5 mL pipettes, 10 mL pipettes, T-25 flasks, 1000 µL barrier tips, 200 µL barrier tips, and 10 µL barrier tips (VWR International, Radnor, PA, USA).
6. Glass coverslips, 22 mm (Fisher Scientific, Pittsburgh, PA, USA): wrap about 30 coverslips in a piece of foil and sterilize them by autoclaving at 121 °C and 15 psi for 15 min (*see Note 2*).
7. 6-well plates (Falcon® Corning, NY, USA) (*see Note 3*).

## **2.3 Dyes**

1. MitoFluor green dye obtained as a 1 mg vial of lyophilized powder (Molecular Probes, Eugene, OR, USA): add 1.65 mL of sterile, anhydrous DMSO to 1 mg of the dye to obtain a solution of 1 mM. Prepare a working dilution of the dye by adding 3 µL of the stock solution to 6 mL complete cell culture medium. Keep the solution protected from light.
2. MitoTracker® Red FM obtained as 50 µg lyophilized powder (Molecular Probes, Eugene, OR, USA): add 69 µL of sterile, anhydrous DMSO to one vial of the dye to obtain a solution of 1 mM. Prepare a working dilution of the dye by adding 1.2 µL of the stock solution to 6 mL complete cell culture medium. Keep the solution protected from light.

3. Hoechst 33342 obtained as a 10 mg/mL solution in water (Thermo Fisher Scientific, Waltham, MA, USA). Prepare a 1 µM solution of Hoechst 33342 by adding 2 µL of the stock to 36 mL of 1× PBS and keep protected from light.

## 2.4 Microscopy

### Components

1. Fine forceps.
2. Frosted slides (VWR International, Radnor, PA, USA).
3. Fluoromount-G® (Southern Biotech, Birmingham, AL, USA).
4. Nail polish.
5. Immersion oil.

## 3 Methods

### 3.1 Preparation of Fluorescently Labeled Liposomes

We prepare unilamellar liposomes using the thin-film hydration technique. A typical liposome preparation is 1 mL at a concentration of 5 mg lipid/mL and contains about 7.7 µmoles of total lipids in the mixture. The molar ratio of the lipids varies for each formulation, as shown in Table 1 (*see Note 4*).

1. Set the temperature of the water bath of the rotary evaporator apparatus to 37 °C.
2. Carefully transfer 5.3 µmoles of PC, 2.3 µmoles of Chol, and 0.04 µmoles of Rh-PE into a 5 mL glass culture tube and lightly mix the contents (*see Note 5*). For preparations that include the drug (Oregon Green Paclitaxel), we prepare 250 µL of total preparation. Hence, scale down the lipid amounts to one fourth of the amount for a 1 mL preparation, transfer 12.5 µL of the 1 mM paclitaxel solution into the tube to obtain a final concentration of 50 µM in the liposome preparation.
3. Mount the culture tube in the rotary evaporator and adjust the height of the apparatus so that the bottom of the tube with the lipids is immersed in the water bath. Evaporate the chloroform

**Table 1**  
Composition and characterization of the liposome formulations

| Liposome  | Composition (molar ratio)               | Size (nm) | Zeta potential (mV) |
|-----------|---|-----------|---------------------|
| Plain     | PC:Chol:Rh-PE (69.5:30:0.5)             | 109 ± 3   | -30 ± 2             |
| Plain-Pxt | PC:Chol(70:30) + 12.5 µL OG Pxt         | 160 ± 2   |                     |
| STPP      | PC:Chol:STPP:Rh-PE (68.5:30:1:0.5)      | 130 ± 1   | 30 ± 5              |
| STPP-Pxt  | PC:Chol:STPP (69:30:1) + 12.5 µL OG Pxt | 179 ± 10  |                     |

in the tube under vacuum while the tube is spinning. This will yield a thin continuous lipid film at the base of the tube once the chloroform evaporates. Verify whether the chloroform has evaporated by checking the absence of chloroform odor in the tube (*see Note 6*).

4. Add 1 mL of PBS 1× to the tube to hydrate the film. For the OG Pxt liposomes, add 250 µL of 1× PBS to the film. Using a probe sonicator (Sonic Dismembrator Model 150, Fisher Scientific, Pittsburgh, PA), set to a continuous pulse mode, sonicate the tube for 10 min; hold for 1 min and sonicate for another 10 min (*see Note 7*). Caution: Wear ear muffs while using the probe sonicator. Ideally, the probe sonicator should be in a hood separate from the main lab work area.
5. Spin the tube at  $1000 \times g$  for 10 min to precipitate any insoluble material, including the titanium shed from the tip of the probe. Wrap the tube in foil to prevent the bleaching of the rhodamine or the OG paclitaxel.
6. Aliquot out three 20 µL samples for particle size determination and estimation of zeta potential. To each aliquot, add 1 mL of water, transfer the mixture to a cuvette, and analyze the size by dynamic light scattering using a particle size analyzer (Brookhaven Instruments Corporation, NY, USA). Thereafter, immerse the zeta electrode in the solution and determine the zeta potential using the Zeta Plus software. Typical sizes observed should be in the range of 100–200 nm with a polydispersity index of less than 0.2. The expected zeta potential of the formulations is shown in Table 1 (*see Note 8*).
7. The liposome preparations are stable for up to 1 week from the date of preparation when stored at room temperature (RT).

### **3.2 Treatment of Cells for Microscopy**

BT-20 cells were maintained in a complete cell culture medium and were used for the assays within 20 passages. Propagate the cells as per American Type Culture Collection (ATCC) instructions.

1. When cells are 80% confluent in a T-25 flask, aspirate the medium from the flask; wash once with 2 mL 1× PBS (sterile), add 2 mL of 0.25% trypsin, and incubate at 37 °C for 5 min to detach the cells from the bottom of the flask (*see Note 9*).
2. While the flask is incubating, using a set of sterile forceps, carefully transfer one coverslip to each well of a 6-well plate (*see Note 10*) and do so for three plates (each of the formulations in triplicate plus one control each (*see Note 11*)) to have a total of 16 coverslips.
3. Add 4 mL of fresh, prewarmed complete cell culture medium to the detached cells and collect the cell suspension into a 15 mL tube. The FBS in the medium will neutralize the trypsin

so that the cells are not disrupted further by the proteolytic enzyme.

4. Using a hemocytometer, count the cells in the suspension and adjust the concentration to 50,000 cells/mL.
5. Transfer 2 mL of the cell suspension to each well of the 6-well plate and let the cells attach for 24 h. Cells should be about 60% confluent before they are treated further for microscopy (*see Note 12*).
6. On the next day, remove the culture medium from the wells and add fresh 1.5 mL complete cell culture medium and 50 µL of the respective liposome preparation. Incubate for 4 h.
7. From the well plates, remove the culture medium containing the liposomes and wash the wells twice with 1× PBS.
8. Add 1.5 mL of the respective working dye solution to each well and incubate for 30 min at 37 °C (*see Note 13*). Keep the plates protected from light.
9. Wash the wells twice with 1× PBS to remove excess dye.
10. Add 1.5 mL of diluted Hoechst solution to each well and incubate at 37 °C for 15 min to stain the nucleus. Wash twice with 1× PBS.
11. Carefully remove each coverslip from the respective well and blot the liquid on the coverslip by holding the edge of the coverslip with Kimwipe.
12. Place a drop of Fluoromount-G® on a slide and carefully place the coverslip (cells facing downward) on the Fluoromount (*see Note 14*). Use the forceps to press down lightly on the coverslip to spread the Fluoromount evenly.
13. Seal the coverslips to the slides by applying nail polish to the edges of the coverslip.
14. Protect the slides from light and immediately proceed to confocal microscopy.

### **3.3 Image Acquisition by Confocal Microscopy**

We use the Zeiss LSM 510 or 700 system for our subcellular distribution analysis. Follow the general guidelines for turning on the microscope and the laser sources and use a setting that will allow the imaging of 4',6-diamidino-2-phenylindole (DAPI, 405 nm excitation, blue emission), fluorescein isothiocyanate (FITC, 488 nm excitation, green emission), and rhodamine (555 nm excitation, red emission) (*see Note 15*).

1. Place a drop of immersion oil on the coverslip.
2. Place the slide with the coverslip facing down on an inverted configuration microscope so that the objective lens touches the coverslip. In an upright microscope, the coverslip should face upward.

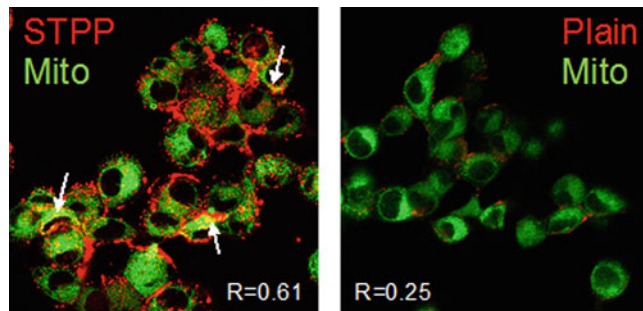


**Fig. 1** Representative composite micrographs of BT-20 cells treated with rhodamine-labeled plain liposomes (Plain) or rhodamine-labeled STPP liposomes (STPP), mitochondria stained green with MitoFluor Green (Mito). The arrows indicate the areas of colocalization, while the *R* values indicate the observed Pearson's correlation coefficient

3. Adjust the focus knobs so that the cells can be seen at 63× magnification (*see Note 16*). Find an area of interest to image.
4. In the ACQUISITION tab of the software, choose the Z-stack mode.
5. Click Live and adjust the exposures of the three channels in the range indicator mode (*see Note 17*).
6. Now, using the focus knob, specify the first slice and the last slice of the stack by looking at the nuclei. Basically, start from the plane where the nuclei begin to appear till the nuclei almost disappear.
7. Adjust the thickness of the optical section based on the degree of resolution required. We generally choose the optimal section that the software computes based on lens magnification and resolution. This is generally 0.35 μm.
8. Once all the parameters are adjusted, click START EXPERIMENT. A typical experiment will take about 4 min to complete (*see Note 18*).
9. Obtain Z-stacks from two to three different regions of each coverslip for analysis. Representative sample images of the distribution of rhodamine-labeled liposomes with MitoFluor Green stained mitochondria are shown in Fig. 1.

### 3.4 Analysis of Subcellular Distribution by Colocalization Analysis

We use ImageJ (National Institutes of Health, Bethesda, MD) to perform colocalization analysis on our images. This software is open access and can be downloaded for both Windows and Macintosh systems from the ImageJ website.

1. Download a plug-in “JACoP” from the ImageJ website and install the plug-in ImageJ.

2. Open the .czi images from the microscope in ImageJ (*see Note 19*). Each image will be in the form of a hyperstack consisting of three channels and several images (corresponding to the number of Z-stacks) in each channel. Note the order of the channels.
3. Now split the single image into three different channels using the Image → Color → Split channels function. The channels can be merged to create a composite at this stage.
4. Using the JACoP plug-in [13], choose the respective image of the corresponding channel and run the macro. One of the values in the result table yields the Pearson correlation coefficient ( $R$ ) (*see Note 20*).
5. Run the macro for each image and obtain the respective  $R$ . Calculate the average and the standard deviation for each formulation and the drug loaded in each formulation (*see Note 21*).

Generally, the  $R$  value for the STPP formulation is significantly higher than the Plain formulation, which indicates a higher degree of colocalization (Fig. 1).

---

## 4 Notes

1. Lipids can be purchased or synthesized as a powder and reconstituted in chloroform to obtain a solution. All the lipids that we use are derived from a natural source, i.e., egg; hence, they are extremely susceptible to oxidation. Hence, store the solution as aliquots, tightly closed, and preferably under a nitrogen atmosphere. Also, tightly seal the vials with parafilm to avoid the evaporation of chloroform.
2. An alternative to sterilizing by autoclaving is to dip the coverslips in a beaker of 70% ethanol and flame sterilize each coverslip inside the biosafety hood.
3. 12-well or 24-well plates may be used with smaller coverslips (18 mm or 15 mm respectively) to conserve reagent and run several samples in one plate. However, a higher degree of skill may be required to manipulate the coverslip at the end of the experiment.
4. A base liposome is considered to be one with a molar ratio of PC:Chol = 70:30. These have been optimized to obtain an adequate balance of stability and phase transition temperature [14]. When introducing other lipids, the molar ratio of cholesterol is kept constant at 30, while the PC molar ratio is adjusted (decreased) to accommodate the other lipids. A decrease of PC below a ratio of 40 is not recommended since that will interfere

with the phase transition temperature and stability of the liposomes, which will then affect the release of the drug from the liposomes [14]. The volume of the liposomes prepared can be scaled down to conserve the reagents, but keep the total concentration of lipids at 5 mg/mL.

5. Due to the low retention of chloroform in the pipette tips, it is better to hold the stock vial and the glass tube close together during transfer to avoid losing the lipid solution. Barrier tips are preferred when pipetting out organic solvents.
6. It is imperative that the chloroform (or other solvent) has completely evaporated so that the lipids when hydrated will form a good liposome preparation. This will take approximately 25 min.
7. Make sure that the tip of the sonicator is in the center of the tube and not touching the sides. Also, adjust the level of sonication so that no bubbles are formed in the tube. The highest level at which a steady, shrill sound is heard with minimal liquid movement is the ideal setting.
8. We use the zeta potential of the liposomal preparations as a quality control parameter and not as an estimate of the absolute surface charge.
9. The optimal incubation time with trypsin required to detach the cells from the flask needs to be determined empirically for each cell line. Check the flask every 2 min for detached cells. Gentle mechanical agitation by rapping on the side of the flask can also help dislodge the cells from the flask bottom.
10. An alternative method to transfer the coverslips is by using a Pasteur pipette attached to the vacuum supply tube. Turn on the suction and use the Pasteur pipette to lift one coverslip and place the coverslip into the well by tapping it against the edge of the well.
11. Adequate controls for fluorescence microscopy experiments include incubating the cells with only one of the fluorophores (rather than the combination used for the experiment) to make adjustments for any bleed-through in the other channels. In this case, the controls include one well each stained with the following fluorophores alone: MitoTracker® Red, MitoFluor Green, Plain liposomes, STPP liposomes, Plain-Pxt liposomes, and STPP-Pxt liposomes. Each of the control wells should be treated in the exact same manner as the respective treatment conditions of the experiment wells. During imaging, these single-stained coverslips should be used to adjust the exposure settings so that the particular fluorophore will only emit fluorescence in the specific channel and not in the other channels; e.g., the MitoTracker Red treated coverslip should exhibit

fluorescence in the red channel but not in the green or blue channel.

12. Most mammalian cells will adhere to glass coverslips and grow well. However, some cells, e.g., human umbilical vein endothelial cells (HUVECs), neuronal cells, etc., will not attach well to the glass. Hence, the coverslip can be treated with either poly-D-lysine (PDL) or 1% gelatin solution before seeding the cells. For treating with PDL, add 200 µL of PDL solution in PBS to each coverslip surface and incubate at 37 °C for 2 h, following which wash the coverslips with PBS and allow to air-dry. For treating with gelatin, add 200 µL of 1% gelatin solution to each coverslip surface and incubate at RT for 1 h, following which wash the coverslips with PBS and allow to air-dry for 1 h.
13. The concentration of the dye and the incubation time to optimally stain the mitochondria will vary for each cell line and will need to be optimized. Before conducting a full-fledged experiment, these conditions must be determined empirically.
14. Other mounting media, such as ProLong Gold antifade reagent and Mowiol, are not very useful in this case since we do not fix our cells but image them within 2 h of mounting.
15. If the microscope is only equipped with one photomultiplier tube (PMT), best-quality images with minimum bleed-through are obtained if the channels are imaged sequentially. If the microscope is equipped with two PMTs, it is feasible to image the blue and red channels together since their spectra are sufficiently apart so as not to interfere with each other. However, the green channel should always be imaged separately to avoid interference with the red channel.
16. It may help to start by focusing the cells at a lower magnification and then move on to the higher magnification lens.
17. The range indicator mode will display the channels as gray-scale images. Make sure there are no red pixels in the image, which are indicative of saturation. Also, ensure that the background (noise) appears blue.
18. Based on the number of stacks and resolution specified, the time of acquisition will vary. Fourteen to sixteen stacks for a cell monolayer at 0.35 µm and 512 × 512 resolution will take 4–5 min.
19. If the images do not open in ImageJ, install the Bio-Formats plug-in from ImageJ, save it into the plug-ins folder, and restart ImageJ. This should enable .czi files to open.
20. JACoP (Just Another Colocalization Plugin) offers a more robust estimate of the correlation coefficient compared to older plug-ins, such as colocalization finder and colocalization

threshold. The iterative methods that determine the thresholding are beneficial in avoiding artifacts that can arise due to the random spatial orientation of pixels in each channel. Although we use Pearson's correlation coefficient ( $R$ ) for our analyses, the other parameters, such as the correlation graph and other correlation coefficients, should also be used to guide one's judgment about the validity of  $R$ .

21. Pearson's correlation coefficient ( $R$ ) determines the correlation of intensities between the red and green pixels.  $R = 1$  indicates a perfect correlation, while a negative  $R$  indicates a lack of correlation. Colocalization is indicated by the degree of correlation. We use  $R$  as a relative indicator of the colocalization only for comparison between formulations and not as an absolute value that describes the characteristic of the formulation.
22. We have established our method for determining the subcellular distribution of liposomes in the mitochondria. Using similar techniques, the distribution of liposomes to the lysosomes can also be studied using lysotracker dyes that preferentially accumulate in the acidic environment of the lysosomes in live cells. We do not fix our cells prior to imaging; however, some applications that require the precise measurement of endocytic mechanisms may require fixations of the cells. In this case, however, the mitotracker or lysotracker dyes used to stain mitochondria or lysosomes in live cells will not suffice since they are not fixable, or even when they claim to be fixable, they do not yield a sufficiently intense signal. In these cases, antibodies toward specific compartments can be utilized following fixation with 4% paraformaldehyde and permeabilization with 0.2% Triton X-100.

## References

1. Rajendran L, Knolker HJ, Simons K (2010) Subcellular targeting strategies for drug design and delivery. *Nat Rev Drug Discov* 9(1):29–42
2. Solomon M, Muro S (2017) Lysosomal enzyme replacement therapies: historical development, clinical outcomes, and future perspectives. *Adv Drug Deliv Rev* 118:109–134
3. Yamada Y, Satrialdi HM, Sasaki D, Abe J, Harashima H (2020) Power of mitochondrial drug delivery systems to produce innovative nanomedicines. *Adv Drug Deliv Rev* 154–155:187–209
4. Khan MM, Filipczak N, Torchilin VP (2021) Cell penetrating peptides: a versatile vector for co-delivery of drug and genes in cancer. *J Control Release* 330:1220–1228
5. Senger K, Haley B (2021) Non-viral alternatives to delivery of CRISPR-Cas gene editing Componenets. In: Vaschetto LM (ed) CRISPR-/Cas9 based genome editing for treating genetic disorders and diseases. CRC Press, Boca Raton, pp 183–223
6. Benien P et al (2015) Hydrophobized triphenyl phosphonium derivatives for the preparation of mitochondriotropic liposomes: choice of hydrophobic anchor influences cytotoxicity but not mitochondriotropic effect. *J Liposome Res* 26:1–7
7. Kohli AG, Kierstead PH, Venditto VJ, Walsh CL, Szoka FC (2014) Designer lipids for drug delivery: from heads to tails. *J Control Release* 190:274–287

8. Bayat F, Hosseinpour-Moghadam R, Mehryab F, Fatahi Y, Shakeri N, Dinarvand R, Ten Hagen TLM, Haeri A (2020) Potential application of liposomal nanodevices for non-cancer diseases: an update on design, characterization and biopharmaceutical evaluation. *Adv Colloid Interf Sci* 277: 102121
9. Solomon MA, Shah AA, D'Souza GG (2013) In vitro assessment of the utility of stearyl triphenyl phosphonium modified liposomes in overcoming the resistance of ovarian carcinoma Ovarc-3 cells to paclitaxel. *Mitochondrion* 13(5):464–472
10. Thekkedath R, Koshkaryev A, Torchilin VP (2013) Lysosome-targeted octadecyl-rhodamine B-liposomes enhance lysosomal accumulation of glucocerebrosidase in Gaucher's cells in vitro. *Nanomedicine (Lond)* 8(7):1055–1065
11. Bayguinov PO, Oakley DM, Shih CC, Geanon DJ, Joens MS, Fitzpatrick JA (2018) Modern laser scanning confocal microscopy. *Curr Protoc Cytom* 85(1):e39
12. Boddapati SV et al (2005) Mitochondriotropic liposomes. *J Liposome Res* 15(1–2):49–58
13. Bolte S, Cordelieres FP (2006) A guided tour into subcellular colocalization analysis in light microscopy. *J Microsc* 224(Pt 3):213–232
14. Briuglia ML, Rotella C, McFarlane A, Lamprou DA (2015) Influence of cholesterol on liposome stability and on in vitro drug release. *Drug Deliv Transl Res* 3:231–242



# Chapter 25

## Liposome Biodistribution via Europium Complexes

Nathalie Mignet and Daniel Scherman

### Abstract

Vector biodistribution is a requirement prior pharmaceutical development. Radioactive tracers allow the most sensitive and quantitative assessment of biodistribution, and conventional fluorophores are widely used in academic laboratories. We propose here to use europium complexes as a label for nanoparticles or biotherapeutics taking liposomes as models. Time-resolved fluorimetry (TRF) has the tremendous advantage of taking into account the fluorescence decay time of the lanthanide chelates, resulting in an improved sensitivity in biological media. The work described aimed following liposome biodistribution by TRF. An octadecyl-DTPA.Eu compound has been prepared and incorporated into liposomes without altering its fluorescence signal. The method has been validated through a comparison with fluorophore-labeled liposomes. The way to proceed when using this method for liposome biodistribution assessment is detailed. It could obviously be applied to other nanosystems, such as lipid nanoparticles.

**Key words** Liposomes, Europium, Time-resolved fluorimetry, Fluorescence, Pharmacokinetics

---

### 1 Introduction

The field of vectorization represents a major goal in formulating drugs, modifying their pharmacokinetic profile, or reducing their toxicity. Hence, following the distribution of the vector is of major interest; however, only a few methods are available for this purpose. Unless the intrinsic properties of the vector allow detecting it, a tracer should be incorporated into the vector. This tracer should be stable, not be released in biological media, and not be exchangeable with lipidic membranes, in the case of a tracer-bearing lipid.

More sensitive tracers so far have been radiolabeled ( $^{14}\text{C}$ ,  $^1\text{H}$ ) and used for liposome biodistribution studies. These tracers are also advantageous since they do not interfere with the liposome bilayer, which fluorophores could do. However, performing experiments with radioactive tracers requires legal authorization and involves experimental constraints, such as safety cautions and waste processing.

Spectrofluorescence is an easier method to handle in the laboratory. Incorporating commercially available labeled lipids into liposomes allowed following them after systemic injection in mice [1]. We used this method by incorporating phosphatidylethanolamine-fluorescein or phosphatidylethanolamine-rhodamine in cationic lipid/deoxyribonucleic acid (DNA) complexes and improved the extraction process to recover the whole lipoplex content injected in the blood [2]. This method is simple and reproducible but requires the extraction of lipids with organic solvents from the biological media to improve the signal-to-noise ratio.

We developed an original method that combines sensitivity in biological media and versatility as it does not require any treatment of the biological tissue in organic solvents. Lanthanides are an interesting class of compounds, thanks to their intrinsic properties, large Stokes shift, narrow emission peak, and optimal emission wavelength, which allow using time-resolved fluorimetry, useful for biological media. Lanthanides suffer from low molar extinction coefficients, but chelates of lanthanides have been developed to transfer energy to the lanthanide ions and limit this drawback. The ability to measure delayed fluorescence in biological media allows getting rid of the medium background and solely measuring the lanthanide-chelate signal. The use of lanthanide chelates for *in vitro* assays has been more studied than the use of *in vivo* tools. Recently, an immunoassay for SARS-COV-2-RNA was proposed [3]. The use of lanthanide-chelates for liposomes or protein detection *in vivo* is less obvious even though it has been reported by us and others [4–6]. Lipid-based chelates have also been shown to amplify the lanthanide signal [7–10]. Based on these previous results, we chose to use lipid-based lanthanide chelates and incorporate them into liposomes. The method to measure directly these liposomes in biological media was worked out. Then the biodistribution of these liposomes post systemic injection was evaluated and compared to rhodamine-labeled liposomes to validate the assay.

---

## 2 Materials

### 2.1 Abbreviations Used

PEG: polyethylene glycol, EPC: egg-phosphatidylcholine, DTPA: diethylenetriaminepentaacetic acid, MRI: magnetic resonance imaging, Eu: europium, DMEM: Dulbecco's Modified Eagle Medium, FBS: fetal bovine serum.

### 2.2 Chemicals Provided or Synthesized

Egg-phosphatidylcholine (EPC), phosphatidylethanolamine rhodamine, phosphatidylethanolamine-poly(ethylene glycol)<sub>45</sub>, and filters for the extruder were purchased from Avanti Polar Lipids. Cholesterol, chloroform, HEPES, Dulbecco's Modified Eagle Medium, and fetal bovine serum were purchased from Sigma. The centrifugal concentrator was purchased from Millipore. The

octadecyl-DTPA used for this study was prepared in three steps from stearic acid, as described by Mignet et al. [11].

### 2.3 Equipment

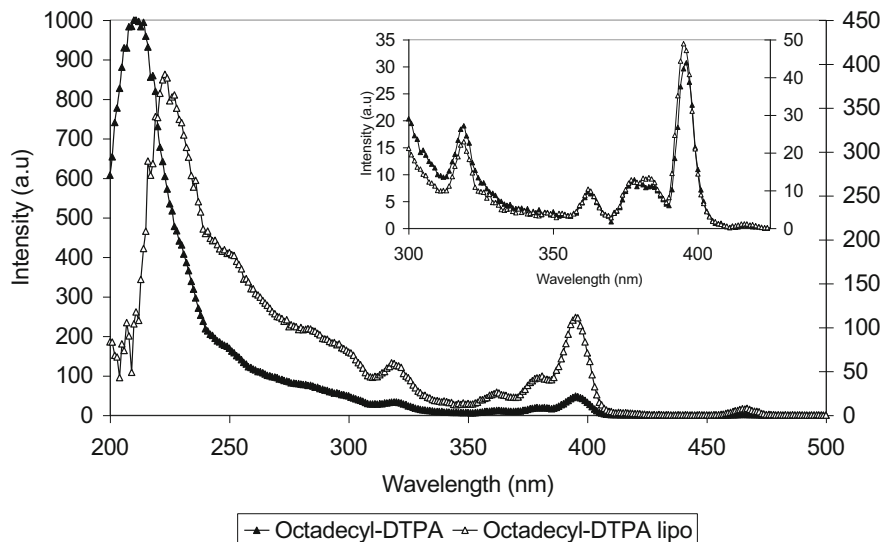
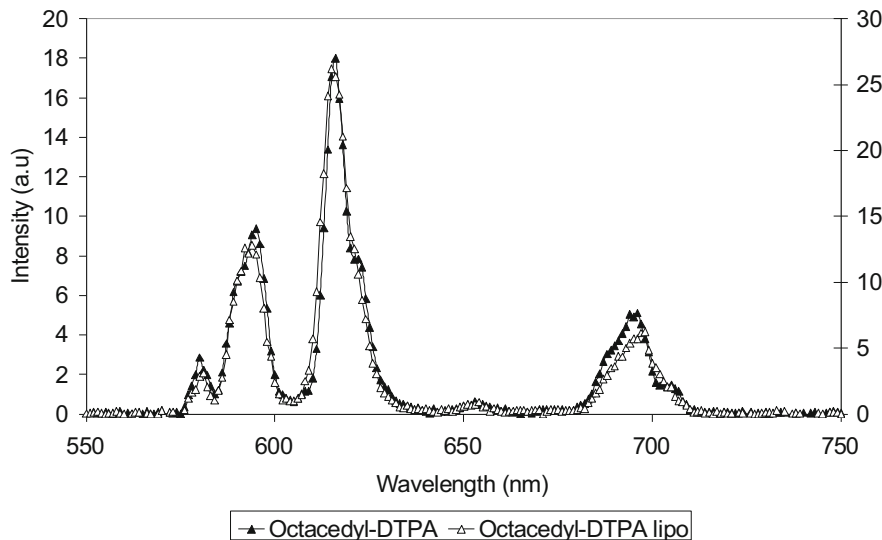
1. Liposomes were prepared through the film method with the use of a rotary evaporator (Heidolph, VWR) equipped with vacuubrand CVC2 to control pressure.
2. *Avanti* Mini-Extruder from Avanti Polar Lipids, Inc.
3. Size and zeta potential measurements were performed on a Zeta Sizer NanoSeries from Malvern Instruments equipped with a 632.8 nm helium-neon laser, 5 mW power, and an angle detection at 173° (noninvasive backscattering).
4. The centrifugator used was Megafuge 1.0 from Heraeus Sepatech.
5. Time-delayed fluorescence was measured on a multilabel plate reader (Wallac Victor2 1420 Multilabel Counter, PerkinElmer, France). The TRF program for europium performs 1000 pulses/sec with excitation light at 320 nm. In the period between flashes, the 615 nm fluorescence of the sample is measured for 400 µs, which allows short-time fluorescence to decay. The photons counted during 1 s were recorded and expressed as counts per second (cps).
6. Phosphorescence spectra were performed on a Varian Cary Eclipse fluorescence spectrophotometer using the phosphorescence mode.

---

## 3 Methods

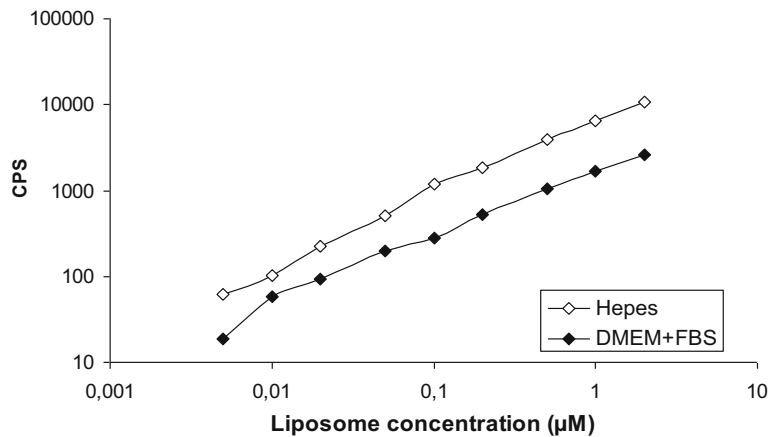
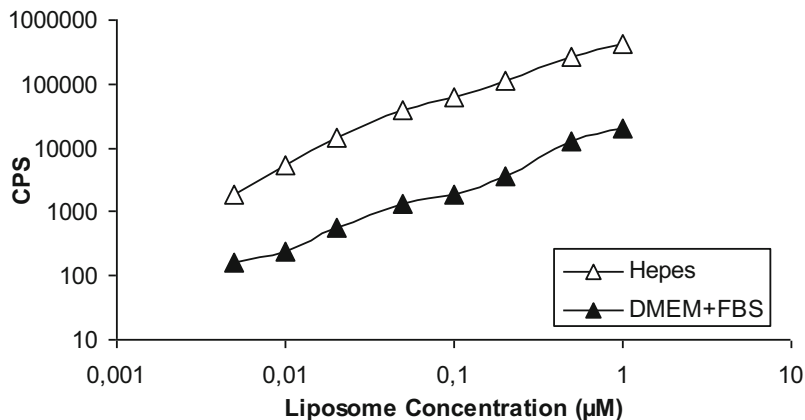
Diethylenetriaminepentaacetic acid (DTPA) is a widely used chelate for a lanthanide, such as europium [12]. We chose to use a lipid bearing the DTPA moiety in order to easily incorporate it into liposomes via hydrophobic interactions between the carbon chains. The DTPA moiety is a big molecule, and the insertion of this lipid, as for all kinds of labeled lipids, into the liposome bilayer might modify the liposome structure, and a first study on the liposome's integrity had to be performed. For this purpose, we did evaluate different kinds of lipids bearing DTPA, such as cholesterol-DTPA and octadecyl-DTPA [10] to follow conventional liposomes. We had also previously developed a cationic spermine-DTPA [13] to introduce it into cationic lipoplexes and follow the biodistribution of these particles using magnetic resonance imaging (MRI). Indeed, the DTPA moiety is able to condense different ions, such as gadolinium, which is a contrast agent used in MRI, and also europium, useful for time-resolved fluorimetry [14].

After lipid-DTPA.Eu insertion into liposomes, the size of the liposome formed was first evaluated through dynamic light scattering, and then excitation and emission phosphorescence

**A****B**

**Fig. 1** Influence of the insertion of octadecyl-DTPA-Eu in liposomes as compared to the free octadecyl-DTPA-Eu on the excitation (a) and emission (b) spectra. The emission spectrum is unchanged when the lipid is inserted in the liposome bilayer. In contrast, the excitation spectrum presents some differences. The characteristic signal of europium [14] at 320 and 396 remain at the same position, but their level is increased upon lipid incorporation. (Reproduced with permission from ref. [11])

measurements were performed to ensure that the europium signal was not modified by the insertion of the lipid [16] (Fig. 1). A liposome concentration range in buffers and biological media was searched to ensure that this label would be useful for *in vivo*

**Medium influence on Europium labelled liposome detection****Medium influence on Rhodamine labelled liposome detection**

**Fig. 2** Influence of the medium on the detection of liposomes. The liposomes were incubated in HEPES 10 mM or DMEM+10% FBS and fluorescence read, either direct fluorescence to read rhodamine content or delayed fluorescence to read europium content. One can see that for the same concentration of liposomes, bearing the same amount of lipid rhodamine or lipid DTPA.Eu, the level is lower when the liposome contains lipid-DTPA.Eu. One can also notice that the fluorescence level is far less influenced by the medium if the liposome is labeled with lipid DTPA.Eu. The fluorescence loss between HEPES and DMEM+SFV was measured as factor  $3 \pm 1$  for the Eu-labeled liposomes and factor  $26 \pm 5$  for the rhodamine-labeled liposomes

experiments. The influence of the biological media on the signal of rhodamine- and europium-labeled liposomes was also evaluated. We could show that the loss on fluorescence was a factor 25, while the loss on time-delayed fluorescence was only a factor 3 when liposomes were incubated in HEPES or a medium containing serum (Fig. 2). Finally, the method was validated for biodistribution experiments by comparing the biodistribution of conventional

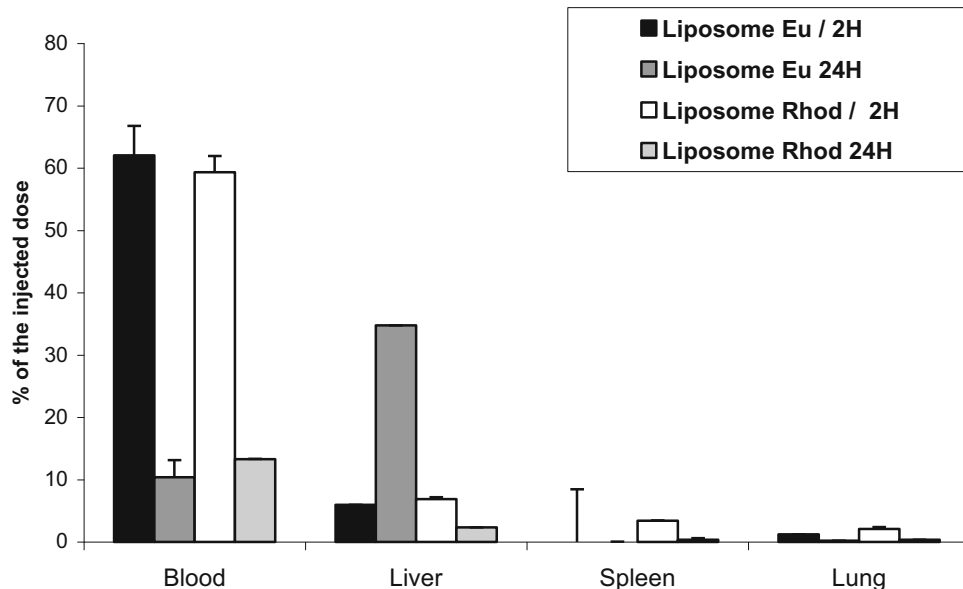


**Fig. 3** Comparison of the biodistribution of rhodamine- and europium-labeled liposomes at 2 and 24 h post systemic injection into C57/Bl6 mice. The levels obtained are comparable to what was previously reported for similar isotopically labeled liposomes [15]

liposomes labeled with a rhodamine lipid and identical liposomes labeled with the octadecyl-DTPA.Eu compound. The data obtained for both liposomes were very similar and correlated with a similar liposome isotopically labeled, which was previously reported (Fig. 3).

### 3.1 Lipid Labeling

- Octadecyl-DTPA is dissolved in H<sub>2</sub>O (1.5 μmol, 1 mg/mL) (*see Notes 1 and 2*).
- Add EuCl<sub>3</sub>,6H<sub>2</sub>O (7.5 μmol, 2.7 mg) to the lipid and stir overnight.
- Separate the excess EuCl<sub>3</sub>,6H<sub>2</sub>O in excess through centrifugal filtration. Load the complex formed on a centrifugal concentrator equipped with a 5 kD polyethersulfone (PES) membrane. Add 4 mL of H<sub>2</sub>O. Centrifuge at 2000 G for 2 min (*see Note 3*) and repeat the operation until no more europium could be detected in the filtrate (*see Note 4*).
- Check whether the lipid is well labeled by taking a sample and reading the associated level of fluorescence as compared to the nonlabeled lipid and the background of EuCl<sub>3</sub>,6H<sub>2</sub>O (*see Note 5*).

### 3.2 Preparation of the Conventional Liposomes Labeled with Europium

- Dissolve separately the lipids egg-phosphatidylcholine (15 μmol, 12 mg), cholesterol (10 μmol, 3.8 mg), and octadecyl-DTPA.Eu (1.5 μmol, 1.5 mg) and phosphatidylethanolamine-poly(ethylene glycol)<sub>45</sub> (1.5 μmol, 4 mg) in chloroform (400 μL for the lipids, 200 μL for the

PEG-lipid). Take care that the lipids are well dissolved separately before mixing them (*see Note 6*).

2. Mix them in a round-bottom flask (10 mL) (*see Note 7*).
3. Put the flask at the rotary evaporator to remove the solvent in a pressure-controlled manner. First, reduce the pressure from 1000 to 200 mbar in approximately 15 min with a middle rotation speed. When the drop forms, increase the rotation speed at its maximum level to drag the drop into the film. Then reduce the pressure from 200 to 5 mbar in 30 min and leave the film under reduced pressure for an additional hour (*see Note 8*).
4. The film being dry, add 1 mL (to afford a final concentration of 28 mM) Milli-Q filtered (0.22 µm) H<sub>2</sub>O and leave the flask under gentle rotation overnight at room temperature (*see Note 9*).
5. Mix gently the mixture on a vortex if the film is not fully detached from the wall.
6. Extrude the liposome ten times successively using polycarbonate filters of 0.44 and 0.22 µm.
7. Control the size through dynamic light scattering. For measurements on a NanoZS (Malvern Instruments), dilute 5 µL of the particles obtained in a 500 µL cuvette and start measuring in the automatic mode. The liposomes should have a size of around 100 nm with a poor polydispersity index (*see Note 10*).

### **3.3 Preparation of the Conventional Liposomes Labeled with Rhodamine**

The same protocol as in Subheading 3.1 was used. Only octadecyl-DTPA.Eu was replaced by phosphatidylethanolamine rhodamine in the same proportions.

### **3.4 Phosphorescence Spectra**

1. Prepare a cuvette containing the octadecyl-DTPA.Eu lipid and another containing europium-labeled liposomes. Put the same amount of europium in both cuvette.
2. In the phosphorescence mode of the system, choose  $\lambda_{\text{em}} = 616$  nm, delay time: 0.1 ms, and gate time: 5 ms; ensure band pass is fixed at 10 nm (*see Note 11*); and scan an excitation spectrum.
3. In the phosphorescence mode of the system, choose  $\lambda_{\text{ex}} = 396$  nm, delay time: 0.1 ms, and gate time: 5 ms; ensure that band pass is fixed at 10 nm; and scan an emission spectrum.
4. Compare the excitation and emission scans of the lipid and the liposome.

**3.5 Test in Buffers**

1. Prepare a concentration range of liposomes to evaluate a straight concentration range useful for quantification (*see Note 12*).
2. Dilute it in the medium of interest for the time of interest. For the measurements presented in Fig. 2, liposomes were diluted in HEPES 10 mM and DMEM+FBS 10% and measured without any incubation.
3. Read the fluorescence level. For phosphorescence, use either of these:  $\lambda_{\text{ex}} = 396$  nm,  $\lambda_{\text{ex}} = 616$  nm, delay time: 0.1 ms, gate-time: 5 ms, and band pass fixed at 10 nm on the Varian Eclipse spectrophotometer or  $\lambda_{\text{ex}} = 320$  nm,  $\lambda_{\text{ex}} = 615$  nm, delay time: 0.4 ms, gate time: 0.4 ms, and 1000 pulses/sec on a multilabel plate reader (Wallac Victor2 1420 Multilabel Counter, PerkinElmer) (the last program used for the measurements is presented in Fig. 2).

For fluorescence, the rhodamine level was read using  $\lambda_{\text{ex}} = 550$  nm and  $\lambda_{\text{ex}} = 590$  nm, with band pass fixed at 5 nm, on the Varian Eclipse spectrophotometer or using filters  $\lambda_{\text{ex}} = 535 \pm 10$  nm and  $\lambda_{\text{ex}} = 570 \pm 10$  nm on the multilabel plate reader Wallac Victor2 (PerkinElmer).

**3.6 Biodistribution In Vivo (See Note 13)**

1. Mice administration: anesthetize the C57Bl/6 mice (Janvier) through intraperitoneal injection of a mix of ketamine (85.8 mg/kg, Centravet) and xylazine (3.1 mg/kg, Bayer) diluted in 150 mM NaCl.
2. Inject europium-labeled liposomes (2  $\mu\text{mol}$ , 200  $\mu\text{L}$ ) or rhodamine-labeled liposomes (2  $\mu\text{mol}$ , 200  $\mu\text{L}$ ) into the mouse tail vein.
3. Euthanize the first group of mice, 2 h post-injection, and the second group 24 h post-injection.
4. Collect the plasma through cardiac puncture.
5. Collect and weigh the liver, spleen, and lungs.
6. Homogenize the organs in pH 7.4 PBS using Ultra Thurax (Dixx 600, Heidolph, Fisher).
7. For europium-labeled lipids, read directly the level of fluorescence in the plasma through TRF with a spectrofluorometer (Victor, PerkinElmer).
8. For europium-labeled lipids in tissue, incubate the tissue homogenates at 2.5 mL/g in a lysis buffer (Roche) 1× (1/1, v/v). Mix it vigorously overnight. Centrifuge (1000 rpm, 5 min).
9. Assay fluorescence intensity on the supernatant through TRF.
10. Perform a calibration curve in each different tissue with the labeled liposomes (*see Note 14*).

11. Calculate the amount of liposomes in the plasma or tissue homogenates with the calibration curve performed in the tissues of interest and expressed as the remaining percentage of injected dose.
12. For rhodamine-labeled lipids, extract the blood or tissues with 3 mL methanol/chloroform (1/1, v/v) through vigorous mixing for 30 min in the blood and overnight for the tissue homogenates. Centrifuge at 3000 rpm for 10 min. Assay the supernatant for rhodamine using  $\lambda_{\text{ex}} = 550$  nm and  $\lambda_{\text{em}} = 590$  nm wavelengths. Perform a calibration curve in each different tissue with the labeled liposomes. Calculate the amount of liposomes in the plasma or tissue homogenates with the calibration curve performed in the tissues of interest and expressed as the remaining percentage of injected dose.

---

#### 4 Notes

1. All buffers and water used should be filtered on 0.22  $\mu\text{m}$  filters since any dust might interfere with the light scattering experiments.
2. Pay attention to the pH. The DTPA lipid will precipitate while the pH remains too acidic. pH has to be adjusted to pH 7 through a dropwise addition of 15  $\mu\text{L}$  NaOH (0.1 M).
3. Adjust the centrifugation speed and length by checking if the lipid is not dry; a minimum of 200  $\mu\text{L}$  should remain to recover it properly.
4. Take a sample (200  $\mu\text{L}$ ) of the filtrate and load it on a 96-well plate (it could be a 1 mL sample in a cuvette) to read the europium content in the filtrate. To increase the signal, you could add ethylenediaminetetraacetic acid (EDTA) in the well (or in a cuvette) to complex Eu.
5. To give an idea of the level range, with the spectrofluorimeter used (Victor, PerkinElmer), we obtained around 3000 CPS at 5  $\mu\text{M}$  lipid.
6. The solubility of the lipids should be checked with intensive care since the presence of nonsoluble entities will appear in the film and reduce particle homogeneity after hydration.
7. The ratio between the volume to be reduced (or the amount of lipids) and the round bottom flask is important since the film should occupy as much flask wall as possible. On the surface of the flask occupied by the film will depend the number of layers in the liposomes.
8. Make sure that the film is not crackled because of too rapid reduction of pressure. If so, dissolve again the lipids in 1 mL

$\text{CHCl}_3$  and start again at **step 3**, Subheading 3.2. It is always preferable to obtain a homogeneous film along the flask wall as this will provide a more homogeneous liposome size after the hydration step.

9. Evaporation and hydration time are usually reported as shorter, but we have found that taking time to do these steps are required to form homogeneous liposome sizes.
10. The polydispersity index reflects the homogeneity of the suspension. It is less than 0.1 for standards such as latex; it should be lower than 0.2 to have homogeneous liposomes.
11. Adjust the band pass according to the signal (dependent on the amount put in the cuvette). If the signal saturates, reduce the band pass or dilute the sample. If the signal is too low, increase the band pass or concentrate the sample.
12. A straight concentration range of interest for the in vivo studies was determined from 10 nM to 1  $\mu\text{M}$  for europium- and rhodamine-labeled liposomes (Fig. 2).
13. Experiments should be conducted following National Institutes of Health (NIH) recommendations and in agreement with a regional ethic committee for animal experimentation. A number is provided upon project presentation, in our case n° P2.PB003.04.
14. The signal of the europium complexes is highly dependent on the environment; a calibration curve should be performed in each medium of interest.

## References

1. Takeuchi H, Kojima H, Yamamoto H, Kawashima Y (2001) Evaluation of circulation profiles of liposomes coated with hydrophilic polymers having different molecular weights in rats. *J Control Release* 75:83–91
2. Nicolazzi C, Mignet N, de la Figuera N, Cadet M, Torero R, Seguin J, Bessodes M, Scherman D (2003) Anionic poly(ethyleneglycol) lipids incorporated into cationic lipoplex increase their circulation time in the blood. *J Control Release* 88:429–443
3. Duan Y, Wang S, Zhang Q, Gao W, Zhang L (2021) Nanoparticle approaches against SARS-CoV-2 infection. *Curr Opin Solid State Mat Sci* 25:100964
4. Laukkonen ML, Orellana A, Keinänen K (1995) Use of genetically engineered lipid-tagged antibody to generate functional europium chelate-loaded liposomes. Application in fluoroimmunoassay. *J Immunol Methods* 185: 95–102
5. Neville M, Richau K, Boni L, Pflug L, Robb R, Popescu M (2000) A comparison of biodistribution of liposomal and soluble IL-2 by a new method based on time-resolved fluorimetry of europium. *Cytokine* 12:1702–1711
6. Salmon H, Gahoual R, Houzé P, Ibrahim T, Bessodes M, Scherman D, Seguin J, Mignet N (2019) Europium labeled lactosylated albumin as a model workflow for the development of biotherapeutics. *Nanomedicine* 18:21–30
7. Jørgensen CK (1962) Electron transfer spectra of lanthanide complexes. *Mol Phys* 5:271–277
8. Roy B, Santos M, Mallik S, Campiglia A (2003) Synthesis of metal-chelating lipids to sensitize lanthanide ions. *J Org Chem* 68:3999–4007
9. Marchi-Artzner V, Brienne MJ, Gulik-Krzywicki T, Dedieu JC, Lehn JM (2003) Selective complexation and transport of europium ions at the interface of vesicles. *Chem Eur J* 10:2342–2350

10. Faulkner S, Pope S, Burton-Pye B (2005) Lanthanide complexes for luminescence imaging applications. *Appl Spectrosc Rev* 40:1–41
11. Mignet N, le Masne de Chermont Q, Randrianarivelo T, Seguin J, Richard C, Bessodes M, Scherman D (2006) Liposome biodistribution by time resolved fluorimetry of lipophilic europium complexes. *Eur Biophys J* 35:155–161
12. Weinmann H, Brasch R, Press W, Wesbey G (1984) Characteristics of gadolinium-DTPA complex: a potential NMR contrast agent. *Am J Roentgenol* 142:619–624
13. Leclercq F, Cohen-Ohana M, Mignet N, Herscovici J, Scherman D, Byk G (2003) Design, synthesis and evaluation of gadolinium cationic lipids as tools for biodistribution studies of gene delivery complexes. *Bioconjug Chem* 14:112–119
14. Elster A, Jackels S, Allen N, Marrache R (1989) Dyke Award. Europium-DTPA: a gadolinium analogue traceable by fluorescence microscopy. *Am J Neuroradiol* 10:1137–1144
15. Parker D, Dickins R, Puschmann H, Crossland C, Howard J (2002) Being excited by lanthanide coordination complexes: aqua species, chirality, excited-state chemistry, and exchange dynamics. *Chem Rev* 102:2389–2403
16. Parr M, Ansell S, Choi L, Cullis P (1994) Factors influencing the retention and chemical stability of poly(ethylene glycol)-lipid conjugates incorporated into large unilamellar vesicles. *Biochim Biophys Acta* 1195:21–30



# Chapter 26

## Quantification of a Fluorescent Lipid DOPE-NBD by an HPLC Method in Biological Tissue: Application to Study Liposomes' Uptake by Human Placenta

Louise Fliedel, Nathalie Mignet, Thierry Fournier, Karine Andrieux, and Khair Alhareth

### Abstract

Nanomedicine offers the possibility of modifying the distribution of encapsulated drugs and biomolecules. Nanomedicine could limit the transplacental passage and/or enhance the concentration of drugs in placental tissue; this approach could be exploited for the treatment of pregnancy disorders. In the context of pregnancy, tackling the biological fate of both the nanocarrier and the drug has high importance in ensuring both the mother's and the fetus' safety.

In this study, we propose a method for quantifying the uptake of liposomes inside placental tissue using covalently labeled liposomes and adapting a high-performance liquid chromatography (HPLC) method using a fluorescent detector. An optimized protocol for liquid-liquid extraction of fluorescent lipids from placental tissue extracts, followed by HPLC analysis, is detailed in this chapter. The HPLC method allows the quantification of fluorescent lipids using a calibration curve, including the biological matrix and extraction procedures. The internalization rate of fluorescent liposomes within human villous placental explants was quantitatively assessed, thanks to the HPLC developed method and suitable analytical tools.

**Key words** Placenta, HPLC, Fluorescence, Liposomes, Ex vivo model, Placental explants

---

### 1 Introduction

The use of nanomedicines for pregnancy-associated disorders raised an important interest in the last years [1–5]. Many types of nanoparticles have been suggested as drug delivery systems for limiting transplacental passage and/or placental targeting. Liposomes appear as promising nanocarriers for this application. Liposomes enable the specific delivery of drugs and therefore ensure safety and efficacy of their usage for pregnant women [6–8].

The communication between the mother and the fetus is governed by the placenta, which connects maternal and fetal blood circulations. The privileged contact between maternal blood and

fetal cells enhances the possible interactions between nanoparticles administered to the mother and the placenta [9–14]. This could be exploited to treat several pregnancy disorders with placental origin. For this specific application, where safety is the main concern, tracking both the nanocarrier and the active pharmaceutical ingredient (API) provides essential information regarding their placental uptake and potential transplacental passage. Fluorescence labeling is one of the strategies to follow nanocarriers in biological media. Fluorescent dyes can be integrated during nanocarrier formulation and enables a specific and highly sensitive tracking of the nanoparticles.

In our previous studies, dually labeled PEGylated liposomes were evaluated on both villous placenta explants and dually perfused placenta models. The carrier contained a lipid that is conjugated to rhodamine and encapsulated carboxyfluorescein, a fluorescent molecule used as a model. Using confocal microscopy, semi-quantitative data on liposome penetration into the external layer of placental villi, the syncytiotrophoblast, were obtained. No detectable passage of fluorescent lipid in the fetal circulation was confirmed using a specific dosage of fluorescent lipid in an aqueous medium. Moreover, the localization of the fluorescent probe in villous explants was concordant with transplacental passage ability. This preliminary work demonstrated that the villous placenta explant model is a relevant model to evaluate the ability of liposomal formulation to penetrate and cross the placental tissue [15]. In a recent study, we developed a high-performance liquid chromatography (HPLC) quantification assay to evaluate the amount of fluorescent liposomes internalized inside villous placental explants. For this purpose, the fluorescent lipid called DOPE-NBD was used to label liposomal formulations, which were then incubated with human villous explants. A liquid-liquid extraction was optimized and validated to extract DOPE-NBD from placenta tissues, and the resulting biological samples were then analyzed using the developed HPLC method [16].

In this chapter, methods are detailed and applied to quantify the uptake of neutral and cationic liposomes inside the placenta using an ex vivo human villous placental explant model. First, liposome preparation using the thin-film hydration method will be described. Then the collection of placental samples and the setup of a human villous placental explants ex vivo model for the study of liposome behavior will be detailed. The steps for liquid-liquid extraction will be thoroughly described to achieve the best yield of extraction before explaining the steps of the HPLC method to quantify the fluorescent lipid DOPE-NBD in biological samples.

## 2 Materials

### 2.1 Lipids for Liposome Preparation

DMAPAP (dimyristoylaminopropylaminopropyl), a cationic lipid, was synthesized in our lab, as mentioned in a previous publication [17]. DSPE-PEG2000 (1,2-distearoyl-sn-glycero-3-phosphoethanolamine-N-polyethylene glycol 2000 ester), cholesterol, DOPE (1, 2-dioleoyl-sn-glycero-3-phosphoethanolamine), and DOPE conjugated to fluorescent NBD, DOPE-NBD, (1, 2-dioleoyl sn-glycero-3-phosphoethanolamine-N-(7-nitro-2-1, 3-benzodiazoxadiazol-4-yl)), were purchased from Avanti Polar Lipids (Alabaster, USA).

### 2.2 Reagents for Placenta Tissue Sampling and Culturing

Hank's balanced salt solution (HBSS), Dulbecco's Modified Eagle Medium (DMEM), penicillin-streptomycin, and glutamine were purchased from Merck (Saint Quentin Fallavier, France). Bovine serum albumin (BSA) was purchased from Interchim (Montluçon, France).

### 2.3 Reagents for Extraction and HPLC Analysis of DOPE-NBD

Triton X-100 was purchased from Merck (Saint Quentin Fallavier, France). All solvents were of HPLC grade and were obtained from Carlo Erba (Val de Reuil, France). Milli-Q system was used to obtain purified water and purchased from Millipore® synergy system (Millipore, Fontenay-sous-Bois, France), Nalgene® filter syringe filters, cellulose acetate, 4 mm (reference: 171-0020) (Thermo Fisher Scientific, Massachusetts, USA),

### 2.4 Equipment

Nano Zeta Sizer (NanoZS) (Malvern Panalytical, Malvern, United Kingdom); rotary evaporator Büchi® Rotavapor R-114 equipped with a v-100 Büchi® vacuum pump and controlled by a Büchi® Interface I-100 vacuum controller (Büchi, Villebon-sur-Yvette, France); Shimadzu LC-20AD high-performance liquid chromatography; Shimadzu fluorescence detector RF-20AXL (Duisburg, Germany); Nova Pak C18 guard column, 60 Å, 4 µm, 20 mm × 3.9 mm (Waters, Milford, Massachusetts, USA); Kromasil, 100-5-C18, 5 µm, 4.6 mm\*250 mm, 100 Å (Nouryon, Amsterdam, Netherlands); HPLC vial with an insert (reference: 12672465) (Thermo Fisher Scientific, Waltham, Massachusetts, USA); and Kimtech® tissue (Kimberly-Clark, Irving, Texas, USA).

## 3 Methods

This method has been developed to assess the placental uptake of liposomes containing the DOPE-NBD fluorescent lipid. Cationic and neutral liposomes were prepared and labeled through the incorporation of the fluorescent lipid DOPE-NBD. Placental tissues were obtained after the dissection of a human placenta (Fig. 1).

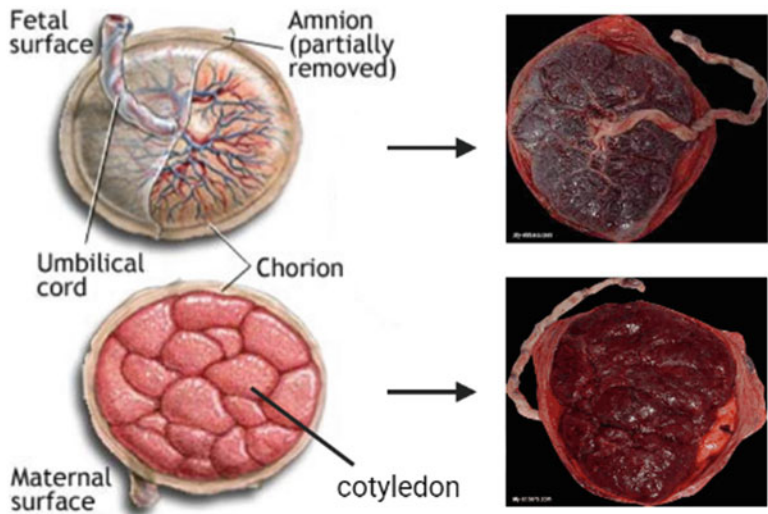


**Fig. 1** Anatomy of the term placenta and graphical presentation of the dissection process to extract human villous placental villi

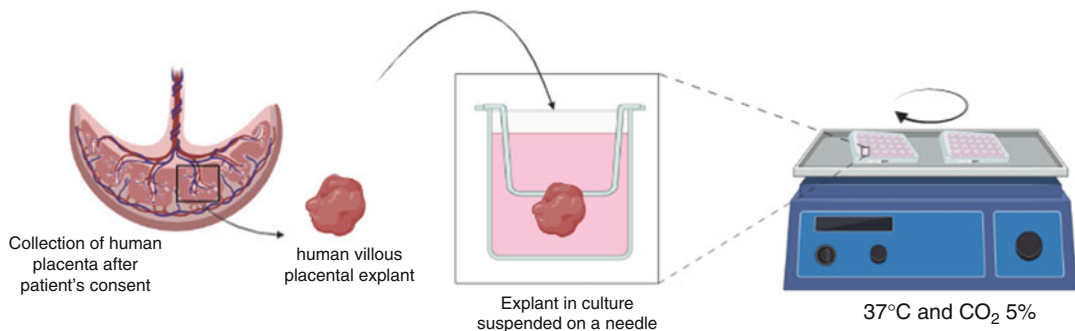


**Fig. 2** Optimized setup of culture techniques of ex vivo placental explants to study nanoparticle internalization

For the incubation of liposomes with placental explants, the culture conditions were adapted and optimized to mimic the *in vivo* situation (Fig. 2). A needle was used to suspend the human villous placenta explant to avoid any interaction with precipitated nano-carriers, and agitation in the incubator simulates the floating of villi into the mother's blood.

The extraction of the fluorescent probe from tissue should be optimized regarding the tissue samples used and the molecule which should be extracted. Chloroform was used in this study to retrieve DOPE-NBD from placental tissue through a liquid-liquid extraction protocol; the organic phase was then evaporated, and the extracted lipids were dissolved in ethanol.

Standard curves using various concentrations of DOPE-NBD in ethanol and containing the extract of control human villous placental tissues were realized to check the linearity and specificity

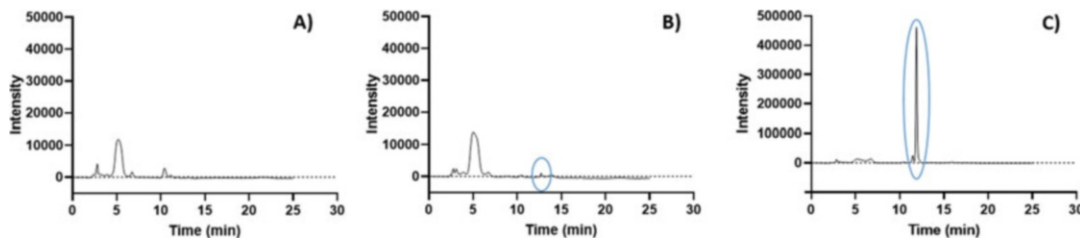


**Fig. 3** Chromatograms of DOPE-NBD inside placental extract. (a) Control sample of explants incubated with medium only, (b) DOPE NBD dosage of explants incubated with neutral liposomes at 0.3 mM for 24 h, (c) DOPE NBD dosage of explants incubated with cationic liposomes at 0.3 mM for 24 h. The Y-axis scale of cationic liposomes in graph c is ten times higher than that in graphs a and b

of the developed HPLC method. A standard curve integrating the extraction process was also performed, and a linear correlation between DOPE concentration and peak area was established. The quantification of neutral and cationic liposomes internalized in placental explants was determined as an application of this methodology. Results confirmed the ability of our method to provide precise information regarding the liposomes' internalization into placental tissue (Fig. 3).

### 3.1 Preparation of Neutral and Cationic Liposomes with Fluorescent Labeling

#### 3.1.1 Preparation of Neutral Liposomes Containing DOPE-NBD

Neutral liposomes were prepared through the thin-film hydration method previously described [18].

1. Prepare the stock solution of lipids, solubilized in a mix of chloroform/ethanol (50/50; v/v) at 10 mg/mL for dioleoyl-phosphatidylcholine (DOPC), 1 mg/mL for cholesterol and DSPE-PEG, and 0.2 mg/mL for DOPE-NBD. Ensure the appropriate dissolution of all lipids before proceeding to the next step.
2. Take the appropriate volume of stock solution to obtain the needed amount of each lipid: DOPC (236  $\mu$ L, 3 mM, 2.36 mg), cholesterol (66  $\mu$ L, 1.7 mM, 0.66 mg), DSPE-PEG (69  $\mu$ L, 0.25 mM, 0.69 mg), and DOPE-NBD (23  $\mu$ L, 0.05 mM, 0.046 mg).
3. Mix all lipids together and transfer them into a round-bottom flask of 5 mL (*see Note 1*).
4. Put the flask, which should be protected from light with aluminum foil, on a rotary evaporator and evaporate the organic solvent step by step to reach the lowest pressure (around 20 mbar). First, decrease the pressure from ambient pressure to 200 mbar in approximately 15 min with a moderated rotation speed. Then reduce the pressure from 200 to 20 mbar in about 30 min and leave the film under reduced pressure for three additional hours to ensure the complete removal of the solvent.

5. Once the film is completely dried, add 1 mL of NaCl 150 mM (filtered on 0.22 µM filters) to obtain a final concentration of lipid of 5 mM, and then leave the flask under rotation overnight at room temperature.
6. After a complete detachment of the lipid film from the walls of the flask, calibrate the liposome suspension using Avanti Polar Lipid Mini Extruder®. Suspension should be passed 11 times successively through filters of 0.8, 0.4, 0.2, and finally 0.1 µM to obtain a homogenized size distribution of particles around 100 nm.
7. The hydrodynamic diameter of liposomes in suspension was measured using dynamic light scattering (DLS) on a NanoZS (Malvern Panalytical). For this purpose, dilute 5 µL of liposome suspension into 500 µL of NaCl 20 mM in a specific cuvette and start the measurement.
8. The zeta potential of the liposomes in suspension was measured by electrophoretic light scattering (ELS) on a NanoZS (Malvern Panalytical). For this purpose, dilute 5 µL of liposome suspension into 500 µL of NaCl 20 mM in a specific cuvette and start the measurement.

### *3.1.2 Preparation of Cationic Liposomes Containing DOPE-NBD*

Cationic liposomes containing a specific cationic lipid, DMAPAP, developed in the laboratory were prepared using the thin-film hydration technique, as previously described [18].

1. Prepare the stock solution of lipids, solubilized in a mix of chloroform/ethanol (50/50; v/v) at 10 mg/mL for DMAPAP and DOPE, 1 mg/mL for DSPE-PEG, and 0.2 mg/mL for DOPE-NBD. Ensure the appropriate dissolution of all lipids before proceeding to the next step.
2. Take the appropriate volume of stock solution to obtain the needed amount of each lipid: DMAPAP (210 µL, 2.5 mM, 2.10 mg), DOPE (164 µL, 2.2 mM, 1.64 mg), DSPE-PEG (69 µL, 0.25 mM, 0.69 mg), and DOPE-NBD (23 µL, 0.05 mM, 0.046 mg).
3. Then repeat steps 3–7, which are detailed in the preparation of neutral liposomes (Subheading 3.1.1).

### **3.2 Dissection of Placental Explants from Human Placenta**

The isolation of tissue explants from the human placenta can be performed on a first-trimester placenta or term placenta obtained from the hospital, after the patient's consent. The collection of placentae from the hospital is possible after the validation of the ethical council. In this study, the collection of samples is framed by the CPP PRB (Comité de Protection des Personnes, Plateforme de Ressources Biologiques), Paris Cochin, N° 14–22, Paris, France. For this study, term placentae obtained after C-section from non-pathological pregnancies were used.

1. The placenta is placed under sterile conditions.
2. The umbilical cord is detached from the chorionic plate, and the decidua is cut on the edge to expose the cotyledons.
3. Several cotyledons are dissected around 25 mm<sup>3</sup> and are washed into three successive warm HBSS 1× baths (37 °C) to remove the maximum of the blood.
4. The first cotyledon is placed inside a large Petri dish (150 mm in diameter) filled with warm HBSS 1×.
5. Using a pair of tweezers, placental villi around 1 mm<sup>3</sup> are detached from the large mesenchymal axis.
6. The isolated villous explants are washed one time in HBSS 1× to ensure the removal of all the blood remaining.
7. Continue with the other cotyledons until none is left.
8. Then the collected villi are either snap frozen in liquid nitrogen and stored at –80 °C for up to 6 months to serve as control villi (*see Note 2*) or kept in culture conditions to be used for further experiments.

### **3.3 Incubation of Liposomes with Placental Explants**

1. Previously dissected placental explants are put in culture conditions in a 24 well-plate in 2 mL of complete DMEM 1× at 5% CO<sub>2</sub> and 37 °C for 24 h (*see Note 3*).
2. After 24 h, villi are hung on needles, and the culture medium is replaced by a dilution of liposomes in the culture at the desired concentration. For example, to incubate the villi with liposomes at 0.3 mM, 200 µL of liposome suspension at 5 mM is diluted inside 1800 µL of complete DMEM 1×. The 24-well plate is placed under agitation in the incubator at 36 rpm (*see Note 4*) for 24 h.
3. Villi are washed three times with warm HBSS 1×, then dried on a tissue, and then snap frozen in liquid nitrogen before processing for liquid-liquid extraction and HPLC quantification.

### **3.4 Liquid-Liquid Extraction of Fluorescent Probe DOPE-NBD from Human Placenta**

The liquid-liquid extraction process was performed following this protocol:

1. Villi are unfrozen at room temperature in a tube and then dried on a tissue and weighed on a precision balance (*see Note 5*).
2. Each villus is retrieved and finely cut with a scalpel on a flat glass surface, ensuring a homogenized mixture of tissue.
3. The mixture is then transferred to a polypropylene 5 mL tube that is resistant to organic solvents.
4. Optional part only for spiking: Here, add 100 µL of DOPE-NBD at the desired concentration and incubated at room temperature for 10 min. Then proceed to the extraction process.

5. Add 400 µL of Milli-Q water and 100 µL of Triton X (10%) to help the disruption of the tissue.
6. Vortex at 2000 rpm for 2 min at room temperature; the sample should be protected from light.
7. Add 3 mL of chloroform inside the tube and proceed to vortex at 2000 rpm for 20 min at room temperature, and ensure the sample is protected from light.
8. Retrieve the tubes and perform centrifugation cycles for 10 min at room temperature.
9. Remove the 3 mL of chloroform with a syringe and a fine and long-enough needle, e.g., 23 G, and 30 mm length (*see Notes 6 and 7*).
10. Add to the same tube another 3 mL of chloroform and perform again **steps 8 and 9**.
11. Collect all 6 mL of organic phases retrieved inside a 25 mL round-bottom flask and place them on a rotary evaporator.
12. Perform the evaporation of the chloroform under 20 mbar until completely dried to retrieve a lipid film at the bottom of the flask. Once all liquid is evaporated, keep it under vacuum for 30 min to ensure all chloroform has been removed.
13. Retrieve the lipid film by adding 500 µL of ethanol and gently vortex until the complete dissolution of the film from the walls of the flask. For the matrix standard curve, the lipid film should be retrieved by 500 µL of DOPE-NBD in absolute ethanol at a known concentration.
14. Filtrate the collected sample on a small acetate cellulose Nalgene® filter (*see Note 8*).
15. Perform the HPLC analysis.

### **3.5 Preparation of Calibration Curves of DOPE-NBD in Placental Tissues**

The idea was to develop a method to quantify the fluorescent lipid contained in liposomes, which means being able to indirectly quantify the number of liposomes inside the studied tissue. For this matter, several calibration curves should be prepared:

- DOPE-NBD dissolved in absolute ethanol
  - DOPE-NBD prepared in absolute ethanol in the presence of a control villous extract, called a “matrix” standard curve
  - DOPE-NBD prepared in absolute ethanol and incubated with control villi before proceeding to the extraction process to consider the extraction yield in the results, called a “spiked” standard curve.
1. Prepare a stock solution of DOPE-NBD at a concentration of 200 mg/L by dissolving 1 mg of DOPE-NBD powder in 5 mL of absolute ethanol, and protect the solution from light. It can be stored at –20 °C for long-term storage.

2. Proceed to the serial dilutions of DOPE-NBD in ethanol to obtain the following concentrations: 2.5, 5, 10, 20, 30, and 60  $\mu\text{g/L}$ . For spiked villi, it should be more concentrated in order to retrieve the same concentrations as the two previous standard curves. During the extraction process, DOPE-NBD is diluted five times; therefore, the concentrations used for DOPE-NBD in this case should be 12.5, 25, 50, 100, 150, and 300  $\mu\text{g/L}$ .
3. Check the linearity of the method using three series of freshly prepared calibration standard samples. Determine the peak area of each chromatogram and plot each curve. Determine the correlation coefficient and the equation of the linear correlation, as presented in Fig. 4.

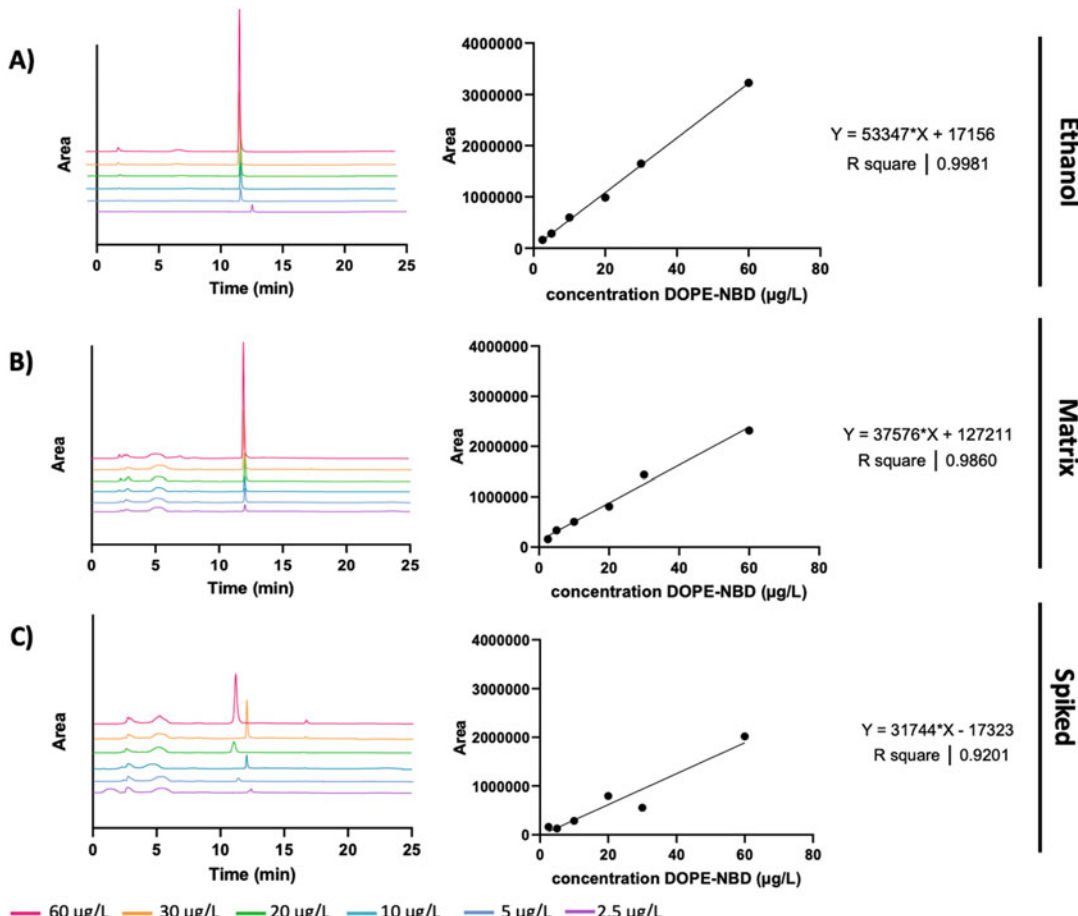


**Fig. 4** (a) Chromatograms of DOPE-NBD quantification in ethanol and the corresponding standard curve, (b) chromatograms of DOPE-NBD quantification of villi spiked after the extraction process and the corresponding “matrix” standard curve, (c) chromatograms of DOPE-NBD quantification of villi spiked before the extraction process and the corresponding “spiked” standard curve

### 3.6 HPLC Quantification of DOPE-NBD in Samples

HPLC analysis was performed on Shimadzu LC-20AD high-performance liquid chromatography completed with a quaternary pump, mobile phase degasser, and autosampler linked to a C18 column. The detection was obtained by Shimadzu fluorescence detector RF-20AXL using excitation and emission wavelengths of 465 nm and 535 nm, respectively. LabSolutions software was used for HPLC monitoring and acquisition.

The gradient mobile phase was composed of water, methanol, and isopropanol. For the first 5 min, a mobile phase of methanol, water, and isopropanol (80%, 10%, and 10%, respectively) was maintained, then changed to isopropanol and methanol (60% and 40%, respectively) in 5 min, and then kept for 5 min; finally, the conditions are returned to the initial ones in 5 min and kept at that for the last 5 min of the run. The total time of the elution gradient was 25 min, exhibiting a flow rate of 1 mL/min and an injection volume of 50 µL (*see Notes 9 and 10*).

1. Install a precolumn (Nova Pak C18 guard column, 60 Å, 4 µm, 20 mm × 3.9 mm) and column (Kromasil, 100-5-C18, 5 µm, 4.6 mm\*250 mm, 100) (*see Note 9*).
2. Fill 1 L glass bottle of mobile phase as follows:
  - Line A: Milli-Q water
  - Line B: Methanol HPLC grade
  - Line C: Isopropanol HPLC grade
3. Open lab solution software and create a new method file. Make sure the pump is off.
4. Purge each line for 5 min to remove any air bubbles in the tubing.
5. Start conditioning the column with 100% methanol. Start the pump at a flow rate of 0.1 mL/min. Leave for 5 min. Increase 0.1 by 0.1 mL/min until you reach 0.5 mL/min. Leave it to equilibrate for 10 min.
6. Start to introduce the isopropanol in the column. Flow the mobile phase at 80% methanol and 20% isopropanol with a flow rate of 0.1 mL/min. Leave it for 5 min. Increase 0.1 by 0.1 mL/min until you reach 0.5 mL/min. Leave it to equilibrate for 10 min.
7. Switch to the mobile phase, which will be used for the analysis of samples. Flow the mobile phase with 80% methanol, 10% isopropanol, and 10% water at 0.1 mL/min and leave it to equilibrate for 5 min. Increase 0.1 by 0.1 mL/min until you reach 1 mL/min. The pressure pump should not exceed 150 mbar (*see Note 11*).

8. When the pressure is equilibrated and the mobile phase is running at 1 mL/min, the apparatus is ready for sample analysis.
9. Take a minimum volume of 100 µL of sample to be analyzed and place it in a specific HPLC vial with an insert for small volumes. Place the vial in the rack.
10. Start a run for the sample and indicate the rack number and the vial number spot on the software. The injection volume should be 50 µL (*see Note 10*).
11. The run lasts for 25 min. After the run, the chromatogram will be available in the post-run section of the software.
12. To estimate the area under the curve of DOPE-NBD, integrate the DOPE-NBD peak at 12.5 min.

### **3.7 Calculation of the Amount of DOPE-NBD Inside Placental Tissue Sample**

1. Calculate the concentration of DOPE-NBD in the sample by using the linear regression equation obtained with the calibration curves:

$$y = ax + b$$

$$\rightarrow x = \frac{y - b}{a}$$

where  $y$  is the peak area and  $x$  is the concentration of DOPE-NBD in µg/L in the sample.

2. Calculate the mass of DOPE-NBD extracted from this sample (m1):

$$m1 = x \times 50.10^{-6}$$

where m1 is the mass of DOPE-NBD extracted in µg from the sample of 50 µL with a concentration of  $x$ .

3. To determine the % of uptake, first, calculate the mass of DOPE-NBD incubated with the explants (m2). DOPE-NBD represents 1% of the total lipid concentration ( $mM$ ) of liposomes ( $c$ ); the incubation volume ( $V$ ) with explants is 1 mL, and the DOPE-NBD molecular weight ( $M$ ) is 927 g/mol:

$$1\% \text{ of } c = \frac{m2_{\text{DOPE-NBD}}}{V \times M}$$

$$\rightarrow m2 = 0.01 * c \times 1 \times 927$$

$$\rightarrow m2 = 9.27 \text{ } c$$

4. Determine the % uptake of DOPE and, therefore, of liposomes in the placental tissue:

$$\% \text{ uptake} = \frac{m1}{m2} \times 100$$

5. Finally, calculate the mass of DOPE-NBD extracted per mg of villus:

$$\frac{m_1}{\text{Weight of the villi (mg)}}$$

This information allows the avoidance of any variability between samples as each villus isolated from the placenta has a specific weight, and all placentae are heterogeneous in terms of density.

---

#### 4 Notes

1. The solubility of each lipid should be carefully studied and well known prior to the experiment. If lipids are not well solubilized, aggregates can form in the lipid film and prevent the homogeneous formation of lipid bilayers.
2. To snap frozen villi with liquid nitrogen, each villus should be well washed and then well dried on a specific tissue Kimtech® to ensure the minimum residues of water, which could prevent the deep freezing of the tissues.
3. After dissection, villi are damaged, and the external cellular layer should reform. Therefore, the villi are maintained for 24 h in culture to restore the layer before performing any experiment to evaluate the internalization of nanoparticles.
4. Hanging villi on needles and placing the plate under agitation is a means to optimize culture conditions to recreate an *in vivo* situation of floating villi in the maternal blood. Moreover, some liposomes tend to aggregate in a medium containing serum. If villi are placed at the bottom of the well also, the sedimentation of liposomes will force contact with the outer layer of explants and induce bias in the internalization results. Therefore, this dynamic setup helps to overcome this situation.
5. It is important to weigh each villus. As they are unique samples and are fully consumed at the end of the experiment, it is important to collect these data, which can be useful afterward, to calculate the uptake of fluorescent probe by mg of tissue.
6. The organic phase to retrieve is below the aqueous phase, and access to this phase is difficult because the layer of cellular component is staying at the surface. With the needle, carefully pass the cellular layer and debris by orienting the tip of the needle toward the tube and sliding it against the wall of the tube straight to the bottom. Aspire almost all the organic phase and stop before the aqueous phase. Pay extra attention not to aspire any cellular debris that could lead to any blockage of the filtration step before HPLC dosage.

7. It is preferable to use a 1 mL syringe and extract the organic phase in three steps, which is easier to handle than a larger syringe to prevent any aspiration of the aqueous phase or cellular debris.
8. The filter selected is adapted for organic solvent and for small volume. You should pay extra attention to hold tight the filter on the syringe because the samples retrieved after the solubilization of lipids in ethanol can contain residues and debris of placental tissues and provoke an overpressure in the filter, leading to a potential loss of the sample.
9. The use of a precolumn is mandatory here to protect the integrity of the column throughout time. As samples contain lipids extracted from biological samples, it is advised to avoid any contamination of the column for further experiments.
10. The volume of injection is critical here; it should be fixed at the beginning of the study and should never change in between experiments.
11. The pressure should not exceed 150 mbar (or the maximum pressure that could be used according to column specification). If the pressure is not equilibrated to the right value, proceed again to **steps 5** and **6** and go slower during **step 7** of Sub-heading **3.6** while increasing the pressure.

## References

1. Fliedel L, Alhareth K, Mignet N, Fournier T, Andrieux K (2022) Placental models for evaluation of nanocarriers as drug delivery systems for pregnancy associated disorders. *Biomedicines* 10:936. <https://doi.org/10.3390/biomedicines10050936>
2. Keelan JA, Leong JW, Ho D, Iyer KS (2015) Therapeutic and safety considerations of nanoparticle-mediated drug delivery in pregnancy. *Nanomedicine* 10:2229–2247. <https://doi.org/10.2217/nnm.15.48>
3. Joshi MD (2017) Drug delivery during pregnancy: how can nanomedicine be used? *Ther Deliv* 8:1023–1025
4. Menezes V, Malek A, Keelan J (2012) Nanoparticulate drug delivery in pregnancy: placental passage and fetal exposure. *Curr Pharm Biotechnol* 12:731–742. <https://doi.org/10.2174/138920111795471010>
5. Valero L, Alhareth K, Gil S, Lecarpentier E, Tsatsaris V, Mignet N, Fournier T, Andrieux K (2018) Nanomedicine as a potential approach to empower the new strategies for the treatment of preeclampsia. *Drug Discov Today* 23:1099–1107. <https://doi.org/10.1016/j.drudis.2018.01.048>
6. Bajoria R, Sooranna SR, Contractor SF (1997) Endocytotic uptake of small unilamellar liposomes by human trophoblast cells in culture. *Hum Reprod* 12:1343–1348. <https://doi.org/10.1093/humrep/12.6.1343>
7. Refuerzo JS, Alexander JF, Leonard F, Leon M, Longo M, Godin B (2015) Liposomes: a nanoscale drug carrying system to prevent indomethacin passage to the fetus in a pregnant mouse model. *Am J Obstet Gynecol* 212:508.e1–508.e7. <https://doi.org/10.1016/j.ajog.2015.02.006>
8. Kaga M, Li H, Ohta H, Taguchi K, Ogaki S, Izumi H, Inagaki M, Tsuchiya S, Okamura K, Otagiri M et al (2012) Liposome-encapsulated hemoglobin (hemoglobin-vesicle) is not transferred from mother to fetus at the late stage of pregnancy in the rat model. *Life Sci* 91:420–428. <https://doi.org/10.1016/j.lfs.2012.08.021>
9. Figueroa-Espada CG, Mitchell MJ, Riley RS, Hofbauer S (2020) Exploiting the placenta for nanoparticle-mediated drug delivery during pregnancy. *Adv Drug Deliv Rev* 160:244–261. <https://doi.org/10.1016/j.addr.2020.09.006>

10. Orendi K, Kivity V, Sammar M, Grimpel Y, Gonen R, Meiri H, Lubzens E, Huppertz B (2011) Placental and trophoblastic in vitro models to study preventive and therapeutic agents for preeclampsia. *Placenta* 32:S49–S54. <https://doi.org/10.1016/j.placenta.2010.11.023>
11. Valero L, Alhareth K, Espinoza Romero J, Viricel W, Leblond J, Chissey A, Dhotel H, Roques C, Campiol Arruda D, Escriou V et al (2018) Liposomes as gene delivery vectors for human placental cells. *Molecules* 23:1085. <https://doi.org/10.3390/molecules23051085>
12. Alfaifi AA, Heyder RS, Bielski ER, Almuqbil RM, Kavdia M, Gerk PM, da Rocha SRP (2020) Megalin-targeting liposomes for placental drug delivery. *J Control Release* 324: 366–378. <https://doi.org/10.1016/j.jconrel.2020.05.033>
13. Renshall LJ, Beards F, Evangelinos A, Greenwood SL, Brownbill P, Stevens A, Sibley CP, Aplin JD, Johnstone ED, Teesalu T et al (2021) Targeted delivery of epidermal growth factor to the human placenta to treat fetal growth restriction. *Pharmaceutics* 13:1778. <https://doi.org/10.3390/pharmaceutics13111778>
14. Yu Q, Qiu Y, Wang X, Tang J, Liu Y, Mei L, Li M, Yang M, Tang L, Gao H et al (2018) Efficient siRNA transfer to knockdown a placenta specific lncRNA using RGD-modified nano-liposome: a new preeclampsia-like mouse model. *Int J Pharm* 546:115–124. <https://doi.org/10.1016/j.ijpharm.2018.05.001>
15. Valero L, Alhareth K, Gil S, Simasotchi C, Roques C, Scherman D, Mignet N, Fournier T, Andrieux K (2017) Assessment of dually labelled PEGylated liposomes transplacental passage and placental penetration using a combination of two ex-vivo human models: the dually perfused placenta and the suspended villous explants. *Int J Pharm* 532:729–737. <https://doi.org/10.1016/j.ijpharm.2017.07.076>
16. Alhareth K, Valero L, Mohamed KE, Fliedel L, Roques C, Gil S, Mignet N, Fournier T, Andrieux K (2019) Qualitative and quantitative analysis of the uptake of lipoplexes by villous placenta explants. *Int J Pharm* 567: 118479. <https://doi.org/10.1016/j.ijpharm.2019.118479>
17. Mignet N, Richard C, Seguin J, Largeau C, Bessodes M, Scherman D (2008) Anionic pH-sensitive pegylated lipoplexes to deliver DNA to tumors. *Int J Pharm* 361:194–201. <https://doi.org/10.1016/j.ijpharm.2008.05.017>
18. Zhang H (2017) Thin-film hydration followed by extrusion method for liposome preparation. In: *Methods in molecular biology*, vol 1522. Humana Press, Clifton, pp 17–22

# INDEX

## A

- Analyses.....109, 171, 201, 203, 214, 222, 228–230, 232–235, 237, 247–250, 270–272, 275, 298, 299  
Anionic.....53, 128–133, 228  
Anionic lipoplexes .....128, 129, 134  
Antibodies .....8–10, 160, 174, 175, 197–199, 204, 205, 275  
Atomic force microscopy (AFM) .....106, 110, 111, 116, 117, 253–261  
Azide-alkyne cycloaddition .....176, 178

## B

- Bacteria .....23, 26, 28, 40, 41  
Bicinchoninic acid (BCA) protein assay .....134  
Bilayers .....2–4, 8, 13, 14, 25, 44, 50, 57, 58, 62, 71, 73, 74, 84, 129, 153, 159, 169, 173, 175, 191, 221, 227, 228, 241–243, 245, 249, 254, 266, 277, 279, 280, 300  
Bioactive molecules .....174, 221, 224, 265  
Bioconjugation chemistry .....186  
Biological membranes .....1, 2, 4, 5, 57, 176  
Biopharmaceuticals .....11, 22, 198  
Biotin .....176, 178, 182, 183, 186  
Bone targeting .....207, 208, 211, 214, 217–219

## C

- Cantilever .....106, 117, 254, 255, 257, 259–261  
Carboxyfluorescein (CF) .....24, 25, 27, 29–31, 34, 41–43, 290  
Cationic .....12, 13, 53, 58, 121–125, 128, 130, 132–135, 279, 290, 291, 293, 294  
Cationic lipids .....12–14, 53, 58, 121, 127–130, 132, 135, 228, 278, 291, 294  
Cholesterol .....6, 7, 13, 14, 25, 27, 53, 57–59, 65, 67, 68, 89, 90, 96, 105, 121, 130, 149, 162, 169, 178, 180, 192, 207–209, 211, 214, 216, 217, 219, 221, 228–230, 232, 233, 237, 247, 255, 272, 278, 291, 293  
Click chemistry .....174–176, 181, 185  
Colloid .....4, 5, 13, 53, 245  
Colocalization .....271, 272, 274, 275  
Confocal microscopy .....218, 266, 270, 290

- Copper-free click chemistry .....176  
Cyclodextrin (CD) .....23, 25–27, 35–37, 44  
Cytosol .....7, 265

## D

- Dehydration-rehydration vesicles (DRVs) .....6, 9, 22, 24–27, 30, 33–37, 39, 43  
Detergents .....3, 13, 43, 50, 52–54, 148, 167, 170, 181  
Dialysis .....39, 41, 50–54, 69, 97–100, 107, 111, 170, 171, 209  
Differential scanning calorimetry (DSC) .....107, 111, 115  
Diffusion .....4, 66, 69, 87, 104, 112, 150, 241  
Distributions .....25, 49, 61, 92, 99, 116, 132, 143, 151, 167, 207, 215, 219, 228, 246, 249, 266, 270, 271, 275, 277, 294  
DNA .....3, 11, 12, 23, 24, 26, 27, 32, 37–40, 44, 50, 103, 121–130, 132, 134, 135, 247, 265, 278  
Doxorubicin .....24, 95–100, 103–117, 202, 205, 247  
Dried reconstituted vesicles (DRV) .....6, 22–44  
Drug carriers .....7, 191  
Drug delivery .....5, 6, 8–10, 13, 14, 49, 58, 65, 71, 73, 104, 139, 140, 159, 173, 175, 197, 208, 228, 245, 247, 254, 265, 266, 289  
Drug/lipid ratio .....54, 92, 133, 205, 221  
Dye exclusion .....122, 124, 125  
Dynamic light scattering (DLS) .....53, 97, 106, 114, 132, 133, 143, 150, 151, 163, 178, 180, 185, 186, 269, 279, 283, 294

## E

- Electron microscopy .....2, 148, 193, 194, 245–250  
  cryo transmission .....148  
  transmission .....106, 110, 111, 193, 194, 245–250  
Emulsion transfer .....74, 77, 78, 83  
Encapsulation efficiencies .....6, 24, 25, 34, 36, 42, 43, 58, 61, 62, 69, 97, 100, 110, 122, 144, 145, 195, 196  
Endocytosis .....121, 174, 191  
Endosomes .....122, 127, 128, 131  
Ethanol injection .....65–67, 69, 99  
Europium .....278–283, 285, 286

Extruder ..... 59, 60, 62, 75, 96, 97, 99, 106, 108, 116, 122, 125, 126, 162, 163, 167, 168, 278  
Extrusion ..... 40, 43, 60–62, 65–67, 80, 81, 99, 116, 163, 166–168, 213–215, 220, 244

**F**

Fab ..... 197–205  
Fatty acid self-assembly ..... 75, 78  
Flame ionization detector (FID) ..... 221–225, 228  
Flow cytometry ..... 154  
Fluidity ..... 69, 73, 167, 169, 228, 241–243  
Fluorescein isothiocyanate (FITC) ..... 216, 217, 219, 270  
Fluorescence ..... 25, 34, 83, 95, 122, 124, 129–131, 134, 154–156, 165, 181, 185, 241–244, 266, 273, 278, 279, 281, 282, 284, 290, 291, 298  
Folic acid ..... 174, 191–196  
Fourier transform infrared spectroscopy ..... 151  
Freeze-thaw ..... 122, 125

**G**

Gene delivery ..... 128, 173  
Giant unilamellar vesicles (GUVs) ..... 58, 71, 76–78, 80–82

**H**

Hemolysis ..... 107, 108, 114  
High Performance Liquid Chromatography (HPLC) ..... 100, 144, 228, 229, 232, 234–237, 289–301  
HPTLC ..... 221–225, 228  
Hydrophilic drugs ..... 23, 29, 65, 69, 141, 218

**I**

Imaging ..... 57, 83, 89, 90, 216, 218, 219, 246–250, 255–261, 270, 273, 275  
Immunoliposomes ..... 197, 199, 200, 202, 203, 205

**L**

Labeling ..... 290  
Laser doppler velocimetry (LDV) ..... 106, 143  
Lipids ..... 2–6, 9, 12–14, 22, 23, 25–43, 50, 52–54, 57–62, 65, 69, 71–78, 80–85, 87–92, 96, 97, 99, 100, 103, 108, 110, 114–117, 121–125, 127–133, 135, 139–145, 147–150, 153–155, 159–171, 174–177, 179–183, 186, 192–195, 200, 202–205, 208, 211, 212, 216, 217, 221, 222, 227–238, 241–244, 247, 249, 254–256, 258, 261, 266, 267, 269, 272, 273, 277–285, 290–294, 296, 299–301  
analysis ..... 228–230, 234

bilayer ..... 2–4, 13, 25, 50, 57, 62, 71, 74, 169, 221, 227, 243, 249, 266, 300

Lipophilic drugs ..... 23, 25, 35, 195

Lipoplexes ..... 13, 58, 121, 122, 125, 126, 128, 130–133, 278, 279

Liposomal bilayers ..... 104, 170

Liposomes ..... 1–14, 22–44, 49, 50, 53, 54, 57, 58, 60–62, 65–71, 87–93, 95–100, 104–117, 121–125, 128–130, 132, 133, 135, 139, 151, 154, 159–161, 163–165, 167–171, 173–178, 180, 181, 183–186, 191–199, 202–205, 207, 208, 211–223, 227–238, 241–250, 254–256, 258, 260, 261, 266–273, 275, 277–286, 289–296, 299, 300

anionic ..... 129, 130, 132–134

cationic ..... 12, 13, 58, 121–126, 131–133, 290, 293, 294

distribution ..... 61, 92, 116, 215, 217–218, 265–275

neutral ..... 11, 58, 228, 290, 293

magnetic ..... 104, 111, 112  
thermosensitive ..... 103–117

Lysolipids ..... 72, 73, 77

Lysotracker ..... 275

**M**

Magnetic ..... 51, 52, 68, 75, 96, 97, 104, 105, 107, 111, 112, 115, 141, 147, 148

Magnetic resonance imaging (MRI) ..... 117, 278, 279

Maleimide ..... 169, 174, 198

Mannose ..... 175, 176, 181, 184, 185

Mass spectrometry (MS) ..... 68, 74, 84, 227–238

Membranes ..... 2–6, 9, 12–14, 24, 26, 44, 50, 58–62, 71–74, 78, 81–84, 97, 100, 103, 106, 108, 114, 121, 122, 125, 126, 128, 147, 154, 160, 163, 167, 168, 173, 175, 176, 191, 193–195, 199, 202, 208, 212, 213, 216, 217, 227, 228, 231, 236, 241–243, 266, 277, 282

models ..... 4, 173

protein ..... 4, 147, 241

translocation ..... 4

transport ..... 4  
fluidity ..... 241–244

Microemulsions ..... 142–145

Microfluidics ..... 67, 87–93, 99

Mitochondria ..... 265, 266, 271, 274, 275

Models ..... 2–6, 25, 57, 71, 73, 95, 123, 147, 151, 153, 173, 176, 183, 235, 290

Multilamellar ..... 3–8, 13, 22,

liposome ..... 13, 22

vesicle ..... 22, 30, 58, 163, 246

**N**

- Nanoparticles ..... 12, 13, 23, 50, 55, 88, 127, 139, 140, 144, 150, 151, 154, 155, 174, 176, 191, 204, 289, 290, 292, 300

Negative staining ..... 245, 247, 248

- Neutral ..... 53, 58, 121, 228, 290, 291, 293, 294

**P**

- Particulates ..... 26, 27, 40, 41, 61
- Pegylated liposomes ..... 9, 130, 160–162, 164, 165, 169–171, 290

- Peptides ..... 6, 8, 9, 22, 23, 26, 27, 29, 37–40, 128, 154, 160, 174–176, 186, 208, 228, 254, 265

Pharmacokinetics ..... 160, 174, 277

Phase transition ..... 107, 111, 115

- Phase transition temperatures ..... 58, 99, 100, 104, 115, 116, 166–169, 195, 241, 272, 273

- Phosphates ..... 6, 12, 27, 35, 38, 67, 89, 108, 122, 123, 164, 168, 180, 242, 247

Phospholipases ..... 76, 81

- Phospholipids ..... 2–5, 8, 13, 14, 25, 28, 34, 35, 37, 38, 53, 57–59, 61, 65, 66, 68, 69, 71, 73, 76, 77, 80, 81, 96, 100, 104, 147–149, 159, 163, 164, 168, 169, 171, 173–175, 178, 180, 184, 185, 191, 195, 225, 228, 229, 237, 241, 244, 245, 247

Photon correlation spectroscopy (PCS) ..... 60, 62

pH-sensitive liposomes ..... 127–135

Placentas ..... 289–292, 294, 300

- Polyethylene glycol (PEG) ..... 7, 28, 39, 54, 128–130, 141, 149, 160, 162, 169–171, 174, 184, 192, 197, 198, 228, 278

- Post insertion ..... 160–162, 164, 166, 168–170, 174, 198

- Proteins ..... 2, 4, 6, 8–11, 22, 24, 26–29, 37–40, 44, 49, 54, 130, 132, 134, 135, 147, 160, 170, 174, 175, 186, 192, 194, 199, 200, 241, 247, 253, 278

Pyrophosphate ..... 208, 214

**R**

Radiolabel ..... 39

Remote loading ..... 95, 99, 109

**S**

- Small interfering ribonucleic acid (siRNA) ..... 127, 204, 265

- Small unilamellar ..... 6, 12, 22, 50, 58, 60, 99, 123, 180, 245

Solid lipid nanoparticles (SLNs) ..... 13, 139–145

- Sonication ..... 6, 26, 29, 30, 38, 42, 49, 54, 60, 61, 67, 69, 97, 116, 129, 167, 180, 220, 257, 273

Steric stabilization ..... 153, 154, 197

Surface modification ..... 88, 175, 191–196

Surfactants ..... 5, 52, 69, 139–144, 147

**T**

- Targeted ..... 6, 9, 10, 144, 145, 174, 175, 185, 191, 227, 236, 266

Thermosensitive ..... 104, 105, 107, 111, 115

- Thin-film hydration ..... 65–67, 76, 108, 123, 125, 192, 193, 267

3D printing ..... 88

Transfection ..... 11, 12, 121, 122, 132, 134

Translocation ..... 4, 176

- Transmission ..... 106, 110, 111, 148, 193, 194, 245–250

**U**

Uranyl acetate ..... 106, 110, 117, 248

**V**

- Vaccines ..... 1–14, 23, 24, 26, 27, 29, 38–40, 44, 57, 173, 175, 186

- Vesicles ..... 3, 4, 6, 7, 12–14, 22, 23, 25, 26, 30, 31, 34, 36–40, 43, 44, 50, 58, 65, 68, 71–77, 79–84, 87, 88, 90, 92, 99, 123, 148, 150–154, 159, 163, 173–176, 180, 181, 184–186, 227, 245, 246, 254, 256

Viscosity ..... 62, 83, 109, 116, 214, 241

**Z**

- Zeta potential ..... 53, 55, 69, 70, 106, 109, 129–131, 133, 143, 165, 167, 171, 194, 228, 269, 273, 279, 294

Z-stack ..... 271